

**SRS Bedrock Probabilistic Seismic Hazard Analysis (PSHA)  
Design Basis Justification (U)**

Geotechnical Engineering  
Technical and Quality Services  
Field Support Services Business Unit

**UNCLASSIFIED**  
DOES NOT CONTAIN  
UNCLASSIFIED CONTROLLED  
NUCLEAR INFORMATION  
ADC &  
Reviewing Bill Mitchell  
Official \_\_\_\_\_  
(Name and Title)  
Date: 12-14-05

Westinghouse Savannah River Company, LLC  
Savannah River Site  
Aiken, SC 29808

---

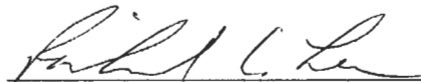
Prepared for the U.S. Department of Energy Under Contract No. DE-AC09-96SR18500



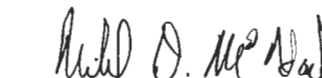
WSRC-TR-2005-00551, Rev. 0

SRS Bedrock Probabilistic Seismic Hazard Analysis (PSHA)  
Design Basis Justification (U)

Prepared by:

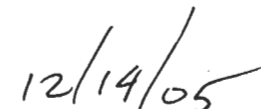
  
\_\_\_\_\_  
R. C. Lee

Verified by:

  
\_\_\_\_\_  
M. D. McHood

Approval by

  
\_\_\_\_\_  
M. R. Lewis  
Manager, Geotechnical Engineering

  
\_\_\_\_\_  
Date

**DISCLAIMER**

This report was prepared as an account of work sponsored by an agency of the United States Government. Neither the United States Government nor any agency thereof, nor any of their employees, nor any of their contractors, subcontractors or their employees makes any warranty, express or implied, or assumes any legal liability or responsibility for the accuracy, completeness, or any third party's use or the results of such use of any information, apparatus, product, or process disclosed, or represents that its use would not infringe privately owned rights. Reference herein to any specific commercial product, process, or service by trade name, trademark, manufacturer, or otherwise does not necessarily constitute or imply its endorsement, recommendation, or favoring by the United States Government or any agency thereof or its contractors or subcontractors. The views and opinions of authors expressed herein do not necessarily state or reflect those of the United States Government or any agency thereof.

## TABLE OF CONTENTS

<b>1.0</b>	<b>Summary.....</b>	<b>1</b>
<b>2.0</b>	<b>Introduction.....</b>	<b>2</b>
<b>3.0</b>	<b>Applicable DOE Guidance and Precedence, Scope .....</b>	<b>3</b>
<b>4.0</b>	<b>EPRI(1988) and LLNL(1993) PSHAs .....</b>	<b>4</b>
<b>5.0</b>	<b>More Recent Data Relevant to the Charleston Seismic Source .....</b>	<b>4</b>
<b>5.1</b>	<b>Paleoliquefaction Investigation.....</b>	<b>5</b>
<b>5.2</b>	<b>Talwani and Schaeffer (2001) Scenarios.....</b>	<b>6</b>
<b>5.3</b>	<b>Geographic Distribution of Inferred Earthquakes.....</b>	<b>8</b>
<b>6.0</b>	<b>Significance of New Data and Interpretations .....</b>	<b>9</b>
<b>6.1</b>	<b>Comparisons of EPRI (1988) Source Definitions to Recent Interpretations.....</b>	<b>9</b>
<b>6.2</b>	<b>Comparison of LLNL (1993) Source Definitions to Recent Interpretations.....</b>	<b>9</b>
<b>6.3</b>	<b>Developments in PSHA Methodologies.....</b>	<b>10</b>
<b>6.4</b>	<b>Comparison of Ground Motion Attenuation Models .....</b>	<b>10</b>
<b>7.0</b>	<b>USGS National Hazard Map Model.....</b>	<b>12</b>
<b>8.0</b>	<b>USGS National Map Source Model with Alternate GMAMs.....</b>	<b>15</b>
<b>8.1</b>	<b>EPRI (2004) .....</b>	<b>15</b>
<b>8.2</b>	<b>Silva et al. (2004) .....</b>	<b>18</b>
<b>9.0</b>	<b>Comparison of Hard-Rock Hazard.....</b>	<b>19</b>
<b>10.0</b>	<b>Considerations for PSHA Weighting .....</b>	<b>20</b>
<b>10.1</b>	<b>Recommended Model Weights .....</b>	<b>21</b>
<b>11.0</b>	<b>SRS Bedrock UHS Based on Model Weights .....</b>	<b>24</b>

<b>12.0 Discussion.....</b>	<b>24</b>
<b>13.0 Acknowledgements .....</b>	<b>25</b>
<b>14.0 References.....</b>	<b>26</b>
<b>15.0 Figures.....</b>	<b>33</b>
<b>Appendix A - Chronology of Probabilistic Seismic Hazard (PSHA) Studies and Use in Establishing the Design Basis Earthquake (DBE)</b>	<b>2 Pages</b>
<b>Appendix B – C. Cramer, Uncertainty in the National Seismic Hazard Maps Near the Savannah River Site, South Carolina, 6/30/04</b>	<b>34 Pages</b>
<b>Appendix C - Development of Regional Hard Rock Attenuation Relations for South Carolina, by W. Silva, N. Gregor and R. Lee, 9/17/04</b>	<b>65 Pages</b>

## 1.0 Summary

This represents an assessment of the available Savannah River Site (SRS) hard-rock probabilistic seismic hazard assessments (PSHAs), including PSHAs recently completed, for incorporation in the SRS seismic hazard update. The prior assessment of the SRS seismic design basis (WSRC, 1997) incorporated the results from two PSHAs that were published in 1988 and 1993. Because of the vintage of these studies, an assessment is necessary to establish the value of these PSHAs considering more recently collected data affecting seismic hazards and the availability of more recent PSHAs. This task is consistent with the Department of Energy (DOE) order, DOE O 420.1B and DOE guidance document DOE G 420.1-2.

Following DOE guidance, the National Map Hazard was reviewed and incorporated in this assessment. In addition to the National Map hazard, alternative ground motion attenuation models (GMAMs) are used with the National Map source model to produce alternate hazard assessments for the SRS. These hazard assessments are the basis for the updated hard-rock hazard recommendation made in this report. The development and comparison of hazard based on the National Map models and PSHAs completed using alternate GMAMs provides increased confidence in this hazard recommendation. The alternate GMAMs are the EPRI (2004), USGS (2002) and a regional specific model (Silva et al., 2004). Weights of 0.6, 0.3 and 0.1 are recommended for EPRI (2004), USGS (2002) and Silva et al. (2004) respectively. This weighting gives cluster weights of .39, .29, .15, .17 for the 1-corner, 2-corner, hybrid, and Greens-function models, respectively. This assessment is judged to be conservative as compared to WSRC (1997) and incorporates the range of prevailing expert opinion pertinent to the development of seismic hazard at the SRS.

The corresponding SRS hard-rock uniform hazard spectra are greater than the design spectra developed in WSRC (1997) that were based on the LLNL (1993) and EPRI (1988) PSHAs. The primary reasons for this difference is the greater activity rate used in contemporary models for the Charleston source zone and proper incorporation of uncertainty and randomness in GMAMs.

## 2.0 Introduction

This represents an assessment of the available Savannah River Site (SRS) hard-rock probabilistic seismic hazard assessments (PSHAs), including PSHAs recently completed, for incorporation in the SRS seismic hazard update. The prior assessment of the SRS seismic design basis (WSRC, 1997) incorporated the results from two PSHAs that were published in 1988 and 1993. Because of the vintage of these studies, an assessment is necessary to establish the value of these PSHAs considering more recently collected data affecting seismic hazards and the availability of more recent PSHAs. This task is consistent with the Department of Energy (DOE) order DOE O 420.1B (approved December 22, 2005), that states in part:

“A review of the state-of-the-art of NPH assessment methodology and of site-specific information must be conducted at least every 10 years. The review should include recommendations to the cognizant secretarial officers on the need for updating the existing NPH assessments based on identification of any significant changes in methods or data. If no change is warranted from earlier assessment, then this only needs to be documented.”

and DOE guidance document, DOE G 420.1-2 (approved March 28, 2000), that states in part:

“In the eastern United States it is recommended that the use of the USGS curves be for hard rock site[s] conditions, and as a result the USGS should be contacted to complete the appropriate computations. Any site whose site-specific hazard curves exceed the USGS curves (for similar site conditions) should continue to use these site-specific curves. If this is not the case, and specifically for the eastern United States, the USGS curves should be appropriately factored into existing assessment of site-specific seismic hazard.”

In addition to documenting new data and assessments relevant to the SRS hard-rock PSHA update, an assessment is made of the available PSHAs and recommendations are made on an appropriate PSHA weighting scheme. These selections and weights are critical to the development of site-specific soil hazard to be developed at a later date. Using these weights, recommended mean uniform hazard spectra are developed that are suitable for hard-rock site conditions. Based on the recommendations herein, site-specific hazard models (for soil surface) will be developed and combined using the same weights developed for the mean hard-rock hazard model.

Since the early Electric Power Research Institute (EPRI) and Lawrence Livermore National Laboratory (LLNL) PSHAs were conducted, a tremendous amount of new data and technologies have developed that bear on any assessment of ground motion in the southeastern United States. A few of the important developments are:

- Geologic evidence on the spatial and temporal characteristics of 1886 Charleston-type earthquakes,
- Geologic data and historic intensity data bearing on the size of the 1886 Charleston-type earthquakes,
- More recently collected eastern United States strong motion data to characterize seismic source models for ground motion characterization,
- Modeling of worldwide strong motion data that improve the general understanding of source and path characterization,
- Development of geophysical models of the crust in the vicinity of the SRS to better define wave propagation affecting the site, and
- Proper incorporation of uncertainty in ground motion attenuation models and in the development of PSHAs.

A total of five hard-rock PSHAs are considered in this assessment, two of the PSHAs are evaluations conducted in the mid-1980s and early-1990s for the electric power industry and the Nuclear Regulatory Commission (NRC) for the purposes of safety evaluation of nuclear power plants. These investigations were completed by EPRI and LLNL for evaluations of the nearby electrical utility (plant Vogtle). The LLNL study was updated in the early 1990s to incorporate more recent attenuation models, improve the rate of exceedence models and to incorporate some of the early geologic data constraining the rate of recurrence of the Charleston seismic source. Following DOE-STD-1023, these hard-rock PSHAs were used exclusively in the mid-1990s to update the SRS site-wide seismic design criteria (WSRC, 1997).

In late 2004, under contract to DOE/SR, three other SRS hard-rock PSHAs were developed by the United States Geological Survey (USGS) (Cramer, 2004). The USGS completed the three hard-rock PSHAs, including sensitivity analysis, based on the USGS National Map seismic source model. One PSHA was completed using the suite of National Map ground motion attenuation models (GMAMs), another PSHA was completed using the composite EPRI (2004) GMAMs (developed for the Early Site Permit study) and the third PSHA was completed using regionally specific GMAMs by Pacific Engineering and Analysis (Silva et al., 2004).

### **3.0 Applicable DOE Guidance and Precedence, Scope**

Most existing SRS facilities require DOE seismic design guidance. However, future SRS facilities, including potential privately owned and DOE waste processing facilities could require NRC seismic design guidance in new or existing facilities. The NRC and DOE guidance are similar in approach to developing design basis but use contrasting criteria to develop the uniform hazard spectrum (UHS). The NRC uses median  $10^{-5}$ /yr versus the DOE mean  $10^{-4}$ /yr probability of exceedence. Our approach with the SRS hard-rock update is to develop PSHA recommendations that can be applicable to either DOE or NRC design criteria. The UHS recommended herein meet DOE design guidance.



A chronology of development of SRS probabilistic design basis is listed in Appendix A. The applicable DOE guidance illustrates an evolution from PSHAs developed by LLNL or EPRI to those conducted by the USGS, reflecting increasing reliance on the National Map hazard model (e.g., see DOE G 420.1-2).

The strengths and weaknesses of these five PSHAs are summarized below and will form the basis of the model selection and weights to be applied for application to the SRS. Recommended hard-rock uniform hazard spectra are developed based on the recommended weights. These evaluations (including weights) incorporate the judgments of outside experts. The outside experts are Professor Martin Chapman of Virginia Polytechnical Institute and Mr. Ivan Wong of URS Corporation of Oakland, California who have reviewed and concur with this document.

The scope of this assessment is to use the reference hard-rock PSHAs to develop site-specific hazard for facilities requiring design criteria with probability of exceedances of the mean hazard ranging from about  $2 \times 10^{-3}$  to  $10^{-5}$ /yr to support engineering design and risk assessments.

#### **4.0 EPRI(1988) and LLNL(1993) PSHAs**

The prior SRS design basis (WSRC, 1997) incorporated two probabilistic seismic hazard studies, commonly referred to as the Lawrence Livermore National Laboratory (LLNL) study (Bernreuter, 1989; LLNL, 1993; USNRC, 1993), and EPRI study (EPRI, 1988) sometimes referred to as the EPRI-SOG study. Because of large differences between the original LLNL and EPRI PSHA results, an update of LLNL was completed and as a result, DOE revised its formal requirements as to how LLNL and EPRI studies should be used, stating that it was acceptable to directly average the LLNL and EPRI PSHA curves to derive the DBE.

The prior SRS design basis (WSRC, 1997) was developed in accordance with USDOE (1996) requirements, specifically, DOE-STD-1023 which provides guidelines for developing site-specific probabilistic seismic hazard assessments, and criteria for determining ground motion parameters for the design earthquakes. It also provides criteria for determination of design response spectra. The LLNL and EPRI hazard assessments used expert judgment and were judged to be state of practice by both the NRC and DOE as evidenced by their recommended use in design guidelines (USNRC, 1997, USDOE, 1996).

#### **5.0 More Recent Data Relevant to the Charleston Seismic Source**

Following the original EPRI and LLNL PSHAs, geological investigations in South Carolina uncovered evidence supporting the earlier occurrence of earthquakes similar to (i.e., location and size) the 1886 Charleston event. Prior to this discovery and interpretation, the 1886 Charleston earthquake was thought by some to be a one-time

event or an event symptomatic of regional crustal deformation and could therefore occur anywhere in the eastern US.

### 5.1 Paleoliquefaction Investigation

Paleoliquefaction studies in South Carolina date back to Cox and Talwani (1983), and Cox (1984), who first discovered evidence for earthquake induced liquefaction preserved in the Coastal Plain sediments (Talwani et al., 1999; Talwani and Cox, 1985). The purpose of these studies was to locate seismically induced sand blows and use geologic and carbon dating techniques in an attempt to date the occurrence of the seismic event that resulted in the development of the sand blow.

At about the same time as the initial Cox effort, the USGS was also locating and investigating sand blows in the southeastern U.S. (SEUS) (Gohn et al., 1984; Obermeier et al., 1985; Weems et al., 1986). In addition the NRC had studies completed for the South Carolina area (Amick et al., 1990) and an extensive study along the eastern seaboard of the United States (Gelinas et al., 1998). In that study, field investigations were conducted at over 1000 sites along the Atlantic coast (including sites in Delaware, Virginia, North Carolina, South Carolina and Georgia) that were potentially susceptible to liquefaction. The purpose of that study was not only to date the paleoliquefaction features and gain an understanding of the hazards posed by the 1886 Charleston-type earthquakes, but also to understand the geographic extent of those features and, if possible, to estimate the magnitudes of pre- 1886 earthquakes.

Two important results of the Amick et al. (1990) investigation (which was also subsequently confirmed later in Gelinas et al., 1998) were: 1) nearly all incidences of liquefaction on the Atlantic seaboard were limited to South Carolina and 2) no conclusive evidence of large prehistoric earthquakes originating outside of South Carolina was found. Thus, an 1886 Charleston-like event was constrained. The NRC (USNRC, 1991) agreed that this result indicated a lower probability that a Charleston-type earthquake could occur randomly along the eastern seaboard. In addition, six dates of large earthquakes were established, five of which could be the result of an 1886 Charleston-type earthquake and one a smaller event near Georgetown, South Carolina. Other findings originating from Amick et al. (1990) were:

- The vast majority of liquefaction features occur either in deposits of late Pleistocene or Holocene age (4,000 to about 240,000 years old).
- None of the identified liquefaction sites were found in deposits older than about 700,000 years.
- Liquefaction sites around Charleston were found primarily in either beach, back-barrier, or fluvial deposits, with the beach setting the most favorable.
- Nearly all sites that had evidence of liquefaction were underlain by at least three meters (about 10 feet) of sand or at least 3 meters of alternating sand, silt and clay beds. The source beds of these features were less than six to seven meters (about 19

to 23 feet) deep and the ground water table was less than one to three meters (about 3 to 10 feet) beneath the present ground surface.

- The majority of the liquefaction sites occurred in soils classified as sands or silty sands under the Unified Soil Classification System.
- The majority of the liquefaction sites associated with the 1886 earthquake were found within 40 kilometers (km) of the known epicenter of that event.
- The thickness of the source bed, the presence or absence of an overlying non-liquefiable cap, and the thickness and strength of the cap material greatly controlled the degree and type of liquefaction feature that formed, and
- The liquefaction features that typify the coastal South Carolina area have been observed to be sand-blow explosion craters and sand vents/fissures.

## 5.2 Talwani and Schaeffer (2001) Scenarios

Talwani and Schaeffer (2001) improved the scenarios for the occurrence of large earthquakes in the SEUS based on the reanalysis of paleoliquefaction investigations conducted in South Carolina. The reanalysis included the calibration of  $^{14}\text{C}$  dates based on the published fluctuation of atmospheric  $^{14}\text{C}$ . Because  $^{14}\text{C}$  has fluctuated for the last several thousand years, previous age estimates made on organic material retrieved from the sandblow could be biased. Talwani and Schaeffer calibrated the date of formation of the sandblows by using a published calibration time scale based on the  $^{14}\text{C}$  fluctuation observed from tree-rings. Following the calibration, grouping of the paleoearthquake dates in time and space was undertaken to roughly estimate the event size, location and return period. Based on the correlation of the liquefaction episodes, seven prehistoric events were found (events A-G, Table 1). Three of which were smaller events ( $M \sim 5-6$ ), two occurring in the northern part of South Carolina (event C and F) and the other occurring at the southern end of South Carolina (event D). The other four events were estimated to be of comparable magnitude and location to the 1886 Charleston earthquake ( $M \sim 7+$ ). Because the paleoearthquake dates were uncertain and in some cases difficult to correlate, an alternate scenario (scenario 2) was devised that combined the two smaller events C and D to a single event (event C') of magnitude about 7+. These events are summarized below in Table 1 (modified from Talwani and Schaeffer).

**Table 1**

Two scenarios for paleoearthquake ages and source zones (taken from Talwani and Schaeffer, 2001)

Liquefaction Episode	Age, years (ybp)	Scenario 1		Scenario 2	
		Source	Magnitude	Source	Magnitude
1886 AD	113	Charleston	7.3	Charleston	7.3
A	546±17	Charleston	7+	Charleston	7+
B	1021±30	Charleston	7+	Charleston	7+
C	1648±74	northern part	~6	-	-
C'	1683±70	-	-	Charleston	7+
D	1966±212	southern part	~6	-	-
E	3548±66	Charleston	7+	Charleston	7+
F	5038±166	northern part	~6	Charleston	7+
G	5800±500	Charleston	7+	Charleston	7+

Cox (1984) and other more recent works are reviewed briefly in Talwani and Schaeffer (2001). Table 2 below summarizes the results of these investigations and indicates inferred return period for large earthquakes in the SEUS.

**Table 2**

Chronology of Charleston source return periods from selected paleoearthquake studies in South Carolina.

<u>Author</u>	<u>Site</u>	<u>Comments/return period (RP)</u>
Cox, 1984	Ravenel, SC	first paleoliquefaction site in SEUS
Gohn et al., 1984	Hollywood, SC site	discovered other sandblows
Obermeier, et al., 1985	Hollywood site	discovered other sandblows and developed sequence of earthquakes
Talwani and Cox, 1985	Hollywood site	1500-1800 years RP
Weems et al., 1986	Hollywood site	1800 years or less RP
Obermeier, et al., 1990	Charleston	inferred three large eqks in past 7200 years
Amick, et al., 1990	1000 sites from New Jersey to Florida paleoliquefaction features predominantly in South Carolina	six events w/ 1000 yrs RP 500-600 yrs RP for recent events; possible smaller event to the north
Talwani & Schaeffer, 2001	Calibrated available data and added new sites in Bluffton	six or seven events with RP 500-600 yrs for recent events; possible smaller events to north and south

### 5.3 Geographic Distribution of Inferred Earthquakes

The geographic distribution of the dated sand boils associated with earthquakes ( $M \sim 7+$ ) in the Charleston vicinity and the possible smaller events ( $M \leq 6$ ) along the coast of South Carolina are illustrated in Figure 1 (modified from Talwani and Schaeffer). Figure 1 shows the South Carolina coastal area, including the intense craterlet area caused by the 1886 earthquake. The paleoliquefaction sites re-evaluated by Talwani and Schaeffer are shown as triangles. Reported liquefaction from the 1886 magnitude ( $M_w$ )  $\sim 7.3$  earthquake is shown by the letter "R". The smaller northern earthquake hypothesized by Talwani and Schaeffer was based on liquefaction detected near Georgetown and the smaller southern earthquake was based on liquefaction detected near Bluffton. Based on the geographic distribution of paleoliquefaction sites, Talwani and Schaeffer believe that events C and D were of  $M \leq 6$ .

The inferred Woodstock and Ashley River faults (Talwani, 1982) together with the 1886 Charleston isoseismals are illustrated in Figure 2. The liquefaction zones northeast and southwest of the 1886 Charleston meizoseismal zone can be accounted for by either of the two Talwani and Schaeffer scenarios.

## 6.0 Significance of New Data and Interpretations

### 6.1 Comparisons of EPRI (1988) Source Definitions to Recent Interpretations

The Charleston source configurations for the available EPRI (1988) teams are illustrated in Figure 3. There were six teams employed by EPRI to develop models for the eastern United States seismic hazards: Dames and Moore, Weston, Law, Bechtel, Rondout and Woodward and Clyde (the Rondout and Woodward Clyde teams source zone geographies were not available for plotting). In addition to the seismic zones selected by the teams, the Modified Mercalli Intensity (MMI) X zone for the 1886 Charleston earthquake is shown. In general, the EPRI zones include the Charleston MMI X zone and tend to be slightly larger and have a NW-SE elongation. The NW-SE trends in the zones are counter to the trends observed in the relic liquefaction data recovered several years later (Figure 2). The EPRI source zone trends are also counter to the trend of the inferred Woodstock fault (Figure 2).

The Charleston source zone magnitude range selected by the EPRI teams was  $m_b$  6.6-7.5 with mean of  $m_b$  6.9. The Charleston recurrence rates ranged from about  $2 \times 10^{-5}$  to  $5 \times 10^{-4}$ /yr with a mean recurrence rate of  $4.9 \times 10^{-5}$ /yr (20,400 years). This exceedence rate is unacceptably low as compared to occurrence rates based on age dating of relic liquefaction features. Based on this, an update of the EPRI Charleston recurrence rates would increase the rate for the Charleston source (factor of approximately 40) thereby increasing the hazard at the SRS. The magnitude distribution would also have changed based on more recent work by Johnston (1994) and Bakun and Hopper (2004). Thus, the EPRI PSHA for the SRS would change if updated. However, the magnitude of this change is unknown at this time, since it was beyond the scope of this effort.

A detailed review of the EPRI SRS-host source zone and other nearby source zones is considered unnecessary in light of the inadequacy of the Charleston source zone and the changes necessary to update that zone with contemporary data. Recommendations relative to the other EPRI source zones are described in the Recommendations Section.

### 6.2 Comparison of LLNL (1993) Source Definitions to Recent Interpretations

The Charleston source zone configurations for the LLNL experts are illustrated in Figure 4 (Expert 10 source zone was unavailable for plotting). Seven of the source zones are similar in nature to the EPRI zones for Charleston- tending to define or outline the 1886 Charleston meizoseismic zone. The other LLNL zones tend to have a NW-SE elongation or are part of a larger SEUS regional zone. The LLNL update (Savy et al., 1993) notes

that Charleston recurrence rates were updated with the new paleoseismic data but that schedule requirements did not allow for changes in the experts zone geometries. Savy et al. (1993) also notes that the experts reported that if given the opportunity that they would have changed the Charleston seismic zones given the new geologic data. Updating the LLNL source zones would have an uncertain effect on the SRS hazard.

The Charleston source zone magnitude range selected by the LLNL experts was  $m_b$  6.5-7.9 with mean of  $m_b$  7.1. The designation of magnitude type ( $m_b$ ) used by the experts is subject to interpretation. The magnitude definitions were not defined in the LLNL report, they were simply presented as “magnitude” or “intensity”. Two of the experts (Expert 1 and 5) used Modified Mercalli intensity which was converted to  $m_b$  for this summary. Expert 6 reported a magnitude range of 7.6-8.4 that was assumed to be  $M_w$  and converted to  $m_b$  for this summary. There is apparently some uncertainty in the LLNL expert’s selection of Charleston source zone magnitude-type. The Charleston recurrence rates ranged from about  $2 \times 10^{-6}$  to  $1 \times 10^{-2}$ /yr with a mean recurrence rate of  $7.8 \times 10^{-4}$ /yr or about 1,300 years. This recurrence rate is about a factor of 2 lower than that used in contemporary models. Updating the LLNL Charleston source recurrence rates would increase the SRS hazard.

### 6.3 Developments in PSHA Methodologies

EPRI (1988) and LLNL (1993) studies were landmark investigations that incorporated expert judgment to model epistemic uncertainty and set the standard for PSHAs at that time. Since that time, the jointly developed guidance to explicitly account for epistemic and aleatory uncertainty were developed by the DOE, NRC, and EPRI (published as LLNL (1997)), commonly referred to as the Senior Seismic Hazard Analysis Committee (SSHAC) report. The SSHAC report provides recommendations for PSHA, specifically guidance on uncertainty and use of experts. This guidance formalizes the process to incorporate ground motion attenuation models and geophysical data supporting the PSHA.

### 6.4 Comparison of Ground Motion Attenuation Models

Kimball (2004) made comparisons of the EPRI (1988) and LLNL (1993) ground motion attenuation models to some contemporary models. His observations have been summarized below.

The LLNL PSHA results were updated in the early 1990’s (LLNL, 1993), and included an update to the ground motion attenuation model termed the “composite model.” The composite model was developed by combining the input from eight members of a ground motion panel into one composite ground motion model that explicitly included an assessment of epistemic uncertainty and random (aleatory) uncertainty. LLNL (1993) developed the composite model by asking each of the ground motion panel members to quantify ground motions for a series of magnitude and distance pairs for hard rock site conditions. Body-wave magnitude scale ( $m_b$ ) and the distance measure of epicentral

distance (or distance to the surface location of the earthquake) were used to develop the composite model. Epistemic uncertainty in the composite model was represented by a series of fractiles for the median composite LLNL ground motion model. LLNL (1993) developed the composite ground motion model for peak ground acceleration, and spectral velocity at frequencies of 25, 10, 5, 2.5 and 1 hertz.

The EPRI (1988) study used three different hard rock ground motion attenuation models to represent the epistemic uncertainty. The three models were selected based on the results of a ground motion workshop, and a report completed by an EPRI consultant. The three models were McGuire et al. (1988), Boore and Atkinson (1987) and one adapted from Nuttli (1986). The McGuire model was given a 50% weight and the other two models were given a 25% weight. Similar to the composite model, the three ground motion models used by EPRI are based on the  $m_b$  scale and epicentral distance, and were developed for peak ground acceleration and spectral velocities at frequencies of 25, 10, 5, 2.5 and 1 hertz. The Nuttli (1986) model was only developed for peak ground acceleration and was combined with the spectral amplifications factors found in Newmark and Hall (1978) to provide the full range of ground motion parameters of interest (spectral velocities).

Kimball (2004) compared the LLNL and EPRI median ground motion attenuation models to eastern US models of Atkinson and Boore (1995), Toro et al. (1997), Somerville et al. (2001), and Campbell (2003). Three of the models (i.e., Atkinson and Boore, 1995; Somerville et al., 2001; and Campbell, 2003) explicitly model the post-critical reflection from the Moho and all use moment magnitude and closest horizontal distance to rupture.

Kimball (2004) concluded that for the vast majority of cases considered, the more recent ground motion models are contained within the epistemic uncertainty captured by the LLNL and EPRI ground motion models. This suggests that a weighted assessment of all the new models would result in a composite attenuation relationship that is within the uncertainty of attenuation relationships used in EPRI and LLNL. Overall, the comparison between the new ground motion models and the LLNL and EPRI models do not indicate a systematic deviation in one direction. It is likely that epistemic uncertainty would be reduced today when compared to that included in the LLNL and EPRI studies.

Kimball (2004) did not discuss comparisons of aleatory uncertainty. However, the EPRI (1988) ground motion uncertainty ( $\sigma_{ln}$ ) was set to 0.5 for all oscillator frequencies, earthquake magnitudes and distances, which is low as compared to contemporary attenuation models (0.6-0.9). This bias in  $\sigma_{ln}$  will significantly reduce the probability of exceedence at lower exceedence rates (higher ground motions) as compared to hazard assessments made with contemporary ground motion attenuation models.



## 7.0 USGS National Hazard Map Model

The National Earthquake Hazard Reduction Program (NEHRP) seismic design recommendations are based on the ground motion inputs from the USGS National Hazard Maps (Frankel et al., 1996; 2002) (hereafter referred to as the National Maps). Both the 1996 and 2002 National Maps were based on the input received at numerous and open workshops; four regional workshops were held prior to the development of the 2002 National Maps. An outside panel of experts also reviewed the National Maps. Briefly, the National Maps for the SEUS are based on a spatially smoothed seismicity model and defined special zones assigned for seismicity occurring in the Charleston, New Madrid and Eastern Tennessee seismic zones. Seismicity is assigned to a geographic grid and seismic activity rates assigned to each grid point. For the site of interest, rates of exceedence are computed for each of the gridpoints. The special Charleston zone incorporates both an area zone and a fault line source, equally weighted (Figures 5 and 6). The area zone is identical to that used for the 1996 National Map. The fault zone approximates the hypothetical Woodstock fault (Figure 2) and zone of river anomalies. Ground motion exceedences are computed for a rupture centered at random within the zone having a strike parallel with the Woodstock fault. The rupture length is specified using correlations of observed earthquake magnitude and fault rupture length.

The mean return period used for the Charleston characteristic earthquake is 550 years based on Talwani and Schaeffer (2001). Five ground motion attenuation models are used. In addition to the Toro et al. (1997) and Frankel et al. (1996) the models of Atkinson and Boore (1995), Campbell (2003) and Somerville et al. (2001) are included. The weights assigned to these models are described below.

The other source component for the CEUS affecting the SRS is the gridded and spatially smoothed seismicity model (Frankel et al., 1996; Frankel et al., 2002). Four seismicity models are developed based on a range of minimum values of magnitude and estimated magnitude completeness of the seismicity catalog. Model 1 a-values were developed by counting all  $m_b \geq 3.0$  since 1924; Model 2 is  $m_b \geq 4.0$  since 1860; Model 3 is  $m_b \geq 5.0$  since 1700. Seismicity is counted in every 0.1-degree intervals (latitude and longitude). The gridded a-values are then spatially smoothed using a Gaussian operator and a smoothing distance of 38, 75 and 150 km. The fourth model is the background zone. This zone was based on the average of all  $m_b \geq 3.0$  occurring within the background zones (extended crust and craton) since 1924. A b-value of 0.95 was used for all four models.  $M_{max}$  for the extended crust was set at  $M_w$  7.5 for all models.

In 2004, the DOE and WSRC procured the services of the USGS to conduct a hazard assessment for the SRS. Unlike the National Map, a full PSHA uncertainty analysis was conducted for hard-rock site conditions at the site center (33.26°N and 81.64°W). Probability of exceedence was computed for spectral accelerations at PGA and periods of 0.04, 0.1, 0.3, 0.5, 1.0 and 2.0 seconds with 5%-damped oscillators.

The description of the uncertainty analysis (Cramer, 2004) is contained in Appendix B. For the recurrence time of the Charleston earthquake, a log-normal distribution is used having a mean of 550 years. This value is based on the last four large Charleston earthquakes (historic and paleoseismic). For the rupture model, the Wells and Coppersmith (1994) model was used. This model allows rupture (maximum of half fault length) outside of the area source. This rupture model is also implemented for the gridded seismicity model.

The magnitude range for the Charleston characteristic earthquake was lowered to reflect the range introduced by Bakun and Hopper (2004). They recommend a 95% confidence interval for the 1886 Charleston earthquake of Mw 6.4-7.1. The weighted magnitudes for the Charleston earthquake are (Frankel et al., 2002):

Mw	Weight
6.8	0.20
7.1	0.20
7.3	0.45
7.5	0.15

This results in a weighted mean magnitude of 7.2, slightly lower than the Mw 7.3 recommended by Johnston (1996) and significantly higher than the Mw 6.8 recommended by Bakun and Hopper (2004).

Because historical seismicity catalogs are characterized using magnitudes defined by  $m_b$ , moment magnitude conversions are made using relationships by Johnston (1996) and Boore and Atkinson (1987). These are given equal weight. These relationships are used for magnitude conversions in the estimate of fault rupture length and ground motion prediction.

The attenuation relations and corresponding weights used for the gridded seismicity model are as follows (Frankel et al., 2002):

Gridded Seismicity Model	Weight
Toro et al. (1997)	0.286
Frankel et al. (1996)	0.286
Atkinson and Boore (1995)	0.286
Campbell (2003)	0.143

The attenuation relations and corresponding weights used for the characteristic New Madrid and Charleston sources are as follows (Frankel et al., 2002):

Model	Weight
Toro et al. (1997)	0.25
Frankel et al. (1996)	0.25
Atkinson and Boore (1995)	0.25
Campbell (2003)	0.125
Somerville et al. (2001)	0.125

Unlike the National Maps, in the evaluation of hazard, there were no truncations either in the ground motion variability or in the absolute value of ground motion. The maximum magnitude used for the background sources is illustrated in Figure 7. Additional description of the analysis and parameter ranges is provided in Appendix B.

Alternate approaches to the spatially smoothed seismicity models could have been developed for the SEUS. For example, the EPRI (1988) and LLNL (1993) (non-Charleston) source zones could be reassessed and updated activity rates could be developed. Alternatively, new models could be developed based on a SSHAC elicitation process similar to the Trial Implementation Program reported by Savy et al. (2002). A new expert elicitation on seismic sources would undoubtedly introduce local fault sources in the vicinity of the SRS such as the Pen Branch fault or other faults along the Dunbarton Basin. The age of significant faulting on these structures has been judged to be older than 500,000 years (Stieve et al., 1994; Stieve and Stephenson, 1995) and the orientation of the fault with respect to the regional stress field is not conducive to reactivation of the faults. We also note that the experts in Savy et al. (2002) heavily favored the “no local source” option of the local region logic tree (a probability of 0.67). We believe that the gridded seismicity model used in the Frankel et al. (2002) model accounts for the low likelihood occurrence of earthquakes along the Dunbarton basin.

We also note that the experts in Savy et al. (2002) heavily favored the localized Charleston source (0.78) over the combined local and floating source (0.2). This weighting is in contrast to the 50-50 weighting of the fault and area source used by Frankel et al. (2002). Although there is a significant body of evidence that points to repeated Charleston earthquakes modeled as a localized or fault source as opposed to a large area source (Silva et al., 2003), the configuration provided by Frankel et al. (2002) may provide a conservative basis for the Charleston source model for the SRS. The Savy et al. (2002) configuration and weights could tend to increase the hazard in the Charleston area and decrease the hazard at the SRS relative to the configuration and weights used by Frankel et al. (2002).

In our judgment there are additional conservatisms contained in the Frankel et al. (2002) Charleston source model. The recent analysis of the 1886 Charleston earthquake by Bakun and Hopper (2004) suggests an Mw 6.8 with a 95% confidence interval of Mw

6.4-7.1. The Bakun and Hopper (2004) magnitude was based on a reassessment of intensities, accommodation of site response and accounting for regional differences in ground motion attenuation in stable continental regions.

## **8.0 USGS National Map Source Model with Alternate GMAMs**

In addition to the National Map attenuation models, the USGS conducted two additional PSHAs at the request of the SRS using alternate GMAMs: the attenuation model set recommended by EPRI (2004) and Silva et al. (2004) were used in separate assessments. In each analysis all other parameters and parameter ranges including sources were identical to the National Map model.

### **8.1 EPRI (2004)**

The EPRI (2004) GMAMs are state of practice models developed specifically for the Early Site Permit (ESP) applications by utilities for licensing of new nuclear power plants in the eastern US. These models were drawn from expert judgement of published and unpublished models. A full uncertainty analysis was completed including point source model adjustments so that re-evaluation at selected utility sites could be completed using the EPRI (1988) source models with the updated attenuation models.

The development of the models followed recommended procedures of the Senior Seismic Hazard Analysis Committee (SSHAC) provided in NUREG/CR-6372 (Budnitz et al., 1997). A Level 3 analysis was completed, which means that a Technical Integrator (TI) is responsible for development of a composite ground motion attenuation model based on available data and the interaction with ground motion experts. In addition to a composite model for the median ground motion and its aleatory variability there were also models for epistemic uncertainty in the median model and the aleatory variability model. The composites were developed for two general areas of the eastern United States, the Gulf Coast and the mid-continent.

Three source categories were developed: (1) earthquakes having  $M_w$  5.0-8.0 within 200 km; (2) large earthquakes,  $M_w > 7.5$ , occurring at greater distances; and (3) nearby large magnitude earthquakes. The composite model provides PGA and spectral accelerations for oscillator frequencies of 0.5, 1.0, 2.5, 5.0, 10 and 25 Hz for hard-rock site conditions.

Based on literature search and expert solicitation, 13 eastern US ground motion attenuation models were identified for incorporation in the model. Four ground motion classes or clusters were devised to combine the models: single- and double-corner, eastern-western United States hybrid, and theoretical (Greens Function) models. The clusters and models were broken down as follows:

Cluster	Model Type	Reference
1	Spectral (Single corner)	Hwang and Huo (1997) Silva et al. (2002)-CS Silva et al. (2002)-CS-S Silva et al. (2003)-VS Toro et al. (1997) Frankel et al. (1996)
2	Spectral (Double Corner)	Atkinson and Boore (1995) Silva et al. (2002) Silva et al. (2002)-S
3	Hybrid	Abrahamson and Silva (2002) Atkinson (2001) & Sadigh et al. (1997) Campbell (2003)
4	Finite Source/Greens fn	Somerville et al. (2001)

Note, CS is constant stress drop and VS is variable stress drop, S denotes model that includes saturation.

Rather than applying weights to define a median model, clusters were used to identify and weight models based on the strength and weakness of the cluster and also evaluate the models individually within the cluster. In this way, the epistemic uncertainty will include uncertainty of the median models within a cluster and include uncertainty of the median between clusters. Table 3 contains the weights applied to each model within a cluster, based on variance of the median model with respect to observed strong motion data. Because only one model was available for Cluster 4 (Somerville), its data variance weight is 1 within that cluster. The data sources are 20 earthquakes with Mw ranging from 4.0-6.4 occurring in the EUS and eastern Canada.

The Atkinson and Boore (1995) model was the highest ranked model (0.714) of the two-corner models. Of the single-corner models, the Silva et al. (2002) variable stress drop model ranked the highest (.56) and the three Silva et al. (2002) models combined had a weight of 0.9. The three hybrid models were equally satisfactory in modeling the observed data.

The TI evaluated the fit of the cluster medians to data to derive weights for the clusters. These weights are also illustrated in Table 3 and show that the two-corner model cluster best fit the observed data. The combined cluster weights for the hybrid and finite source models were less than 0.05.

Because of the limited EUS data, particularly for larger magnitudes, the TI also sought to subjectively weight clusters by “seismological principals” used to construct the model.

Seismological principals include an assessment of the degree to which aleatory and epistemic uncertainty were incorporated and the degree to which physical principles were used in developing the model. On this basis (Table 3) each of the four clusters received about the same weighting. A composite weighting for each cluster was derived by combining the data consistency weight and the seismological principal weight. Data consistency was assigned a weight of 0.25 and seismological principals were assigned a weight of 0.75. The composite weights for each cluster using this scheme are shown in Table 3 and range from about 0.2 to 0.3 for each cluster.

For this study, the product of the composite cluster weight with the weight assigned for each model (based on data consistency) was computed to derive an approximate model contribution to the composite model (Table 3). This procedure illustrates that the Silva et al. (2002) models have a combined weight of 0.34 (Abrahamson and Silva hybrid model not included). The highest individually weighted models are Somerville (2001) (0.217), Atkinson and Boore (1995) (0.223) and the Silva et al. (2002) variable stress drop model (0.154). The lowest weighted models were Frankel et al. (1996) (0.009) and Toro et al. (1997) (0.008).

**TABLE 3**

		EPRI (2004) model weights by:				
Cluster Type	Models	data agreement within cluster	data agreement by cluster	seismological principals	composite of data and seismological principals	combined weight for each GMAM
<u>Spectral, 1-corner</u>						
	Hwang and Huo (1997)	.037	.3639	.245	.275	.010
	Silva et al. (2002)-SCCS	.192	.3639	.245	.275	.053
	Silva et al. (2002)-SCCSS	.148	.3639	.245	.275	.041
	Silva et al. (2002)-SCVS	.560	.3639	.245	.275	.154
	Toro et al. (1997)	.029	.3639	.245	.275	.008
	Frankel et al. (1996)	.034	.3639	.245	.275	.009
<u>Spectral, 2-corner</u>						
	Atkinson and Boore (1995)	.714	.5869	.221	.312	.223
	Silva et al. (2002)-DC	.154	.5869	.221	.312	.048
	Silva et al. (2002)-DCS	.132	.5869	.221	.312	.041
<u>Hybrid</u>						
	Abrahamson and Silva (2002)	.336	.0135	.257	.196	.066
	Atkinson (2001)	.363	.0135	.257	.196	.071
	Campbell (2003)	.301	.0135	.257	.196	.059
<u>Finite Source/Greens fn</u>						
	Somerville et al. (2001)	1	.0357	.277	.217	.217

Aleatory uncertainty in the composite model includes dependencies on earthquake magnitude, distance and oscillator frequency. This new model incorporates much higher aleatory uncertainty than the early EPRI model. For 1-Hz, Mw 7.5 ranges from about 0.6-0.7 (lognormal) depending on source distance.

## 8.2 Silva et al. (2004)

The Silva et al. (2004) hard-rock attenuation models were developed specifically for application to the South Carolina Coastal Plain and used available regional crustal models to constrain geometrical attenuation. The model includes single and double corner source models, variable and constant stress drop correlation to magnitude, and models with explicit dependency on stress drop. Coefficients are provided for PGA, PGV and 26 oscillator frequencies from 100 to 0.1 Hz for hard-rock site conditions (Appendix C).

The Silva et al. (2004) crustal model is based on available models developed for the crustal structure between the SRS and Charleston, SC. A Charleston crustal model was constrained by interpretations made from deep borehole velocity logs and structural models required for consistent earthquake location models by the University of South Carolina. For the SRS, the regional seismic refraction model of Leutgert et al. (1994) was used. That model, based on the reflected and refracted P-wave arrivals from several subsurface explosive sources, constrains the crust from New Ellenton, SC to Walterboro, SC. The South Georgia Basin and crystalline rock were averaged in this model. The average SRS to Charleston crustal model used by Silva et al. (2004) is described in the table below.

**Crustal Model Used in the Silva et al. (2004) GMAM**

Depth (km)	Thickness (km)	Shear Velocity (km/sec)	Density (gm/cc <sup>3</sup> )
0.0	0.13	2.53	2.62
0.13	0.15	3.09	2.78
0.28	1.90	3.29	2.85
2.18	7.10	3.43	2.93
9.28	8.50	3.62	2.99
17.8	16.7	3.75	3.04
34.5	-	4.54	3.42

The crustal model is used to incorporate region-specific site amplification factors for the computation of hard-rock response. The region-specific crustal model is also used to evaluate appropriate crossover distance for body wave and surface wave attenuation.

The Q (f) model ( $Q(f) = 1052f^{0.22}$ ) was taken from Benz et al. (1997) and is based on crustal models in the northeastern United States and southeastern Canada that are most representative of the Appalachian Piedmont province. A hard-rock kappa ( $\kappa$ ) of 0.006 seconds is used.

Magnitude dependent and independent stress drop models are used. The magnitude dependent stress drop model decreases with increasing magnitude (160 bars for Mw 5.5 to 90 bars for Mw 7.5). A stress drop of 120 bars is used for the magnitude independent stress drop model. Epistemic uncertainty in the stress drop model is developed using median, high (2 x median) and low (1/2 of median) stress drop models.

The following weights were applied to the models (“SD Weight” refers to the weight applied to models containing epistemic uncertainty in stress drop).

Model Description	Class Weight	SD Weight	Total Weight
Single corner, variable median $\sigma$	1/2	2/3	1/3
Single corner, variable low $\sigma$	1/2	1/6	1/12
Single corner, variable high $\sigma$	1/2	1/6	1/12
Single corner, constant median $\sigma$	1/4	2/3	1/6
Single corner, constant low $\sigma$	1/4	1/6	1/24
Single corner, constant high $\sigma$	1/4	1/6	1/24
Double corner	1/4	1	1/4

## 9.0 Comparison of Hard-Rock Hazard

Comparisons of the mean and fractile hazard for the three models (USGS National Map, USGS-EPRI (2004) and USGS-Silva et al. (2004)) are illustrated in Figures 8 through 13. Figure 8 illustrates the 100-Hz mean, 10<sup>th</sup> and 90<sup>th</sup> fractile hard-rock hazard curves. Also shown are the mean LLNL and EPRI hazard curves for the SRS used in the prior assessment (WSRC, 1997). Figures 9 through 13 illustrate the hazard comparisons for oscillator frequencies of 25, 10, 5, 2.5 and 1-Hz respectively. The 10<sup>th</sup> and 90<sup>th</sup> fractiles were selected to illustrate the dispersion in the range of computed hazard curves and represent an approximate  $\pm 1.3 \sigma$  range of the distribution of hazard curves. Each of the three models exhibit substantially increasing uncertainty with increasing ground motion. For example, comparison of 10 gals (.01g) to 1000 gals (1.0g) there is an approximate 6-fold increase in the range of probability of exceedence. For each of the oscillator frequencies illustrated, there is a rapid change of slope of the mean hazard that occurs at the exceedence rate of about 10<sup>-3</sup>/yr. The slope change represents the relative decrease in site hazard with increasing ground motion as a result of the distribution and rates of seismic sources affecting the SRS. There is significant uncertainty in the rate of exceedence where this slope change occurs as is evident by the range in ground motion observed in the 10<sup>th</sup> and 90<sup>th</sup> percentile fractile hazard. Of the three models, the USGS-EPRI (2004) model exhibits the greatest range of uncertainty followed by USGS-Silva (2004) model and then the National Map model. The mean models exhibit the largest differences at high oscillator frequencies (25, 100 Hz) and lowest frequencies (f<1-Hz) and probably represent differences assumed in source stress-drop and weights of 1- and 2-corner source models respectively.



Comparison of the means of the three models to the EPRI (1988) and LLNL (1993) mean hazard models illustrates a low-bias in the EPRI (1988) model that is clearly a result of the low rates of exceedence assigned to the Charleston seismic zone in the earlier study. As discussed above, the EPRI (1988) PSHA predated much of the paleoliquefaction data that was subsequently available. For higher oscillator frequencies (25, 100-Hz) and lower exceedence rates ( $< 10^{-3}/\text{yr}$ ), the mean and slope of the mean LLNL (1993) hazard is lower than the mean of the USGS-based models. This could be caused by a high-bias in the crustal attenuation parameter  $\kappa$  used in the earlier attenuation models.

## 10.0 Considerations for PSHA Weighting

Most weighting schemes are subjective by nature, however, carefully describing the basis for the scheme with review and concurrence by outside reviewers can provide a defensible basis for the models. We considered the following factors in judging the PSHAs:

1. Epistemic uncertainty incorporated and quantified in model.
2. Dependency in models (e.g., the three USGS models all have the same source models).
3. Incorporation of attenuation model class (RVT, empirical/RVT hybrid, finite source).
4. Attenuation model sub-class (single, double-corner, magnitude-dependent stress drop, stress-drop class (high, medium, low)).
5. Attenuation models most consistent with CEUS data.
6. Regional crustal model considered in development.
7. PSHA source models incorporate available seismological and paleoseismological data.
8. PSHA attenuation models fully incorporate epistemic uncertainty in attenuation models.
9. PSHA attenuation models fully incorporate aleatory uncertainty in attenuation models.
10. Published and peer reviewed.
11. SSHAC level of PSHA

Based on the available PSHAs, a matrix of weights corresponding to the attributes above is unnecessary. The EPRI and LLNL PSHAs were state-of-the-art for the mid-to-late 1980s, and were landmark investigations accounting for expert uncertainty in probabilistic seismic hazard. The LLNL (1993) was much improved by the update of the ground motion attenuation models and the incorporation of some of the more recent geologic data. However, the new geologic, geophysical and seismological data collected in the nearly 20 years since these studies were completed continues to date these investigations for application to the SRS. The EPRI and LLNL models would be significantly down-weighted in factors 3, 4, 5, 6, 7, 8 and 9. For example, the LLNL and EPRI models are too dated in their Charleston source configuration and rates of recurrence to be seriously considered for adoption in this assessment. This attribute alone

is considered sufficient to reject those two PSHAs. By giving zero weight to the EPRI and LLNL PSHAs the issue of combining the remaining models is considerably simplified since the source models in the remaining three models is identical.

The USGS source models were built on consensus from open and well-attended subject matter meetings and were the subject of numerous peer-reviewed publications. The USGS source models are the basis for the National Maps that currently control the design of some SRS facilities and nearby critical facilities such as hospitals and dams through the International Building Code (IBC), which is currently invoked for SRS PC-1 and PC-2 facilities. We consider the development of the USGS source models to be SSHAC Level 2-3 and appropriate for ground motions at the SRS having probabilities of exceedence of  $10^{-4}$  to  $10^{-5}$ /yr. We acknowledge that this is not an ideal situation since some experts could recommend seismic sources in the near-SRS region and so those potential sources would not be explicitly accounted for in this study. However, this is not expected to have any significant impact at design levels of motion but could be expected to impact motions appropriate for risk and liquefaction assessments. For example a SSHAC level 3-4 assessment of seismogenic zones could result in a number of local faults or zones, having low probability of activity that at exceedences of  $10^{-5}$ /yr or lower could result in possibly greater ground motions than generated by the USGS model. However, additional conservatisms present in the USGS source model (discussed below) would likely offset these lower exceedence rate increases.

### 10.1 Recommended Model Weights

Based on the strengths and weaknesses of the five PSHAs, a weighting scheme is developed in this section that will be used to develop hard-rock UHS and be used for the site response corrections to develop fully probabilistic site-specific hazard. EPRI (1988) and LLNL (1993) models are given zero weight for reasons cited above. The three remaining PSHAs are based on the USGS source model (Frankel et al., 2002). Because there are no other independently developed PSHAs to combine with these models at this time, the three USGS models will be weighted on the merits of the attenuation models used in each of the models.

The EPRI (2004) composite GMAM was conducted with SSHAC Level 3 guidance and with full accounting for epistemic uncertainty and model type. The USGS-Silva et al. (2004) PSHA, incorporating regional-specific crustal models is desirable from the perspective of reducing potential bias by incorporating site-specific regional crustal structure, however, these models have not been fully peer reviewed and do not incorporate some of the other available model classes (e.g., hybrid model). The USGS National Map PSHA is desirable from the perspective that it has received considerable review and acceptance in the seismological community and is a basis for the various building codes such as the IBC, which is used at the SRS. More importantly, it is also recommended by DOE (see DOE G 420.1-2).

In order to develop weights for these three sets of models, we use a ground motion model ranking scheme that gives the greatest merit to models developed with the intent of fully accounting for expert uncertainty that also includes full documentation and review of the models. This results in a ranking of the models as follows: (1) EPRI (2004); (2) USGS (2002) and (3) Silva et al. (2004). This ranking follows from the detailed documentation of the SSHAC Level 3 approach taken in EPRI (2004), the open-meeting and review and comment process taken by the USGS in developing the models in USGS (2002). The Silva (2004) model has the lowest ranking because it is influenced by one author and because Silva is included as an author in the EPRI (2004) models.

Another consideration for development of a weighting scheme is to account for the net weight by author to insure that there is not an excessive bias. The contribution of the Silva et al. (2002) models to the EPRI (2004) composite has a combined weight of 0.34 (Table 3). This weight for a single group of authors was acceptable to the TI in the EPRI (2004) study. In our opinion, this single authorship weight can be considered an upper-bound target weight for the Silva et al. (2002, 2004) models used in this PSHA update. Assigning comparable weights (1/3, 1/3, 1/3) for each of the three models results in a net cumulative contribution of the Silva et al. (2002, 2004) models of 0.45. This value is well in excess of the target value. Because the EPRI (2004) model is the most desirable of the three ground motion attenuation models for this application, only a reduction of the weight on the region-specific model will reduce the authorship bias in these three models. Consideration of residuals for selection of model weights for the regionally specific model is not possible because of the paucity of strong motion data in the SEUS.

Another consideration is the total model weight by model cluster. EPRI (2004) has a single corner model weight of 0.27 and a two-corner model weight of 0.31 (Hybrid model weight of .20 and Somerville model weight of 0.22). The USGS (2002) model has a single corner model weight of 0.5 and a two-corner model weight of 0.25 (Hybrid model weight of .125 and Somerville model weight of 0.125) for the large source model. The Silva et al. (2004) model has a single corner model weight of 0.75 and a two-corner model weight of 0.25 with no cluster contribution for Greens function and hybrid models. Equal weighting of the attenuation models results in cluster weights of 0.51, 0.27, 0.11, 0.11 for the 1-corner, 2-corner, hybrid, and Greens function models respectively.

After considering several alternatives, a weighting scheme of 0.6, 0.3 and 0.1 for EPRI (2004), USGS (2002) and Silva et al. (2004) was selected. This weighting results in a model ranking and cluster weights of .39, .29, .15, .17 for the 1-corner, 2-corner, hybrid, and Greens function models, respectively. This weighting also results in a desirable combined Silva et al. (2002, 2004) model weight of 0.3 for the three PSHAs. If authorship was not an issue, a higher weight for the Silva et al. (2004) would have resulted in a higher 1-corner model weighting. Our recommended weighting scheme results in a 1-corner source model weight between the USGS (2002) and EPRI (2004) model weights. Also, for an exceedence of  $10^{-4}$ /yr, the region-specific mean hazard is lower than the EPRI (2004) and the USGS (2002) mean hazard models and consequently, reduction of the region-specific model weight will slightly increase the hazard for the

SRS. This judgment results in a somewhat more conservative result but avoids the risk of overweighting one particular group of experts. The selection of cluster and authorship weights by any one expert could be considered biased and therefore a consensus opinion was reached. This weighting scheme is reasonably consistent with the authorship and model cluster combination precedents set in the EPRI (2004) and USGS (2002) ground motion model assessments. This consistency of model and cluster weights with these SSHAC level 2 and 3 investigations, both having received prior NRC and DOE review and approval provides further justification of this weighting scheme. The peer reviewers are also in agreement with the weighting scheme.

We note that the three mean models do not differ to a large degree (10-25%) for most oscillator frequencies (2.5-10 Hz) and for ground motions important to the design of critical facilities (rates of exceedence of  $10^{-3}$  to  $10^{-4}$ /yr). Only at higher oscillator frequencies where means may differ because of preferences on source stress drop and at lower oscillator frequencies where single and two-corner source model weights affect the mean will the weights have a meaningful impact on the bedrock UHS.

Some criticism of the EPRI (2004) models has been made recently by Cramer (2005). His concern relates to the comparison of the National Map attenuation models (Frankel et al., 2002) to the EPRI (2004) models at larger distances and at long period (1-Hz) where he notes that the EPRI (2004) models under-predict spectra. He argues that a subset of the EPRI (2004) (1- and 2-corner models of Silva, 2002) under-predict long-period spectra because of the lower Q-model used in those evaluations. We agree that the Q model is critical to the prediction of long-period spectra, however, other factors are also critical such as the bedrock velocity, kappa and the geometrical spreading model. These factors in combination result in attenuation model coefficients that match observed data in Silva et al. (2002). Consequently, isolating one model parameter to the exclusion of others to assess the validity of a model is not appropriate. In this context, Cramer (2005) compares the Silva et al. (2002) 1-corner model to the Frankel et al. (1996) and Toro et al. (1993) models. Although there is only limited EUS strong motion data bearing on this issue, an important aspect of any ground motion attenuation model is its predictive ability. The Silva et al. (2002) 1-corner variable stress drop best fit the observed data of any 1-corner model evaluated in the EPRI (2004) study. The Silva et al. (2002) median 1-Hz model over-predicts observed spectra by about 18% in the hypocentral distance range of 75-150 km and under-predicts by about 22% in the distance range 150-500 km. In contrast, the Frankel (1996) 1-Hz median model over-predicts by a factor of 2.7 in the 75-150 km distance range and over-predicts by a factor of 3.5 in the 150-500 km distance range. The Silva (2002) 2-corner model does under-predict the 1-Hz observations in the 150-500 km distance range, however this model is down-weighted in EPRI (2004). Because the EUS strong motion data are limited to about Mw 6, we would argue the Silva et al. (2002) and Frankel et al. (1996) models reflect epistemic uncertainty in the prediction of long-period motions for large (Mw 7) earthquakes, and both models are appropriately retained in this recommendation.

## 11.0 SRS Bedrock UHS Based on Model Weights

The model weights described in Section 10 are used to derive mean bedrock UHS for the central site location. Bedrock UHS are illustrated for return periods of 500, 2500, 5000 and 10,000 years using the USGS-EPRI (2004), USGS-Silva et al. (2004) and USGS National Map models in Figures 14, 15 and 16 respectively. Figure 17 compares the three PSHAs for a 2000-yr return period. Similarly Figure 18 compares the three PSHAs for a 10,000-yr return period. Figures 19 and 20 illustrate the weighted UHS for return periods of 500, 2000, 5000 and 10000 years on log-log and log-linear ordinates respectively. Also shown are the mean EPRI (1988) and LLNL (1993) bedrock UHS used to develop the PC-3 and PC-4 SRS bedrock envelope spectra.

Because the PSHAs were derived for the SRS site center, and because there is a significant spatial dependence of the hazard owing to the proximity of the Charleston source, an estimate of the spatial derivative of the hard-rock hazard will be established from the available National Map gridded 2,500 year ground motion values. These corrections will be derived for the available range in oscillator frequencies. The site gradient in ground motion hazard can be used to correct the central site hazard to other more remote areas of the site if desired.

## 12.0 Discussion

This recommendation considers the appropriateness of the early EPRI and LLNL PSHAs, together with the more recent USGS National Map PSHA. In addition, alternative GMAMs are used with the National Map source model to produce PSHAs. Based on the new data and methods developed since the early EPRI and LLNL PSHAs were completed, we recommend that the EPRI and LLNL studies no longer be used for design purposes. This is consistent with current DOE direction (see DOE G 420.1-2). As replacements for these PSHAs, a new PSHA following the recommendations of SSHAC Level 4 guidelines would be the most desirable and defensible solution for the SRS but is beyond the scope of this study. Nevertheless, development and comparison of hazard based on the National Map models and PSHAs completed using alternate GMAMs provides increased confidence in this hazard recommendation and we believe is defensible. It is our judgment that this assessment is conservative relative to WSRC (1997) and incorporates the prevailing expert opinion pertinent to the development of seismic hazard at the SRS.

The source model and the alternate suites of ground motion attenuation models were developed using differing levels of expert input and technical integration as well as documentation. It is our judgment that this recommendation represents a SSHAC Level 2-3 assessment based on the documentation and participation of outside experts involved on the various elements of this recommendation.

We note from Figures 17 and 18 that the recommended SRS hard-rock UHS (2000- and 10000-yr) are greater than the design spectra developed in WSRC (1997) that were based on the LLNL (1993) and EPRI (1988) PSHAs. This follows from Section 6 where we observed that the EPRI (1988) activity rate for the Charleston source zone is underestimated based on more recent data. This would tend to increase the low frequency portions of the design spectra. Higher frequency portions of the UHS are also considerably greater than the design spectra developed in WSRC (1997). This increase is likely a result of greater aleatory uncertainty used in the contemporary ground motion attenuation models and possibly a result of greater activity assumed in the local area of the SRS.

### **13.0 ACKNOWLEDGEMENTS**

Chris Cramer of the USGS conducted the PSHAs and uncertainty analysis and continues to provide guidance and support. Brent Gutierrez of DOE/SR made considerable efforts to procure services of subcontractors. Technical reviews by Martin Chapman and Ivan Wong greatly improved our approach.

## 14.0 REFERENCES

Abbott, J., Gelinas, R., and Amick, D., 1999. "Investigations of liquefaction features at the Savannah River Site, South Carolina"; In the Proceedings, Techniques for Identifying Faults and Determining Their Origins, NUREG/CR-5503, NRC, Washington, D.C., July 1999.

Abrahamson, N.A., and W.J. Silva, 2002. Hybrid model-empirical attenuation relations for central and eastern U.S. hard and soft rock and deep soil site conditions: presentation slides, CEUS Ground Motion Project Workshop, September 24-25, 2002, Las Vegas, NV.

Amick, D., Gelinas, R., Maurath, G., Cannon, R.; Moore, D., Billington, E., Kemppinen, H., 1990. Paleoliquefaction features along the Atlantic Seaboard, NUREG/CR-5613 RA, Prepared for U. S. Nuclear Regulatory Commission by Ebasco Services Inc., 146 pp.

Amick, D. and Gelinas, R. 1991. The Search for evidence of large prehistoric earthquakes along the Atlantic Seaboard. American Assoc. for the Advancement of Science, Feb. 1991, p.655-658, v. 251.

Atkinson, G.M., and D.M. Boore, 1990. Recent Trends in Ground Motion and Spectral Response Relations for North America, *Earthquake Spectra*, Vol. 6, No.1, pp 15-35.

Atkinson, G.M., and D.M. Boore, 1995. New ground motion relations for eastern North America, *Bull. Seis. Soc. Am.*, Vol. 85, 17-30.

Atkinson, G.M., and D.M. Boore, 1998. Evaluation of Models for Earthquake Source Spectra in Eastern North America, *Bull. Seis. Soc. Am.*, Vol. 88, 917-934.

Atkinson, G.M., 2001. An alternative to stochastic ground-motion relations for use in seismic hazard analysis in eastern North America, *Seis. Res. Lett.*: 72(2), 299-306.

Bakun, W.H. and M.G. Hopper, 2004. Magnitudes and locations of the 1811-1812 New Madrid, Missouri, and the 1886 Charleston, South Carolina, earthquakes. *Bull. Seis. Soc. Am.*, 94, no. 1, 64-75.

Benz, H., A. Frankel and D.M. Boore 1997. Regional Lg Attenuation for the Continental United States, *Bull. Seis. Soc. Am.*, 87, no. 3, 606-619.

Bernreuter, D.L., J.B. Savy, R.W. Mensing and J.C. Chen, 1989a. Seismic Hazard Characterization of 69 Nuclear Power Plant Sites East of the Rocky Mountains, NUREG/CR-5250, UCID-21517.

Bernreuter, D. L., et al., 1989b. Seismic Hazard Characterization of 69 Nuclear Plant Sites East of the Rocky Mountains, NUREG/CR-1582, vols. 1-8.

Bernreuter, D.L., 1997. Letter report from Don Bernreuter to Jeff Kimball. Lawrence Livermore National Laboratory, Fission Energy and Systems Safety Program, May 15, 1997, NTFS97-123.

Bollinger, G.A., 1977. Reinterpretation of the intensity data for the 1886 Charleston, South Carolina earthquake: in Rankin, D.W., ed., Studies Related to the Charleston, South Carolina, earthquake of 1886--A Preliminary Report, U.S.G.S. Prof. Paper 1028, p. 17-32.

Boore, D.M., 1983. Stochastic simulation of high-frequency ground motions based on seismological models of the radiated spectra, *Bull. Seis. Soc. Am.*, vol. 73, 1865-1894.

Boore, D. M., and G. M. Atkinson, 1987. Stochastic Prediction of Ground Motion and Spectral Response Parameters at Hard-rock Sites in Eastern North America, *Bulletin of the Seismological Society of America*, Vol. 77, p. 440.

Budnitz, R.J., G. Apostolakis, D.M. Boore, L.S. Cluff, K.J. Coppersmith, C.A. Cornell and P.A. Morris, 1997. Recommendations for Probabilistic Seismic Hazard Analysis: Guidance on Uncertainty and Use of Experts, NUREG/CR-6372, UCRL-ID-122160.  
Campbell, K. W., 2003. Prediction of Strong Ground Motion Using the Hybrid Empirical Method and Its Use in the Development of Ground-Motion (Attenuation) Relations in Eastern North America, *Bulletin of the Seismological Society of America*, Vol. 93, p. 1012.

Cox, J.H.M., 1984. Paleoseismology studies in South Carolina, M.S. Thesis, Univ. of S.C., Columbia.

Cox, J., and P. Talwani, 1983. Paleoseismic studies in the 1886 Charleston earthquake meizoseismal area (abstract), *Geol. Soc. Am. Abstr. Programs*, 16, 130.

Cramer, C. 2004. Uncertainties in the National Seismic Hazard Maps near the Savannah River Site, South Carolina, Prepared for US Dept. of Energy, June 30, 2004.

Cramer, C., 2005. An Assessment of the Impact of the EPRI (2003) Ground Motion Prediction Models on the USGS National Seismic Hazard Maps, manuscript submitted for publication in the *Bulletin of the Seismological Society of America*, 2005.

Electric Power Research Institute, 1986. Methods of Earthquake Ground-Motion Estimation for the Eastern United States, prepared by Risk Engineering, EPRI Project RP2556-16.

Electric Power Research Institute, 1988. Seismic Hazard Methodology for the Central and Eastern United States, Vol. 1-10, NP-4726.



Electric Power Research Institute, 1989. Probabilistic Seismic Hazard Evaluations at Nuclear Power Plant Sites in the Central and Eastern United States: Resolution of the Charleston Earthquake Issue, EPRI Report NP-6395-D, based on EPRI, 1988, Seismic Hazard Methodology for the Central and Eastern United States, EPRI NP-4726.

Electric Power Research Institute, 1993. Guidelines for determining design basis ground motions, EPRI TR-102293, Nov. 1993.

Electric Power Research Institute, 2004. CEUS Ground Motion Project, Model Development and Results, EPRI Report No. 1008910, December 2004.

Frankel, A., C. Mueller, T. Barnhard, D. Perkins, E.V. Leyendecker, N. Dickman, S. Hanson, and M. Hopper, 1996. National Seismic Hazard Maps, June 1996, U.S. Geol. Surv. Open-File Report 96-532.

Frankel, A. 1999. Letter report of calculation results to R.C. Lee, March 9, 1999.

Frankel, A., M. Petersen, C. Mueller, K. Haller, R. Wheeler, E. Leyendecker, R. Wesson, S. Harmsen, C. Cramer, D. Perkins, and K. Rukstales, 2002. Documentation for the 2002 Update of the National Seismic Hazard Maps, U.S. Geol. Surv. Open-File Report 02-420.

Gelinas, R., Cato, K., Amick, D., and Kemppinen, H., 1998. Paleoseismic studies in the Southeastern United States and New England, NUREG/CR-6274, Office of Nuclear Regulatory Research, U.S. Nuclear Regulatory Commission, August 1998.

Geyh, M.A., and H. Schleicher, 1990. Absolute age determination: Physical and chemical dating methods and their application. Springer-Verlag, Germany, 503 pp.

Gohn, G.S., R.E. Weems, S.F. Obermeier, and R.L. Gelinas, 1984. Field studies of earthquake-induced, liquefaction-flowage features in the Charleston, South Carolina, area, preliminary report U.S. Geol. Surv. Open File Report 84-670, 26 pp.

Hwang, H. and J.R. Huo, 1997. Attenuation Relations of Ground Motion for Rock and Soil Sites in Eastern United States, Soil Dynamics and Earthquake Engineering: ch.16, pp. 363-372.

Johnston, A., 1994. Moment Magnitude Assessment of Stable Continental Earthquakes, Part I: instrumental seismicity, pre-print (published with revised relations in Geophys. J. Int., [1996], v. 124, pp. 381-414).

Johnston, A., 1996. Seismic moment assessment of earthquakes in stable continental regions. Geophys. J. Intl., Vol. 124, pp. 381-414 (Part I); Vol. 125, pp. 639-678 (Part II); Vol. 126, pp. 314-344 (Part III).

Kimball, J, 2004. Comparison of Ground Motion Attenuation Models Used to Complete Savannah River Site Probabilistic Seismic Hazard Assessment (Lawrence Livermore National Laboratory, Electric Power Research Institute), and Recently Published Ground Motion Attenuation Models, Report in support of the MFFF Project 2004.

Lawrence Livermore National Laboratory, 1993, Eastern U. S. Seismic Hazard Characterization Update, UCRL-ID-115111.

Lawrence Livermore National Laboratory, 1997, Recommendation for Probabilistic Seismic Hazard Analysis: Guidance on Uncertainty and Use of Experts, Senior Seismic Hazard Analysis Committee (SSHAC) report, NUREG/CR-6372.

Leutgert, J.H., H.M. Benz and S. Madabhushi 1994. Crustal Structure Beneath the Atlantic Coastal Plain of South Carolina, *Seis. Res. Lett.*, vol. 65, pp. 180-191.

McGuire, R.K., Toro, G.R., and W.J. Silva, 1988. Engineering Model of Earthquake Ground Motion for Eastern North America, Technical Report NP-6074, prepared by Risk Engineering, Inc. for the Electric Power Research Institute.

NEI, 1994. Nuclear Energy Institute, Washington, D.C., Seismic Siting Decision Process, May 24, 1994.

Newmark, N. M., and W. J. Hall, 1978. Development of Criteria for Seismic Review of Selected Nuclear Power Plants, NUREG/CR-0098.

Nuttli, O.W., 1985. Appendix C-A. Seismic Hazard Characterization of the Eastern United States, Volume 2: Questionnaires. Letter to D. Chung, Lawrence Livermore National Laboratory, UCID-20421. Prepared for the U.S. Nuclear Regulatory Commission, March 1986.

Nuttli, O. W., 1986. Letter dated September 19, 1986 to J. B. Savy. Reproduced in: NUREG/CR-5250, Seismic Hazard Characterization of 69 Nuclear Plant Sites East of the Rocky Mountains, prepared by Lawrence Livermore National Laboratory.

Obermeier, S.F., G.S. Gohn, R.E. Weems, R.L. Gelinas, and M. Rubin, 1985. Geological evidence for recurrent moderate to large earthquakes near Charleston, South Carolina. *Science*, vol. 227, pp. 408-411.

Obermeier, S.F., R.B. Jacobson, J.P. Smout, R.E. Weems, G.S. Gohn, J.E. Monroe, and D.S. Powars, 1990. Earthquake induced liquefaction features in the coastal setting of South Carolina and in the fluvial setting of the New Madrid Zone, U.S. Geological Survey Prof. Paper 1504.

Sadigh, K., C.Y. Chang, J.A. Egan, F. Makdisi and R.R. Youngs, 1997. Attenuation relationships for shallow crustal earthquakes based on California strong motion data, *Seis. Res. Lett.*, vol. 68 (1), pp. 180-189.

Savy, J.B., A.C. Boissonnade, R.W. Mensing and C.M. Short, 1993. Eastern U.S. Seismic Hazard Characterization Update, Lawrence Livermore National Laboratory, July 20, 1993.

Savy, J.B., 1996. Fission Energy and Systems Safety Program, April 24, 1996, SANT96-147JBS, letter from J.B. Savy, Deputy Associate Program Leader Natural Phenomena Hazards to Jeff Kimball, DOE.

Savy, J.B., Foxall, W., Abrahamson, N., and D. Bernreuter, 2002. Guidance for Performing Probabilistic Seismic Hazard Analysis for a Nuclear Plant Site: Example Application to the Southeastern United States, NUREG/CR-6607, UCRL-ID-133494, Prepared by Lawrence Livermore National Laboratory Livermore, CA for U.S. Nuclear Regulatory Commission, Washington, D.C.

Silva, W., N. Gregor and R. Darragh, 2002. Development of Regional Hard Rock Attenuation Relations for Central and Eastern North America, Pacific Engineering and Analysis, El Cerrito, CA.

Silva, W., I. Wong, T. Siegel, N. Gregor, R. Darragh and R. Lee, 2003. Ground Motion and Liquefaction Simulation of the 1886 Charleston, South Carolina, Earthquake, *Bulletin of the Seismological Society of America*, Vol.93, pp. 2717-2736.

Silva, W., N. Gregor and R. Lee, 2004. Development of Regional Hard Rock Attenuation Relations for South Carolina, Pacific Engineering and Analysis, El Cerrito, CA.

Somerville, P., N. Collins, N. Abrahamson, R. Graves and C. Saikia, 2001. Ground motion attenuation relations for the Central and Eastern United States, Final Report, June 30, 2001 to the U.S. Geol. Surv., Award Number: 99HQGR0098 by URS Group, Inc., Pasadena, CA.

Stieve, A.L., C. Coruh, and J. Costain 1994. Confirmatory Drilling Project Final Report, WSRC-RP-94-0136, Rev. 0, October 1994.

Stieve, A., and D. Stephenson, 1995. Geophysical Evidence for Post Late Cretaceous Reactivation of Basement Structures in the Central Savannah River Area, *Southeastern Geology*, Vol. 35, No. 1, March 1995.

Talwani, P. 1982. Internally consistent pattern of seismicity near Charleston, South Carolina: *Geology*, vol. 10, pp. 654-658.

Talwani, P., and J. Cox, 1985. Paleoseismic evidence for recurrence of earthquakes near Charleston, South Carolina, *Science*, vol. 229, pp. 379-381.

Talwani, P., D.C. Amick, and W.T. Schaeffer, 1999. Paleoliquefaction studies in the South Carolina Coastal Plain, Tech. Rep. NUREG/CR-6619, 109 pp., Nucl. Regul. Comm., Washington, D.C.

Talwani, P., and W.T. Schaeffer, 2001. Recurrence rates of large earthquakes in the South Carolina Coastal Plain based on paleoliquefaction data, *J. Geophys. Res.*, vol. 106, no. B4, pp. 6621-6642.

Toro, G., N. Abrahamson, and J. Schneider, 1993. Engineering model of strong ground motions from earthquakes in the central and eastern United States, in *Guidelines for determining design basis ground motions*, EPRI TR-102293, J.F. Schneider, ed., Electric Power Research Institute.

Toro, G., N. Abrahamson, and J. Schneider, 1997. Model of strong ground motion in eastern and central North America: best estimates and uncertainties, *Seism. Res. Lett.* Vol. 68, pp. 41-57.

Weems, R.E., S.F. Obermeier, M.J. Pavich, G.S. Gohn, and M. Rubin, 1986. Evidence for three moderate to large prehistoric Holocene earthquakes near Charleston, South Carolina, in *Proceedings of the 3<sup>rd</sup> U.S. National Conference on Earthquake Engineering*, Charleston, South Carolina, vol. 1, pp.3-13, Earthquake Eng. Res. Inst., Oakland, Calif.

Wells, D.L. and K.J. Coppersmith, 1994. New empirical relationships among magnitude, rupture length, rupture width, and surface displacements, *Bull. Seism. Soc. Am.*, vol. 84, pp.974-1002.

U.S. Department of Energy, 1989. General Design Criteria, DOE Order 6430.1A, Washington, D.C.

U.S. Department of Energy, 1992. Natural Phenomena Hazards Design Requirements, Draft DOE Order 5480.NPH, Washington, D.C.

U.S. Department of Energy, 1989. General Design Criteria, DOE Standard 1020, Natural Phenomena Hazards Design and Evaluation Criteria for Department of Energy Facilities, U.S. Department of Energy, Washington, D.C.

U.S. Department of Energy, 1992. General Design Criteria, DOE Standard 1024. Guidelines for Use of Probabilistic Seismic Hazard Curves at Department of Energy Sites, U.S. Department of Energy, Washington, D.C.

U.S. Department of Energy, 1996. DOE Standard: Natural Phenomena Hazards Assessment Criteria, DOE-STD-1023-95, Change Notice #1, Washington, D.C., January 1996.

U.S. Department of Energy, 2000. Guide for the Mitigation of Natural Phenomena Hazards for DOE Nuclear Facilities and Nonuclear Facilities, DOE G 420.1-2, Office of Environment, Safety and Health, Approved 3/28/00.

U.S. Geological Survey, 2002. USGS national seismic hazard maps, USGS web site: <http://geohazards.cr.usgs.gov/eq/>, January, 2002.

U.S. Nuclear Regulatory Commission, 1977. Regulatory Guide 1.60 Design Response Spectra for Seismic Design of Nuclear Power Plants, Washington, D.C.

U.S. Nuclear Regulatory Commission, 1991. Policy Issue, Conclusions of the probabilistic seismic hazard studies conducted for nuclear power plants in the eastern United States, SECY-91-135, May 1991.

U.S. Nuclear Regulatory Commission, 1993. Revised Livermore Seismic Hazard Estimates for 69 Nuclear Power Plant Sites East of the Rocky Mountains, (P. Sobel), NUREG-1488.

U.S. Nuclear Regulatory Commission, 1997. Regulatory Guide 1.165, Identification and Characterization of Seismic Sources and Determination of Safe Shutdown Earthquake Ground Motion, March 1997.

WSRC, 1997. SRS Seismic Response Analysis and Design Basis Guidelines, by R.C. Lee, M.E. Maryak, and M.D. McHood, WSRC-TR-97-0085, Rev. 0, March 1997.

**FIGURES**

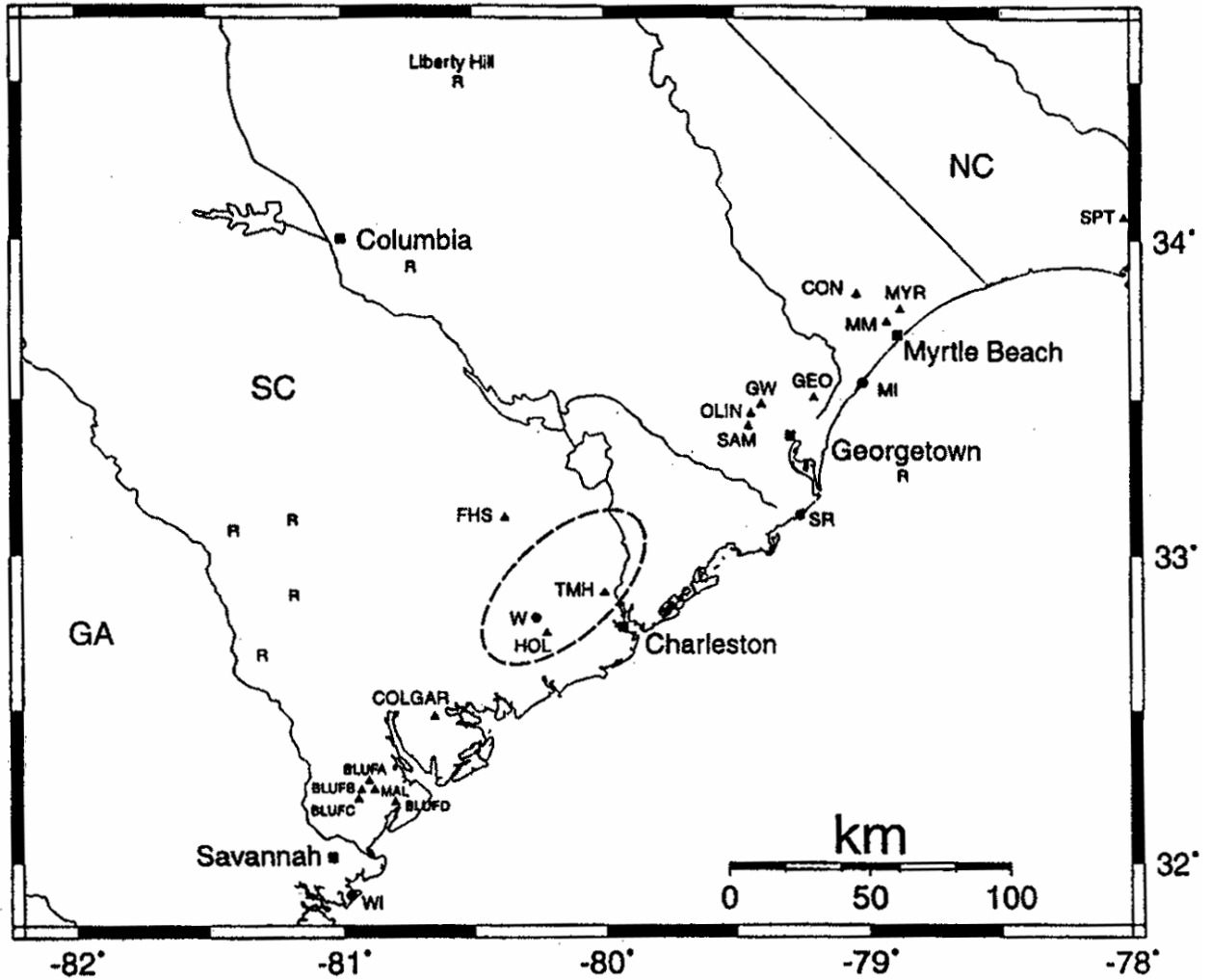


Figure 1. South Carolina Coastal Area showing Geographic Distribution of dated sand boils (taken from Talwani and Schaeffer, 2001)

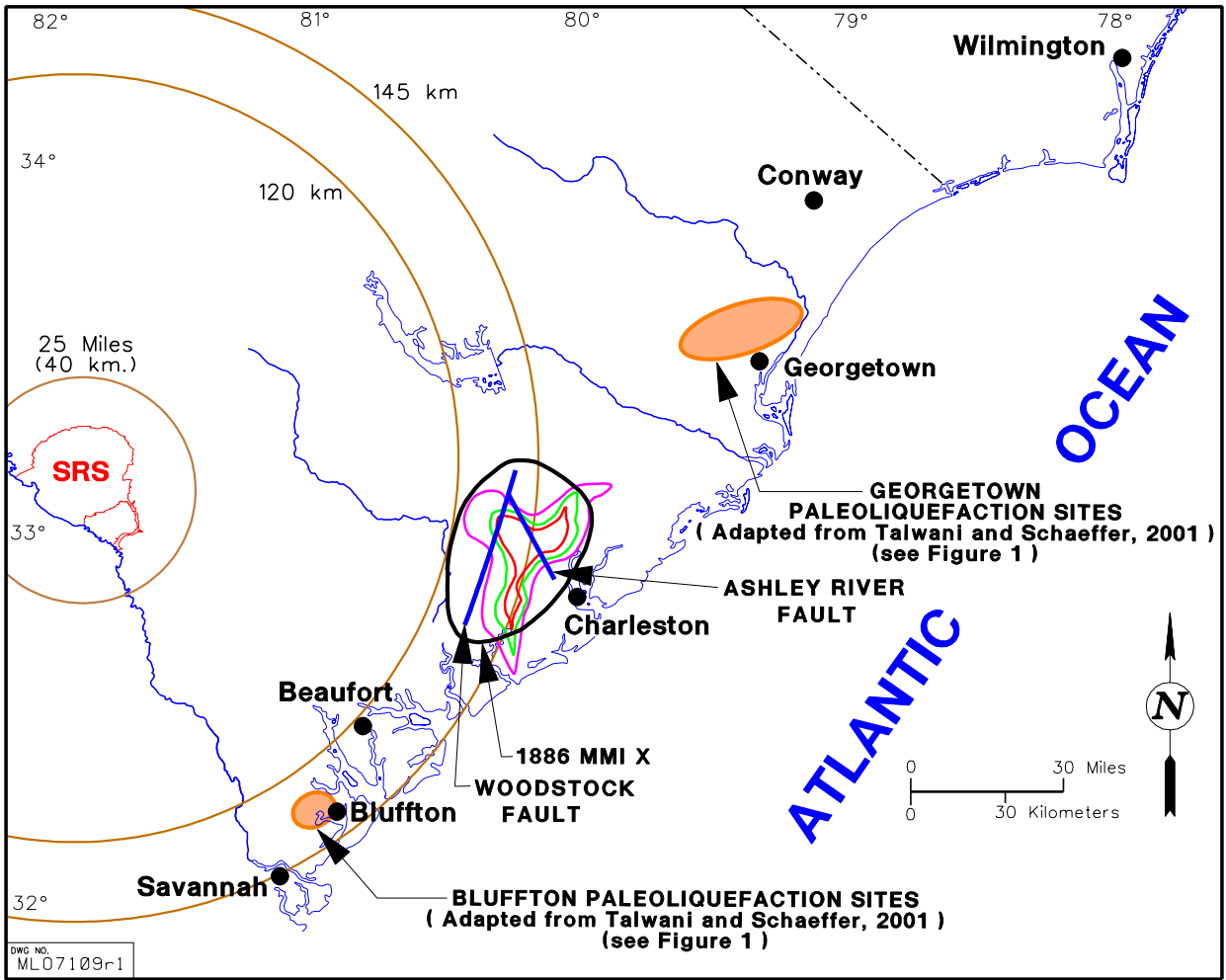


Figure 2. Bluffton and Georgetown paleoliquefaction sites relative to the SRS



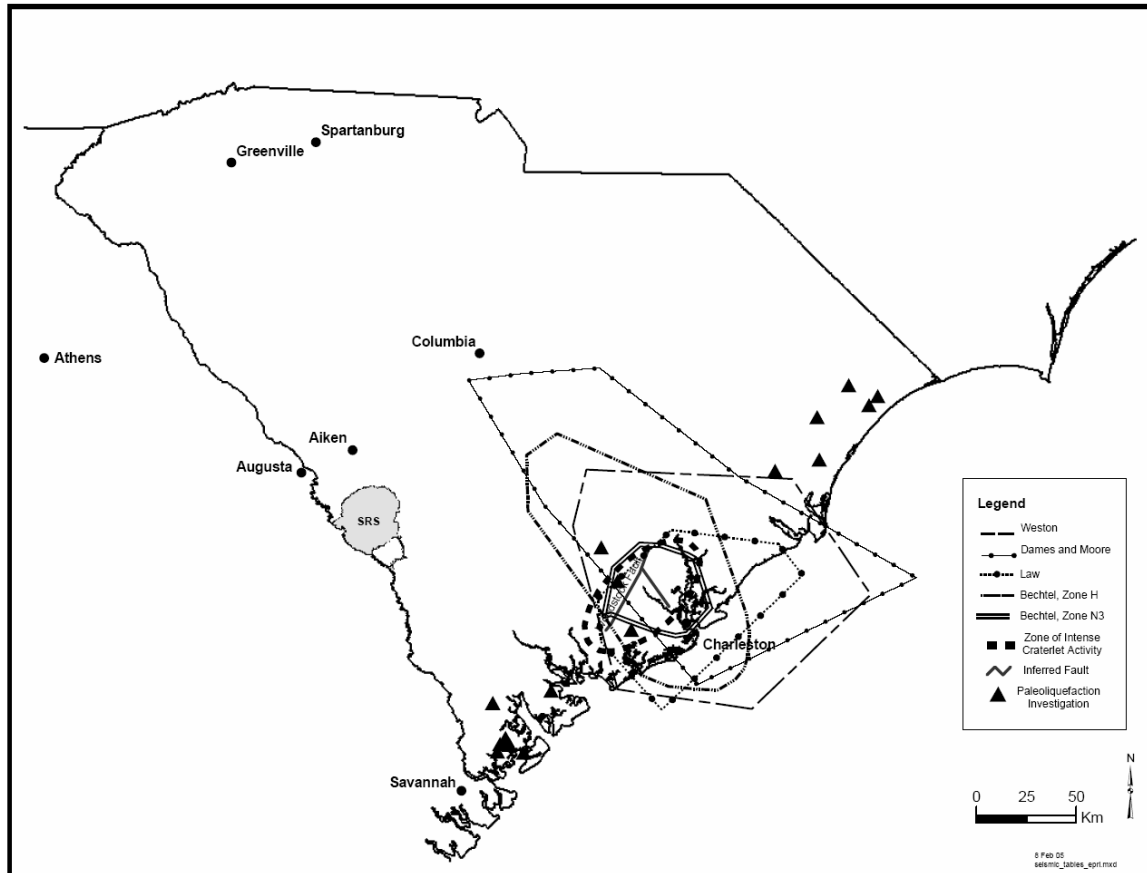


Figure 3. Illustration of available EPRI Team models for the Charleston seismic zone.

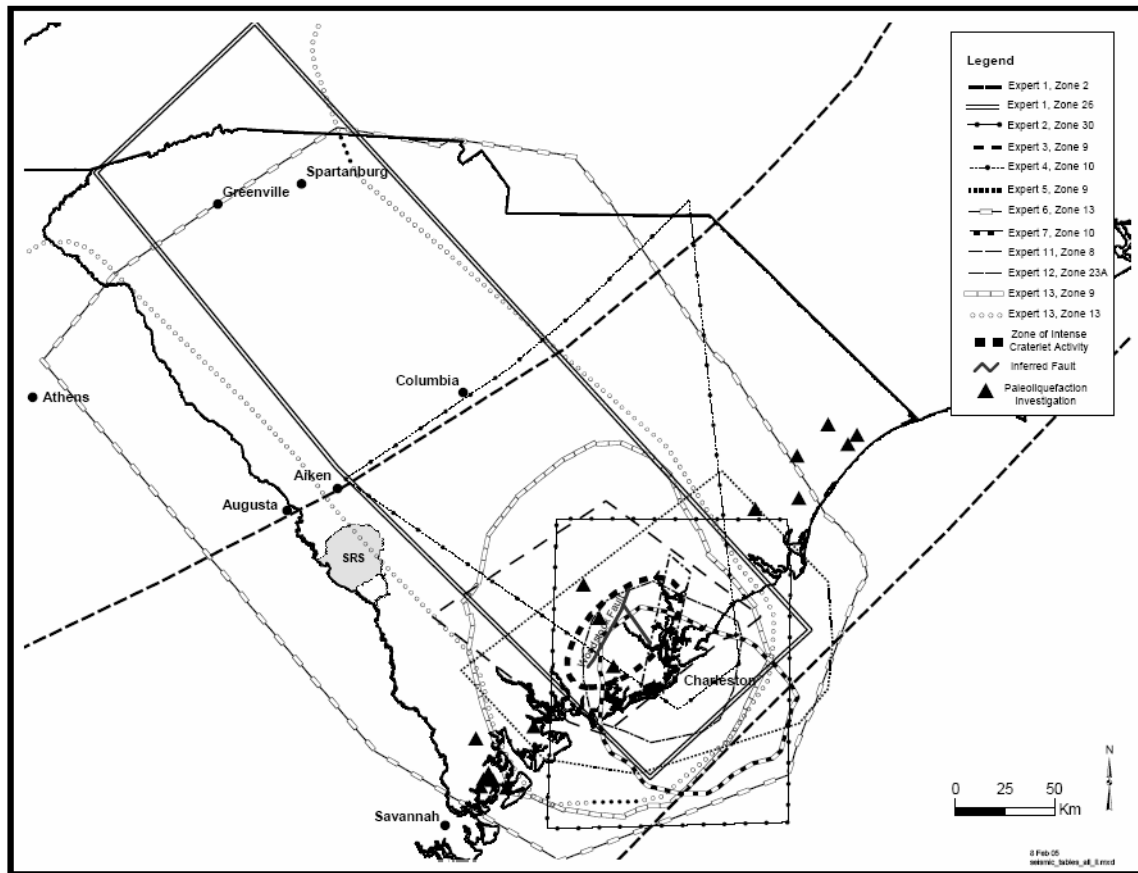


Figure 4. Illustration of LLNL expert models for the Charleston seismic zone.

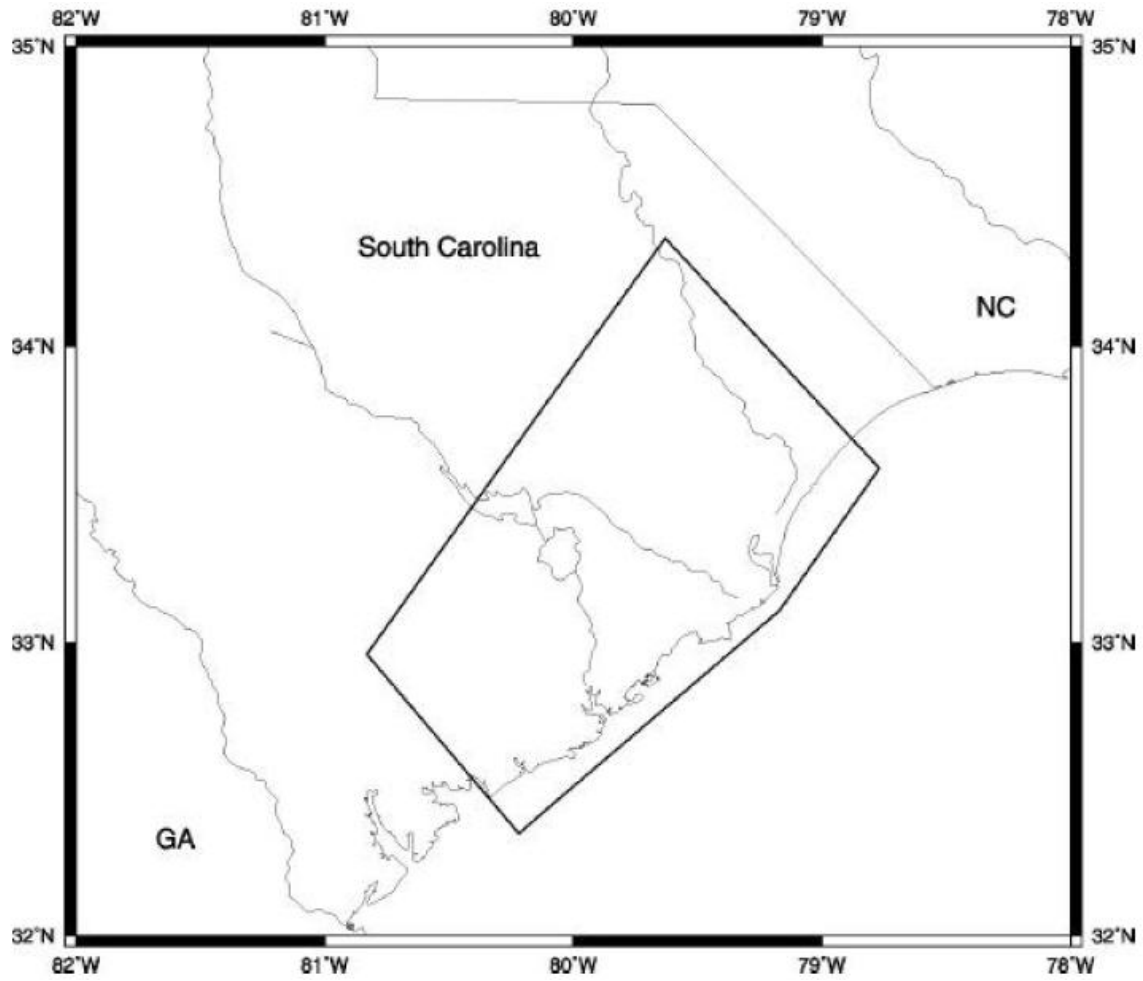


Figure 5. Charleston area source used in USGS National Map model (Frankel et al., 2002)

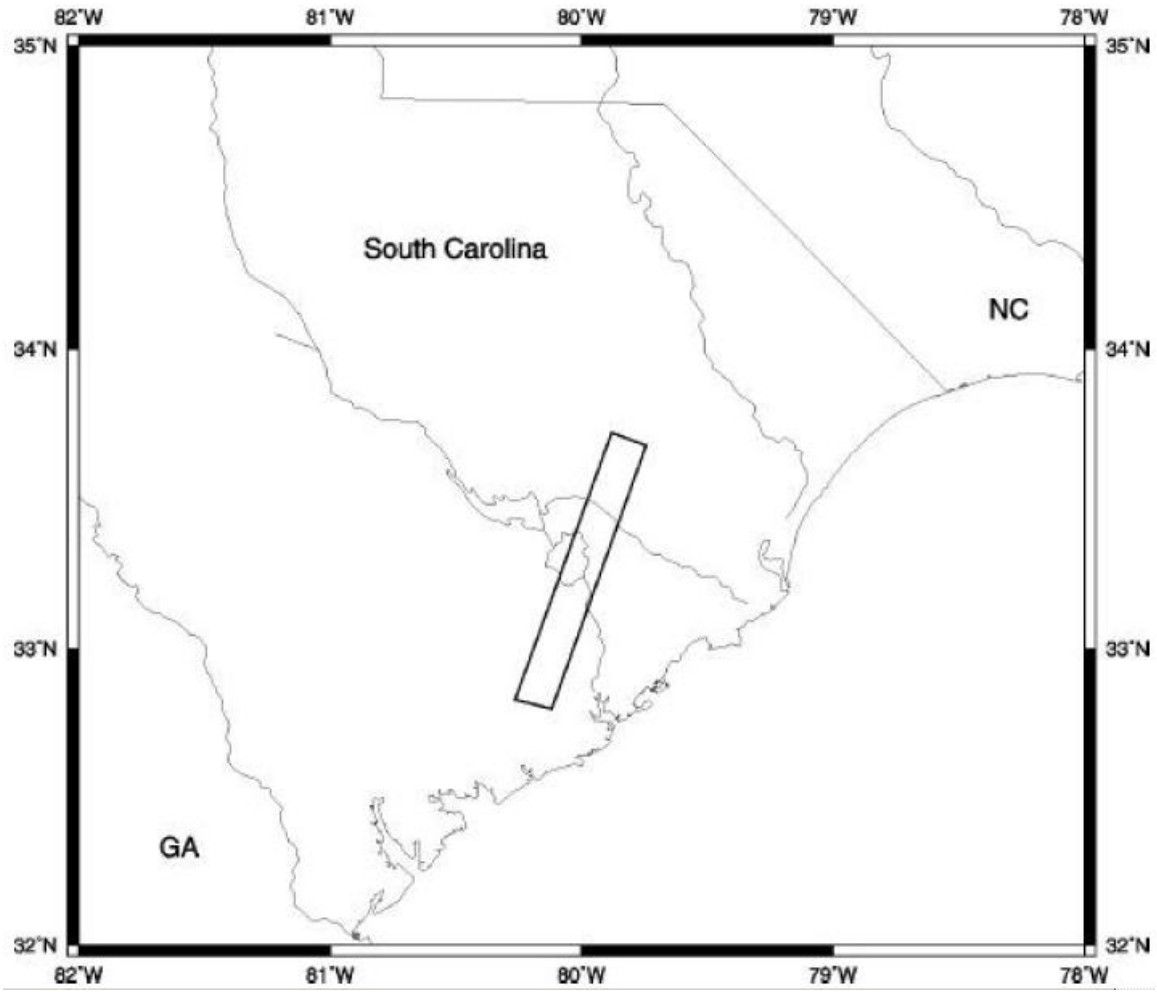


Figure 6. Charleston "fault" source used in USGS National Map model (Frankel et al., 2002)

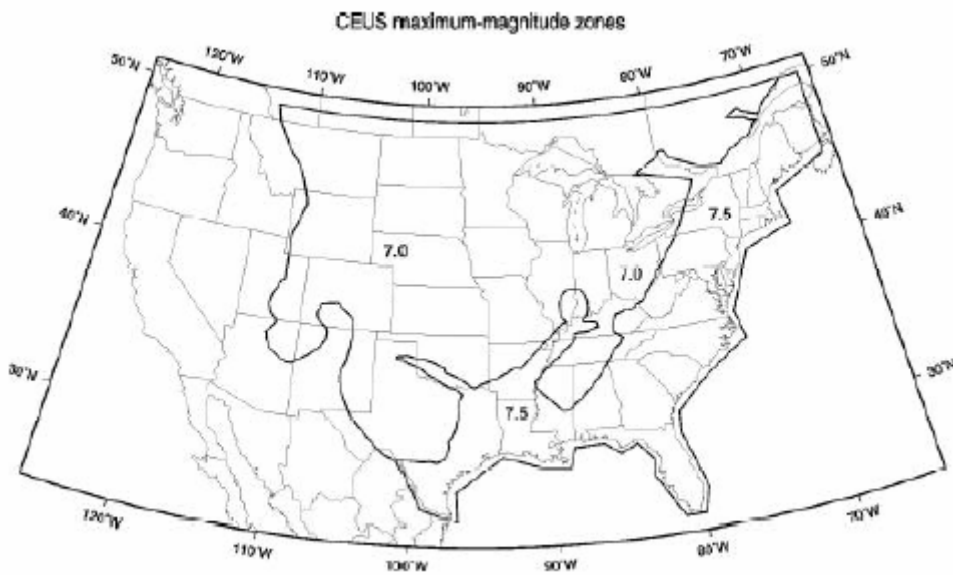


Figure 7. Maximum magnitudes used in the USGS National Map model (Frankel et al., 2002)

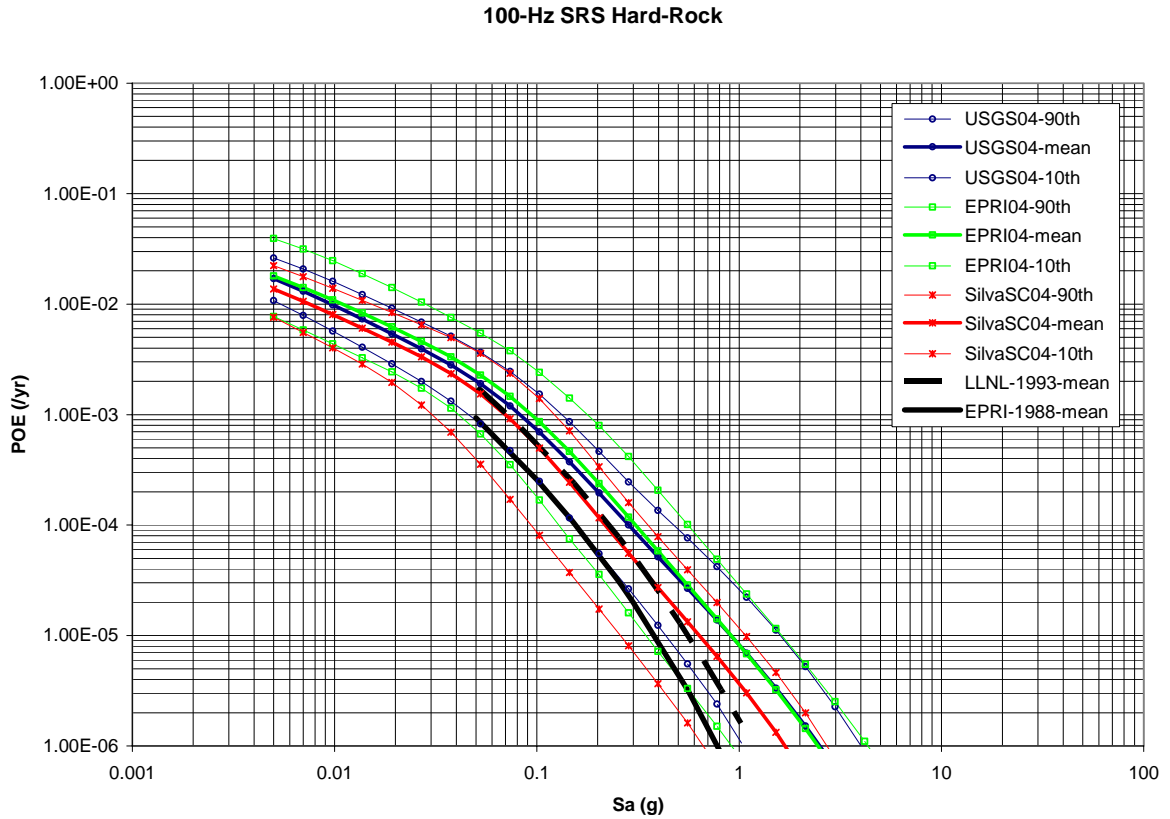


Figure 8. Comparison of SRS mean, and fractile PGA hard-rock hazard for USGS National Map model (USGS04-blue lines), the National Map model and EPRI (2004) attenuation model (EPRI04- green lines) and the National Map model and Silva et al. (2004) regional attenuation model (SilvaSC04-red lines). EPRI (1988) and LLNL (1993) mean hazard curves are illustrated with the solid and dashed thick lines respectively.

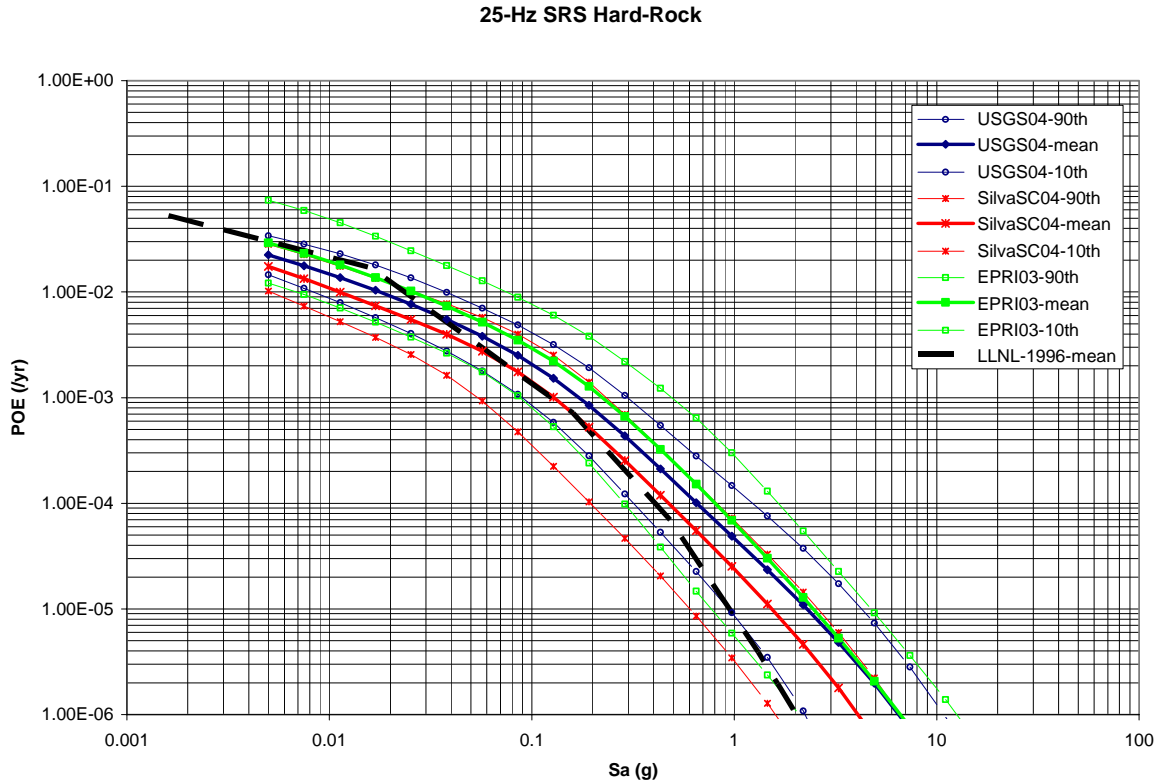


Figure 9. Comparison of SRS mean, and fractile 25-Hz hard-rock hazard for USGS National Map model (USGS04-blue lines), the National Map model and EPRI (2004) attenuation model (EPRI04- green lines) and the National Map model and Silva et al. (2004) regional attenuation model (SilvaSC04-red lines). EPRI (1988) and LLNL (1993) mean hazard curves are illustrated with the solid and dashed thick lines respectively.

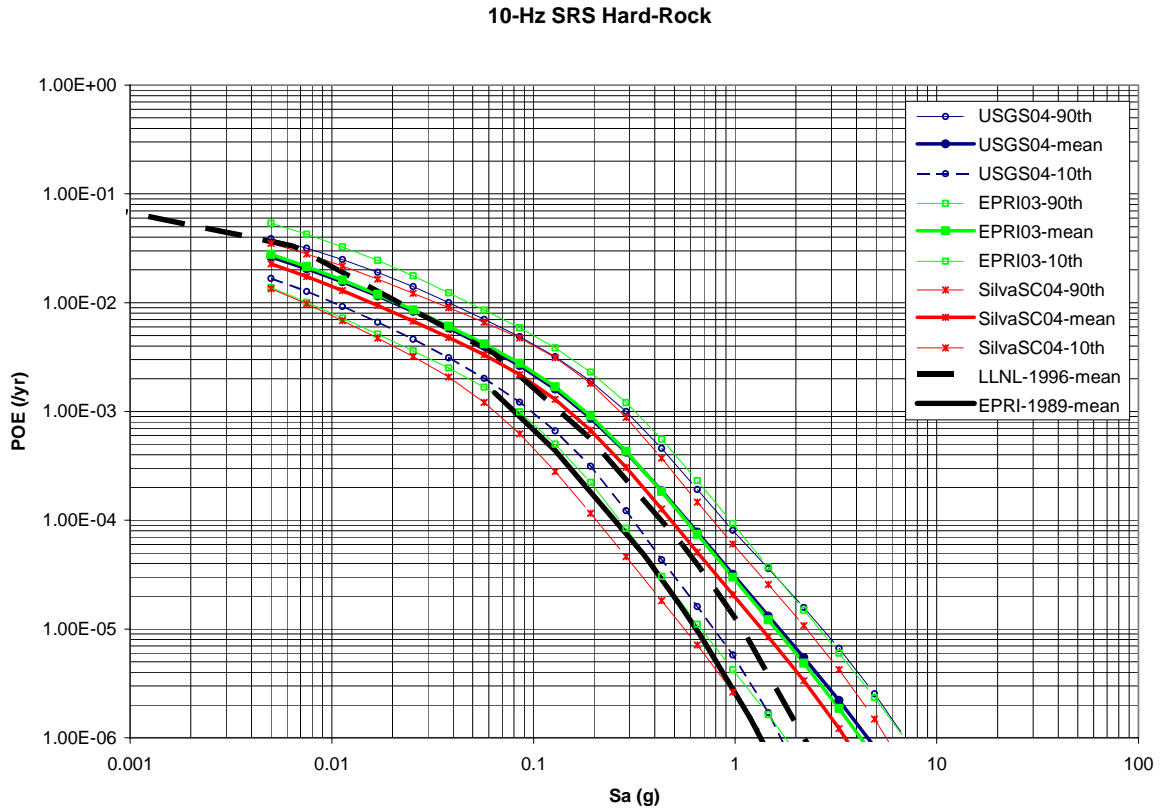


Figure 10. Comparison of SRS mean, and fractile 10-Hz hard-rock hazard for USGS National Map model (USGS04-blue lines), the National Map model and EPRI (2004) attenuation model (EPRI04- green lines) and the National Map model and Silva et al. (2004) regional attenuation model (SilvaSC04-red lines). EPRI (1988) and LLNL (1993) mean hazard curves are illustrated with the solid and dashed thick lines respectively.



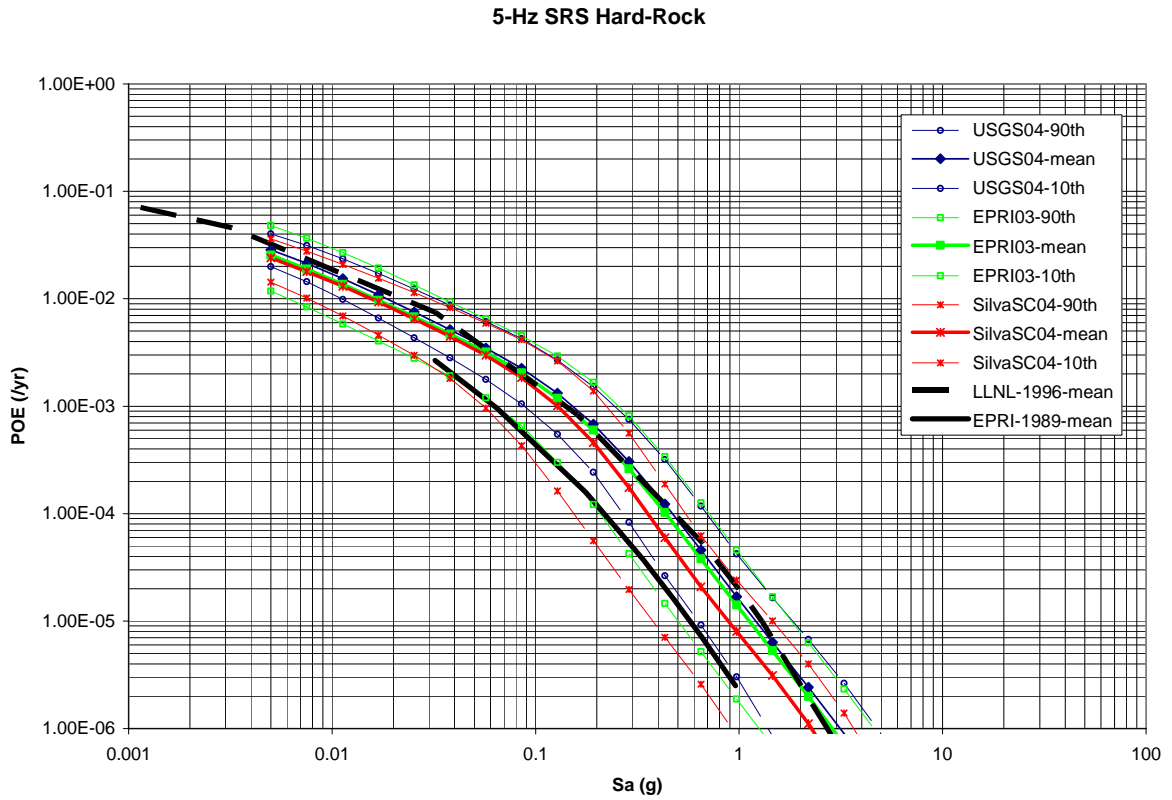


Figure 11. Comparison of SRS mean, and fractile 5-Hz hard-rock hazard for USGS National Map model (USGS04-blue lines), the National Map model and EPRI (2004) attenuation model (EPRI04- green lines) and the National Map model and Silva et al. (2004) regional attenuation model (SilvaSC04-red lines). EPRI (1988) and LLNL (1993) mean hazard curves are illustrated with the solid and dashed thick lines respectively.

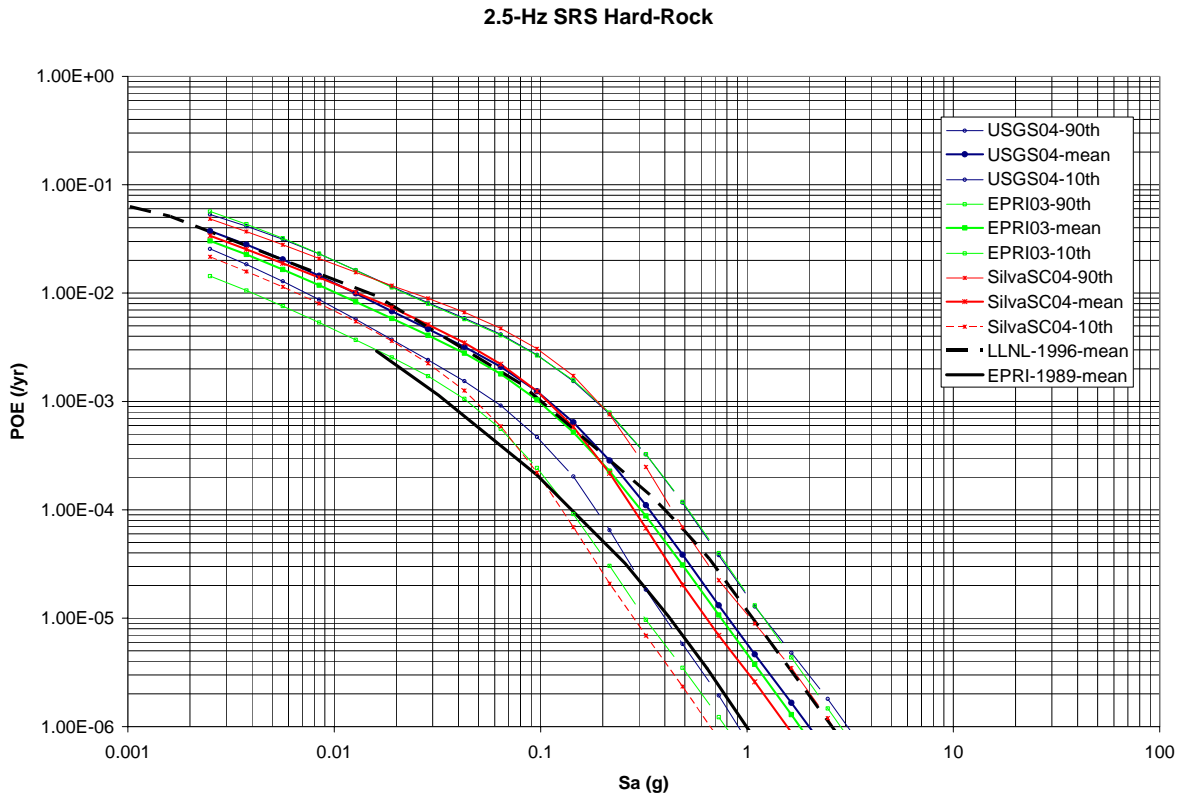


Figure 12. Comparison of SRS mean, and fractile 2.5-Hz hard-rock hazard for USGS National Map model (USGS04-blue lines), the National Map model and EPRI (2004) attenuation model (EPRI04- green lines) and the National Map model and Silva et al. (2004) regional attenuation model (SilvaSC04-red lines). EPRI (1988) and LLNL (1993) mean hazard curves are illustrated with the solid and dashed thick lines respectively.

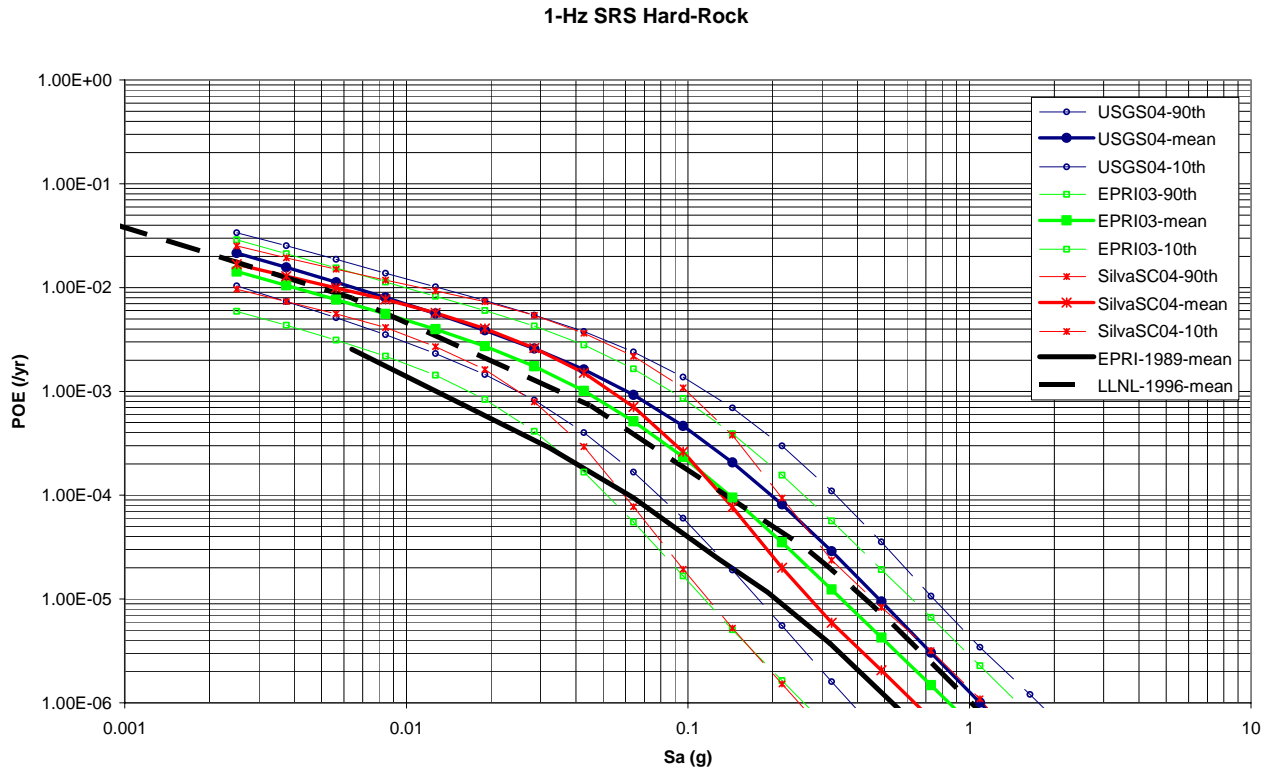


Figure 13. Comparison of SRS mean, and fractile 1-Hz hard-rock hazard for USGS National Map model (USGS04-blue lines), the National Map model and EPRI (2004) attenuation model (EPRI04- green lines) and the National Map model and Silva et al. (2004) regional attenuation model (SilvaSC04-red lines). EPRI (1988) and LLNL (1993) mean hazard curves are illustrated with the solid and dashed thick lines respectively.

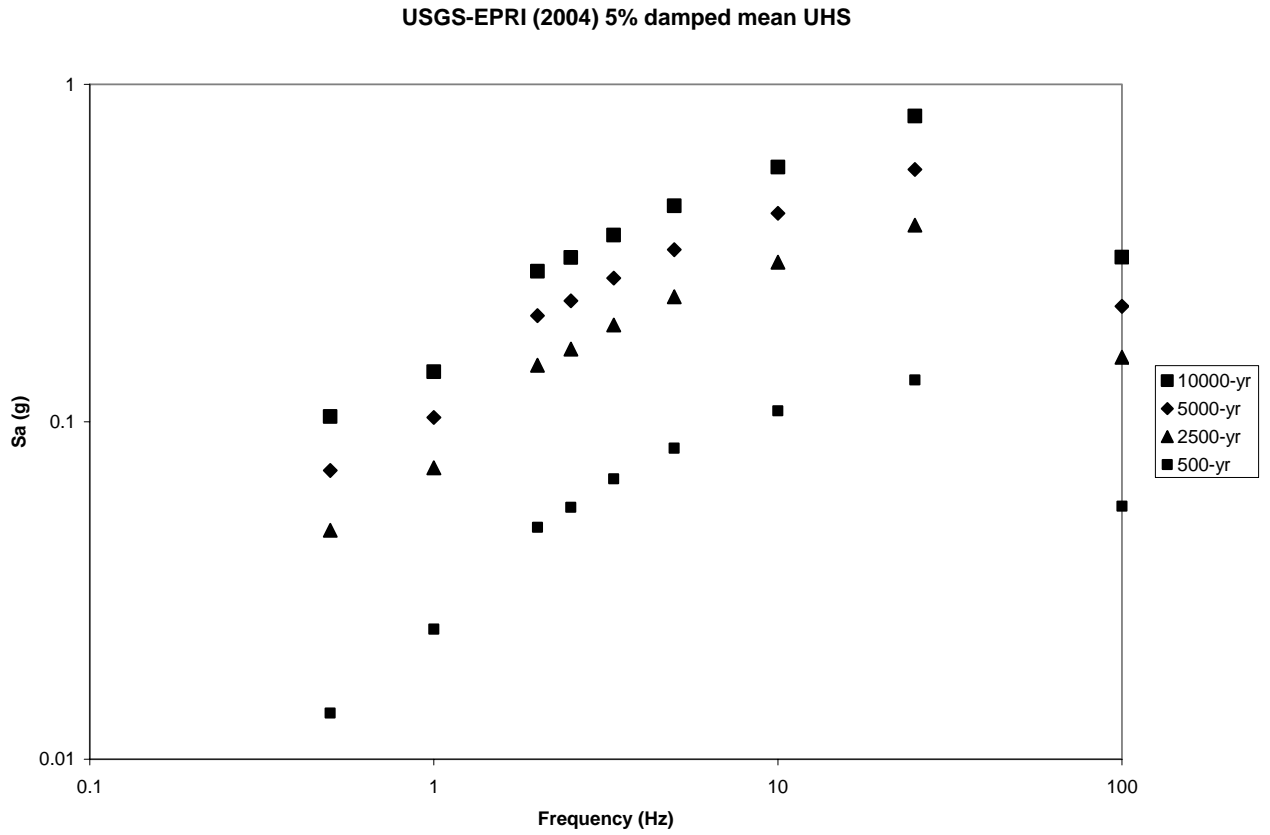


Figure 14. Mean horizontal component uniform hazard spectra for National Map source model and EPRI (2004) attenuation model. Shown are return periods of 500, 2500, 5000 and 10000 years.

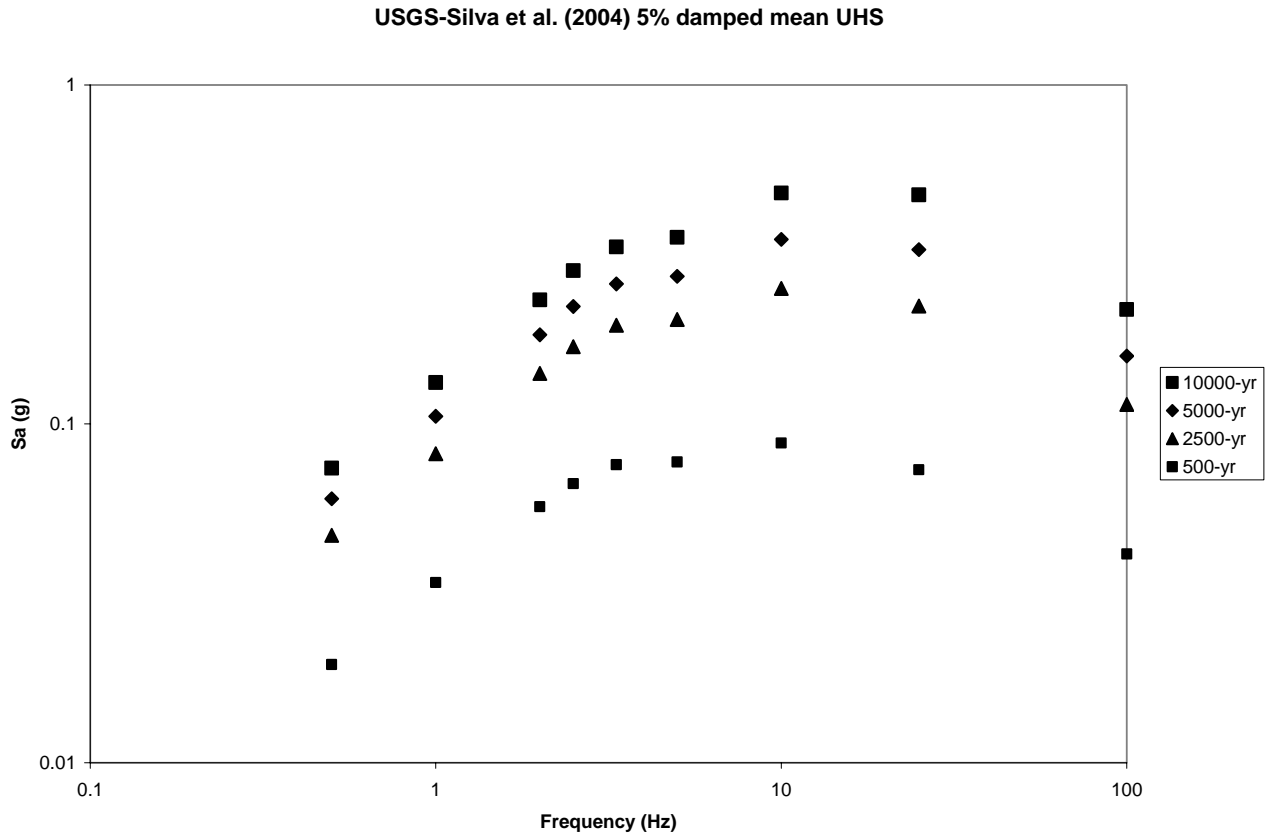


Figure 15. Mean horizontal component uniform hazard spectra for National Map source model and Silva et al. (2004) attenuation model. Shown are return periods of 500, 2500, 5000 and 10000 years.

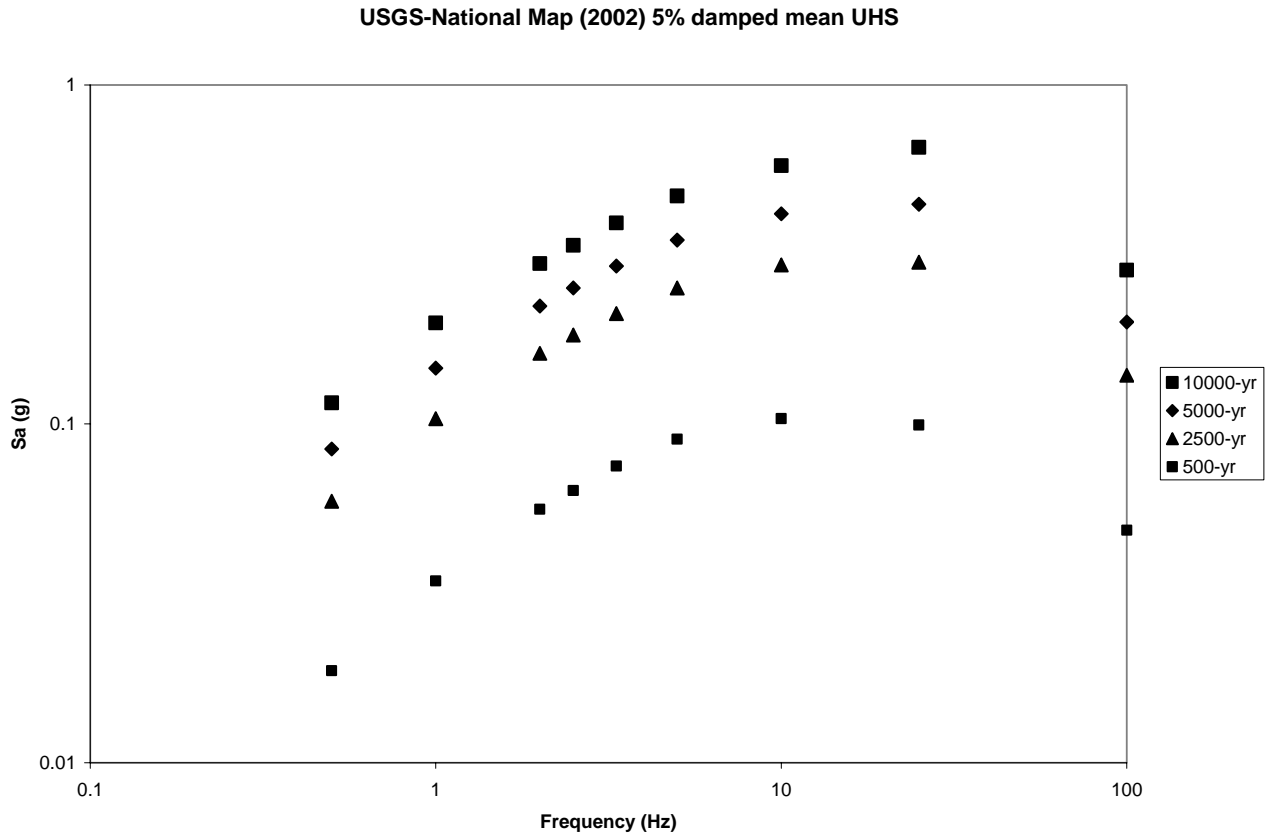


Figure 16. Mean horizontal component uniform hazard spectra for National Map source model and National Map (USGS, 2002) attenuation models. Shown are return periods of 500, 2500, 5000 and 10000 years.

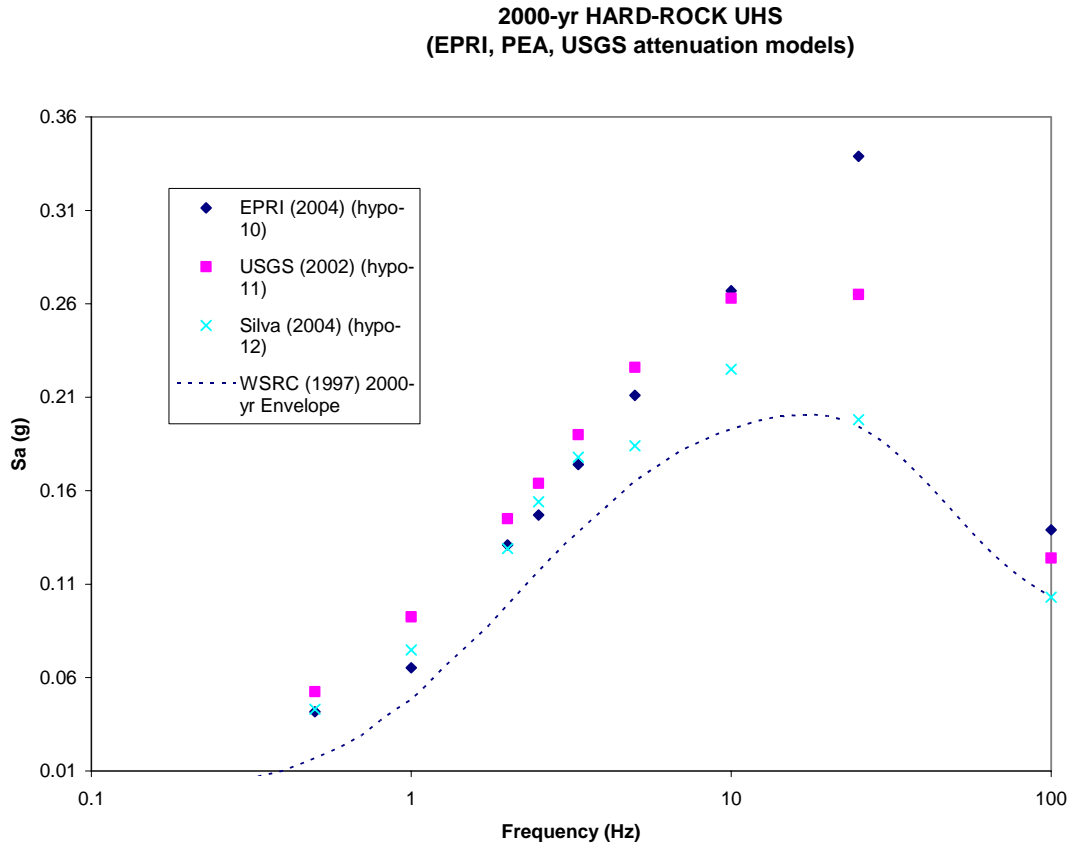


Figure 17. Comparison of National Map source model using attenuation models EPRI (2004), USGS (2002) and Silva et al. (2004) based UHS for 2000-year return period. Also shown is the 2000-year design spectrum based on EPRI (1988) and LLNL (1993) (WSRC, 1997).

**10000-yr HARD-ROCK UHS  
 (EPRI, PEA, USGS attenuation models)**

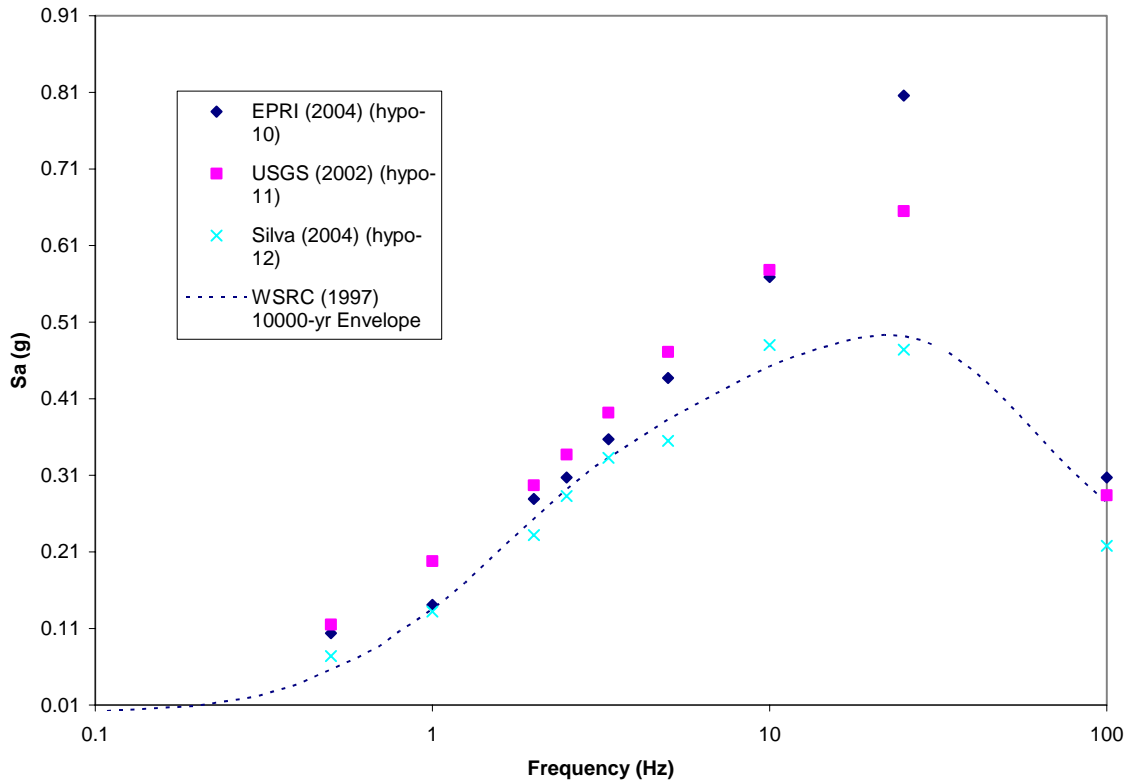


Figure 18. Comparison of National Map source model using attenuation models EPRI (2004), USGS (2002) and Silva et al. (2004) based UHS for 10000-year return period. Also shown is the 10000-year design spectrum based on EPRI (1988) and LLNL (1993) (WSRC, 1997).



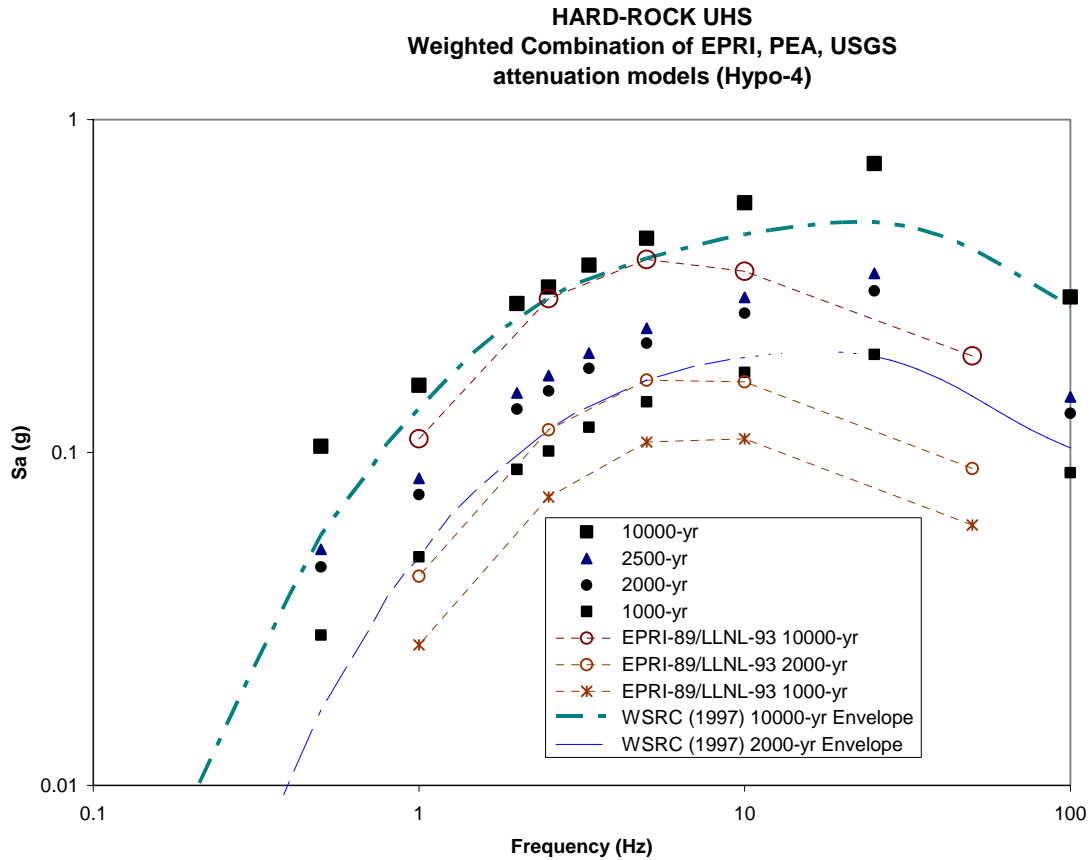


Figure 19. Combined mean horizontal component uniform hazard spectra using weighting scheme described in Section 9. Shown are return periods of 1000, 2000, 2500 and 10000 years. Also shown are the corresponding three uniform hazard spectral values based on the mean of EPRI (1988) and LLNL (1993) (connected by dashed lines for visualization). These spectral values were the basis for the 10,000 and 2,000 year envelopes (WSRC, 1997).

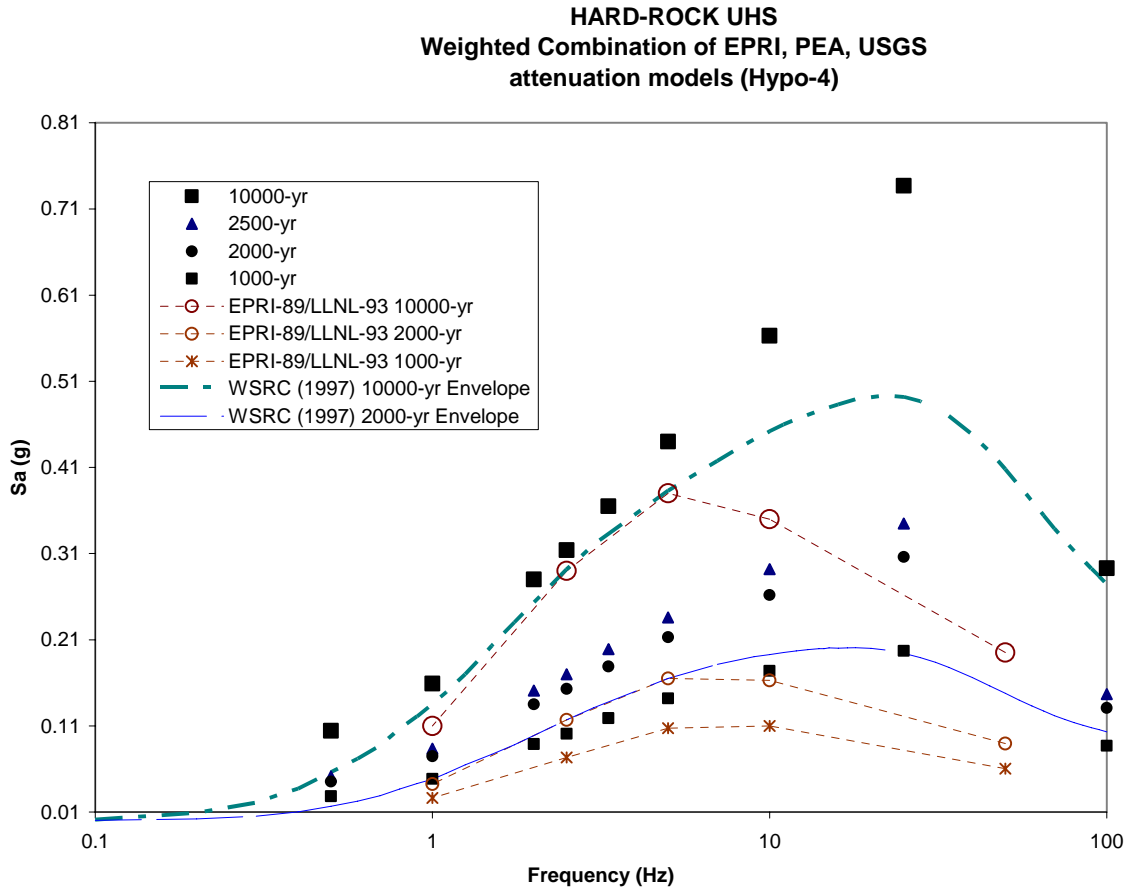


Figure 20. Combined mean horizontal component uniform hazard spectra using weighting scheme described in Section 9. Shown are return periods of 1000, 2000, 2500 and 10000 years. Also shown are the corresponding three uniform hazard spectral values based on the mean of EPRI (1988) and LLNL (1993) (connected by dashed lines for visualization). These spectral values were the basis for the 10,000 and 2,000 year envelopes (WSRC, 1997).

**Appendix A**  
**Chronology of Probabilistic Seismic Hazard (PSHA) Studies**  
**and Use in Establishing the Design Basis Earthquake (DBE)**

1. **Bernreuter (1981 – NUREG/CR-1582): Initial U.S. Nuclear Regulatory Commission (NRC) PSHA completed by Lawrence Livermore National Laboratory (LLNL) as part of NRC Systematic Evaluation Program.**
2. **Coats and Murray (1984 – UCRL-53582 Rev. 1): Initial PSHA studies of DOE sites.**
3. **U. S. DOE Order 6430.1A, General Design Criteria (1989): Initial requirements to establish the DBE based on PSHA.**
4. **Bernreuter et al. (1989 – NUREG/CR-5250): NRC sponsored updated LLNL PSHA for 69 reactor sites in Eastern United States (EUS), commonly referred to as the Livermore study.**
5. **Electric Power Research Institute {EPRI} (1989 – NP-6395-D): Industry sponsored PSHA for Nuclear Power Plants in EUS, commonly referred to as the EPRI study.**
6. **Kennedy et al. (1990 – UCRL-15910): Establishes design and evaluation guidelines for DOE facilities. The concept of facility usage category is introduced that eventually becomes performance category.**
7. **U. S. DOE Standard 1024 (1992): DOE guidelines for how to use LLNL and EPRI PSHA results to establish DBE at DOE sites.**
8. **U. S. DOE Order 5480.28 (1993): Established natural phenomena hazard mitigation requirements for DOE sites, supersedes DBE requirements in DOE Order 6430.1A.**
9. **U. S. DOE Standard 1021 (1993): Established performance categorization for structures, systems and components at DOE facilities.**
10. **U. S. DOE Standard 1020 (1994): Established natural phenomena design and evaluation criteria for DOE facilities, replacing UCRL-15910. Following DOE standard 1021 the concept of performance category is used and the DBE is based on PSHA, following DOE Standard 1024 in the EUS.**
11. **U. S. DOE Standard 1022 (1994): Established natural phenomena site characterization criteria for DOE facilities.**
12. **Sobel (1994 – NUREG-1488): Presents updated LLNL PSHA results for the EUS, partly to address issues identified as part of ongoing PSHA review of Savannah River Site. Commonly referred to as the updated LLNL study.**
13. **U. S. DOE Standard 1023 (1995): Established natural phenomena hazards assessment criteria including how a site should complete a PSHA. In the EUS states that the updated LLNL PSHA can be directly averaged with the EPRI PSHA to set the DBE, and includes spectral shape checks and a deterministic historic earthquake check.**
14. **U. S. DOE Order 420.1 (1995, Facility Safety): Establishes DOE facility safety requirements, replacing DOE Order 6430.1A.**
15. **U. S. Geological Survey {USGS} (1996, Open File Report 96-532): Provides documentation for USGS national seismic hazard maps.**

- 16. U. S. Nuclear Regulatory Commission (1996): NRC publishes final rules amending criteria for seismic and geologic siting and earthquake engineering, including the use of PSHA to set the DBE at reactor sites. In 1997 NRC publishes several supporting documents including Regulatory Guide 1.165 that includes method to set the DBE based on either updated LLNL or EPRI PSHA.**
- 17. Senior Seismic Hazard Analysis Committee (1997 – NUREG/CR-6372). Recommendation for PSHA: Guidance on Uncertainty and Use of Experts.**
- 18. McGuire et al. (2001 – NUREG/CR-6728): NRC sponsored study providing technical basis for revision of regulatory guidance on design ground motions.**
- 19. DOE G 420.1-2 (2000, Nuclear Facility Guidance) Establishes USGS National Map should be incorporated when implementing DOE-STD-1023.**
- 20. DOE recommends USGS National Map hard-rock PSHA for the Oak Ridge National Laboratory Seismic Hazard Update, 2003.**

Uncertainty in the National Seismic Hazard Maps near the Savannah River Site, South  
Carolina

Chris H. Cramer  
U.S. Geological Survey  
3876 Central Ave Ste 2  
Memphis, TN 38152-3050

June 30, 2004

Revised February 13, 2006 after review (minor revisions)

Work done under contract for the Department of Energy

# Uncertainty in the National Seismic Hazard Maps near the Savannah River Site, South Carolina

Chris H. Cramer

## SUMMARY

As part of a Department of Energy (DOE) funded study of seismic hazard at the Savannah River Site, South Carolina (33.26N, 81.64W), an uncertainty analysis of seismic hazard based on the U.S. Geological Survey (USGS) 2002 National Seismic Hazard Maps (Frankel et al., 2002) has been performed. Knowledge-based uncertainty used in the 2002 update of the national seismic hazard maps are represented in logic trees for the three major seismic sources affecting the study site: New Madrid, Charleston, and the local seismicity (smoothed seismicity model). For peak ground acceleration (PGA), and 0.04, 0.1, 0.2, 0.3, 0.4, 0.5, 1.0, and 2.0 s spectral acceleration (Sa), the mean and 5%, 15%, 50% (median), 85%, and 95% hazard curves are estimated using Monte Carlo sampling of these logic trees. 200 Monte Carlo samples were used in calculating the hazard curves (see Appendices for numerical values). The calculations were done for hard-rock site conditions. Overall uncertainty, as represented by the coefficient of variation (cv – standard deviation divided by mean) for 0.01 to 0.0000001 annual probability of exceedance (PE), ranges from 0.3 to 10.0. Four major contributors to this overall uncertainty are (1) the choice of ground-motion attenuation relation used in the seismic hazard calculations, (2) the uncertainty in maximum and characteristic magnitudes, (3) the uncertainty in earthquake rates as represented by catalog resampling, (4) and the choice of M<sub>blg</sub> to M<sub>w</sub> conversion relation. All other branch-points have very small contributions to overall uncertainty at the Savannah River Site. Additionally, deaggregation of the hazard at four points per decade of PE has been performed and summarized at each decade. Local seismic sources dominate the hazard at low PE's (0.00001 and less) while the Charleston characteristic source becomes more prominent at higher PE's. The New Madrid seismic zone contributes very little to the seismic hazard except at long periods (1.0 s and greater) and high PE's (0.01), where the contribution is small.

## APPROACH

Overall uncertainty and sensitivity to model parameters has been determined via Monte Carlo sampling of model-parameter logic trees (Cramer, 2001a). Standard USGS national seismic hazard mapping project models and computer codes were used in the analysis (Frankel et al., 2002). The three central and eastern US (CEUS) hazard models affecting the Savannah River Site (SRS) are the Charleston and New Madrid characteristic earthquake models, and the CEUS smoothed seismicity model. The CEUS smoothed seismicity model contains the seismic hazard model for the East Tennessee seismic zone.

In this study, the uncertainty analysis was conducted in three alternative ways. The first conformed to the NRC 29-site study conducted for the Nuclear Regulatory Commission (National Seismic Hazard Project, 2004) and includes the 2002 hazard curve truncations and caps (Frankel et al., 2002). The second and third alternatives removed all truncations and caps from the hazard calculations, and modified the Charleston characteristic magnitude alternative from 6.8 to 6.9 to better model the final preferred value of Bakun and Hopper (2004) at SRS staff's request. For the second alternative, the fractile deaggregations are composed of actual single fractile values at each ground motion level that makes up the hazard curve. For the third (and also the first) alternative, fractile deaggregations are the result of averaging fractile values within 5% of the desired fractile at each ground motion level per Norm Abrahamson (personal communication, 2003).

### LOGIC TREES

Figures 1 – 3 present the logic trees for the three CEUS models used in the analysis. Previous work (Cramer, 2001b; Cramer et al., 2002; National Seismic Hazard Project, 2004) enabled the logic trees shown here to contain only those elements that contribute to the overall uncertainty in the CEUS. Common to all the logic trees is the ground-motion attenuation relation branch-point involving five relations for the characteristic models and four relations for the smoothed-seismicity model. For the New Madrid characteristic earthquake model (Figure 1), the logic tree contains the fault rupture and characteristic magnitude alternatives of the 2002 national model (Frankel et al., 2002). Along strike uncertainty in the characteristic rupture model is represented by pseudo-fault end-point alternatives of +25 km (NE), 0 km, and -25 km (SW) variations relative to those used in the 2002 national model (weighted 0.2, 0.6, 0.2 respectively). Variation about the 500 year mean recurrence interval of the 2002 national model is represented by a continuous lognormal distribution with a ln-sigma of 0.5, implying a median recurrence interval of 440 years (see Cramer, 2001b).

For the Charleston characteristic earthquake model (Figure 2), the logic tree uses the 2002 national model alternatives for the fault rupture zones and characteristic magnitudes. Like the New Madrid model, the Charleston model variability about a 550-year mean recurrence interval is represented by a lognormal distribution with a ln-sigma of 0.5 (median recurrence interval of 485 years).

As shown in Figure 3, besides the ground-motion attenuation relation alternatives already discussed, the logic tree for the smoothed-seismicity model contains alternatives for the seismicity model, catalog (via resampling), maximum magnitude, seismicity model alternatives, smoothing distance, and M<sub>blg</sub> to M<sub>w</sub> conversion relation. These alternatives are taken from the 2004 NRC 29-site study (National Seismic Hazard Project, 2004).

It is important for interpreting the results to understand how the East Tennessee seismic zone is represented within the smoothed-seismicity model. As related in Wheeler and Frankel (2000), the East Tennessee seismic zone is treated as a seismicity area source instead of the usual manner. Within the areal representation of the East Tennessee

seismic zone, the seismicity rate since 1976 is evenly distributed by counting all the  $M \geq 3$  earthquakes within the zone and averaging that rate over the area of the zone. Prior to smoothing, this value for the seismicity rate is then substituted for the actual gridded rate for those grid points that fall within the East Tennessee zone. In the Monte Carlo procedure, the rate of seismicity within the zone is varied by catalog resampling, but the rate of  $M \geq 3$ ,  $M \geq 4$ , and  $M \geq 5$  earthquakes are derived from the same a-value as determined in each randomized model selected via Monte Carlo sampling. As shown, in Cramer et al. (2002), this forcing of the rate to be uniform within a seismicity zone reduces the variability from regional completeness, seismicity model, and smoothing distance branch-points to very low levels at sites within that seismicity zone. It is important to remember this is not the case for sites distant from a seismicity zone and this is why the branch-points are retained in the CEUS smoothed-seismicity logic tree shown in Figure 3, except regional completeness, which has an insignificant contribution to seismic hazard (Cramer et al., 2002).

## RESULTS

Two kinds of sensitivity tests were conducted: one for the sensitivity of the mean and fractile hazard curves to the number of Monte Carlo samples of the logic trees, and the other for individual branch-point contributions to the uncertainty in hazard estimates. Figures 4 and 5 present the results of the first sensitivity test. Figure 4 shows that the PGA mean hazard curve is well represented by 100 or more Monte Carlo samples of the logic trees. The PGA median hazard curve is well represented by 200 or more Monte Carlo samples as shown in Figure 5. The other PGA fractile hazard curves need at least 200 and possibly a minimum of 500 Monte Carlo runs, particularly for the 5%, 15%, and 95% fractile curves at low probabilities of exceedance (PE). Similar results for the other periods of interest are presented in the Appendix (mncmp\*.ps and frm\*.ps files in the main directory of the appendix CD).

The sensitivity of each branch-point's contribution to the overall uncertainty was determined by only letting the branch-point of interest vary among its alternatives while the remaining branch-points are held at one fixed value at or near its mean alternative. The results of these tests for PGA are shown in Figures 6 through 15. The major contributors to uncertainty are the choice of attenuation relations (Figure 6), catalog resampling (Figure 7), Charleston characteristic recurrence interval (Figure 8), alternative seismicity models (Figure 9), and Charleston characteristic magnitude (Figure 10). There is some sensitivity to the  $M_{blg} \rightarrow M_w$  conversion used (Figure 11) and, at PE's below  $1E-5$ , to the Gutenberg-Richter maximum magnitude for the smoothed seismicity models (Figure 12). There is very little or no sensitivity to the seismicity smoothing distance (Figure 13), alternative Charleston characteristic rupture models (Figure 14), and New Madrid fault length variability (Figure 15). Similar results for the other periods of interest are presented in the Appendix (hazc\*.ps files in appendix CD subdirectories Alt, Attn, Cnvt, Len, Mag, Mmax, Ri, Rsmpl, Rup, and Smth). For 1.0s and 2.0s  $S_a$ , the sensitivity to the choice of attenuation relations increases due to the variability among



one and two corner source models in the various relations that is not present at shorter periods.

Based on the first sensitivity test described above, the overall uncertainty was calculated using 200 Monte Carlo samples of the logic trees shown in Figures 1 – 3. The calculations were done for hard-rock site conditions for peak ground acceleration (PGA) and 0.04, 0.1, 0.2, 0.3, 0.4, 0.5, 1.0, and 2.0 s spectral acceleration (Sa). Mean, 5%, 15%, median, 85%, and 95% hazard curves are estimated from the resulting 200 alternative-model hazard curves for the Savannah River site (33.26N, 81.64W). As discussed in the Approach section above, the analysis was done three alternative ways: 1) according to the USGS's NRC 29-site report (National Seismic Hazard Project, 2004), using the logic trees of Figures 1 through 3 with single fractile hazard curve deaggregation, and using the logic trees of Figures 1 through 3 with averaged fractile hazard deaggregation. A further difference between the NRC approach and the other two alternatives is the use of hazard curve truncation/capping for the "NRC" runs and no truncation/capping in the SRS specific runs.

Figures 16 through 18 present the PGA mean and fractile hazard curves for each analysis alternative. Each hazard curve has been calculated to a PE level below  $10^7$ . Figure 16 shows the effect of the truncation used in the National Seismic Hazard maps while Figures 17 and 18 have no hazard curve truncation. The effect of truncation in Figure 16 becomes significant at about a PE of  $10^4$ . The difference between the hazard curves of Figure 17 (single fractile estimate) and Figure 18 (averaged fractile estimate) is very small, which is also seen in the two red curves of Figures 3 and 4, which are from these two alternative analyses.

In Figure 16, the mean PGA hazard curve of the Monte Carlo sampling of the logic trees varies somewhat from the mean PGA hazard curve for the national maps. The variance increases with decreasing PE. As explained in the NRC 29-site report (National Seismic Hazard Project, 2004), this is due to the procedure used to generate model activity rates from the resampled catalog not adequately representing the original procedure used to generate the standard activity rates used in the national map calculations. Basically, the  $M \geq 5$  seismicity model creates a lower hazard bias that imparts an asymmetry from the smoothed-seismicity-model branch-point. The seismicity model alternatives incorporated the NRC and SRS logic trees are felt to better represent the epistemic uncertainty in the national maps for this branch-point.

The Appendix presents the hazard curve results for the other periods of interest [hazc\*.ps files in appendix CD subdirectories NRCanal, Fulls (single fractile estimate), and Full (averaged fractile estimate)]. Additionally, digital versions of the hazard curves are also available in these Appendix subdirectories (see descriptions in Appendix description section below).

Deaggregations of PGA hazard for the NRC-style analysis and the two SRS analyses are presented in Figures 19 through 21 for a PE of  $10^5$ . The deaggregations were done at 25 km distance and 0.5 magnitude-unit increments. Six deaggregation plots are shown in

each figure, one for the mean and each fractile (5%, 15%, 50%, 85%, and 95%) hazard curve at the stated PE. The height of each column represents the probability density for that magnitude and distance bin (the sum of the column values in each plot has been normalized to one).

Figure 19 shows the NRC-style results, which uses the average of fractiles within 5% of the target fractile deaggregation. Figure 20 shows the SRS single fractile deaggregations and Figure 21 shows the SRS averaged fractile deaggregations. Generally, the local (smoothed seismicity) sources dominate the hazard at PE's of  $10^{-5}$  and below. At higher PE's the Charleston characteristic source becomes more dominant, and only near a PE of 0.01 does the New Madrid characteristic source make some contribution to the hazard (see the dma3ds[3-14].ps files in the appendix CD subdirectory Full). At a PE of  $10^{-5}$ , Figure 19 and 21 show similar results, except for the subtle effects of truncation in Figure 19. Obviously at lower PE's the differences become less subtle. In Figure 20 the differences from Figure 21 are striking at 5% and 15% fractile deaggregations for PGA. In Figure 20, each fractile deaggregation is for a single fractile hazard curve, while in Figure 21, each fractile deaggregation is for the average of all fractile hazard curve deaggregations within 5% of the desired fractile value. Although suggested, but not fully demonstrated here, the single fractile deaggregation approach can lead to neighboring fractile deaggregations that are very different from each other due to the variations among hazard models that produce similar hazard results. Our recommendation is to use the averaged results.

The deaggregation results for other periods of interest are presented in the Appendix (dma3ds\*.ps files in subdirectories NRCAnal, Fulls, and Full). The results are similar to those for PGA discussed above, except at longer periods (1.0 and 2.0 s) the characteristic sources become more prominent (Figure 22). At PE's near 0.01 the New Madrid characteristic source becomes predominant at these long periods. Additionally, the digital deaggregations at four PE points per decade (1.0, 1.78, 3.16, and 5.62) between  $10^{-2}$  and  $10^{-7}$  are available in the appendix CD subdirectories Full and Fulls. Please see the Appendix section below for details.

## REFERENCES

- Atkinson, G.M. and D.M. Boore (1995). Ground motion relations for eastern North America, *Bull. Seism. Soc. Am.* **85**, 17-30.
- Boore, D.M., and G.M. Atkinson (1987). Stochastic prediction of ground motion and spectral response parameters at hard-rock sites in eastern North America, *Bull. Seism. Soc. Am.* **77**, 440-467.
- Campbell, K.W. (2003). Prediction of strong ground motion using the hybrid empirical method and its use in the development of ground-motion (attenuation) relations in eastern North America, *Bull. Seism. Soc. Am.* **93**, 1012-1033.

- Cramer, C.H. (2001a). The New Madrid seismic zone: Capturing variability in seismic hazard analyses, *Seism. Res. Lett.* **72**, 664-672.
- Cramer, C.H. (2001b). A seismic hazard uncertainty analysis for New Madrid, *Eng. Geol.* **62**, 251-266.
- Cramer, C.H., R.L. Wheeler, and C.S. Mueller (2002). Uncertainty analysis for seismic hazard in the southern Illinois basin, *Seism. Res. Lett.* **73**, 792-805.
- Frankel, A., C. Mueller, T. Barnhard, D. Perkins, E.V. Leyendecker, N. Dickman, S. Hanson, and M. Hopper (1996). *National Seismic-Hazard Maps: Documentation June 1996*, U.S. Geological Survey, Open-File Report 96-532.
- Frankel, A.D., M.D. Petersen, C.S. Mueller, K.M. Haller, R.L. Wheeler, E.V. Leyendecker, R.L. Wesson, S.C. Harmsen, C.H. Cramer, D.M. Perkins, and K.S. Rukstales (2002). *Documentation for the 2002 update of the national seismic hazard maps*, U.S. Geological Survey, Open-File Report 02-420.
- Johnston, A.C. (1994). Seismotectonic interpretations and conclusions for the stable continental region seismicity database, in J.F. Schneider (editor), *The Earthquakes of Stable Continental Regions – v. 1, Assessment of Large Earthquake Potential*, Palo Alto, CA, Electric Power Research Institute, 4-1 – 4-103.
- Johnston, A.C. (1996). Seismic moment assessment of earthquakes in stable continental regions – I. Instrumental seismicity, *Geophys. J. Int.* **124**, 381-414.
- National Seismic Hazard Project (2004). *Evaluation of 2002 USGS National Seismic Hazard Assessment*, Final Report to the NRC, U.S. Geological Survey, 22 pp.
- Somerville, P., N. Collins, N. Abrahamson, R. Graves, and C. Saikia (2001). Ground motion attenuation relations for the central and eastern United States, Final Report to the USGS, June 30, 2001, URS Group, Inc., Pasadena, CA, 36 pp.
- Toro, G., N. Abrahamson, and J. Schneider (1997). Model of strong ground motions from earthquakes in central and eastern North America: best estimates and uncertainties, *Seism. Res. Lett.* **68**, 41-57.
- Wheeler, R.L., and A. Frankel (2000). Geology in the 1996 USGS seismic-hazard maps, central and eastern United States, *Seism. Res. Lett.* **71**, 273-282.

## APPENDIX

The accompanying CD appendix contains postscript plot files and digital data files for the Savannah River site derived from the uncertainty analyses and sensitivity tests of this report. The subdirectories of this appendix are for the single parameter sensitivity tests (Alt, Attn, Cnvt, Len, Mag, Mmax, Ri, Rsmpl, Rup, and Smth), for the number of Monte Carlo samples sensitivity test (Full500, Full, Fulls, Full100, Full150, and Full20), and for the three uncertainty analyses (NRCanal, Fulls, and Full). The subdirectories Full and Fulls are used for both analyses and one sensitivity test.

Generally, **.ps** files are postscript plot files, **.hzdt** files are hazard curve files, and **dma.** and **dmd.** files are deaggregation files. **dma.** files are deaggregation files whose probabilities sum to the indicated PE for the deaggregation (retain probabilities that aggregate into the PE of the hazard). **dmd.** files are probability density files whose probabilities sum to 1.0 and are used in the deaggregation plots (**dma3ds\*.ps** files).

Naming conventions for **.hzdt** files are pga for PGA, s04 for 0.04 s Sa, a01 for 0.1 s Sa, a02 for 0.2 s Sa, a03 for 0.3 s Sa, a04 for 0.4 s Sa, a05 for 0.5 s Sa, a10 for 1.0 s Sa, and a20 for 2.0 s Sa. The type of hazard curve is identified by mean, minus90cl (5%), minus70cl (15%), median, plus70cl (85%), and plus90cl (95%). The file naming convention is **mapunc.type.ppp.hzdt**. Type indicates the type of hazard curve and ppp represents the ground motion period.

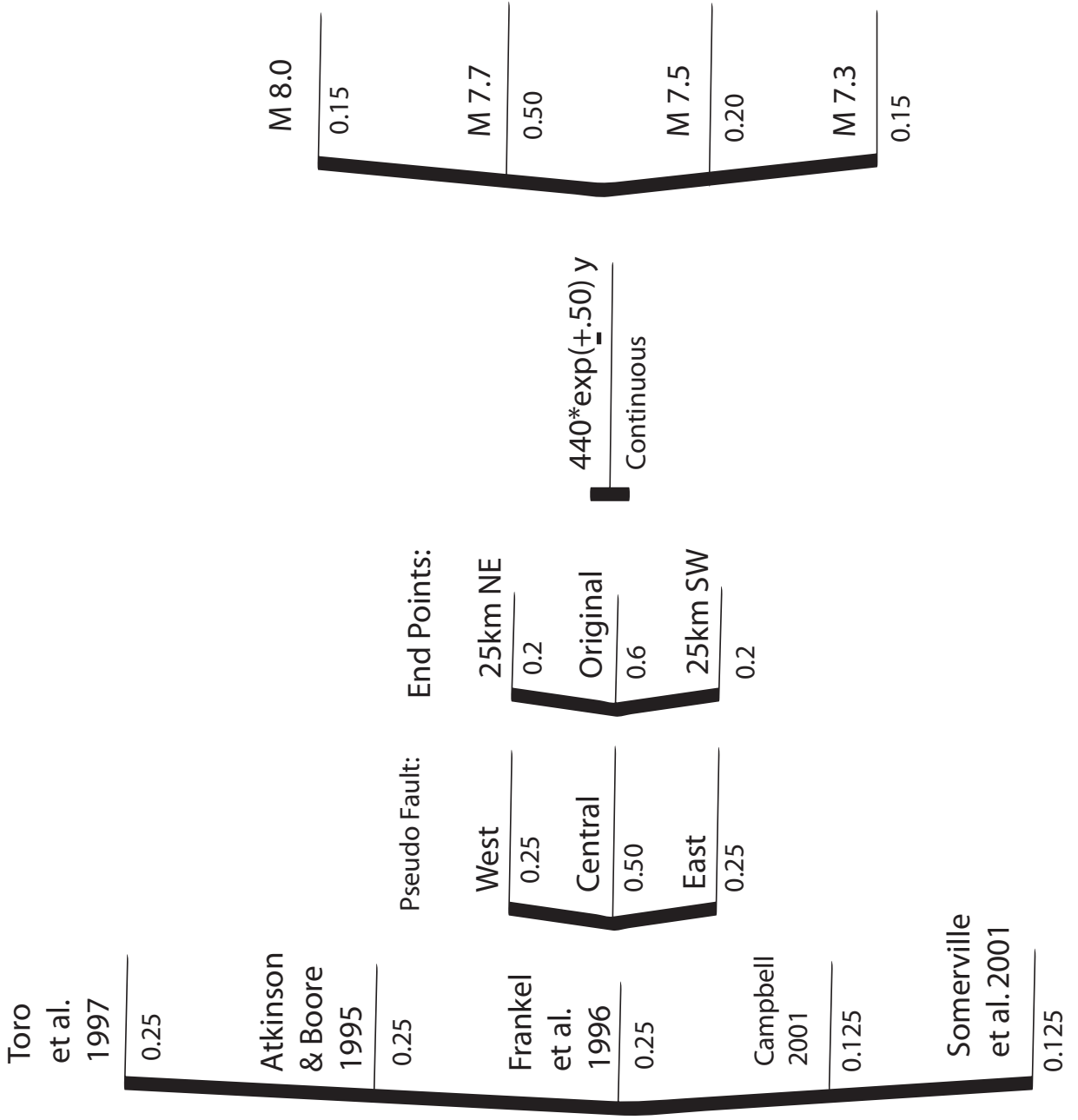
In the subdirectory NRCanal, there are additional **.hzdt** files for the national maps mean hazard curves. They have the naming convention of **natlhrppp.hzdt**. As before ppp represents the ground motion period.

All hazard curve files contain pairs of ground motion level and probability of exceedance. There is only one data pair per line but a variable number of entries depending on the ground motion type.

All deaggregation files contain triplets of distance, magnitude, and probability. Again there is only one data triplet per line. The number of entries is fixed at 130.

# CEUS New Madrid Logic Tree

Attenuation | Rupture | Fault Length | Recurrence | Characteristic  
 Relation | Model | Variability | Interval | Magnitude



# SRS Charleston Logic Tree

Attenuation | 1886 | Recurrence | Characteristic  
 Relation | Rupture Model | Interval | Magnitude

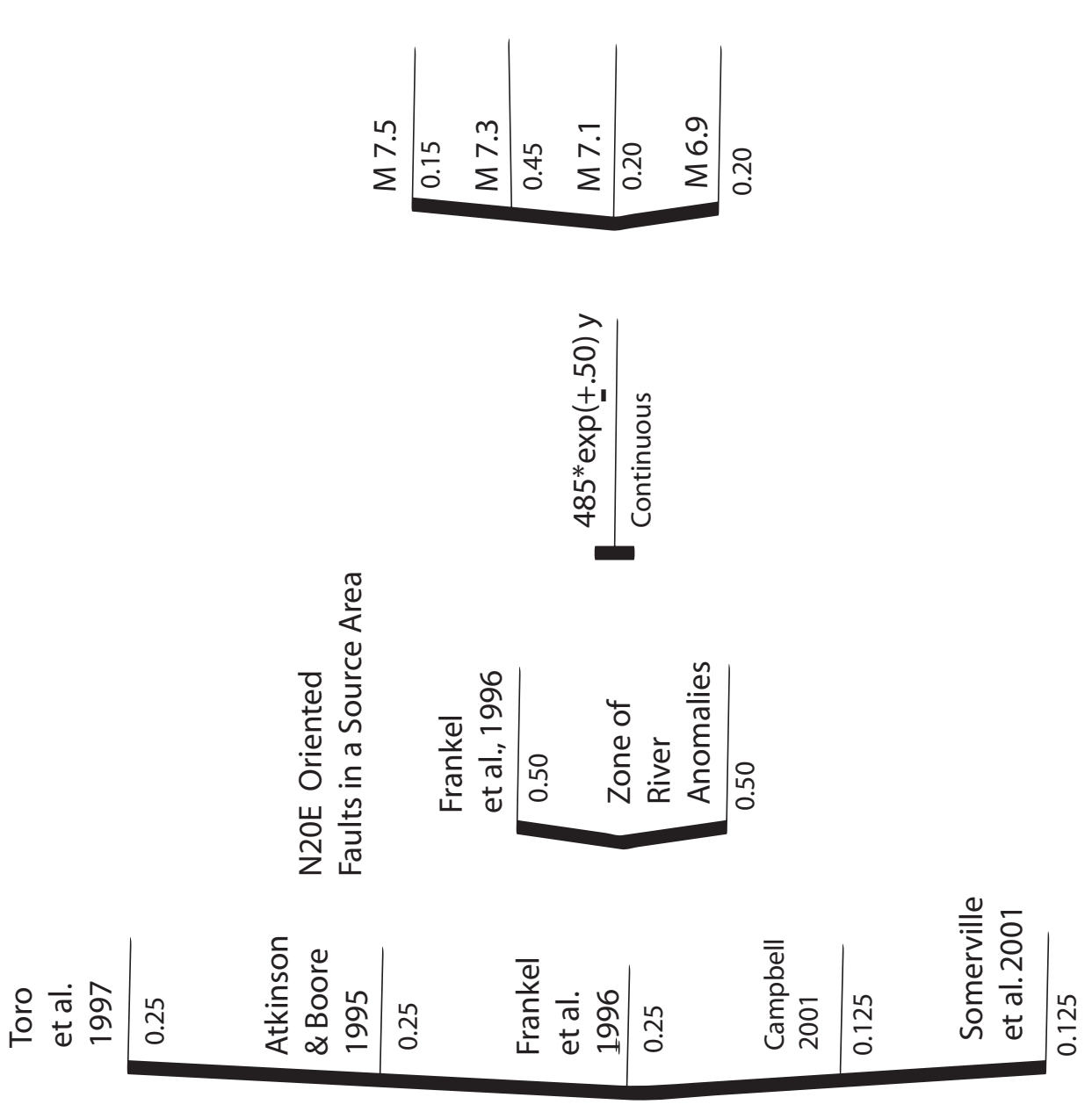


Figure 2

# CEUS Smoothed Seismicity Logic Tree

Attenuation | Catalog | Regional | Seismicity | Smoothing | Mblg -> Mw  
 Relation | Resampling | Maximum | Model | Distance | Conversion  
 | (activity & | Magnitude |  
 | b-value ) |

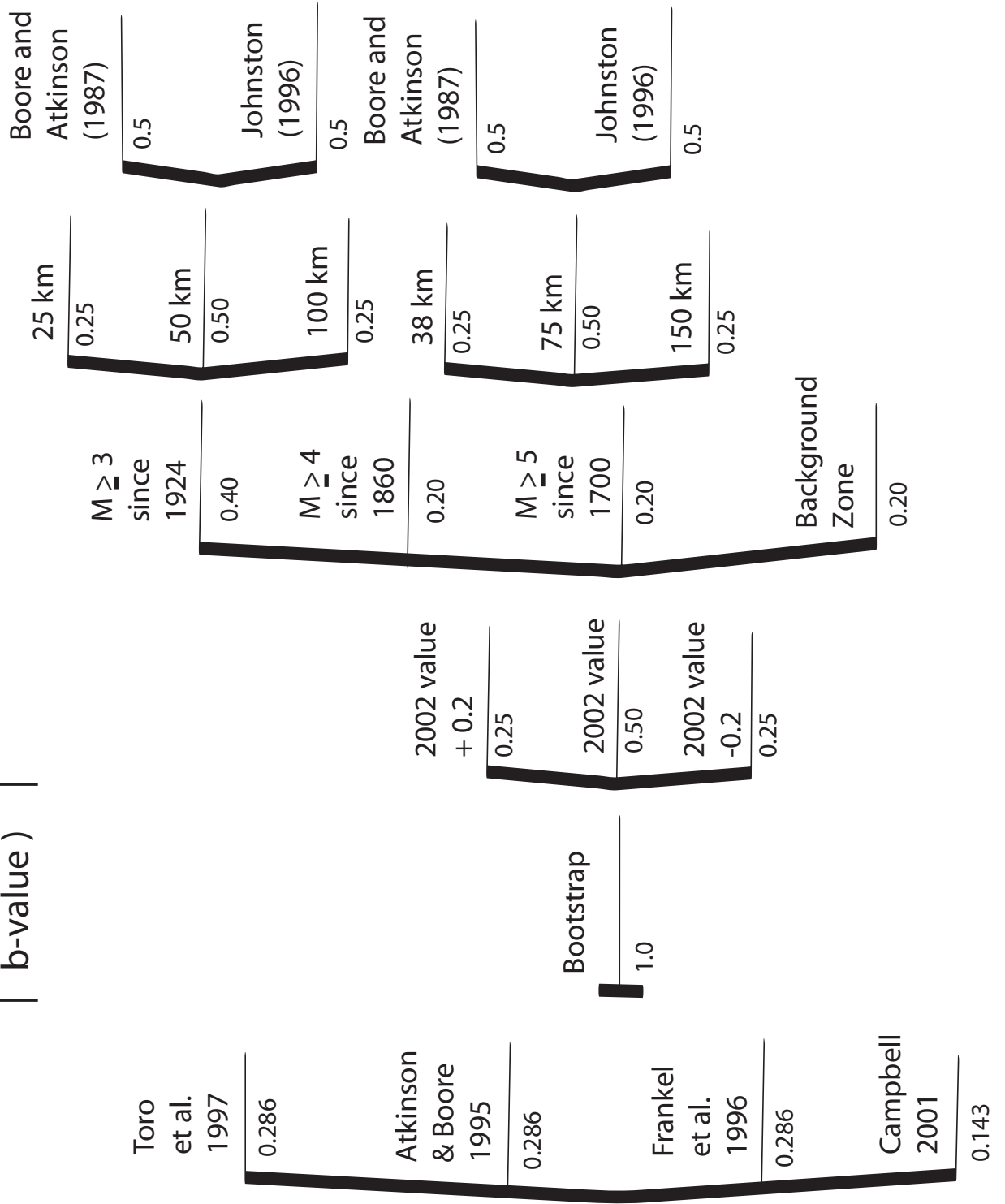


Figure 3

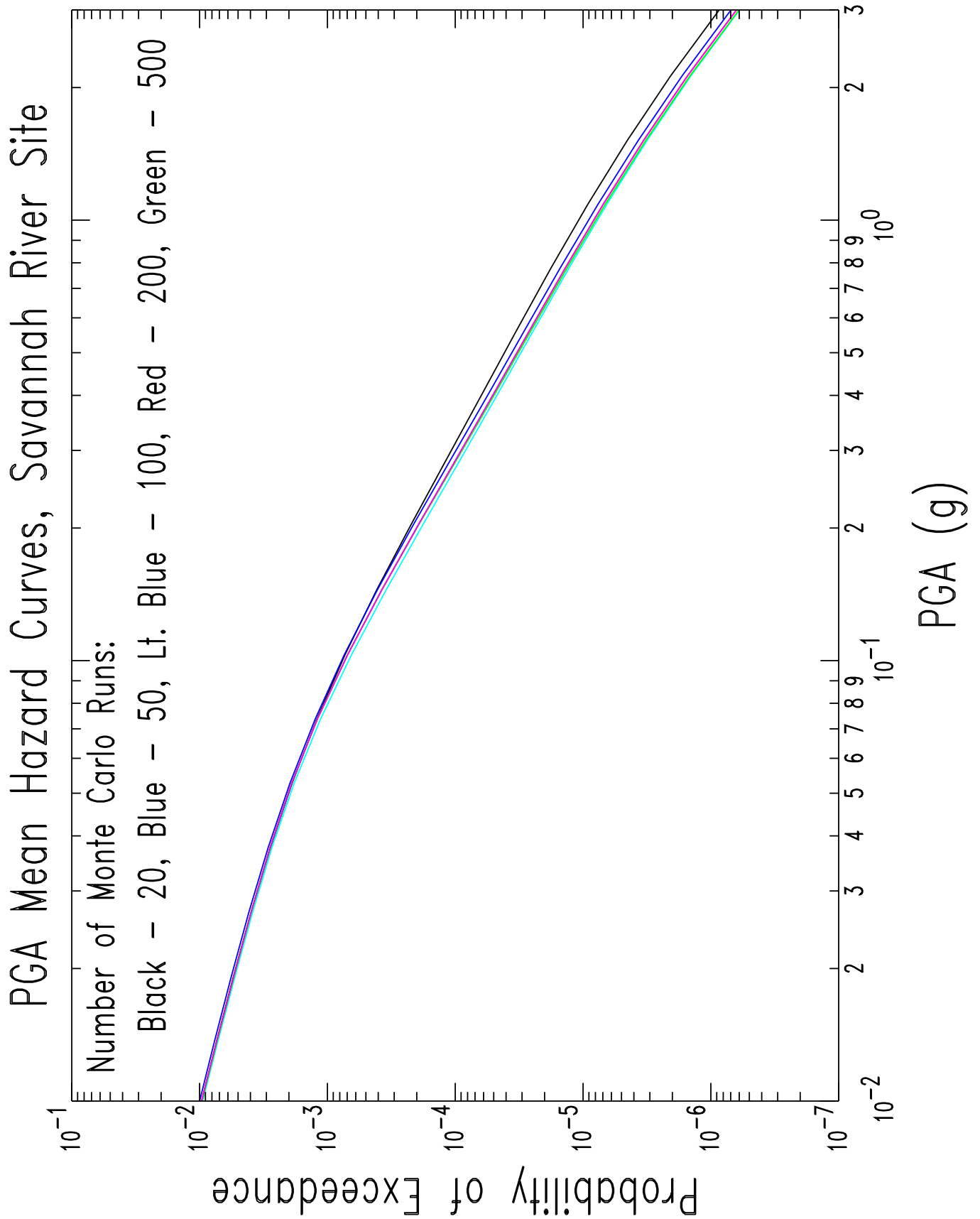


Figure 4



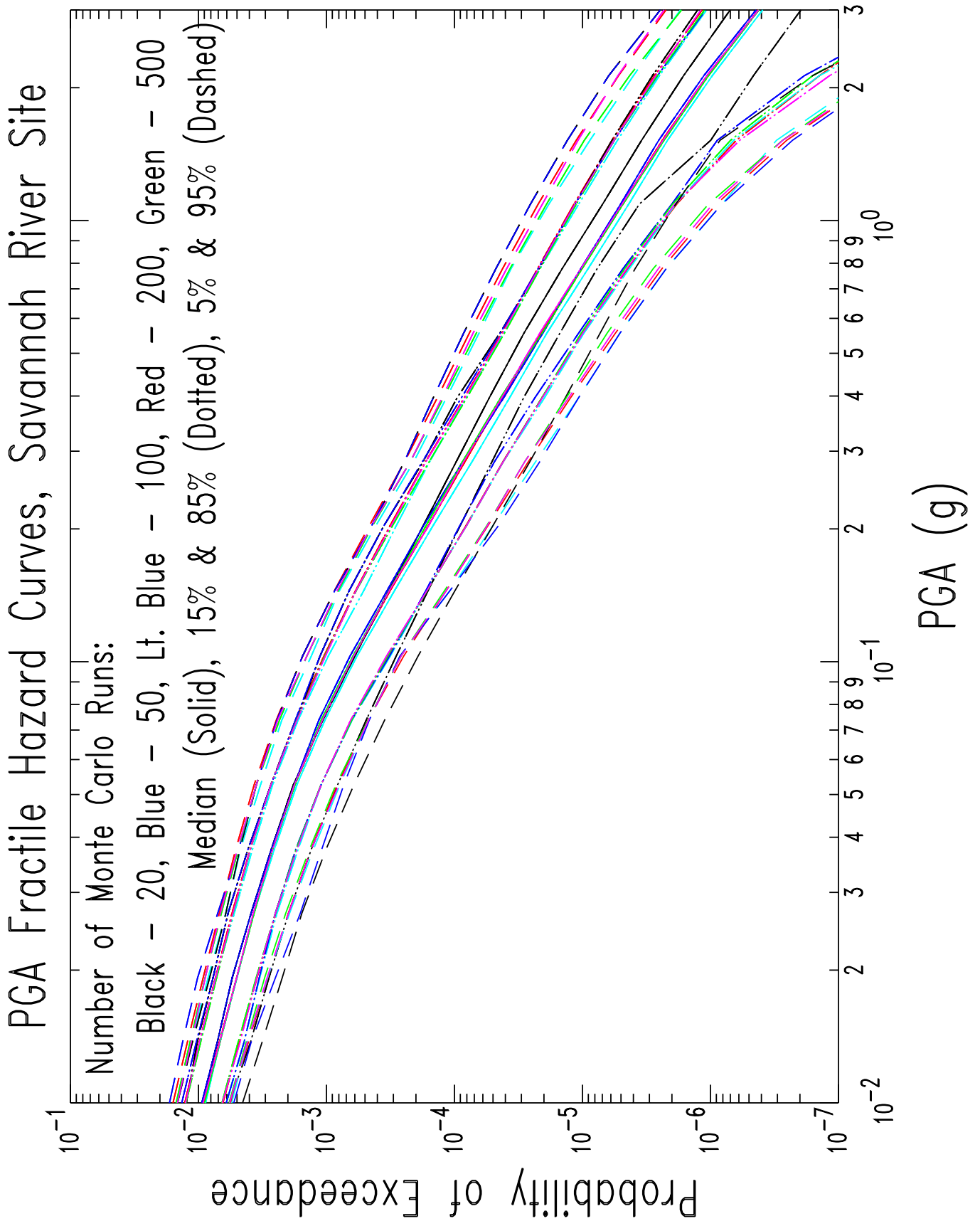


Figure 5

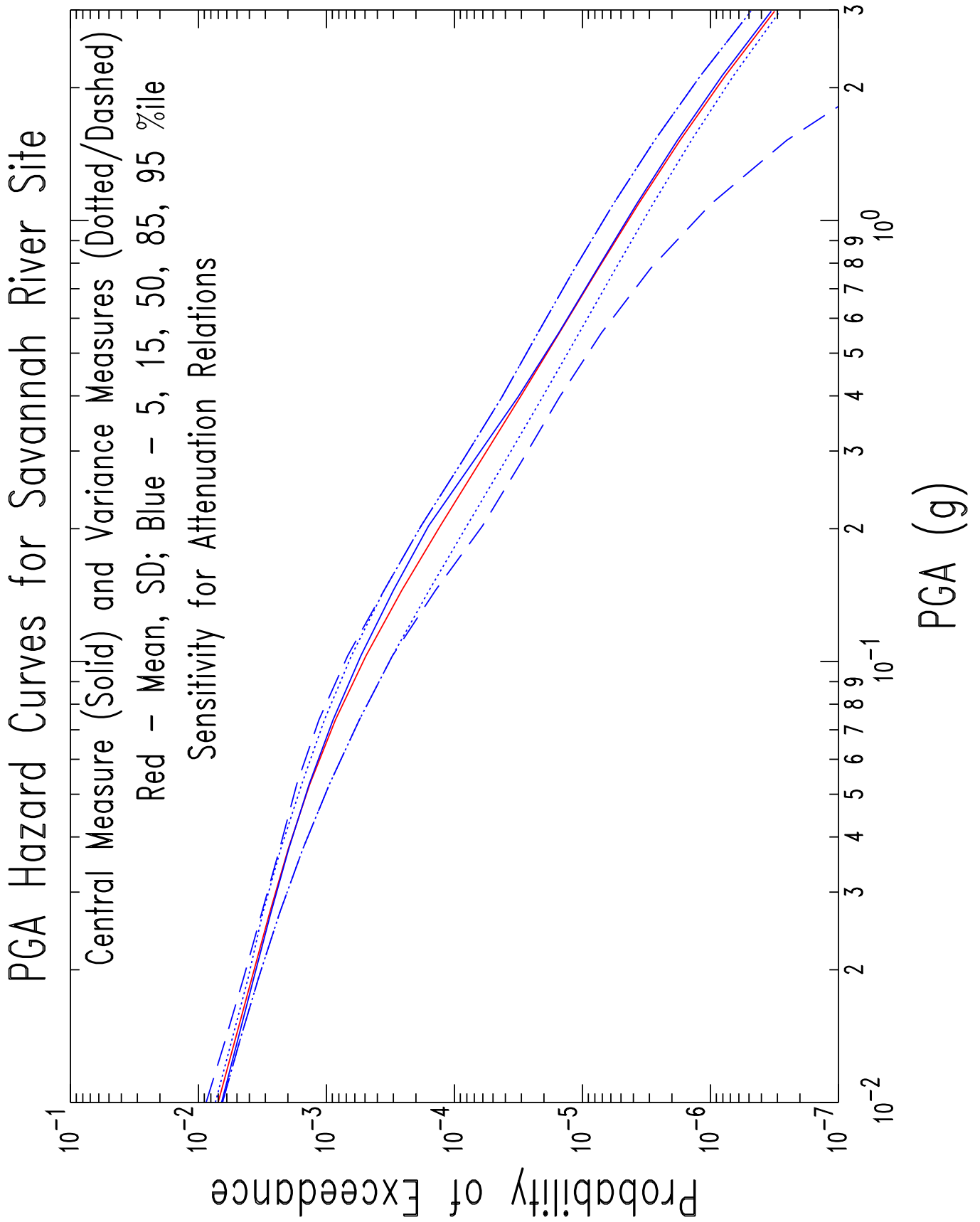


Figure 6

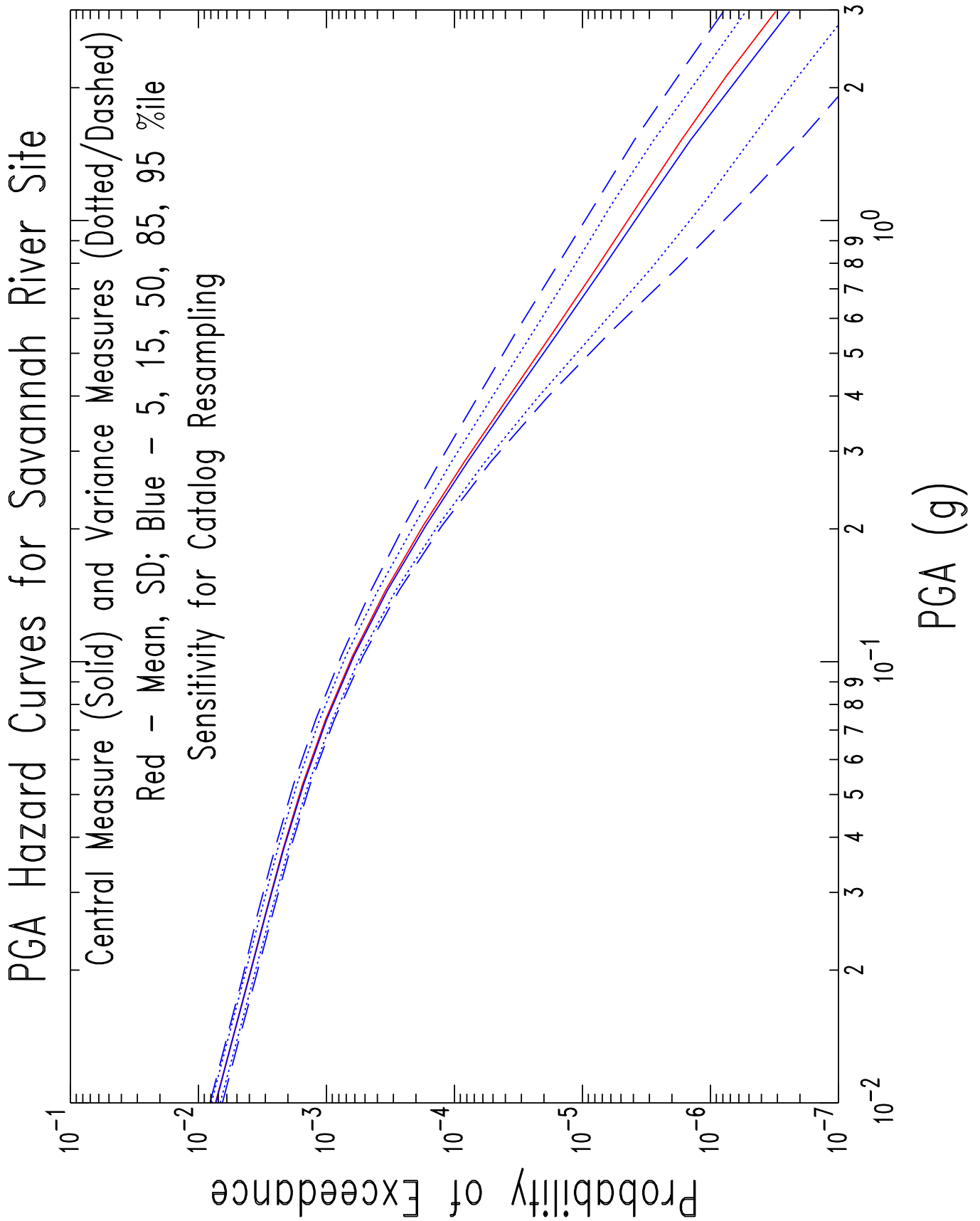


Figure 7

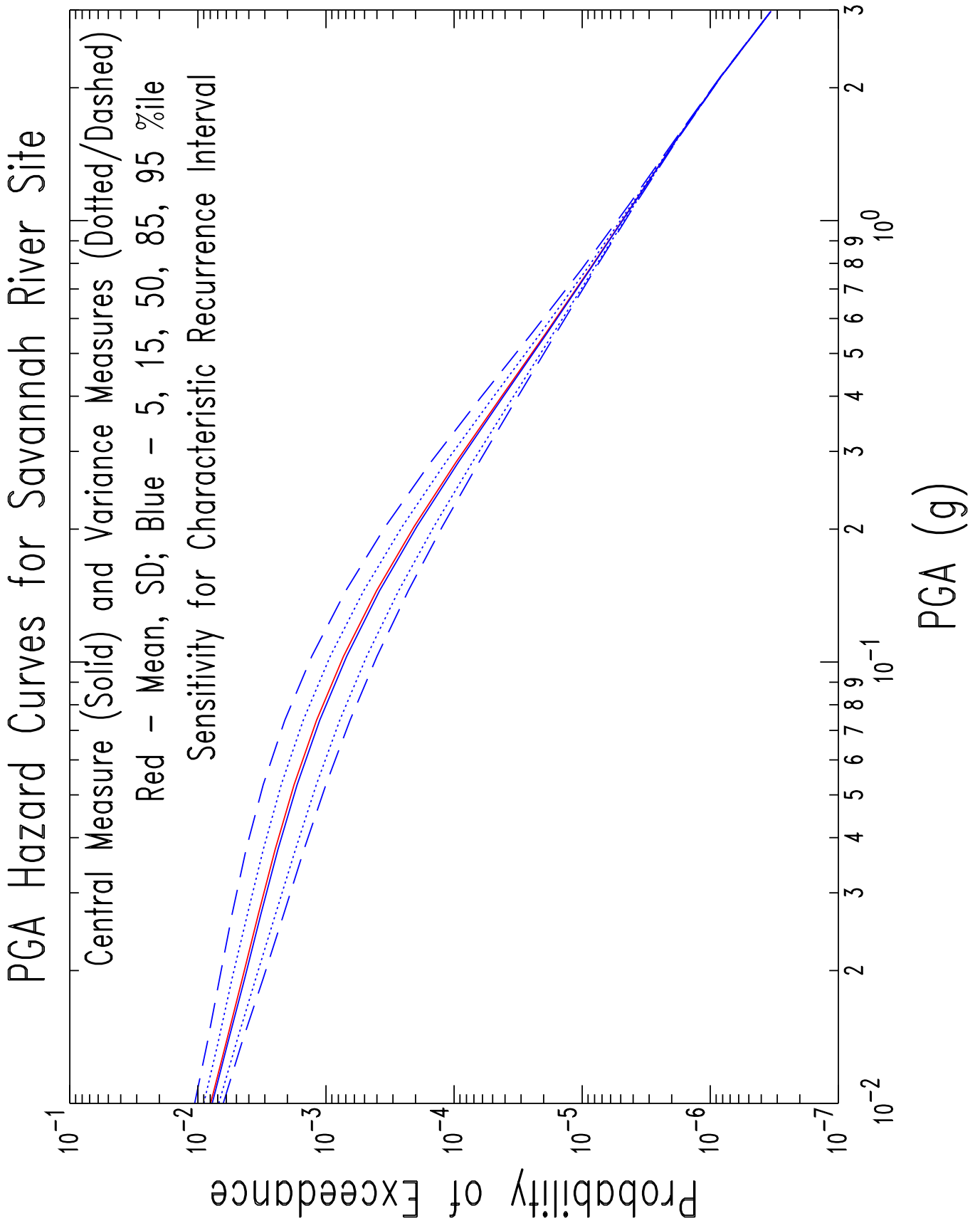


Figure 8

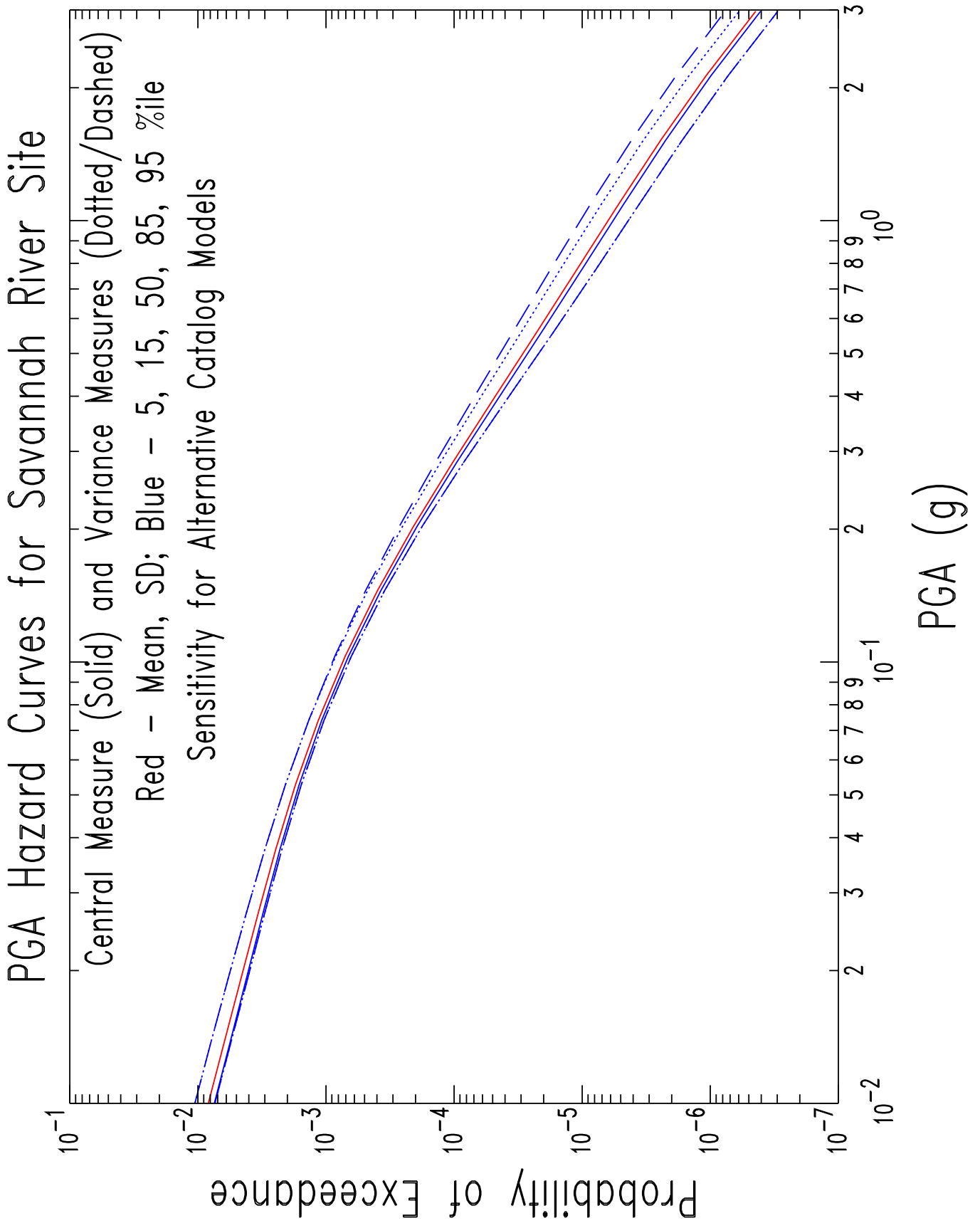


Figure 9

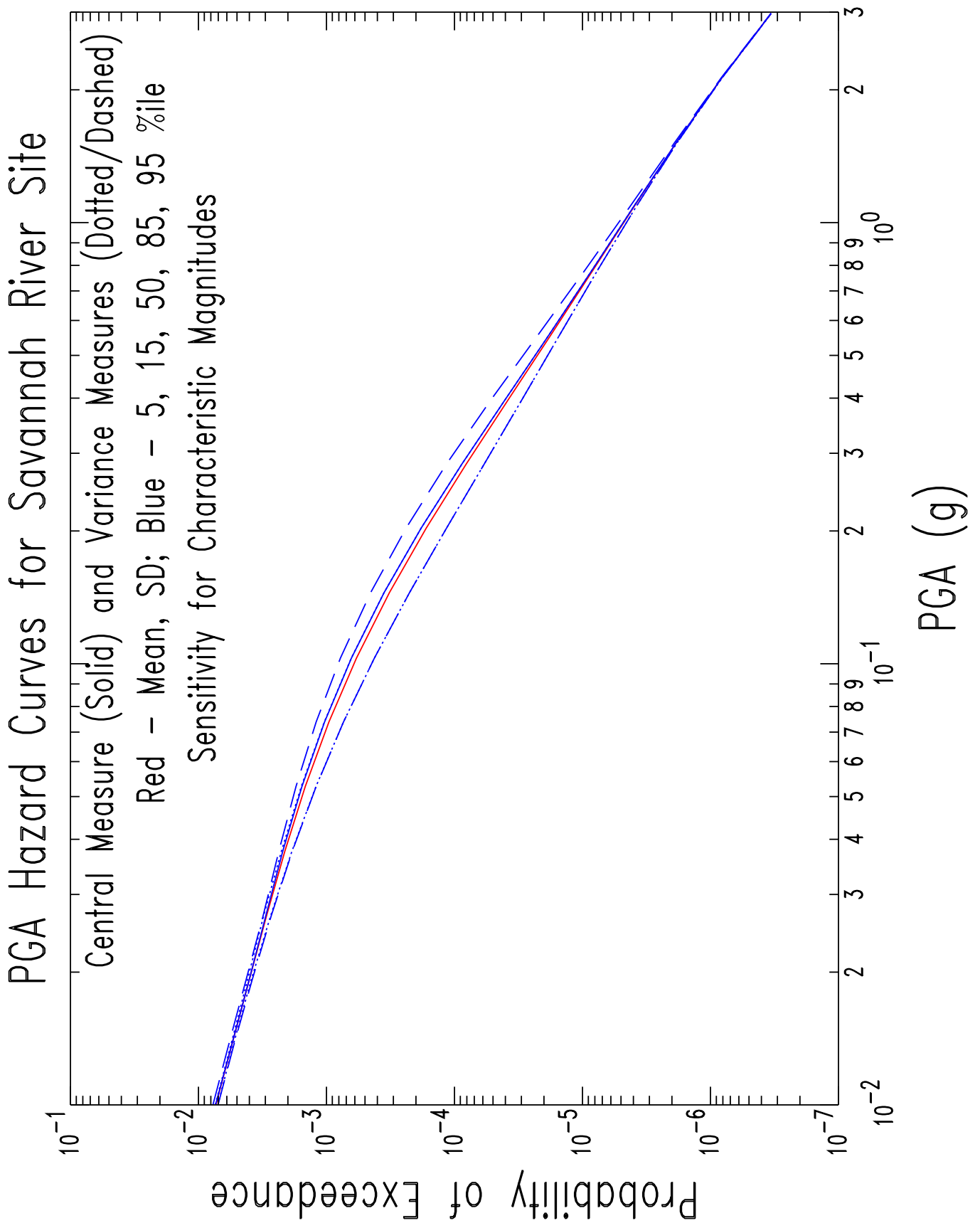


Figure 10

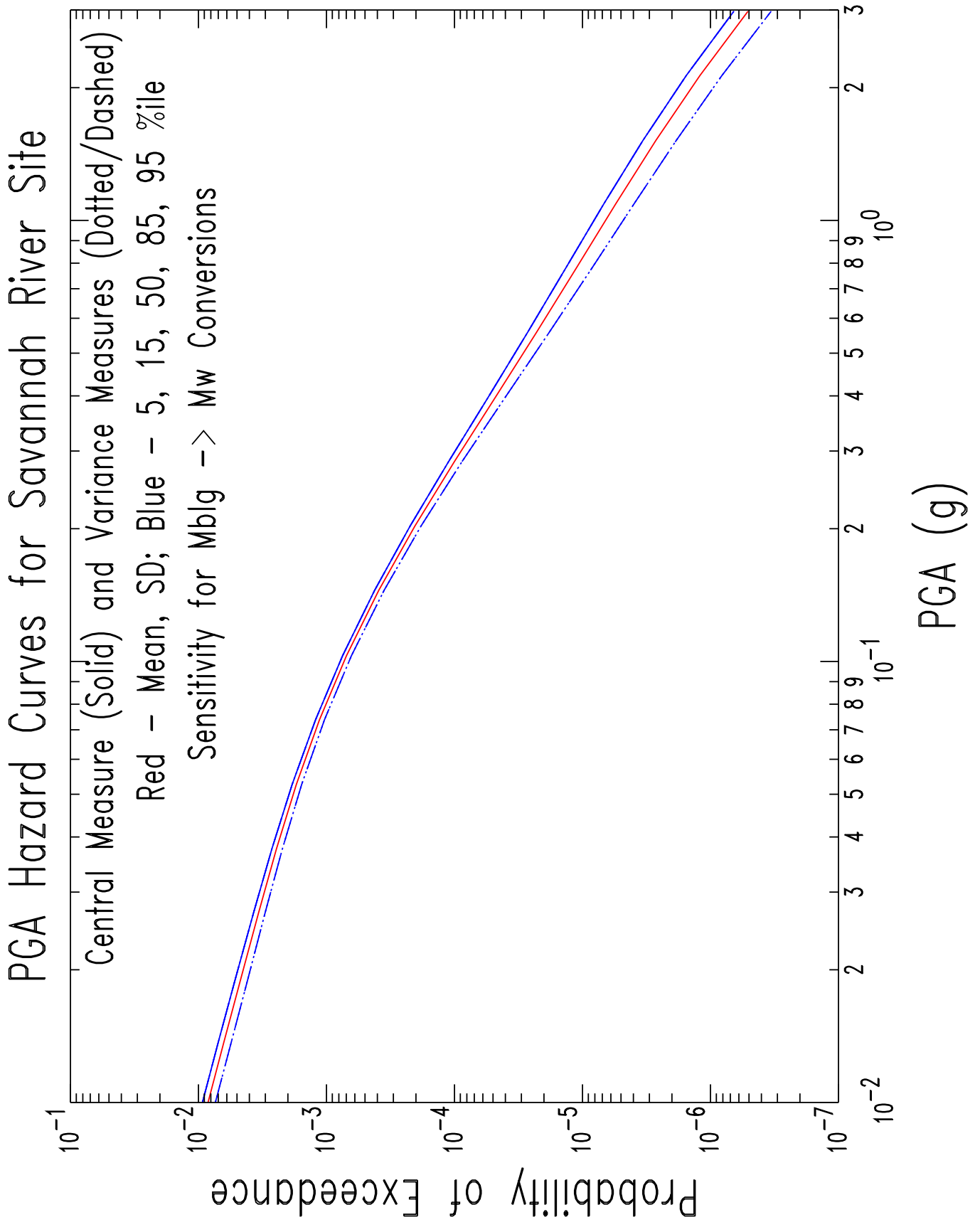


Figure 11

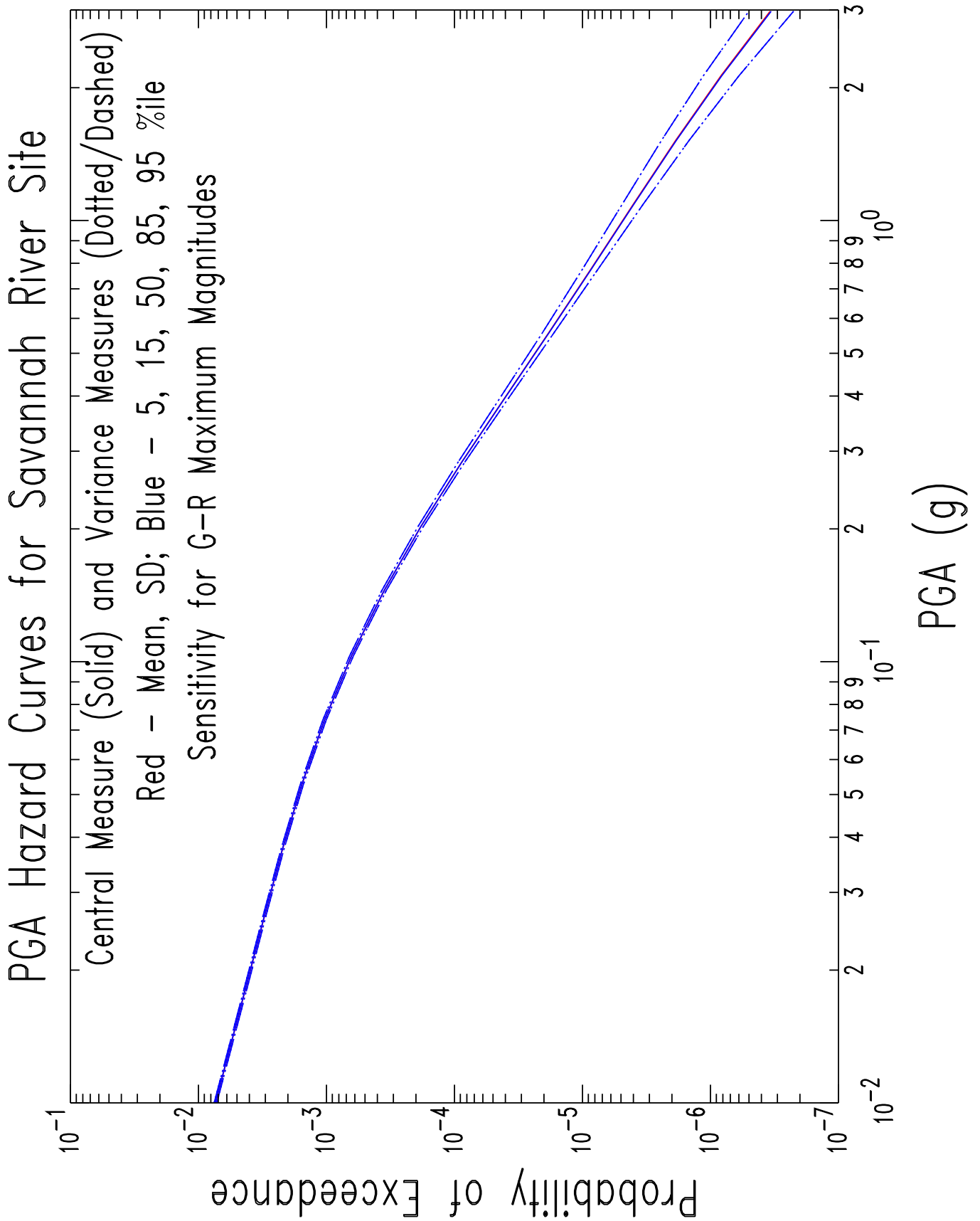


Figure 12



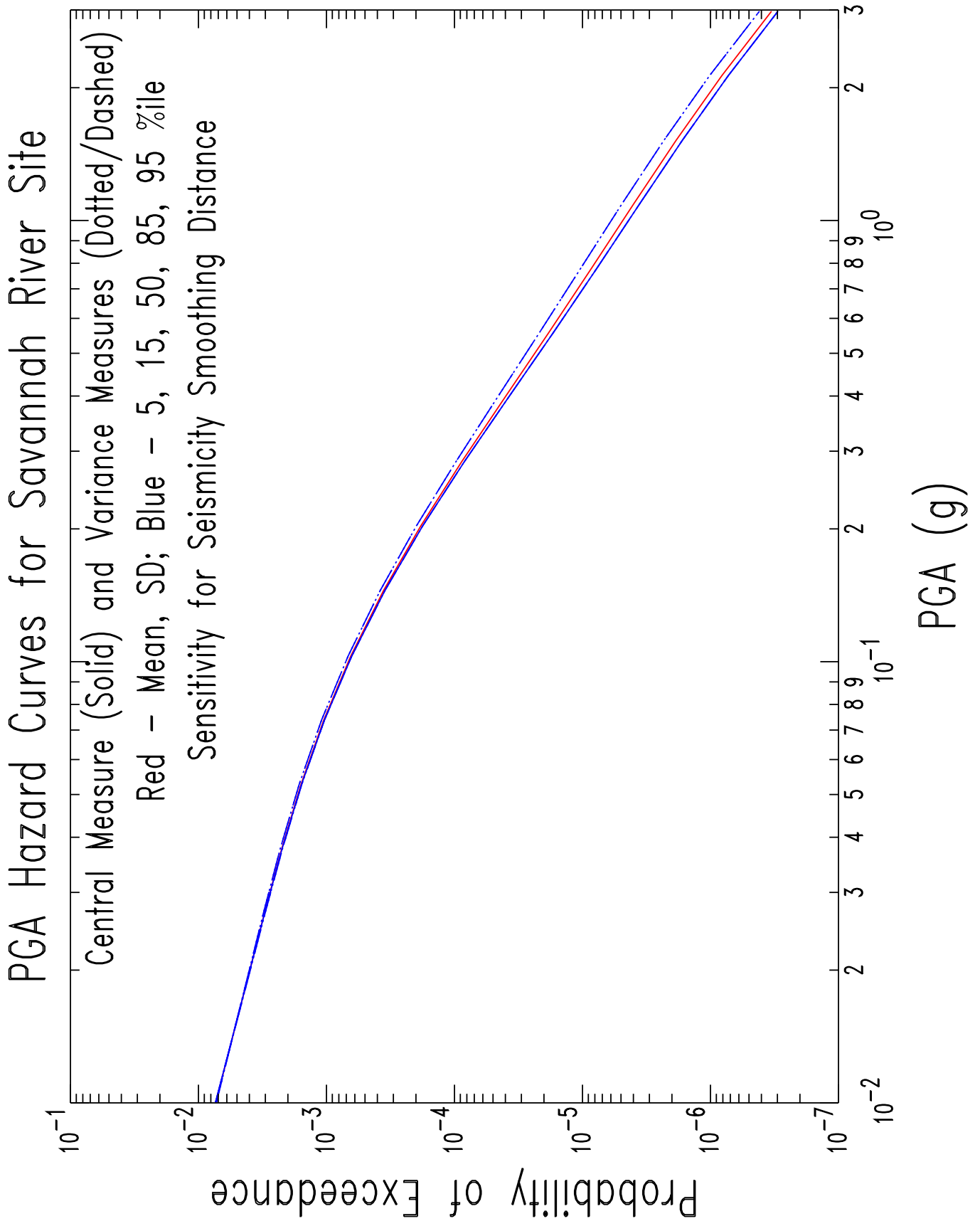


Figure 13

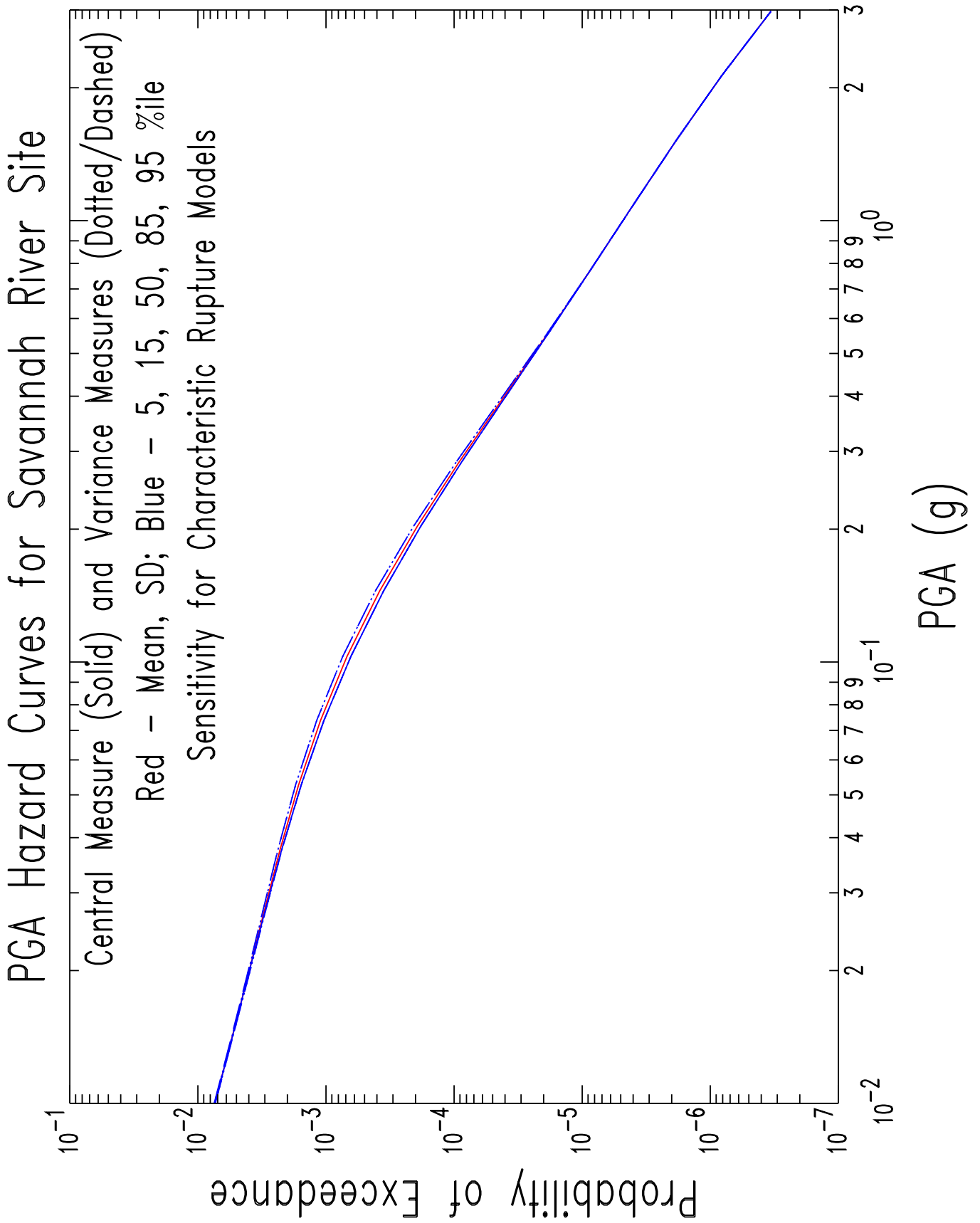


Figure 14

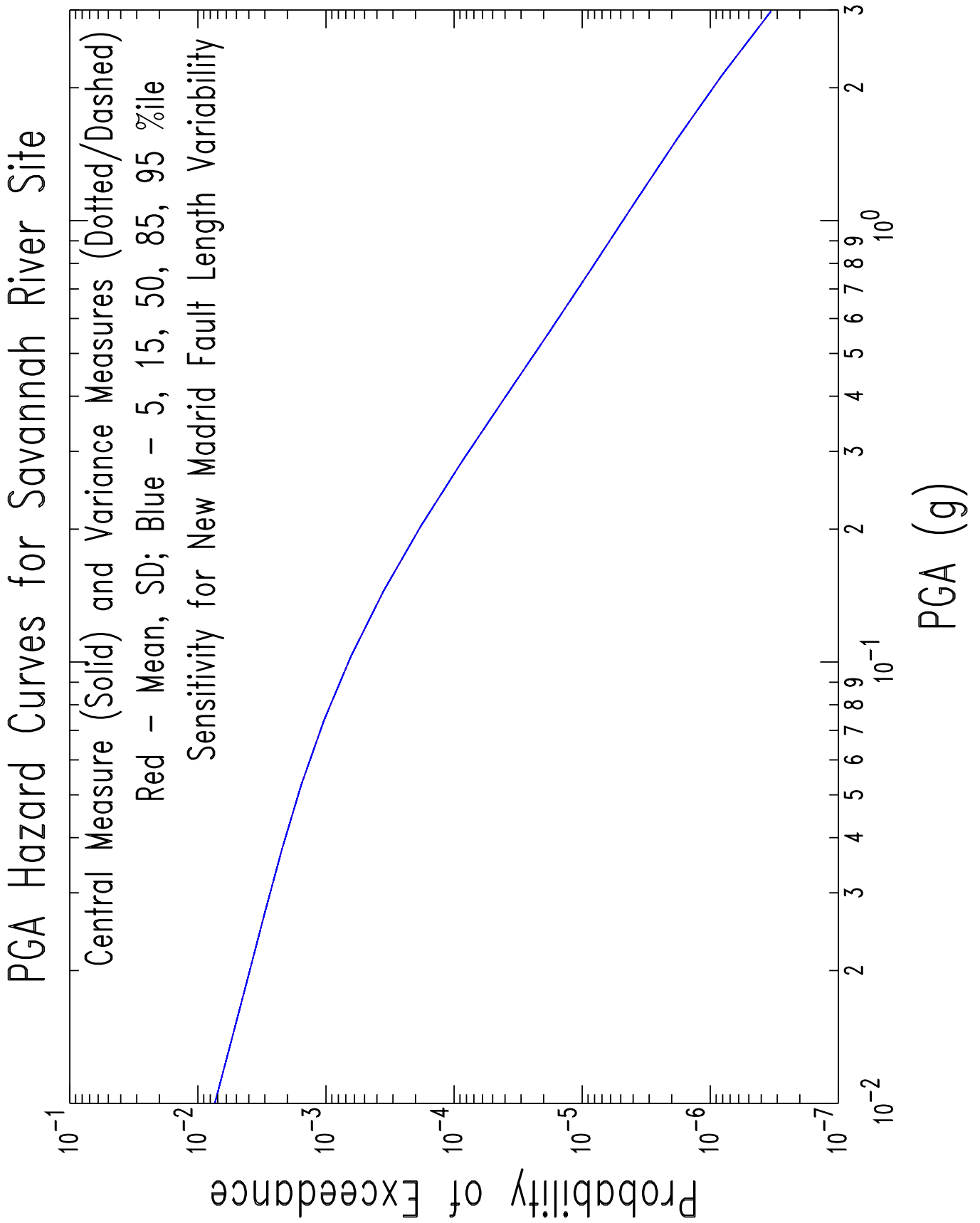


Figure 15

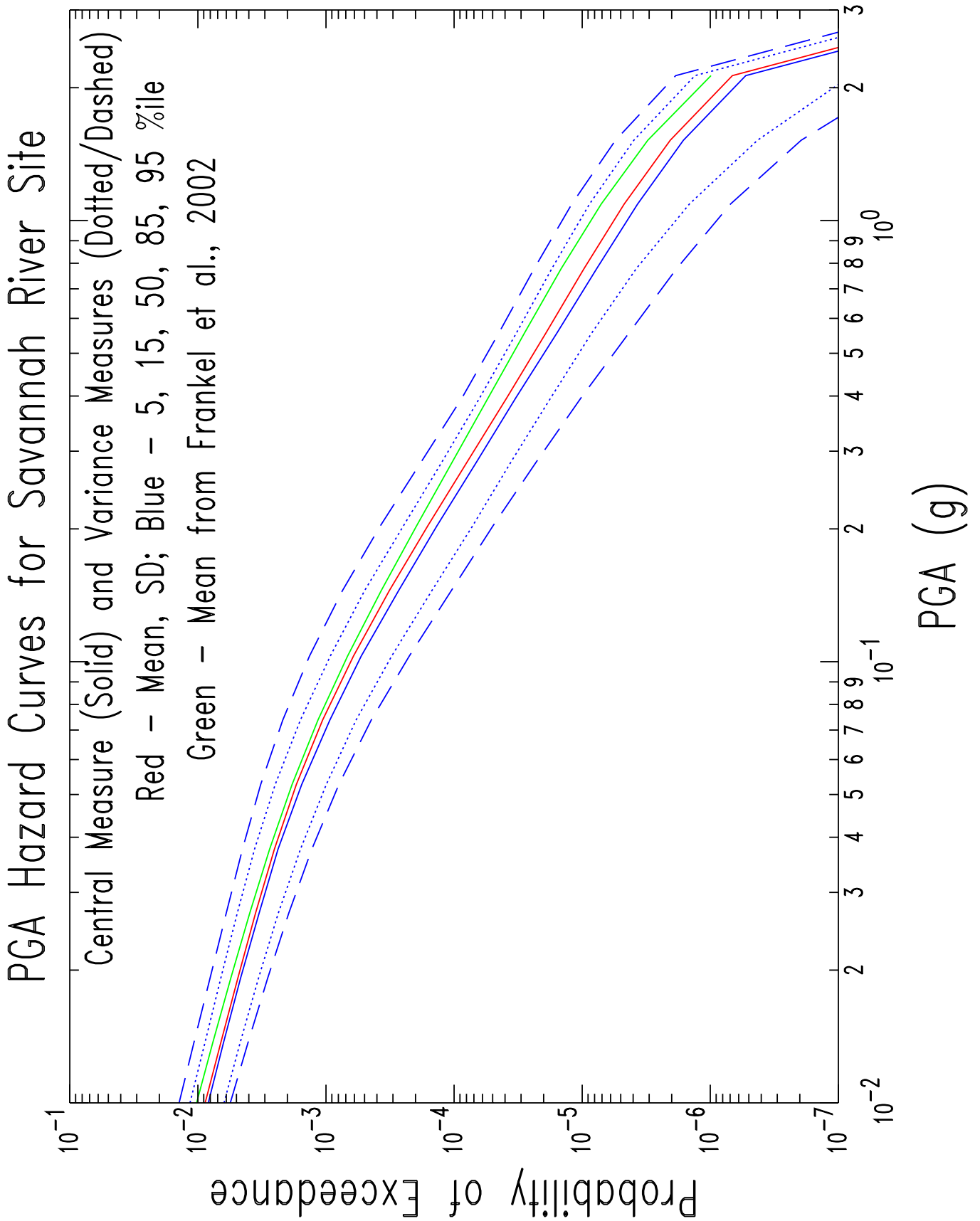


Figure 16

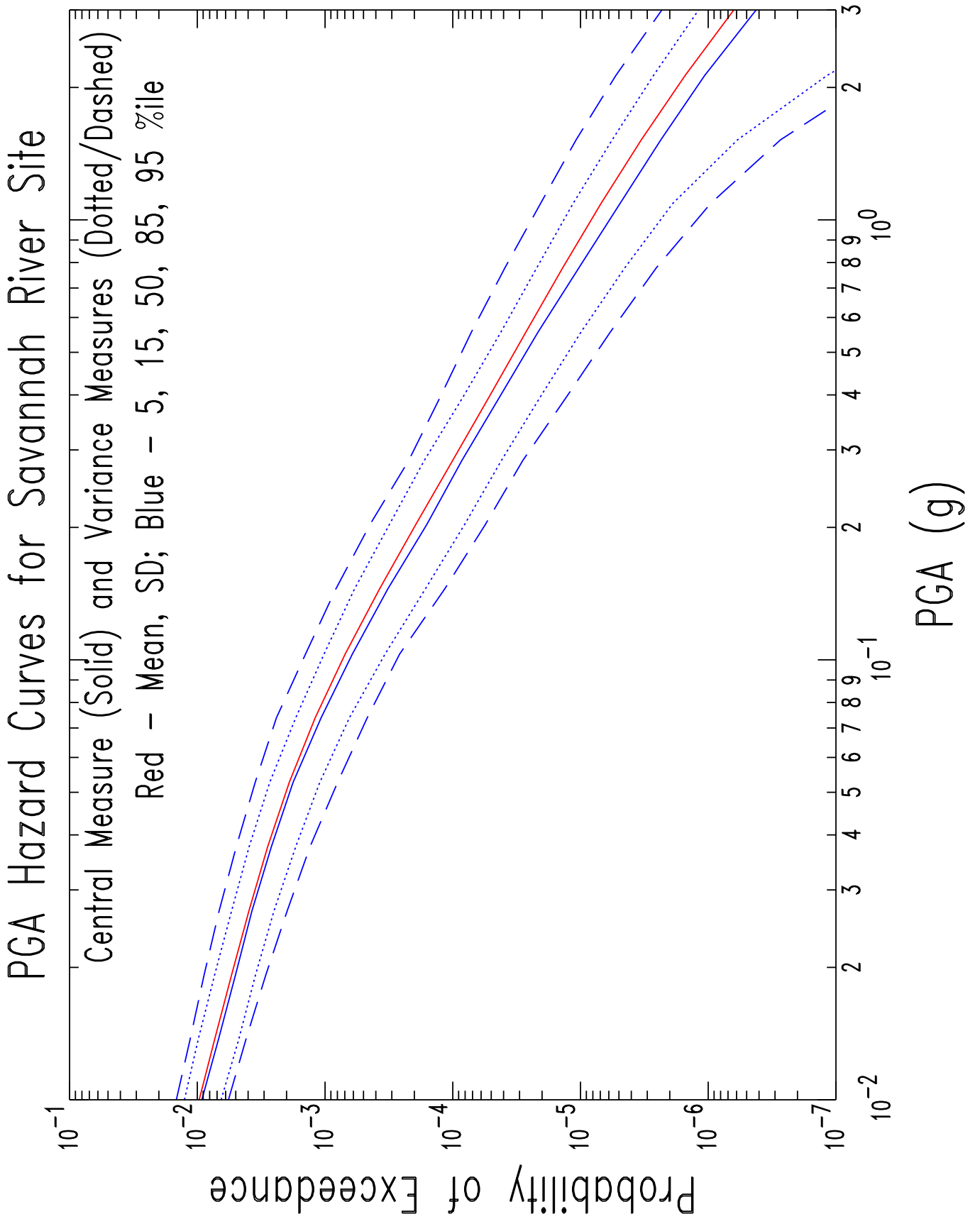


Figure 17

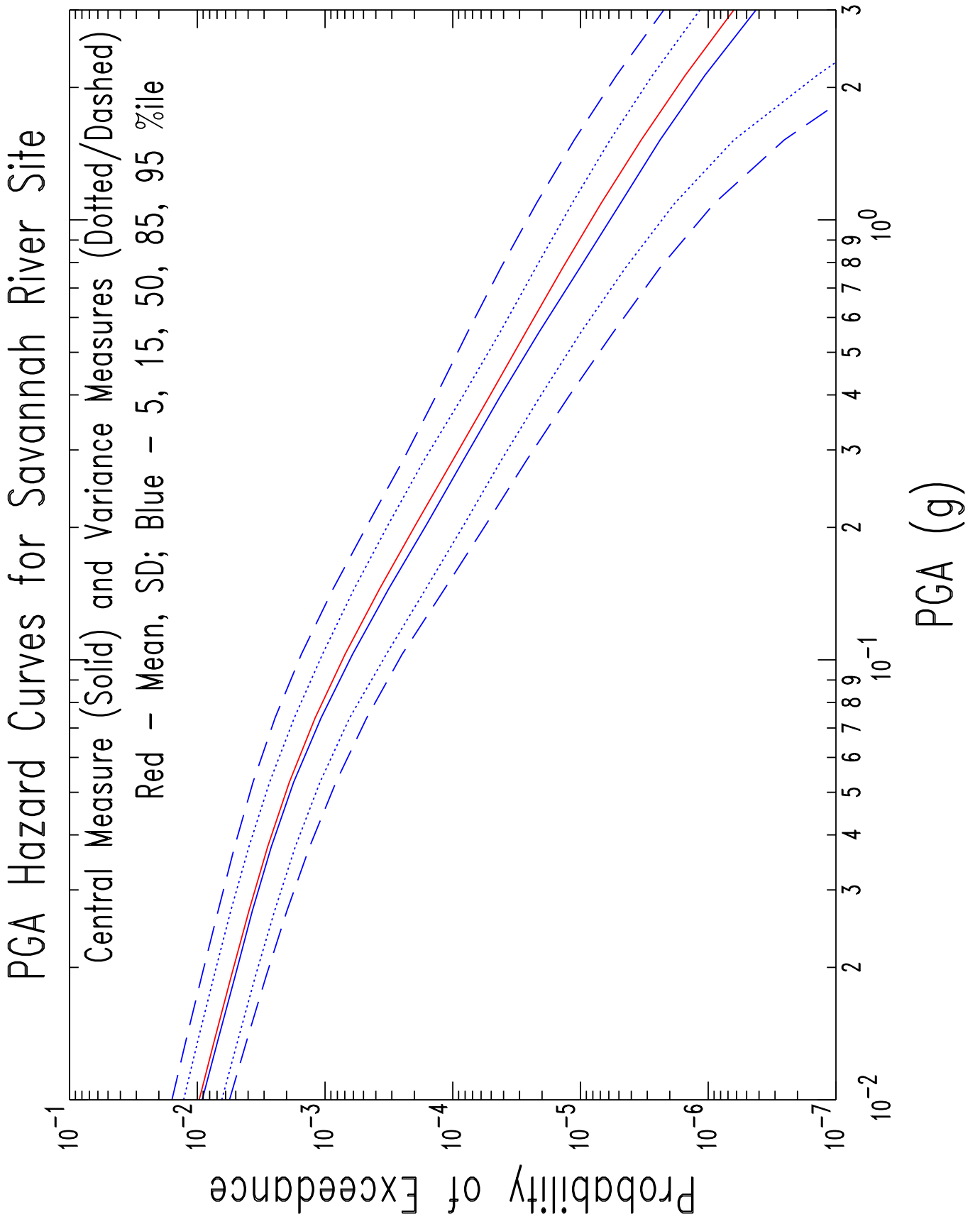


Figure 18

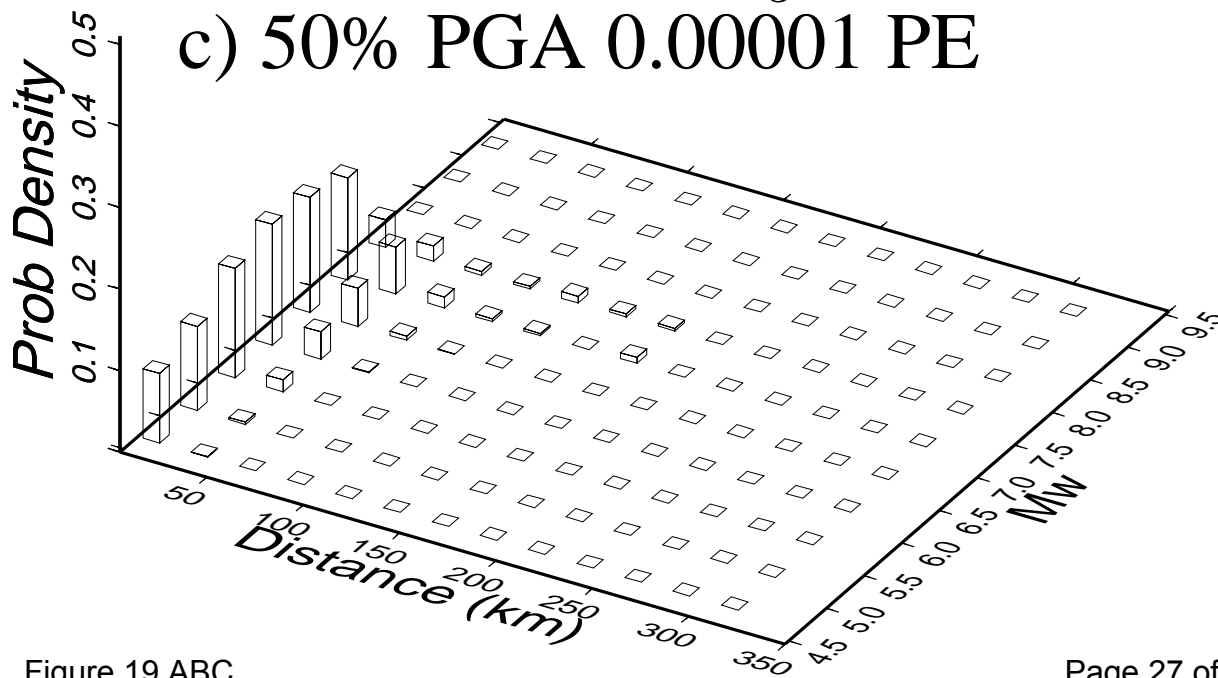
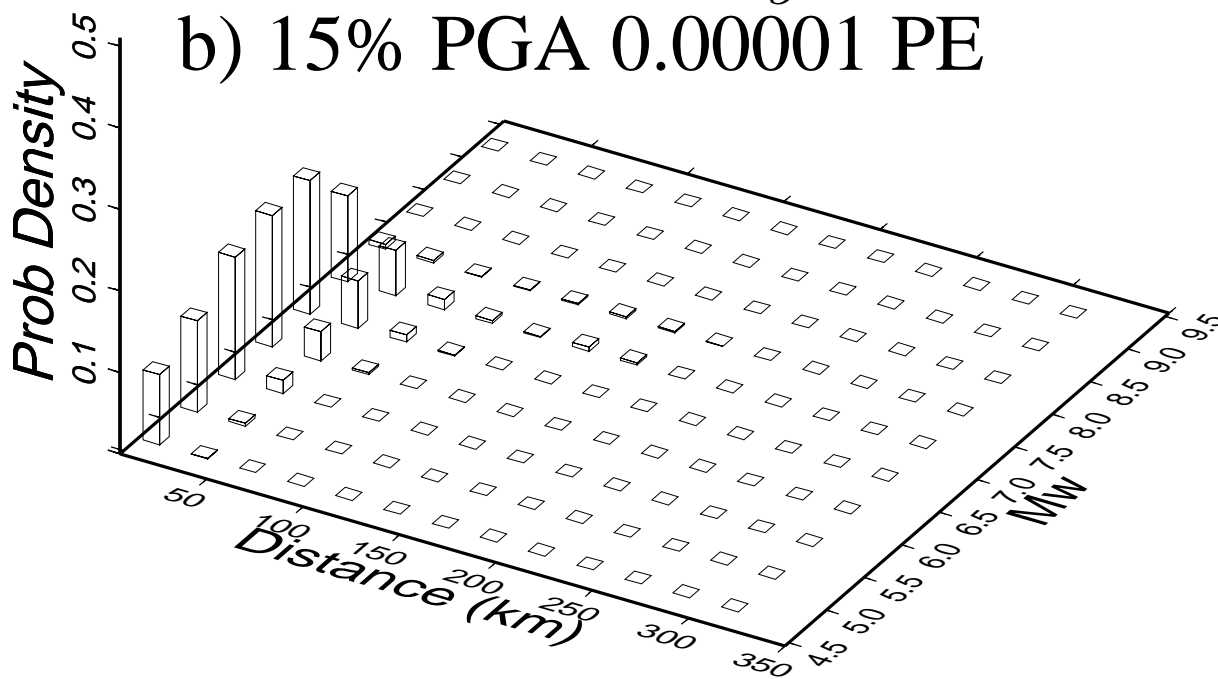
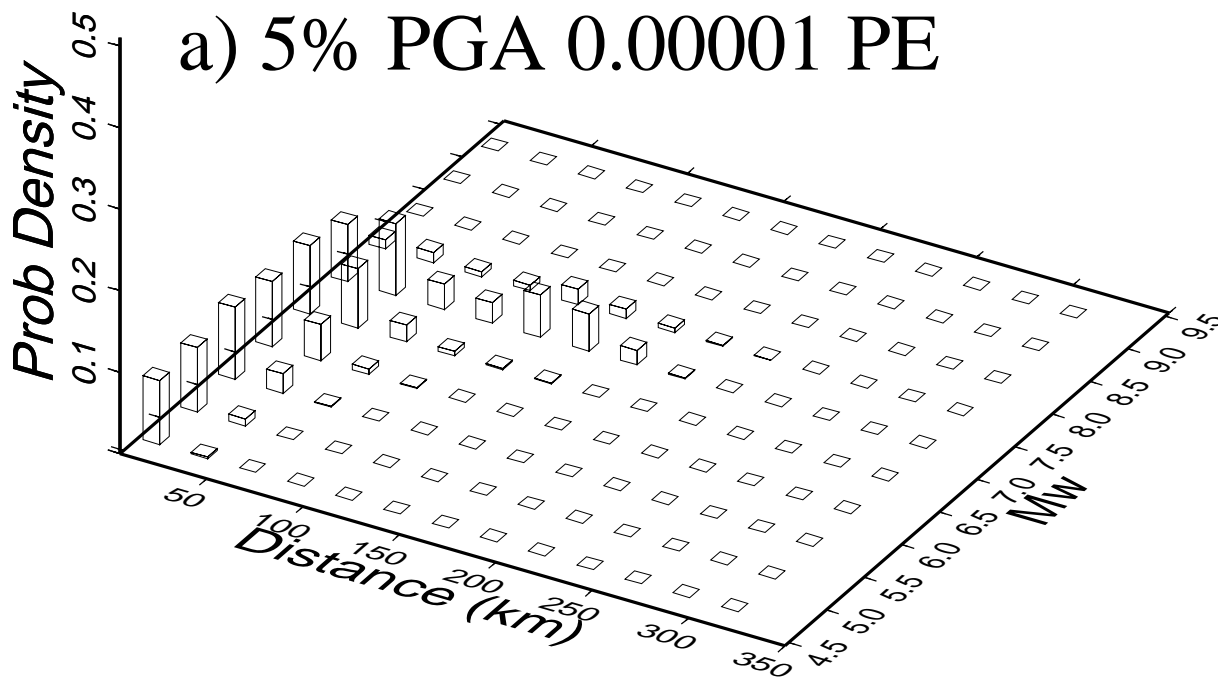
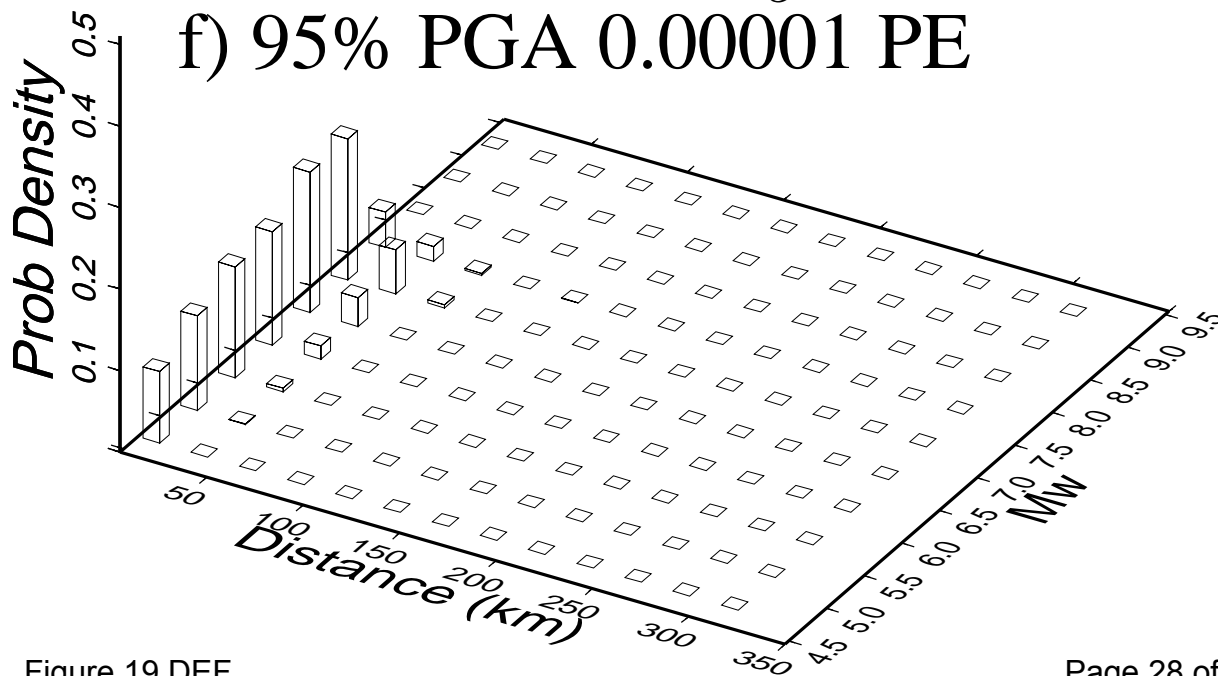
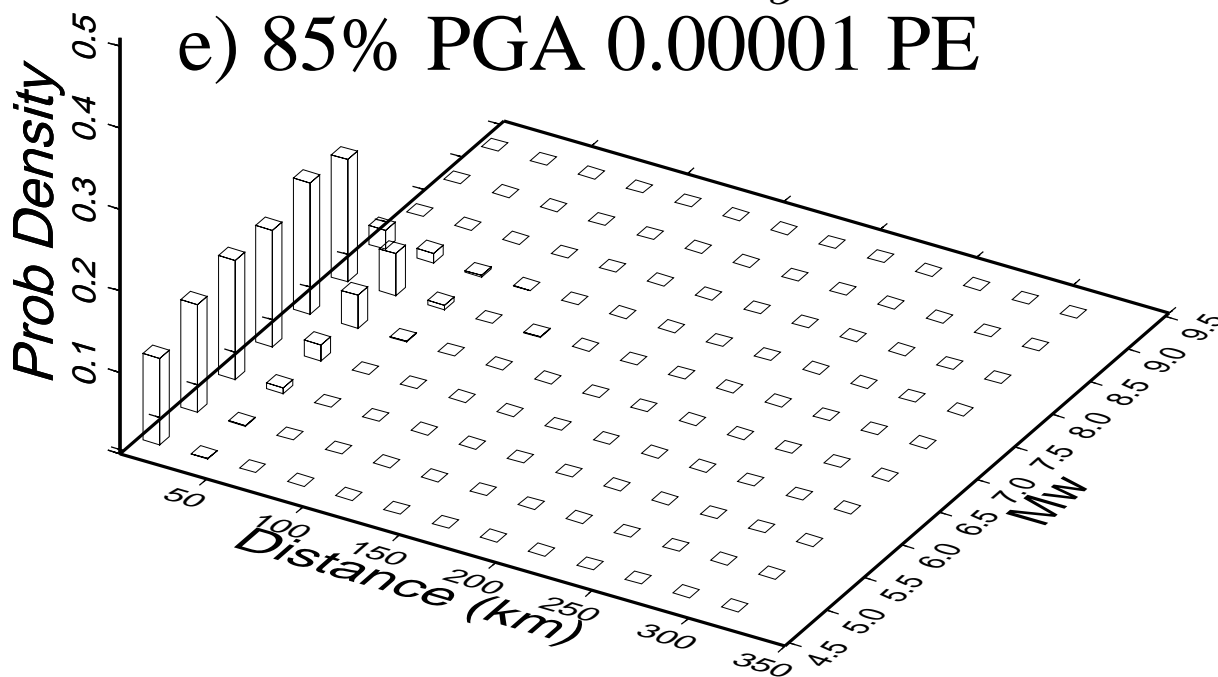
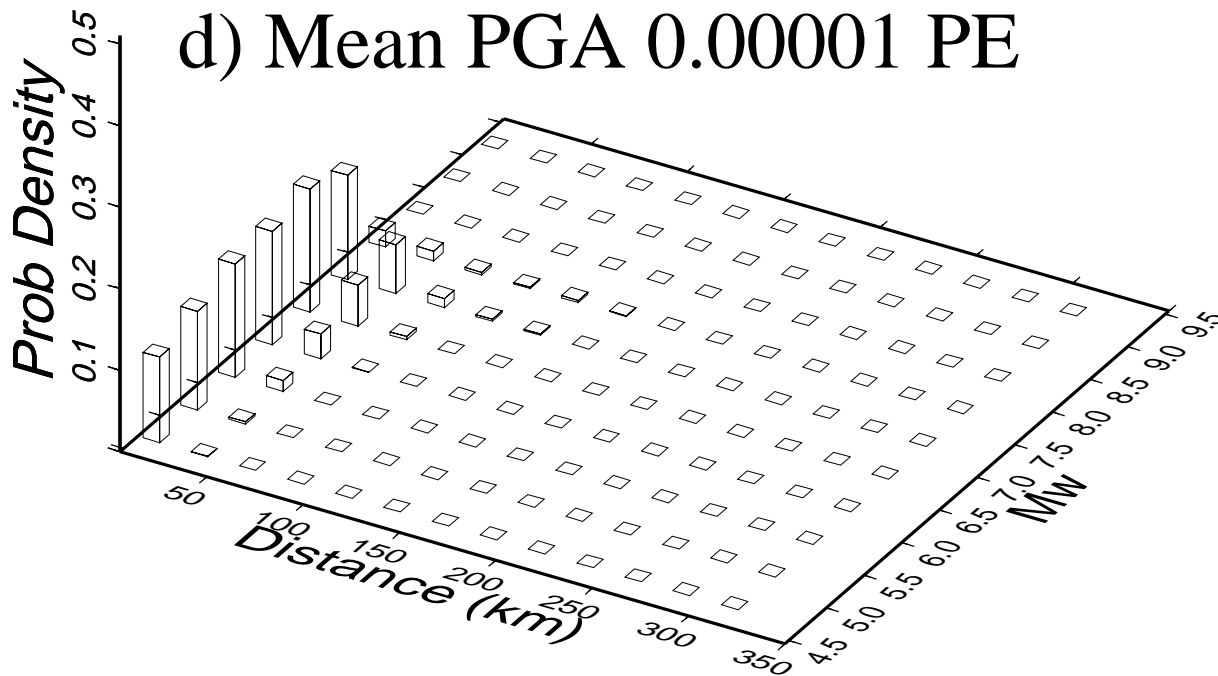


Figure 19 ABC





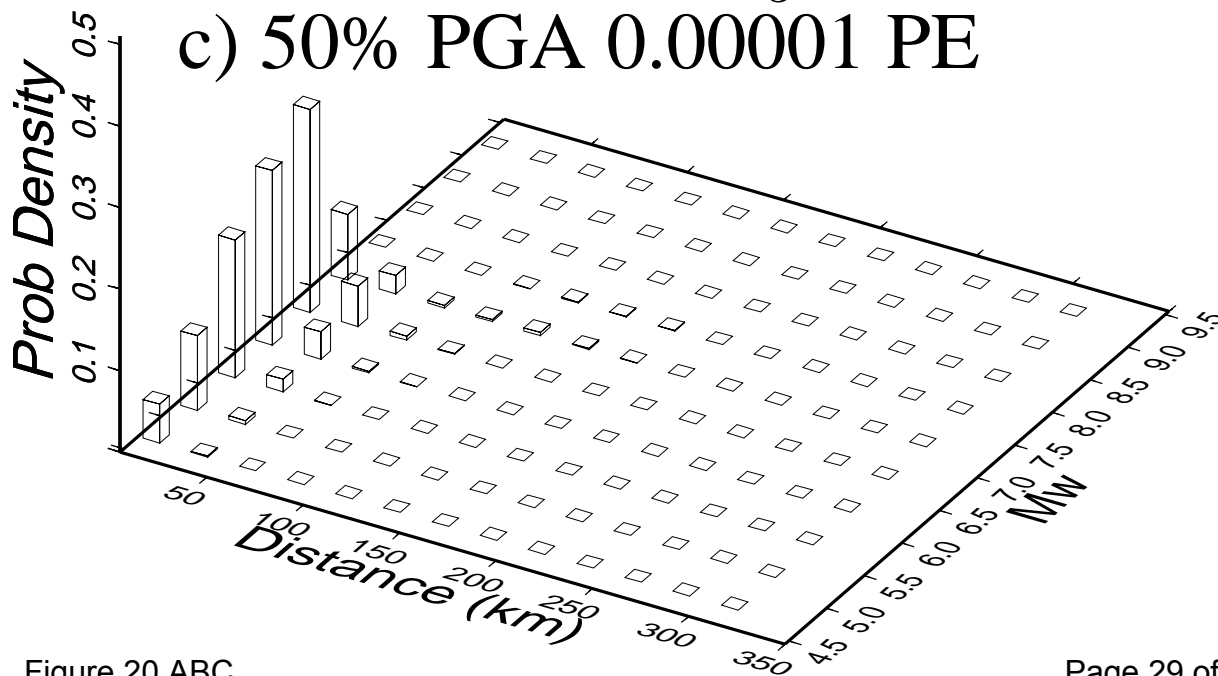
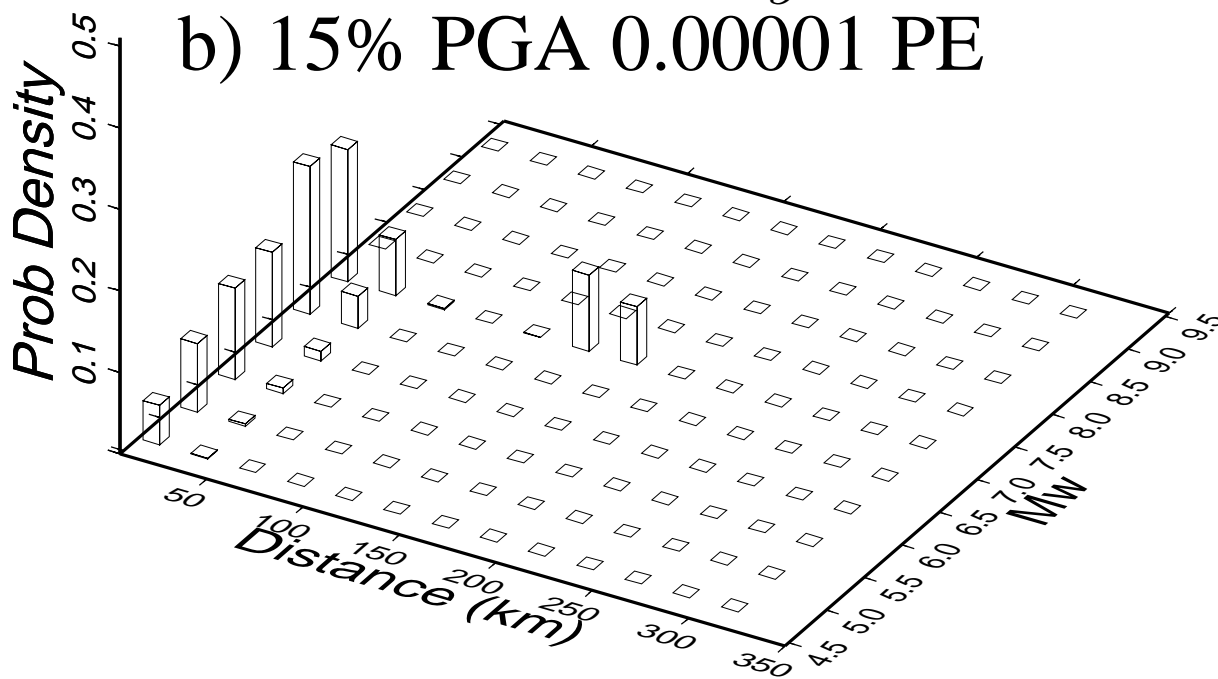
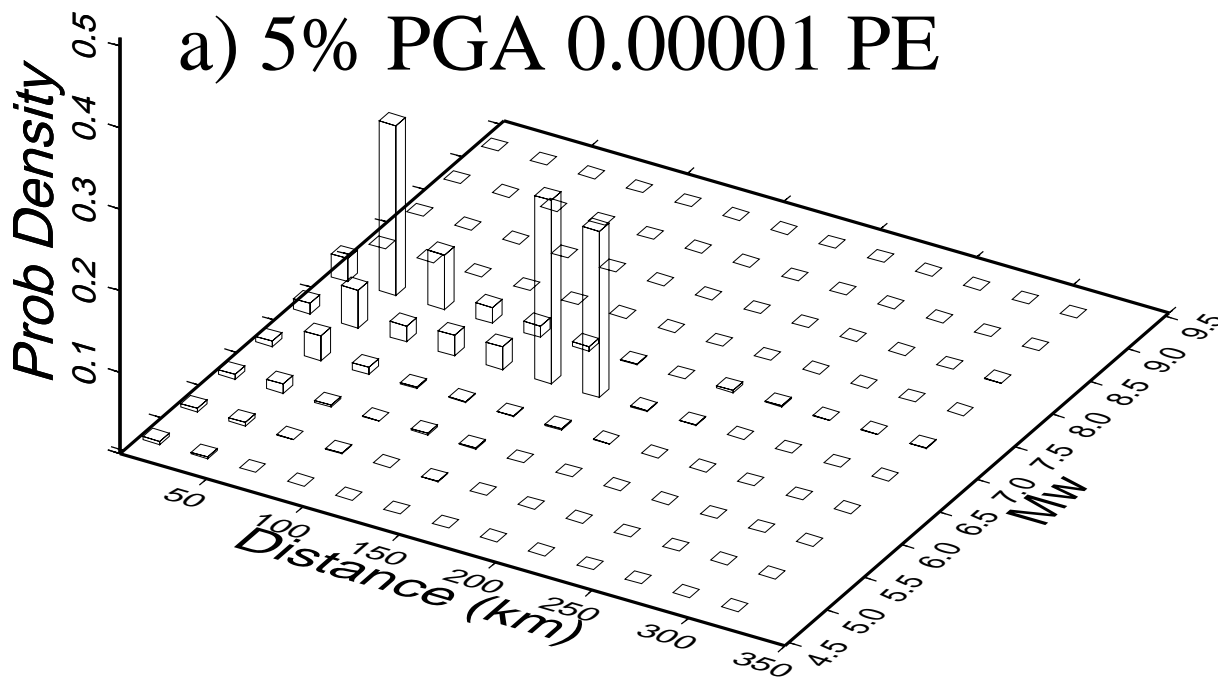
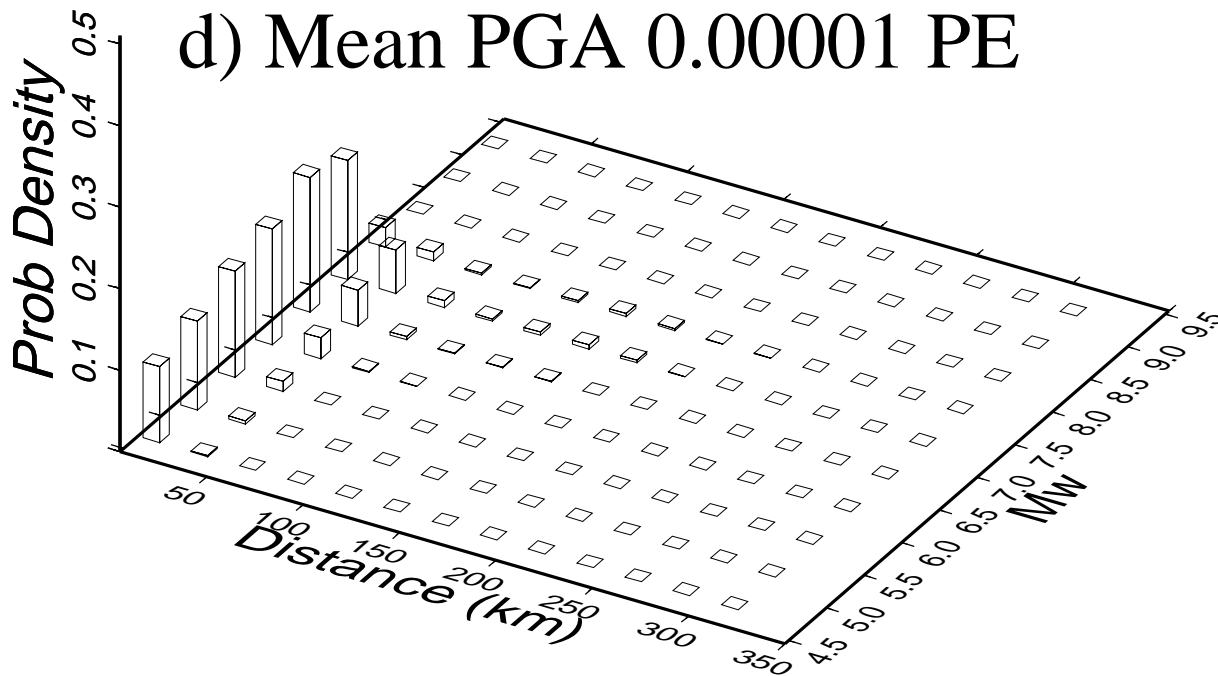
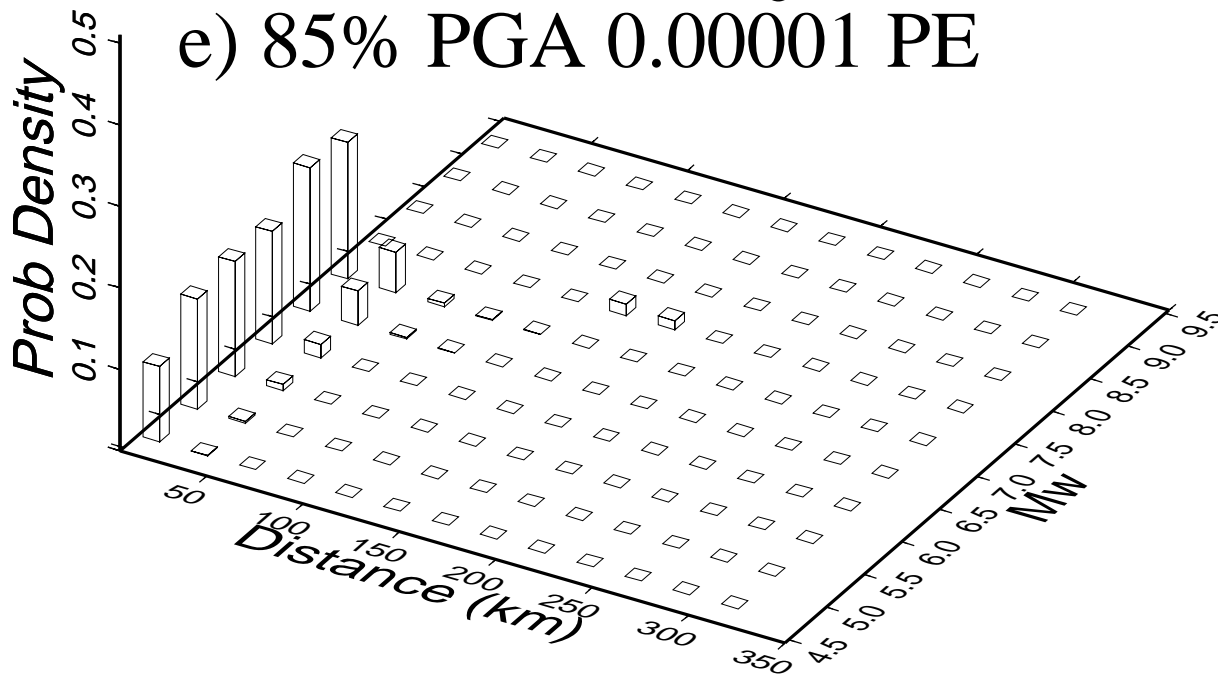


Figure 20 ABC

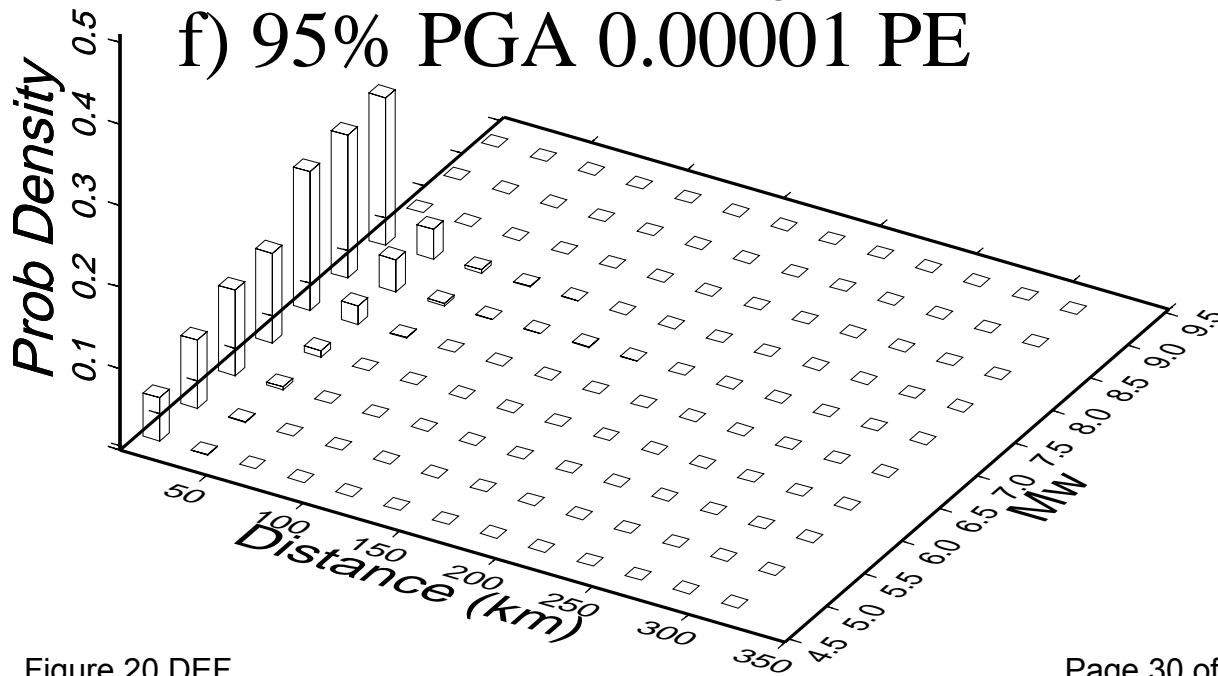
### d) Mean PGA 0.00001 PE



### e) 85% PGA 0.00001 PE



### f) 95% PGA 0.00001 PE



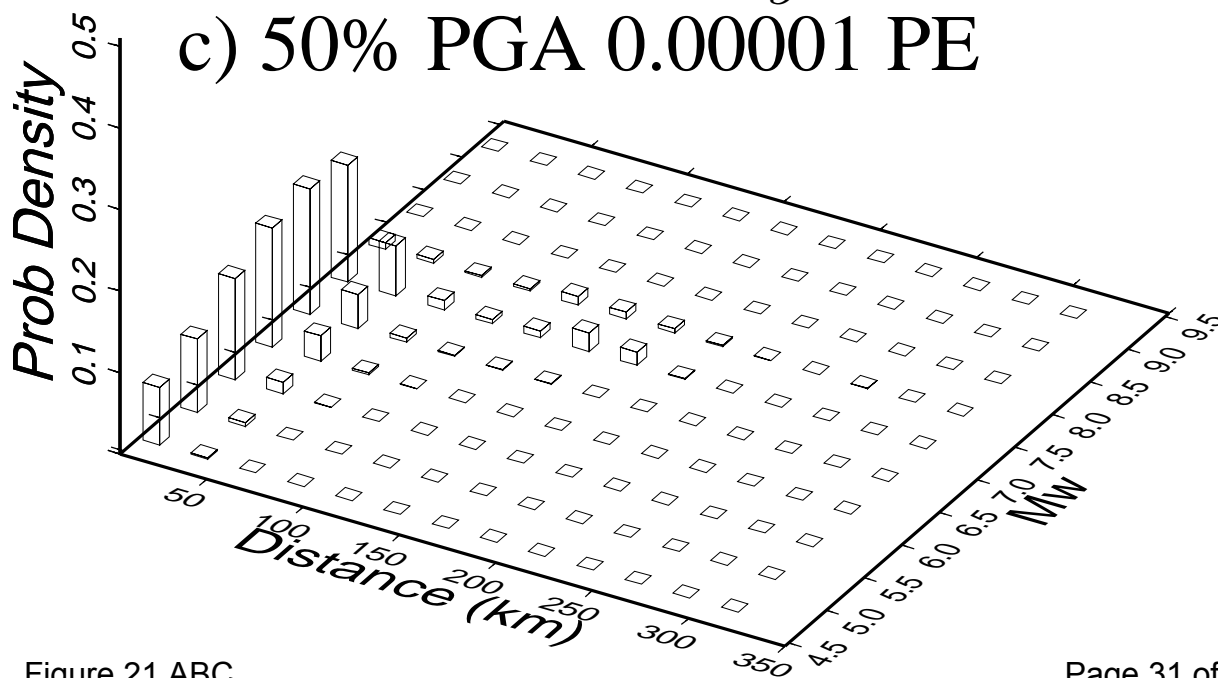
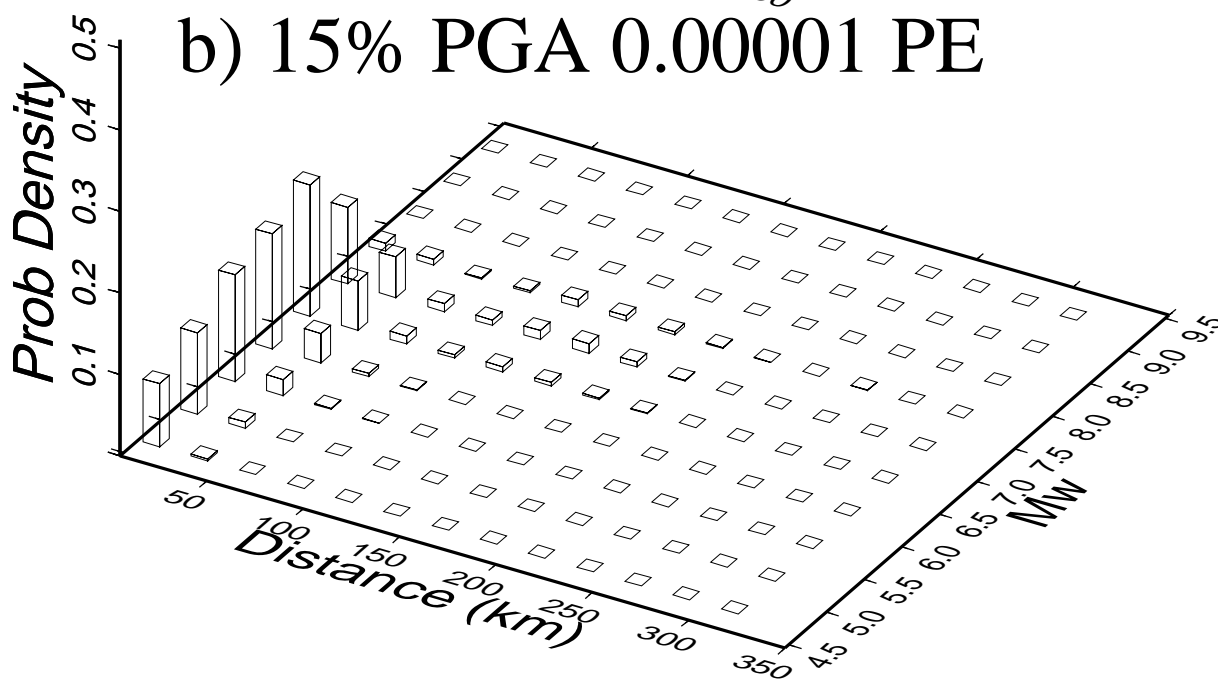
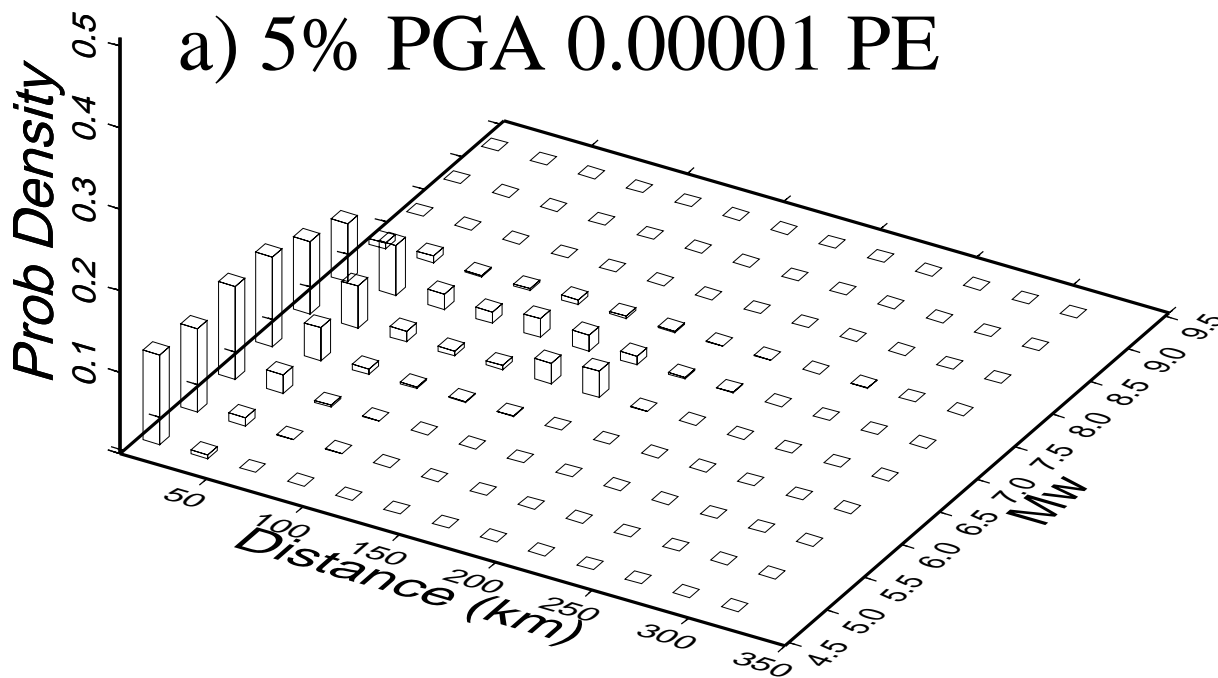


Figure 21 ABC

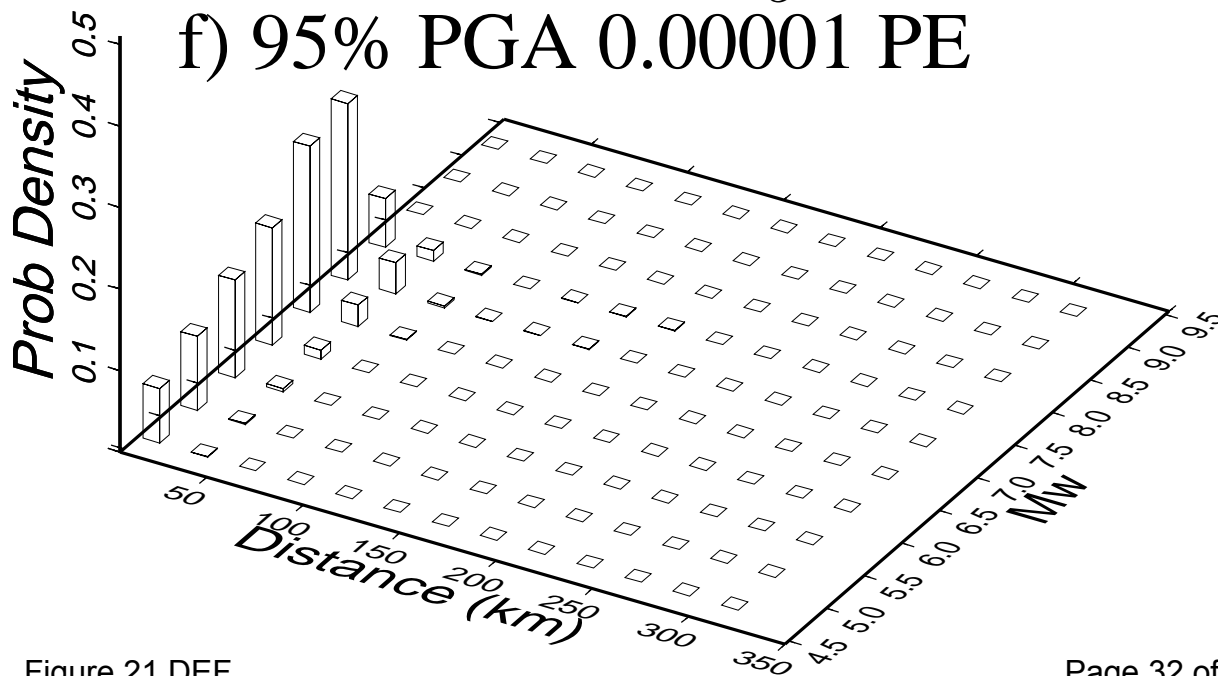
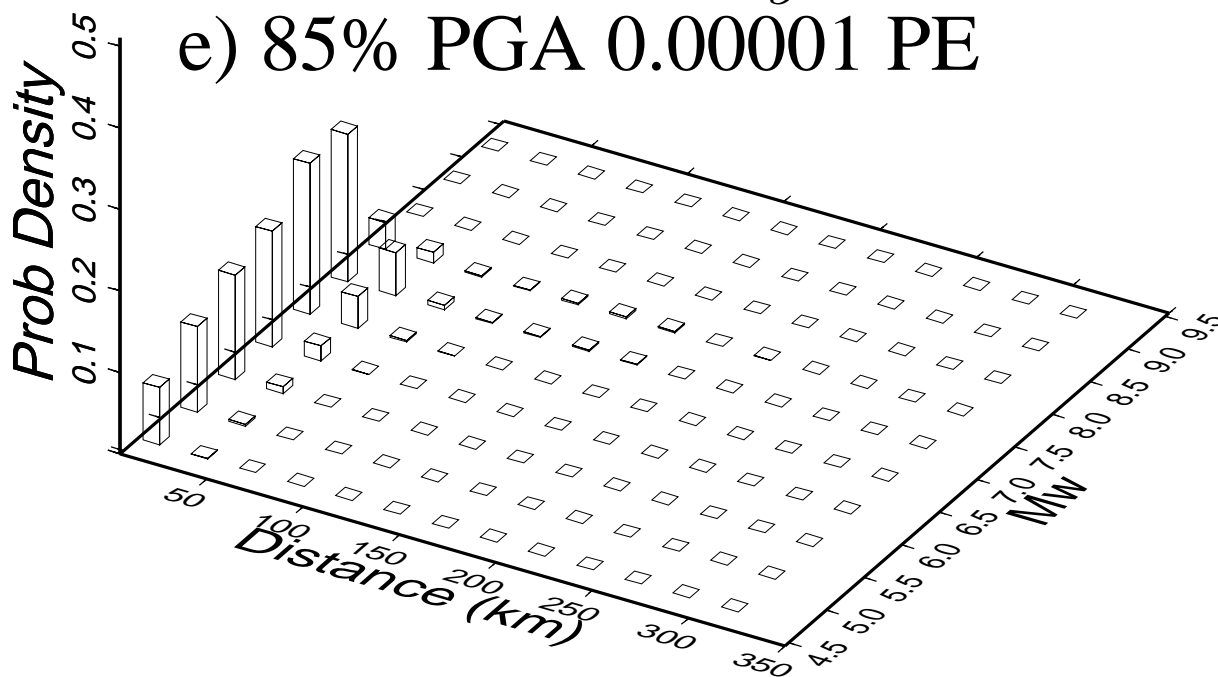
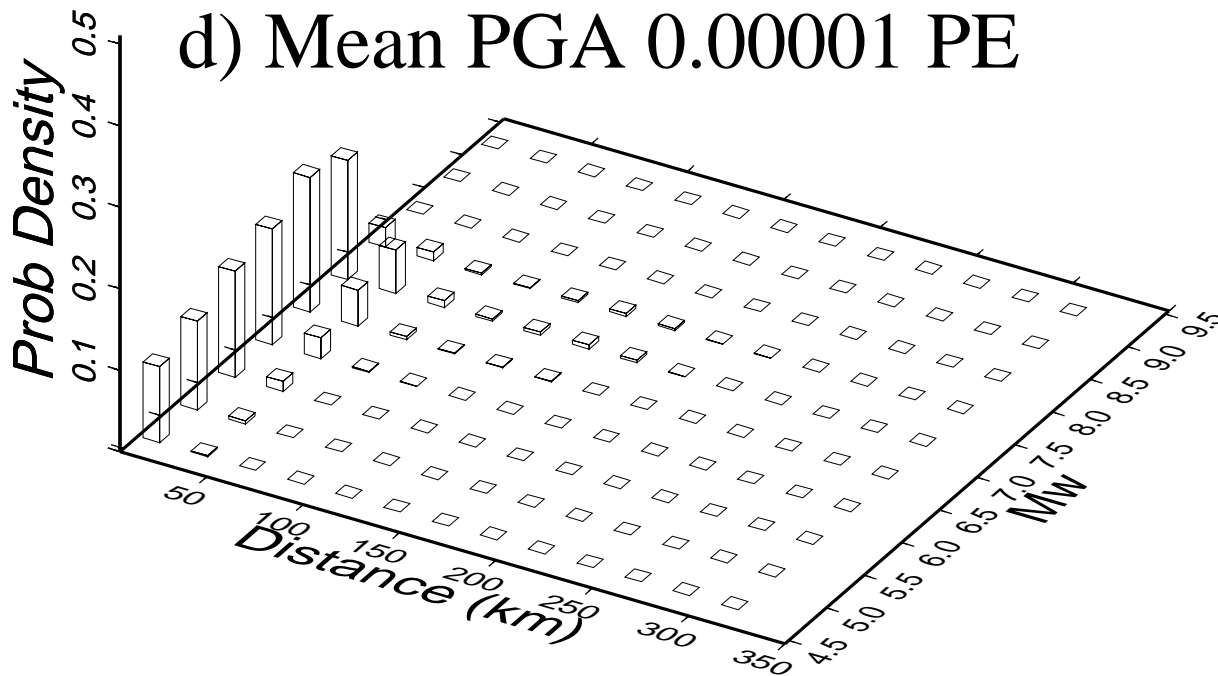


Figure 21 DEF

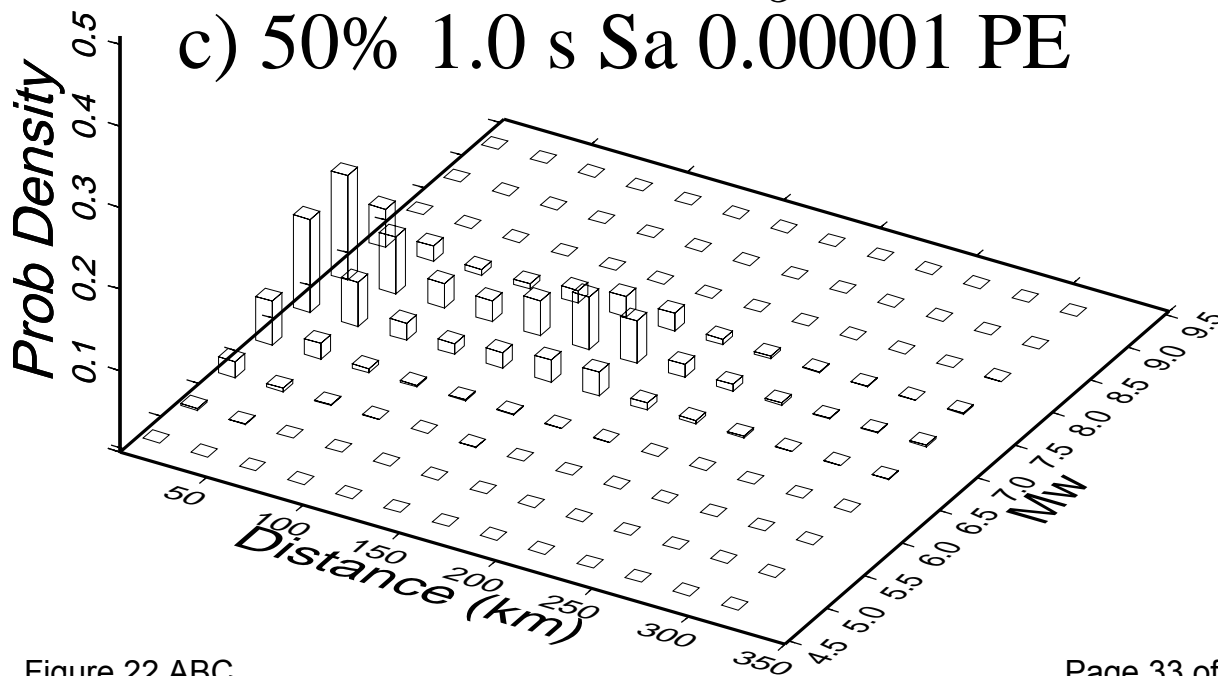
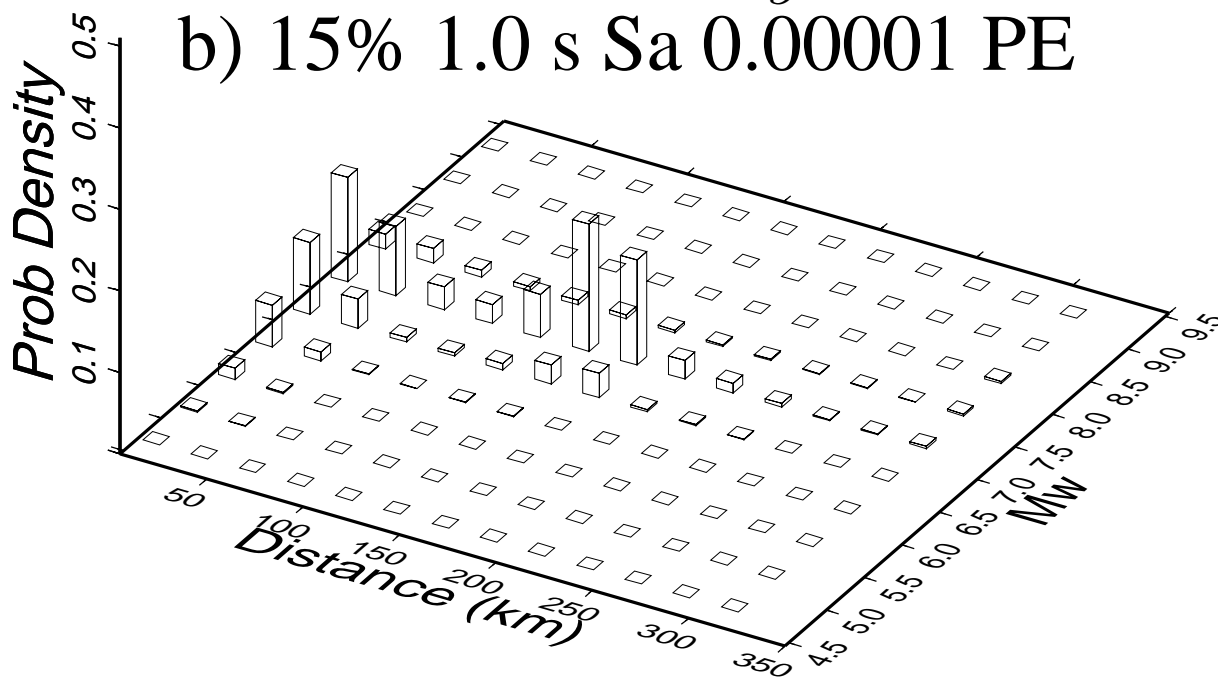
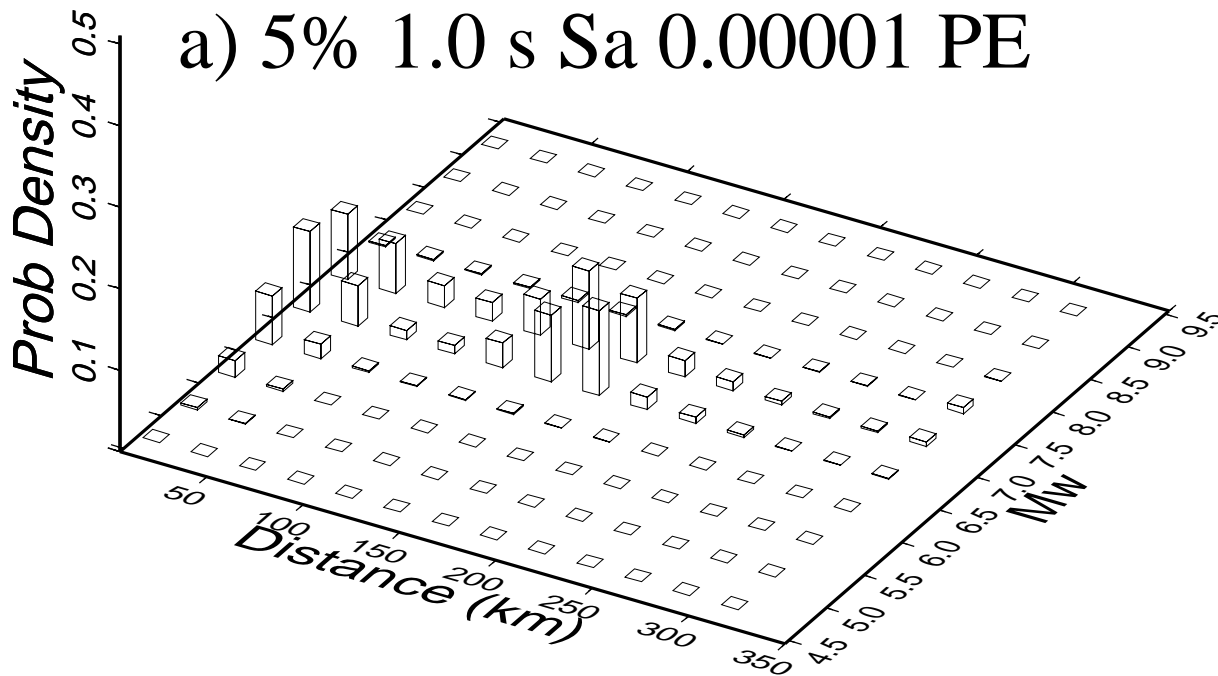
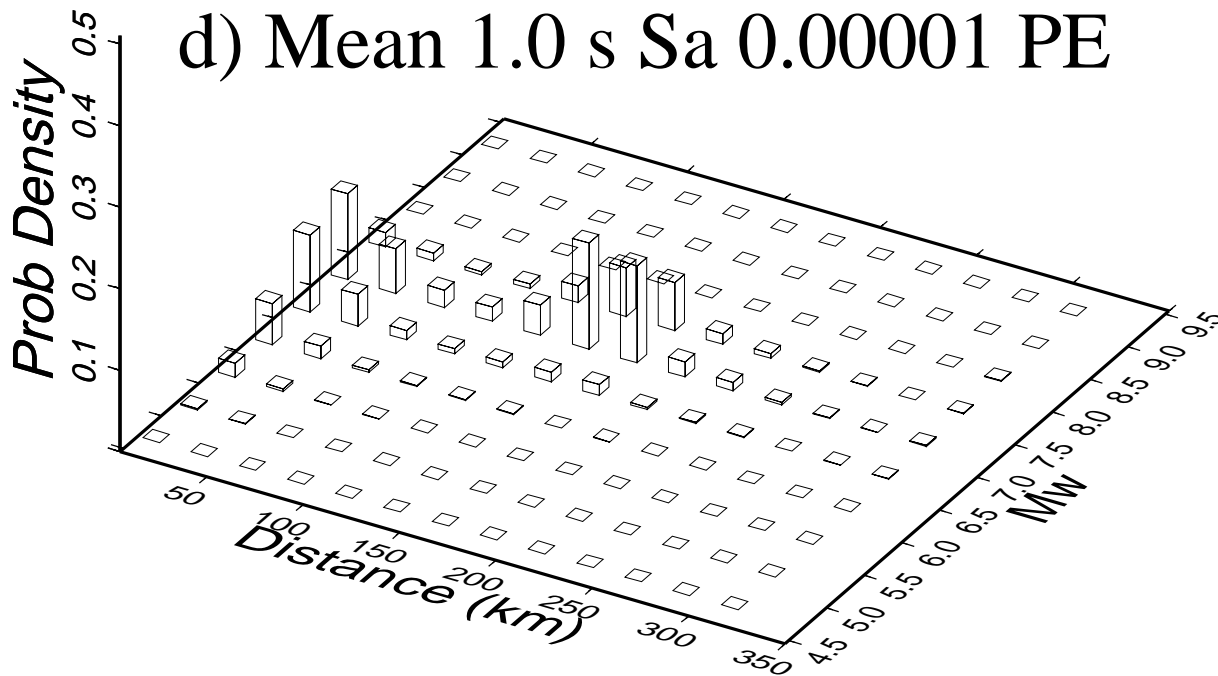
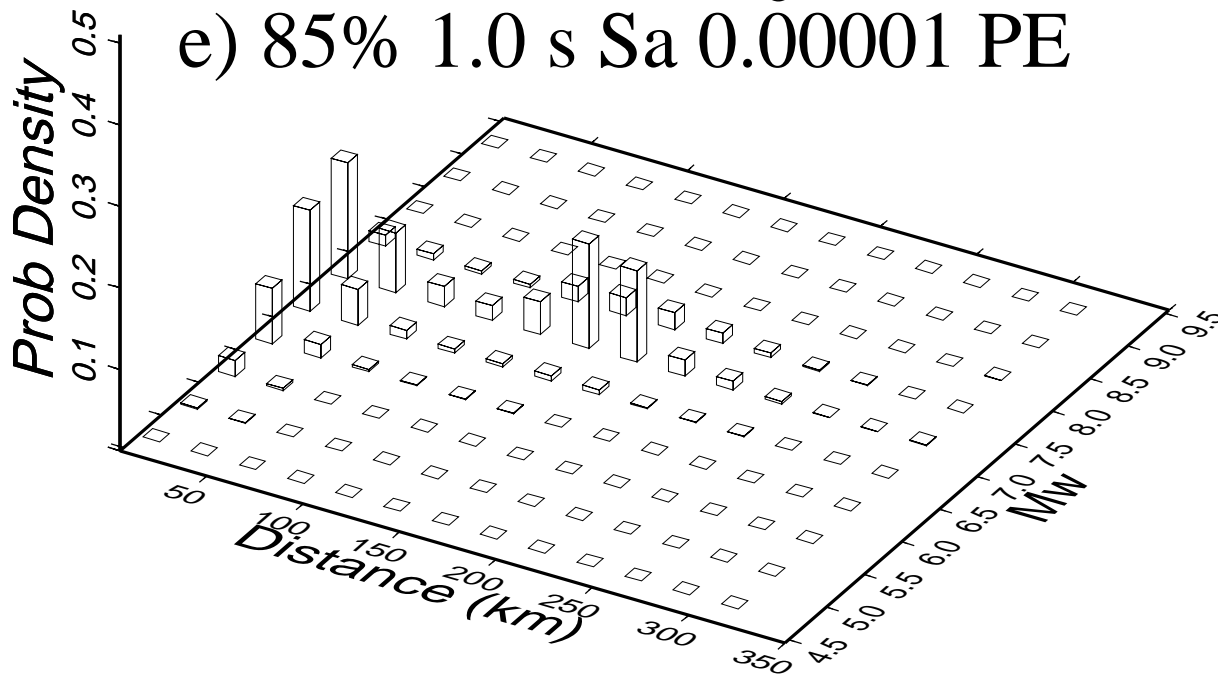


Figure 22 ABC

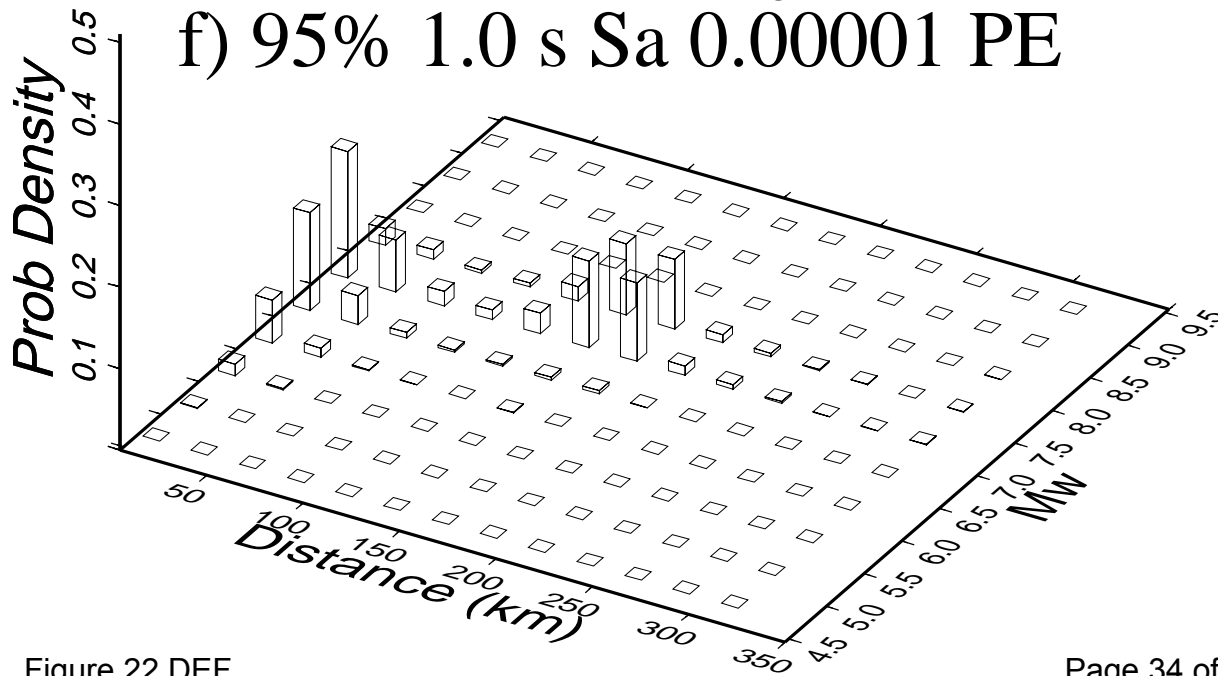
### d) Mean 1.0 s Sa 0.00001 PE



### e) 85% 1.0 s Sa 0.00001 PE



### f) 95% 1.0 s Sa 0.00001 PE



## DEVELOPMENT OF REGIONAL HARD ROCK ATTENUATION RELATIONS FOR SOUTH CAROLINA

Walter Silva\*, Nick Gregor\*, Richard Lee\*\*

### Background

Due to the low rates of seismicity, a significant and currently unresolvable issue exists in the estimation of strong ground motions for specified magnitude, distance, and site conditions in central and eastern North America (CENA). The preferred approach to estimating design ground motions is through the use of empirical attenuation relations, perhaps augmented with a model based relation to capture regional influences. For western North America (WNA), particularly California, seismicity rates are such that sufficient strong motion recordings are available for ranges in magnitudes and distances to properly constrain regression analyses. Naturally, not enough recorded data are available at close distances ( $\approx 10$  km) to large magnitude earthquakes ( $M \approx 3/4$ ) so large uncertainty exists for these design conditions but, in general, ground motions are reasonably well defined. For CENA however, very few data exist and nearly all are for  $M \approx 5.8$  and distances exceeding about 50 km. This is a fortunate circumstance in terms of hazard but, because the potential exists for large, though infrequent, earthquakes in certain areas of CENA, the actual risk to life and structures is comparable to that which exists in seismically active WNA. As a result, the need to characterize strong ground motions is significant and considerable effort has been directed to developing appropriate attenuation relations for CENA conditions (Boore and Atkinson, 1987; Toro and McGuire, 1987; EPRI, 1993; Toro et al., 1997; Atkinson and Boore, 1997). Because the strong motion data set is sparse in the CENA, numerical simulations represent the only available approach and the stochastic point-source model (Appendix A) has generally been the preferred model used to develop attenuation relations. The process involves repeatedly exercising the model for a range in magnitude and distances as well as expected parameter values, adopting a functional form for a regression equation, and finally performing regression analyses to determine coefficients for median predictions as well as variability about the median. Essential elements in this process include: a physically realistic, reasonably robust and well-validated model (Silva et al., 1997; Schneider et al., 1993); appropriate parameter values and their distributions; and a statistically stable estimate of model variability (Appendix A). The model variability is added to the variability resulting from the regression analyses (parametric plus regression variability) to represent the total variability associated with median estimates of ground motions (Appendix A).

---

\*Pacific Engineering and Analysis, 311 Pomona Ave., El Cerrito, CA 94530  
[www.pacificengineering.org](http://www.pacificengineering.org); e-mail: [pacificengineering@juno.com](mailto:pacificengineering@juno.com)

\*\*Bechtel Savannah River, Inc.

## Model Parameters

For the point-source model implemented here, parameters include stress drop ( $\Delta\sigma$ ), source depth ( $H$ ), path damping ( $Q(f) = Q_0 f^{\eta}$ ), shallow crustal damping ( $\kappa$ ), and crustal amplification. For the South Carolina crust, the model is based on an average of the crustal velocity in the coastal area of South Carolina near Charleston (Talwani, personal communication) and the region in the vicinity of the Savannah River Site (Leutgert et al., 1994). This crustal combination averages the velocities of the South Georgia Basin and crystalline bedrock. The crustal model is listed in Table 1. The Moho is at a depth of about 34 km. Geometrical attenuation is assumed to be magnitude dependent, using a model based on inversions of the Abrahamson and Silva (1997) empirical attenuation relation with the point-source model. The model for geometrical attenuation is given by

$$R^{-(a+b(M-6.5))}, R \leq 65 \text{ km}; \quad R^{-(a+b(M-6.5))/2}, \quad R > 65 \text{ km} \quad (1)$$

where  $a = 1.0296$ ,  $b = -0.0422$ , and 65 km reflects about twice the crustal thickness (Table 1).

The duration model is taken as the inverse corner frequency plus a smooth distance term of 0.05 times the hypocentral distance (Herrmann, 1985). Monotonic trends in both the geometrical attenuation and distance duration models produced no biases in the validation exercises using WNA and CENA recordings (Appendix A) and are considered appropriate when considerable variability in crustal structure that may exist over a region, as well as variability in source depth. Additionally, extensive modeling exercises have shown that the effects of source finiteness, coupled with variability in source depth and crustal structure, result in smooth attenuation with distance, accompanied by a large variability in ground motions (EPRI, 1993). More recently, regressions for peak acceleration, peak particle velocity, and peak displacement on WNA strong motion data (over 50 earthquakes,  $M \approx 5.0$  to 7.6), including the recent Chi-Chi, Taiwan and Koaceli and Duzce, Turkey earthquakes using a smooth monotonic distance dependency (Equation 3) showed symmetric distributions of residuals about zero (Silva et al., 2002). These results suggest a monotonic distance dependency adequately reflects strong motion distance attenuation when considering multiple earthquakes and variable crustal conditions and is an appropriate assumption for estimating strong ground motions for the next earthquake.

To model shallow crustal damping, a  $\kappa$  value of 0.006 sec is assumed to apply for the crystalline basement and below (Silva and Darragh, 1995; EPRI, 1993). The  $Q(f)$  model is from Benz et al. (1997), based on inversions of the NE United States and SE Canada recordings and is given by  $Q(f) = 1,052 f^{0.22}$  for the region. Both magnitude independent and magnitude dependent stress drop models are used. For the magnitude dependent stress drop model, the stress drop varies from 160 bars for  $M$  5.5 to 90 bars for  $M$  7.5 and 70 bars for  $M$  8.5 (the range in magnitudes for the simulations). The magnitude scaling of stress drop is based on point-source inversions of the Abrahamson and Silva (1997) empirical attenuation relation (Silva et al., 1997) and is an empirically driven mechanism to accommodate the observed magnitude saturation due to source finiteness. Similar point-source stress drop scaling has been observed by Atkinson and Silva (1997) using



(WNA) recordings of strong ground motions and from inversions of the Sadigh et al., (1997) attenuation relation (EPRI, 1993). For the CEUS, the stress drop values are constrained by the **M** 5.5 stress drop of 160 bars. This value is from recent work of Gail Atkinson (personal communication, 1998) who determined CENA stress drops based on instrumental and intensity data. Since the majority of her data are from earthquakes below **M** 6 (**M** 4 to 7), it was assumed her average stress drop (. 180 bars adjusted for the regional crustal model to 160 bars) is appropriate for **M** 5.5. Table 2 shows the magnitude dependent as well as magnitude independent stress drops. The magnitude independent stress drop of 120 bars reflects the log average of the **M** 5.5, **M** 6.5, and **M** 7.5 stress drops (Table 2).

The single corner frequency model was also run with a constant stress drop for all magnitudes. A stress drop of 120 bars was applied to all four magnitudes. This is the same constant stress drop used in the Toro et al. (1997; EPRI, 1993) CEUS rock relations. To accommodate uncertainty (epistemic) in median stress drop (parameters) for CEUS earthquakes, both high and low median values were run using a 100% variation on the constant and variable stress drop models (Table 2). The high stress drop model is taken as 2 times the base case values with the low stress drop as the base case values divided by 2.

Source depth is also assumed to be magnitude dependent and is based on the depth distribution of stable continental interiors and margins (EPRI, 1993). The magnitude dependent depth distribution is shown in Table 2.

Another source model considered appropriate for CENA ground motions is the double corner model (Atkinson and Boore, 1995). In this model there is no variation of the stress drop with magnitude. Additionally, stress drop is not explicitly defined for this model and no uncertainties are given for the corner frequencies (which are magnitude dependent). As a result, the parametric uncertainty obtained from the regression analysis will underrepresent the total parametric uncertainty. For this reason, the total parametric uncertainty for the two-corner model is taken as the total parametric uncertainty from the single corner model with variable stress drop, which is slightly larger than the parametric uncertainty for the single corner model with constant stress drop scaling (to avoid underestimating the two-corner parametric uncertainty).

To accommodate magnitude saturation in the double-corner and single-corner constant stress drop models, magnitude dependent fictitious depth terms were added to the source depths for simulations at **M** 6.5 and above. The functional form is given by

$$H = H' e^{a + bM} \quad (2)$$

with

$$a = -1.250, \quad b = 0.227.$$

H and H' are the fictitious and original source depths respectively and the coefficients are based on the Abrahamson and Silva (1997) empirical attenuation relation. The magnitude saturation built into the constant stress drop single corner and double corner models is then constrained empirically, accommodating source finiteness in a manner consistent with the WUS strong motion database. This approach to limiting unrealistically high ground motions for large magnitude earthquakes at close distances is

considered more physically reasonable than limiting the motions directly, which can be rather arbitrary with specific limiting values difficult to defend on a physical basis.

Because of the manner in which the model validations were performed ( $\Delta\sigma$ ,  $Q(f)$ , and  $H$  were optimized), parametric variability for only  $\Delta\sigma$ ,  $Q(f)$  and  $H$  are required to be reflected in the model simulations (Appendix B; EPRI, 1993; Roblee et. al., 1996). For source depth variability, a lognormal distribution is used with a  $\sigma_{\ln} = 0.6$  (EPRI, 1993). Bounds are placed on the distribution to prevent nonphysical realizations (Table 2).

The stress drop aleatory variability,  $\sigma_{\ln} = 0.5$  is from Silva et al. (1997) and is based on inversions of ground motions for stress drop using WNA earthquakes with  $M \geq 5$ . The variability in  $Q(f)$  is taken in  $Q_0$  alone ( $\sigma_{\ln} = 0.4$ ) and is based on inversions in WNA for  $Q(f)$  models (Silva et al., 1997).

## Attenuation Relations

To generate data, which consists of 5% damped spectral acceleration, peak acceleration, peak particle velocity, and peak displacements, for the regression analyses, 30 simulations reflecting parametric variability are made at distances of 1, 5, 10, 20, 50, 75, 100, 200, and 400 km. At each distance, five magnitudes are used:  $M$  4.5, 5.5, 6.5, 7.5, and 8.5 (Table 2).

The functional form selected for the regressions which provided the best overall fit (from a suite of about 25) to the simulations is given by

$$\ln y = C_1 + C_2 M + (C_6 + C_7 M)^* \tag{3}$$

$$\ln (R + e^{C_4}) + C_{10} (M - 6)^2,$$

where  $R$  is taken as a closest distance to the surface projection of the rupture surface, consistent with the validation exercises (Silva et al., 1997).

Figure 1 shows the simulations for peak accelerations as well as the model fits for the single corner model with variable (medium, Table 2) stress drops for  $M$  7.5 and the South Carolina parameters. In general, the model fits the central trends (medians) of the simulations. Figure 2a summarizes the magnitude dependency of the peak acceleration estimates and saturation is evident, primarily due to the magnitude dependent stress drop. Also evident is the magnitude dependent far-field fall off with a decrease in slope as  $M$  increases (easily seen beyond 100 km). This feature is especially important in the CEUS where large contributions to the hazard can come from distant sources. The model predicts peak accelerations at a distance of 1 km of about 0.30, 0.70, 1.10, 1.50g for  $M$  4.5, 5.5, 6.5, and 7.5, respectively.

Figure 2b illustrates the effect of median stress drop on the peak accelerations, about a factor of 2 (closer to 1.7 overall) at close distances and decreasing with increasing distance (likely due to a decrease in frequency content with increasing distance).

Examples of response spectra at 1 km for  $M$  4.5, 5.5, 6.5, 7.5, and 8.5 are shown in Figure 3. For  $M$  7.5, the peak acceleration ( $S_a$  at 100 Hz) is about 2g with the peak in the spectrum near 0.03 sec. The jagged nature of the spectra is due to unsmoothed coefficients. Figure 3 also shows the effect of median stress drop on the spectra for the South Carolina parameters. As expected the maximum effect is at high frequency, decreasing with increasing period, and approaching no effect at the magnitude dependent corner period.

The model regression coefficients are listed in Table 3 along with the parametric and total variability. The modeling variability is taken from Appendix A. The total variability (medium stress drop model), solid line in Figure 4, is large at long period. It ranges from about 2 at short periods to about 4 at a period of 10 sec, where it is dominated by modeling variability.

The large long period uncertainty is due to the tendency of the point-source model to overpredict low frequency motions at large magnitudes ( $M > 6.5$ ; EPRI, 1993). This trend led Atkinson and Silva (1997, 2000) to introduce a double-corner point-source model for WUS crustal sources, suggesting a similarity in source processes for WUS and CEUS crustal sources, but with CEUS sources being more energetic by about a factor of two (twice WUS stress drops), on average.

The results for the single corner frequency model with constant stress drop scaling are shown in Figures 5 to 8. The same plots are shown as were described for the previous model. These two models estimate similar values with the variable stress drop motions exceeding the constant stress drop motions at the lower magnitudes ( $M \leq 6.5$ ). The constant stress drop of 120 bars will result in about 30% to 50% higher rock motions at high frequency ( $> 1$  Hz) for  $M$  7.5 than the variable stress drop model, with a corresponding stress drop of 95 bars (EPRI, 1993). At small  $M$ , say  $M$  5.5, the variable stress drop motions are higher, reflecting the 160 bar results of Atkinson for CEUS earthquakes with average  $M$  near 5.5. Also shown are the results for the model with saturation, reducing the large magnitude, close-in motions. The saturation reduces the  $M$  7.5 and  $M$  8.5 motions by 30 to 50% within about 10 km distance. The parametric variability is also similar to that of the variable stress drop model. The regression coefficients are given in Tables 4 and 5.

The regression results for the double corner frequency model are listed in Tables 6 and 7. The regression model fit to the peak acceleration data as shown in Figure 9. The PGA model is shown in Figure 10, and Figure 12 is a plot of the uncertainty. Figure 11 shows the spectra at a distance of 1 km. At long period ( $> 1$  sec) and large  $M$  ( $\geq 6.5$ ) the motions are significantly lower than those of the single-corner models (Figures 3a and 7). The parametric variability was taken as the same as the single corner model with variable stress drop as distributions are not currently available to apply to the two corner frequencies associated with this model (Atkinson and Boore, 1997). Since the two corner frequency source model was not available when the validations were performed (Silva et al., 1997), the model variability for the single corner frequency source model was used. This is considered conservative as the total aleatory variability for the two corner model is likely to be lower than that of the single corner model, as comparisons using WUS data show it provides a better fit to recorded motions at low frequencies ( $\leq 1$  Hz; Atkinson and

Silva, 1997, 2000). This is, of course, assuming the aleatory parametric variability associated with the two corner frequencies is not significantly larger than that associated with the single corner frequency stress drop.

At long period ( $> 1$  sec) the total variability for all the models is largely empirical, being driven by the modeling component or comparisons to recorded motions. While this variability may be considered large, it includes about 17 earthquakes with magnitudes ranging from  $M$  5.3 to  $M$  7.4, distances out to 500 km, and both rock and soil sites. The average  $M$  for the validation earthquakes is about  $M$  6.5, near the magnitude where empirical aleatory variability has a significant reduction (Abrahamson and Shedlock, 1997). The magnitude independent point-source variability may then reflect the generally higher variability associated with lower magnitude ( $M \leq 6.5$ ) earthquakes, being conservative for larger magnitude earthquakes.

Epistemic variability or uncertainty in mean estimates of ground motions is assumed to be accommodated in the use of the three mean stress drop single corner models and the double corner model, all with appropriate weights. This assumption assumes the epistemic uncertainty in the spectral levels of the two corner frequency model are small (indeed zero) and can be neglected. This approach assumes the major contributors to epistemic uncertainty (variability in mean motions) for the CEUS are in single corner mean stress drop and shape of the source spectrum, as well as differences in crustal structure between the Midcontinent and Gulf Coast regions (Toro et al., 1997; Silva et al., 2003). As a guide to estimating appropriate weights for the low, medium, and high median stress drops to accommodate epistemic variability in median CEUS single corner stress drops, the EPRI (1993) value for total variability (epistemic plus aleatory) of 0.7 at large magnitude ( $M \geq 6.5$ ) may be adopted. Based on the WUS aleatory value of 0.5 (Table 2; Silva et al., 1997), assuming similar aleatory variability in median stress drop for the CEUS, the remaining variability of 0.49 may be attributed to epistemic variability in the medium stress drop. For the factors of two above and below the medium stress drop (Table 2), an approximate three point weighting would have weights of 1/6, 2/3, 1/6 (Gabe Toro, personal communication).

## REFERENCES

- Abrahamson, N.A. and W.J. Silva (1997). "Empirical response spectral attenuation relations for shallow crustal earthquakes." *Seismological Research Let.*, 68(1), 94-127.
- Ackerman, H.D (1983). "Seismic refraction study in the area of the Charleston, South Carolina, 1886 earthquake, in studies related to the Charleston, South Carolina, earthquake of 1886 - tectonics and seismicity." G.S. Gohn, ed., *U.S. Geological Survey Professional Paper*, 1313-F, 20p.
- Atkinson, G.M and W.J. Silva (2000). "Stochastic modeling of California ground motions." *Bull. Seism. Soc. Am.* 90(2), 255-274.
- Atkinson, G.M. and D.M. Boore (1997). "Some comparisons between recent ground-motion relations." *Seism. Res. Lett.* 68(1), 24-40.
- Atkinson, G.M and W.J. Silva (1997). "An empirical study of earthquake source spectra for California earthquakes." *Bull. Seism. Soc. Am.* 87(1), 97-113.
- Benz, H.M., A. Frankel and D.M. Boore (1997). "Regional Lg Attenuation for the Continental United States." *Bull. Seism. Soc. Am.* 87(3), 606-619.
- Boore, D.M. and G.M. Atkinson (1987). "Stochastic prediction of ground motion and spectral response parameters at hard-rock sites in eastern North America." *Bull. Seism. Soc. Am.*, 77(2), 440-467.
- Campbell, K W. (1997). "Empirical near-source attenuation relationships for horizontal and vertical components of peak ground acceleration, peak ground velocity, and pseudo-absolute acceleration response spectra." *Seismological Research Let.*, 68(1), 154-176.
- Electric Power Research Institute (1993). "Guidelines for determining design basis ground motions." Palo Alto, Calif: Electric Power Research Institute, vol. 1-5, EPRI TR-102293.
- vol. 1: Methodology and guidelines for estimating earthquake ground motion in eastern North America.
  - vol. 2: Appendices for ground motion estimation.
  - vol. 3: Appendices for field investigations.
  - vol. 4: Appendices for laboratory investigations.
  - vol. 5: Quantification of seismic source effects.
- Herrmann, R.B. (1985). "An extension of random vibration theory estimates of strong ground motion to large distance." *Bull. Seism. Soc. Am.*, 75, 1447-1453.
- Luetgert, J.H., H.M. Benz and S. Madabhushi (1994). "Crustal Structure Beneath the Atlantic Coastal Plain of South Carolina." *Seis. Res. Lett.*, 65, 180-191.

- Roblee, C.J., W.J. Silva, G.R. Toro, and N. Abrahamson (1996). "Variability in Site-Specific Seismic Ground-Motion Predictions." *Uncertainty in the Geologic Environment: From Theory to Practice, Proceedings of "Uncertainty '96" ASCE Specialty Conference*, Edited by C.D. Shackelford, P.P. Nelson, and M.J.S. Roth, Madison, WI, Aug. 1-3, pp. 1113-1133
- Sadigh, K., C.-Y. Chang, J.A. Egan, F. Makdisi, and R.R. Youngs (1997). "Attenuation relationships for shallow crustal earthquakes based on California strong motion data." *Seism. Soc. Am.*, 68(1), 180-189.
- Schneider, J.F., W.J. Silva, and C.L. Stark (1993). Ground motion model for the 1989 M 6.9 Loma Prieta earthquake including effects of source, path and site. *Earthquake Spectra*, 9(2), 251-287.
- Silva, W., N. Gregor, R. Darragh (2003). "Development of regional hard rock attenuation relations for Central and eastern North America, Mid-Continent and Gulf Coast Areas".
- Silva, W.J., N. Abrahamson, G. Toro, and C. Costantino (1997). "Description and validation of the stochastic ground motion model." Submitted to Brookhaven National Laboratory, Associated Universities, Inc. Upton, New York.
- Silva, W.J. and R. Darragh (1995). "Engineering characterization of earthquake strong ground motion recorded at rock sites." Palo Alto, Calif:Electric Power Research Institute, TR-102261.
- Toro, G.R. and R.K. McGuire (1987). "An investigation into earthquake ground motion characteristics in eastern North America." *Bull. Seism. Soc. Am.*, 77(2), 468-489.
- Toro, G.R., N.A. Abrahamson, and J.F. Schneider (1997). "A Model of strong ground motions from earthquakes in Central and Eastern North America: Best estimates and uncertainties." *Seismological Research Let.*, 68(1), 41-57.

Table 1  
CRUSTAL MODEL  
SOUTH CAROLINA

Thickness (km)	V <sub>s</sub> (km/sec)	Density (cgs)
0.13	2.53	2.62
0.15	3.09	2.78
1.90	3.29	2.85
7.10	3.43	2.93
8.50	3.62	2.99
16.70	3.75	3.04
----	4.54	3.42

Table 2 PARAMETERS FOR SEDIMENTARY ROCK OUTCROP ATTENUATION SIMULATIONS				
<b>M</b>	4.5, 5.5, 6.5, 7.5, 8.5			
D (km)	1, 5, 10, 20, 50, 75, 100, 200, 400			
300 simulations for each <b>M</b> , <i>R</i> pair				
Randomly vary source depth, $\Delta\sigma$ , kappa, $Q_0$ , $\eta$ , profile				
<u>Depth</u> , $\sigma_{lnH} = 0.6$ , Intraplate Seismicity (EPRI, 1993)				
<b>M</b>	$m_{blg}$	Lower Bound (km)	$\bar{H}$ (km)	Upper Bound (km)
4.5	4.9	2	6	15
5.5	6.0	2	6	15
6.5	6.6	4	8	20
7.5	7.1	5	10	20
8.5	7.8	5	10	20
$\Delta\sigma$ , $\sigma_{ln\Delta\sigma} = 0.5$ (Silva et al., 1997)				
<b>M</b>	$m_{blg}$	$\Delta\sigma$ (bars) Base Case Values	AVG. $\Delta\sigma$ (bars) = 123; Assumes <b>M</b> 5.5 = 160 bars (Atkinson, 1993) with magnitude scaling taken from WUS (Silva et al., 1997); constant stress drop model has $\Delta\sigma$ (bars) = 120. High and low stress drop models are 100% higher and 100% lower than base case values.	
4.5	4.9	160, 120*		
5.5	6.0	160, 120*		
6.5	6.6	120, 120*		
7.5	7.1	90, 120*		
8.5	7.8	70, 120*		
<u>Q(s)</u> , $1,052$ , $\eta = 0.22$ , $\sigma_{lnQ_0} = 0.4$ (Benz et al. 1997) Varying $Q_0$ only sufficient, $\pm 1 \sigma$ covers range of CEUS inversions from 1 to 20 Hz				
Kappa, $\bar{\kappa} = 0.006$ sec (EPRI, 1993)				
<u>Profile</u> , Crystalline Basement, randomize top 100 ft				
Geometrical attenuation	$R^{-(a+b(M-6.5))}$ , $R^{-(a+b(M-6.5))/2}$ ,		$a = 1.0296$ , $b = -0.0422$ $R > 65$ km, approximately twice crustal thickness (Table1)	
Based on inversions of the Abrahamson and Silva (1997) relation				

\*Constant Stress Drop Model



Table 3a  
SOUTH CAROLINA  
REGRESSION COEFFICIENTS FOR THE SINGLE CORNER MODEL WITH  
VARIABLE MEDIUM STRESS DROP AS A FUNCTION OF MOMENT MAGNITUDE (M)

Freq. Hz	C1	C2	C4	C5	C6	C7	C8	C10	Parametric	Total
									Sigma	Sigma
0.1000	-20.34111	2.60194	1.40000	.00000	-1.08558	.04640	.00000	-.30371	.3573	1.3246
0.2000	-16.73900	2.30757	1.50000	.00000	-1.16565	.05178	.00000	-.37951	.3696	1.1942
0.3333	-13.57757	2.00261	1.70000	.00000	-1.29760	.06226	.00000	-.38860	.3852	1.0446
0.5000	-10.98377	1.72186	1.80000	.00000	-1.42212	.07357	.00000	-.36699	.4102	.9565
0.6250	-9.47360	1.55395	1.90000	.00000	-1.51379	.08160	.00000	-.34549	.4239	.8842
1.0000	-6.45963	1.20847	2.00000	.00000	-1.68824	.09795	.00000	-.28426	.4531	.8027
1.3333	-4.85330	1.01608	2.00000	.00000	-1.78223	.10744	.00000	-.24230	.4684	.8090
2.0000	-2.60478	.76905	2.10000	.00000	-1.94949	.12195	.00000	-.18473	.4972	.7714
2.5000	-1.40255	.64885	2.20000	.00000	-2.06185	.13054	.00000	-.15738	.5207	.7677
3.3333	-.08110	.52001	2.30000	.00000	-2.19330	.13926	.00000	-.12919	.5309	.7689
4.1667	.62132	.44430	2.30000	.00000	-2.26314	.14359	.00000	-.11198	.5314	.7524
5.0000	1.42947	.37165	2.40000	.00000	-2.38047	.15104	.00000	-.10052	.5373	.7481
6.2500	2.34666	.29538	2.50000	.00000	-2.52530	.16033	.00000	-.08963	.5514	.7509
6.6667	2.51220	.28131	2.50000	.00000	-2.55233	.16215	.00000	-.08711	.5555	.7547
8.3333	3.82298	.19666	2.70000	.00000	-2.78523	.17649	.00000	-.08022	.5755	.7742
10.0000	4.74102	.13857	2.80000	.00000	-2.94210	.18510	.00000	-.07565	.5996	.7801
12.5000	5.32022	.09551	2.80000	.00000	-3.04406	.19102	.00000	-.07192	.6155	.7857
14.2857	6.08837	.04583	2.90000	.00000	-3.19714	.20084	.00000	-.07142	.6062	.7783
16.6667	6.40243	.01563	2.90000	.00000	-3.27602	.20733	.00000	-.07091	.6069	.7804
18.1818	6.58201	-.00612	2.90000	.00000	-3.31878	.21133	.00000	-.07040	.6057	.7755
20.0000	6.74549	-.01996	2.90000	.00000	-3.36106	.21467	.00000	-.07031	.6044	.7772
25.0000	6.56386	-.01385	2.80000	.00000	-3.35824	.21579	.00000	-.07078	.6152	.7830
31.0000	6.88238	-.04115	2.80000	.00000	-3.43310	.22124	.00000	-.07027	.6271	.7892
40.0000	6.62198	-.04194	2.70000	.00000	-3.40938	.22240	.00000	-.07041	.6282	.7869
50.0000	6.13592	-.02753	2.60000	.00000	-3.34276	.22097	.00000	-.07204	.6231	.7845
100.000	3.80314	.07060	2.40000	.00000	-2.96769	.20791	.00000	-.08054	.5625	.7374
PGA	3.49839	.08928	2.40000	.00000	-2.91374	.20455	.00000	-.08156	.5568	.7334
PGV	1.78500	.69725	1.90000	.00000	-2.38690	.19158	.00000	-.12481	.4470	-----

Table 3b  
SOUTH CAROLINA  
REGRESSION COEFFICIENTS FOR THE SINGLE CORNER MODEL WITH  
VARIABLE LOW STRESS DROP AS A FUNCTION OF MOMENT MAGNITUDE (M)

Freq. Hz	C1	C2	C4	C5	C6	C7	C8	C10	Parametric	Total
									Sigma	Sigma
0.1000	-20.05231	2.53227	1.40000	.00000	-1.07453	.04458	.00000	-.33586	.3615	1.3257
0.2000	-16.27482	2.19486	1.50000	.00000	-1.16205	.05129	.00000	-.38905	.3781	1.1970
0.3333	-13.04615	1.86751	1.70000	.00000	-1.29847	.06256	.00000	-.38046	.4007	1.0503
0.5000	-10.45871	1.57792	1.80000	.00000	-1.42382	.07424	.00000	-.34646	.4264	.9635
0.6250	-9.12302	1.41677	1.80000	.00000	-1.48739	.08097	.00000	-.31954	.4380	.8914
1.0000	-6.23478	1.08031	1.90000	.00000	-1.65772	.09727	.00000	-.25183	.4608	.8067
1.3333	-4.55982	.89047	2.00000	.00000	-1.78241	.10846	.00000	-.21021	.4732	.8119
2.0000	-2.50090	.66910	2.10000	.00000	-1.94421	.12242	.00000	-.15772	.5006	.7733
2.5000	-1.40924	.56460	2.20000	.00000	-2.05286	.13061	.00000	-.13451	.5242	.7704
3.3333	-.21574	.45412	2.30000	.00000	-2.17973	.13883	.00000	-.11152	.5346	.7716
4.1667	.40330	.39049	2.30000	.00000	-2.24641	.14281	.00000	-.09787	.5351	.7552
5.0000	1.14750	.32686	2.40000	.00000	-2.36017	.14988	.00000	-.08899	.5408	.7502
6.2500	1.99242	.26076	2.50000	.00000	-2.49951	.15853	.00000	-.08081	.5542	.7531
6.6667	2.13993	.24927	2.50000	.00000	-2.52505	.16018	.00000	-.07896	.5579	.7562
8.3333	3.38857	.17291	2.70000	.00000	-2.75163	.17382	.00000	-.07400	.5771	.7757
10.0000	4.26612	.12018	2.80000	.00000	-2.90389	.18190	.00000	-.07059	.6009	.7808
12.5000	4.80280	.08289	2.80000	.00000	-2.99953	.18704	.00000	-.06781	.6163	.7865
14.2857	5.53531	.03755	2.90000	.00000	-3.14600	.19608	.00000	-.06765	.6068	.7783
16.6667	5.81659	.01153	2.90000	.00000	-3.21804	.20171	.00000	-.06737	.6073	.7812
18.1818	5.47728	.02280	2.80000	.00000	-3.16765	.19979	.00000	-.06693	.6058	.7755
20.0000	5.61769	.01155	2.80000	.00000	-3.20499	.20256	.00000	-.06689	.6043	.7772
25.0000	5.92208	-.01071	2.80000	.00000	-3.28678	.20844	.00000	-.06736	.6149	.7822
31.0000	6.21793	-.03527	2.80000	.00000	-3.35589	.21317	.00000	-.06677	.6266	.7884
40.0000	5.94977	-.03501	2.70000	.00000	-3.32883	.21388	.00000	-.06674	.6277	.7861
50.0000	5.46547	-.02078	2.60000	.00000	-3.26088	.21226	.00000	-.06814	.6227	.7837
100.000	3.19108	.06980	2.40000	.00000	-2.89257	.19998	.00000	-.07545	.5626	.7374
PGA	2.89680	.08717	2.40000	.00000	-2.84056	.19685	.00000	-.07632	.5571	.7337
PGV	1.36709	.68365	1.90000	.00000	-2.31521	.18396	.00000	-.12869	.4495	-----

Table 3c  
SOUTH CAROLINA  
REGRESSION COEFFICIENTS FOR THE SINGLE CORNER MODEL WITH  
VARIABLE HIGH STRESS DROP AS A FUNCTION OF MOMENT MAGNITUDE (M)

Freq. Hz	C1	C2	C4	C5	C6	C7	C8	C10	Parametric	Total
									Sigma	Sigma
0.1000	-20.56146	2.65753	1.40000	.00000	-1.10167	.04890	.00000	-.26749	.3524	1.3233
0.2000	-17.04411	2.40199	1.60000	.00000	-1.19448	.05392	.00000	-.36235	.3633	1.1924
0.3333	-14.08074	2.12859	1.70000	.00000	-1.30133	.06256	.00000	-.38948	.3726	1.0399
0.5000	-11.50960	1.86114	1.80000	.00000	-1.42361	.07335	.00000	-.38115	.3938	.9494
0.6250	-9.98850	1.69698	1.90000	.00000	-1.51498	.08117	.00000	-.36609	.4078	.8766
1.0000	-6.91188	1.35161	2.00000	.00000	-1.68784	.09700	.00000	-.31470	.4427	.7966
1.3333	-5.02927	1.13995	2.10000	.00000	-1.81934	.10857	.00000	-.27482	.4618	.8050
2.0000	-2.58923	.87023	2.20000	.00000	-1.99500	.12371	.00000	-.21494	.4938	.7688
2.5000	-1.50326	.74863	2.20000	.00000	-2.06874	.13013	.00000	-.18415	.5176	.7657
3.3333	-.04550	.60048	2.30000	.00000	-2.20452	.13930	.00000	-.15077	.5273	.7668
4.1667	1.03708	.49374	2.40000	.00000	-2.32982	.14711	.00000	-.12963	.5276	.7495
5.0000	1.63054	.42844	2.40000	.00000	-2.39747	.15166	.00000	-.11513	.5338	.7452
6.2500	2.62840	.34072	2.50000	.00000	-2.54671	.16141	.00000	-.10088	.5485	.7487
6.6667	2.81493	.32360	2.50000	.00000	-2.57508	.16340	.00000	-.09749	.5528	.7525
8.3333	4.19608	.22940	2.70000	.00000	-2.81360	.17833	.00000	-.08805	.5737	.7727
10.0000	5.16133	.16491	2.80000	.00000	-2.97485	.18742	.00000	-.08187	.5981	.7793
12.5000	5.79219	.11474	2.80000	.00000	-3.08363	.19418	.00000	-.07674	.6146	.7849
14.2857	6.60146	.05996	2.90000	.00000	-3.24392	.20485	.00000	-.07571	.6057	.7775
16.6667	6.95517	.02462	2.90000	.00000	-3.33066	.21231	.00000	-.07480	.6068	.7804
18.1818	7.15547	.00024	2.90000	.00000	-3.37781	.21686	.00000	-.07413	.6058	.7755
20.0000	7.34032	-.01632	2.90000	.00000	-3.42473	.22078	.00000	-.07392	.6048	.7772
25.0000	7.73231	-.04885	2.90000	.00000	-3.52618	.22900	.00000	-.07428	.6159	.7830
31.0000	7.53570	-.04513	2.80000	.00000	-3.51127	.22923	.00000	-.07380	.6280	.7900
40.0000	7.28719	-.04751	2.70000	.00000	-3.49198	.23099	.00000	-.07411	.6292	.7877
50.0000	6.80166	-.03323	2.60000	.00000	-3.42745	.22986	.00000	-.07599	.6239	.7845
100.000	4.80627	.04540	2.50000	.00000	-3.11897	.22107	.00000	-.08595	.5626	.7374
PGA	4.48217	.06607	2.50000	.00000	-3.06158	.21737	.00000	-.08717	.5568	.7334
PGV	2.45098	.69142	2.00000	.00000	-2.50898	.20312	.00000	-.12192	.4447	-----

Table 4a  
SOUTH CAROLINA  
REGRESSION COEFFICIENTS FOR THE SINGLE CORNER MODEL WITH  
CONSTANT MEDIUM STRESS DROP (M)

Freq. Hz	C1	C2	C4	C5	C6	C7	C8	C10	Parametric	Total
									Sigma	Sigma
0.1000	-20.75572	2.66436	1.40000	.00000	-1.08036	.04575	.00000	-.26225	.3507	1.3227
0.2000	-17.19667	2.37874	1.50000	.00000	-1.15935	.05081	.00000	-.33621	.3670	1.1936
0.3333	-14.06689	2.07919	1.70000	.00000	-1.28989	.06096	.00000	-.34445	.3828	1.0435
0.5000	-11.50543	1.80276	1.80000	.00000	-1.41313	.07203	.00000	-.32162	.4058	.9544
0.6250	-10.01702	1.63758	1.90000	.00000	-1.50425	.07995	.00000	-.29941	.4178	.8813
1.0000	-7.05566	1.29873	2.00000	.00000	-1.67870	.09627	.00000	-.23741	.4440	.7977
1.3333	-5.49548	1.11266	2.00000	.00000	-1.77199	.10566	.00000	-.19612	.4587	.8033
2.0000	-3.32938	.87752	2.10000	.00000	-1.93695	.11987	.00000	-.14101	.4886	.7656
2.5000	-2.17689	.76471	2.20000	.00000	-2.04747	.12821	.00000	-.11553	.5132	.7630
3.3333	-.91426	.64469	2.30000	.00000	-2.17662	.13662	.00000	-.08967	.5249	.7647
4.1667	-.25005	.57474	2.30000	.00000	-2.24507	.14078	.00000	-.07407	.5265	.7488
5.0000	.52720	.50677	2.40000	.00000	-2.36056	.14798	.00000	-.06377	.5331	.7452
6.2500	1.40962	.43574	2.50000	.00000	-2.50272	.15689	.00000	-.05410	.5473	.7479
6.6667	1.56684	.42291	2.50000	.00000	-2.52910	.15864	.00000	-.05189	.5512	.7518
8.3333	2.84539	.34310	2.70000	.00000	-2.75855	.17249	.00000	-.04589	.5704	.7705
10.0000	3.74250	.28811	2.80000	.00000	-2.91299	.18076	.00000	-.04184	.5949	.7762
12.5000	4.30142	.24798	2.80000	.00000	-3.01204	.18629	.00000	-.03854	.6114	.7826
14.2857	5.05068	.20098	2.90000	.00000	-3.16171	.19564	.00000	-.03820	.6016	.7744
16.6667	5.34872	.17298	2.90000	.00000	-3.23737	.20169	.00000	-.03779	.6020	.7773
18.1818	5.51993	.15239	2.90000	.00000	-3.27833	.20546	.00000	-.03730	.6010	.7723
20.0000	5.67485	.13971	2.90000	.00000	-3.31873	.20854	.00000	-.03723	.5994	.7733
25.0000	5.48446	.14693	2.80000	.00000	-3.31359	.20937	.00000	-.03769	.6096	.7783
31.0000	5.79121	.12122	2.80000	.00000	-3.38561	.21443	.00000	-.03713	.6215	.7844
40.0000	5.52760	.12078	2.70000	.00000	-3.36044	.21541	.00000	-.03717	.6227	.7821
50.0000	5.04282	.13496	2.60000	.00000	-3.29331	.21392	.00000	-.03869	.6175	.7798
100.000	2.73988	.22873	2.40000	.00000	-2.92178	.20135	.00000	-.04661	.5568	.7328
PGA	2.44059	.24664	2.40000	.00000	-2.86879	.19811	.00000	-.04758	.5512	.7292
PGV	.89599	.82861	1.90000	.00000	-2.34455	.18556	.00000	-.08813	.4429	-----

Table 4b  
SOUTH CAROLINA  
REGRESSION COEFFICIENTS FOR THE SINGLE CORNER MODEL WITH  
CONSTANT LOW STRESS DROP

Freq. Hz	C1	C2	C4	C5	C6	C7	C8	C10	Parametric	Total
									Sigma	Sigma
0.1000	-20.55815	2.60017	1.30000	.00000	-1.05537	.04356	.00000	-.29353	.3564	1.3243
0.2000	-16.73947	2.26764	1.50000	.00000	-1.15760	.05052	.00000	-.34549	.3760	1.1964
0.3333	-13.65946	1.95051	1.60000	.00000	-1.27073	.06054	.00000	-.33566	.3974	1.0491
0.5000	-10.99282	1.66012	1.80000	.00000	-1.41718	.07304	.00000	-.30030	.4203	.9608
0.6250	-9.68073	1.50191	1.80000	.00000	-1.48069	.07973	.00000	-.27288	.4303	.8875
1.0000	-6.85855	1.17422	1.90000	.00000	-1.65049	.09595	.00000	-.20544	.4512	.8016
1.3333	-5.24001	.99240	2.00000	.00000	-1.77350	.10692	.00000	-.16520	.4640	.8067
2.0000	-3.26924	.78397	2.10000	.00000	-1.93239	.12049	.00000	-.11585	.4929	.7681
2.5000	-2.22508	.68658	2.20000	.00000	-2.03913	.12843	.00000	-.09454	.5175	.7657
3.3333	-1.08416	.58402	2.30000	.00000	-2.16376	.13636	.00000	-.07370	.5293	.7682
4.1667	-.49842	.52540	2.30000	.00000	-2.22892	.14015	.00000	-.06141	.5307	.7516
5.0000	.21762	.46599	2.40000	.00000	-2.34043	.14691	.00000	-.05349	.5368	.7473
6.2500	1.03212	.40443	2.50000	.00000	-2.47694	.15518	.00000	-.04627	.5502	.7501
6.6667	1.17253	.39399	2.50000	.00000	-2.50179	.15673	.00000	-.04465	.5538	.7532
8.3333	2.39286	.32183	2.70000	.00000	-2.72488	.16988	.00000	-.04034	.5721	.7720
10.0000	3.25258	.27171	2.80000	.00000	-2.87481	.17765	.00000	-.03729	.5963	.7778
12.5000	3.77291	.23675	2.80000	.00000	-2.96790	.18244	.00000	-.03480	.6122	.7834
14.2857	4.48907	.19370	2.90000	.00000	-3.11130	.19106	.00000	-.03473	.6022	.7752
16.6667	4.75723	.16948	2.90000	.00000	-3.18064	.19633	.00000	-.03449	.6024	.7773
18.1818	4.41709	.18082	2.80000	.00000	-3.12981	.19436	.00000	-.03406	.6011	.7723
20.0000	4.55068	.17049	2.80000	.00000	-3.16561	.19693	.00000	-.03402	.5994	.7733
25.0000	4.84204	.15000	2.80000	.00000	-3.24440	.20240	.00000	-.03447	.6094	.7783
31.0000	5.12821	.12675	2.80000	.00000	-3.31113	.20681	.00000	-.03383	.6211	.7844
40.0000	4.85835	.12717	2.70000	.00000	-3.28306	.20739	.00000	-.03371	.6223	.7821
50.0000	4.37562	.14114	2.60000	.00000	-3.21479	.20573	.00000	-.03501	.6173	.7798
100.000	2.12732	.22793	2.40000	.00000	-2.84970	.19389	.00000	-.04184	.5571	.7336
PGA	1.83761	.24466	2.40000	.00000	-2.79850	.19087	.00000	-.04268	.5515	.7294
PGV	.46600	.81692	1.90000	.00000	-2.27508	.17831	.00000	-.09206	.4459	-----

Table 4c  
SOUTH CAROLINA  
REGRESSION COEFFICIENTS FOR THE SINGLE CORNER MODEL WITH  
CONSTANT HIGH STRESS DROP

Freq. Hz	C1	C2	C4	C5	C6	C7	C8	C10	Parametric	Total
									Sigma	Sigma
0.1000	-20.96056	2.71675	1.40000	.00000	-1.09530	.04814	.00000	-.22730	.3442	1.3212
0.2000	-17.49443	2.47125	1.60000	.00000	-1.18623	.05274	.00000	-.31935	.3598	1.1912
0.3333	-14.56214	2.20380	1.70000	.00000	-1.29165	.06102	.00000	-.34577	.3703	1.0392
0.5000	-12.02019	1.94074	1.80000	.00000	-1.41253	.07152	.00000	-.33650	.3906	.9481
0.6250	-10.51906	1.77922	1.90000	.00000	-1.50306	.07918	.00000	-.32073	.4034	.8748
1.0000	-7.48613	1.43919	2.00000	.00000	-1.67573	.09494	.00000	-.26795	.4347	.7922
1.3333	-5.64199	1.23261	2.10000	.00000	-1.80682	.10642	.00000	-.22804	.4524	.7998
2.0000	-3.49702	.98628	2.10000	.00000	-1.93942	.11890	.00000	-.16965	.4844	.7630
2.5000	-2.23447	.85817	2.20000	.00000	-2.05340	.12760	.00000	-.14044	.5092	.7603
3.3333	-.83895	.71930	2.30000	.00000	-2.18694	.13646	.00000	-.10939	.5205	.7620
4.1667	.19834	.61938	2.40000	.00000	-2.31041	.14402	.00000	-.09000	.5221	.7460
5.0000	.75953	.55896	2.40000	.00000	-2.37683	.14842	.00000	-.07686	.5290	.7423
6.2500	1.71843	.47717	2.50000	.00000	-2.52375	.15785	.00000	-.06412	.5441	.7457
6.6667	2.24624	.44033	2.60000	.00000	-2.61513	.16354	.00000	-.06112	.5483	.7496
8.3333	3.24012	.37282	2.70000	.00000	-2.78683	.17423	.00000	-.05284	.5685	.7690
10.0000	4.18107	.31199	2.80000	.00000	-2.94569	.18298	.00000	-.04739	.5934	.7755
12.5000	4.78769	.26535	2.80000	.00000	-3.05138	.18933	.00000	-.04289	.6105	.7818
14.2857	5.57485	.21375	2.90000	.00000	-3.20785	.19946	.00000	-.04210	.6011	.7744
16.6667	5.90954	.18105	2.90000	.00000	-3.29094	.20644	.00000	-.04136	.6019	.7766
18.1818	6.09980	.15805	2.90000	.00000	-3.33603	.21072	.00000	-.04075	.6010	.7723
20.0000	6.27420	.14292	2.90000	.00000	-3.38074	.21434	.00000	-.04059	.5997	.7733
25.0000	6.64603	.11313	2.90000	.00000	-3.47773	.22196	.00000	-.04099	.6103	.7791
31.0000	6.44287	.11766	2.80000	.00000	-3.46082	.22193	.00000	-.04049	.6223	.7852
40.0000	6.18975	.11580	2.70000	.00000	-3.43970	.22346	.00000	-.04070	.6236	.7829
50.0000	5.70463	.12993	2.60000	.00000	-3.37433	.22223	.00000	-.04245	.6182	.7806
100.000	3.73644	.20458	2.50000	.00000	-3.06845	.21379	.00000	-.05171	.5568	.7328
PGA	3.41869	.22434	2.50000	.00000	-3.01216	.21025	.00000	-.05284	.5510	.7290
PGV	1.56942	.82163	2.00000	.00000	-2.46320	.19656	.00000	-.08546	.4401	-----

Table 5a  
SOUTH CAROLINA  
REGRESSION COEFFICIENTS FOR THE SINGLE CORNER MODEL  
WITH CONSTANT MEDIUM STRESS DROP AND SATURATION

Freq. Hz	C1	C2	C4	C5	C6	C7	C8	C10	Parametric	Total
									Sigma	Sigma
0.1000	-19.49851	2.44358	1.60000	.00000	-1.33851	.09176	.00000	-.27226	.3535	1.3235
0.2000	-15.76713	2.14489	1.80000	.00000	-1.44976	.09921	.00000	-.34622	.3736	1.1955
0.3333	-12.68162	1.84290	1.90000	.00000	-1.57135	.10979	.00000	-.35445	.3918	1.0469
0.5000	-10.05969	1.55925	2.00000	.00000	-1.70560	.12218	.00000	-.33162	.4162	.9591
0.6250	-8.51490	1.38716	2.10000	.00000	-1.80673	.13133	.00000	-.30941	.4286	.8866
1.0000	-5.47426	1.03910	2.20000	.00000	-1.99534	.14929	.00000	-.24741	.4556	.8039
1.3333	-3.89260	.85098	2.20000	.00000	-2.09267	.15905	.00000	-.20613	.4708	.8102
2.0000	-1.64473	.60671	2.30000	.00000	-2.27192	.17484	.00000	-.15102	.5011	.7739
2.5000	-.41821	.48551	2.40000	.00000	-2.39510	.18462	.00000	-.12553	.5259	.7711
3.3333	.92932	.35642	2.50000	.00000	-2.53880	.19457	.00000	-.09967	.5377	.7737
4.1667	1.61284	.28534	2.50000	.00000	-2.61087	.19894	.00000	-.08407	.5392	.7580
5.0000	2.47822	.20789	2.60000	.00000	-2.74128	.20773	.00000	-.07378	.5456	.7538
6.2500	3.46248	.12632	2.70000	.00000	-2.90065	.21841	.00000	-.06411	.5599	.7568
6.6667	3.62759	.11304	2.70000	.00000	-2.92848	.22023	.00000	-.06190	.5639	.7606
8.3333	5.11216	.01138	2.90000	.00000	-3.19187	.23767	.00000	-.05589	.5844	.7809
10.0000	6.13834	-.05642	3.00000	.00000	-3.36770	.24805	.00000	-.05185	.6093	.7878
12.5000	6.73520	-.09898	3.00000	.00000	-3.47378	.25405	.00000	-.04855	.6243	.7928
14.2857	7.61948	-.15985	3.10000	.00000	-3.64537	.26565	.00000	-.04820	.6149	.7846
16.6667	7.94524	-.19015	3.10000	.00000	-3.72601	.27212	.00000	-.04780	.6154	.7874
18.1818	7.51087	-.16870	3.00000	.00000	-3.66142	.26868	.00000	-.04730	.6137	.7817
20.0000	7.67232	-.18185	3.00000	.00000	-3.70297	.27185	.00000	-.04724	.6121	.7834
25.0000	8.02069	-.20800	3.00000	.00000	-3.79370	.27856	.00000	-.04769	.6224	.7886
31.0000	8.35117	-.23555	3.00000	.00000	-3.86993	.28396	.00000	-.04714	.6345	.7948
40.0000	7.41237	-.18438	2.80000	.00000	-3.72699	.27609	.00000	-.04718	.6346	.7917
50.0000	6.86192	-.16191	2.70000	.00000	-3.64908	.27323	.00000	-.04870	.6289	.7885
100.000	4.84985	-.08535	2.60000	.00000	-3.33178	.26390	.00000	-.05662	.5686	.7420
PGA	4.53538	-.06647	2.60000	.00000	-3.27599	.26049	.00000	-.05758	.5630	.7382
PGV	2.58628	.55455	2.10000	.00000	-2.68278	.24143	.00000	-.09813	.4489	-----

Table 5b  
SOUTH CAROLINA  
REGRESSION COEFFICIENTS FOR THE SINGLE CORNER MODEL  
WITH CONSTANT LOW STRESS DROP AND SATURATION

Freq. Hz	C1	C2	C4	C5	C6	C7	C8	C10	Parametric	Total
									Sigma	Sigma
0.1000	-19.22315	2.37688	1.60000	.00000	-1.32848	.09002	.00000	-.30354	.3601	1.3254
0.2000	-15.44147	2.04218	1.70000	.00000	-1.42322	.09738	.00000	-.35549	.3837	1.1986
0.3333	-12.16021	1.70907	1.90000	.00000	-1.57394	.11033	.00000	-.34567	.4072	1.0529
0.5000	-9.54716	1.41649	2.00000	.00000	-1.70958	.12320	.00000	-.31030	.4309	.9653
0.6250	-8.22053	1.25676	2.00000	.00000	-1.77592	.13019	.00000	-.28289	.4412	.8929
1.0000	-5.32394	.92033	2.10000	.00000	-1.95912	.14797	.00000	-.21544	.4625	.8078
1.3333	-3.63748	.73048	2.20000	.00000	-2.09406	.16035	.00000	-.17521	.4756	.8131
2.0000	-1.58622	.51303	2.30000	.00000	-2.26702	.17549	.00000	-.12585	.5049	.7759
2.5000	-.46884	.40732	2.40000	.00000	-2.38628	.18485	.00000	-.10455	.5296	.7738
3.3333	.75586	.29579	2.50000	.00000	-2.52527	.19430	.00000	-.08371	.5415	.7765
4.1667	1.36003	.23615	2.50000	.00000	-2.59389	.19828	.00000	-.07141	.5428	.7602
5.0000	2.16308	.16737	2.60000	.00000	-2.72013	.20662	.00000	-.06349	.5488	.7560
6.2500	3.07766	.09545	2.70000	.00000	-2.87355	.21662	.00000	-.05627	.5622	.7590
6.6667	3.22568	.08459	2.70000	.00000	-2.89981	.21825	.00000	-.05466	.5660	.7628
8.3333	4.64940	-.00917	2.90000	.00000	-3.15639	.23494	.00000	-.05034	.5857	.7816
10.0000	5.63634	-.07192	3.00000	.00000	-3.32739	.24478	.00000	-.04729	.6102	.7885
12.5000	6.19239	-.10902	3.00000	.00000	-3.42712	.24999	.00000	-.04480	.6248	.7928
14.2857	7.04069	-.16563	3.10000	.00000	-3.59195	.26081	.00000	-.04473	.6152	.7853
16.6667	7.33406	-.19183	3.10000	.00000	-3.66580	.26644	.00000	-.04450	.6155	.7874
18.1818	6.89341	-.16928	3.00000	.00000	-3.59932	.26271	.00000	-.04406	.6135	.7817
20.0000	7.03853	-.18041	3.00000	.00000	-3.63716	.26541	.00000	-.04403	.6118	.7826
25.0000	7.35482	-.20260	3.00000	.00000	-3.72031	.27118	.00000	-.04447	.6220	.7886
31.0000	7.06323	-.18554	2.90000	.00000	-3.68550	.26862	.00000	-.04383	.6339	.7940
40.0000	6.73104	-.17676	2.80000	.00000	-3.64741	.26785	.00000	-.04371	.6339	.7909
50.0000	6.18299	-.15452	2.70000	.00000	-3.56843	.26482	.00000	-.04502	.6284	.7885
100.000	4.21704	-.08408	2.60000	.00000	-3.25598	.25607	.00000	-.05184	.5685	.7420
PGA	3.91273	-.06646	2.60000	.00000	-3.20209	.25288	.00000	-.05268	.5631	.7382
PGV	2.14049	.54448	2.10000	.00000	-2.61030	.23387	.00000	-.10207	.4513	-----



Table 5c  
SOUTH CAROLINA  
REGRESSION COEFFICIENTS FOR THE SINGLE CORNER MODEL  
WITH CONSTANT HIGH STRESS DROP AND SATURATION

Freq. Hz	C1	C2	C4	C5	C6	C7	C8	C10	Parametric	Total
									Sigma	Sigma
0.1000	-19.69964	2.49541	1.60000	.00000	-1.35424	.09427	.00000	-.23731	.3464	1.3217
0.2000	-16.16105	2.24103	1.80000	.00000	-1.45825	.10047	.00000	-.32935	.3653	1.1930
0.3333	-13.17561	1.96739	1.90000	.00000	-1.57341	.10989	.00000	-.35578	.3785	1.0421
0.5000	-10.39119	1.68495	2.10000	.00000	-1.73909	.12390	.00000	-.34651	.4005	.9523
0.6250	-9.01636	1.52890	2.10000	.00000	-1.80570	.13054	.00000	-.33074	.4139	.8794
1.0000	-5.90447	1.17978	2.20000	.00000	-1.99249	.14792	.00000	-.27796	.4465	.7988
1.3333	-3.98706	.96465	2.30000	.00000	-2.13635	.16089	.00000	-.23804	.4648	.8067
2.0000	-1.53095	.69527	2.40000	.00000	-2.32575	.17750	.00000	-.17966	.4974	.7714
2.5000	-.47383	.57909	2.40000	.00000	-2.40142	.18398	.00000	-.15044	.5223	.7691
3.3333	1.00761	.43107	2.50000	.00000	-2.54967	.19440	.00000	-.11939	.5339	.7709
4.1667	2.13449	.32163	2.60000	.00000	-2.68835	.20357	.00000	-.10000	.5354	.7552
5.0000	2.71500	.26001	2.60000	.00000	-2.75836	.20818	.00000	-.08687	.5421	.7517
6.2500	3.77719	.16754	2.70000	.00000	-2.92274	.21940	.00000	-.07412	.5572	.7553
6.6667	4.39753	.12042	2.80000	.00000	-3.02933	.22679	.00000	-.07112	.5616	.7591
8.3333	5.51538	.04067	2.90000	.00000	-3.22165	.23948	.00000	-.06285	.5830	.7801
10.0000	6.58742	-.03320	3.00000	.00000	-3.40224	.25038	.00000	-.05740	.6082	.7870
12.5000	7.23410	-.08251	3.00000	.00000	-3.51535	.25724	.00000	-.05290	.6238	.7920
14.2857	8.15944	-.14834	3.10000	.00000	-3.69429	.26969	.00000	-.05210	.6147	.7846
16.6667	8.52466	-.18367	3.10000	.00000	-3.78287	.27715	.00000	-.05137	.6156	.7874
18.1818	8.73233	-.20849	3.10000	.00000	-3.83113	.28176	.00000	-.05076	.6140	.7825
20.0000	8.92221	-.22488	3.10000	.00000	-3.87857	.28560	.00000	-.05060	.6127	.7834
25.0000	8.66995	-.21066	3.00000	.00000	-3.86665	.28566	.00000	-.05100	.6232	.7893
31.0000	9.02849	-.24163	3.00000	.00000	-3.94975	.29191	.00000	-.05050	.6354	.7956
40.0000	8.68242	-.23353	2.90000	.00000	-3.91406	.29188	.00000	-.05071	.6356	.7925
50.0000	7.53592	-.16817	2.70000	.00000	-3.73234	.28177	.00000	-.05246	.6298	.7893
100.000	5.47014	-.08443	2.60000	.00000	-3.40962	.27179	.00000	-.06172	.5689	.7420
PGA	5.14426	-.06415	2.60000	.00000	-3.35183	.26815	.00000	-.06285	.5632	.7383
PGV	3.01933	.56635	2.10000	.00000	-2.75593	.24888	.00000	-.09546	.4467	-----

Table 6  
SOUTH CAROLINA  
REGRESSION COEFFICIENTS FOR THE DOUBLE CORNER MODEL

Freq. Hz	C1	C2	C4	C5	C6	C7	C8	C10	Parametric	Total
									Sigma	Sigma
0.1000	-18.93236	2.27993	1.40000	.00000	-1.06291	.04229	.00000	-.31157	.3573	1.3246
0.2000	-15.32941	1.96381	1.60000	.00000	-1.16602	.04855	.00000	-.28613	.3696	1.1942
0.3333	-12.69571	1.72502	1.70000	.00000	-1.28057	.05826	.00000	-.22678	.3852	1.0446
0.5000	-10.65171	1.53696	1.80000	.00000	-1.41349	.07071	.00000	-.17758	.4102	.9565
0.6250	-9.46782	1.43351	1.90000	.00000	-1.51015	.07943	.00000	-.15705	.4239	.8842
1.0000	-7.11822	1.23406	2.00000	.00000	-1.69182	.09700	.00000	-.13487	.4531	.8027
1.3333	-5.79677	1.11610	2.00000	.00000	-1.78608	.10679	.00000	-.12968	.4684	.8090
2.0000	-3.73490	.93677	2.10000	.00000	-1.94936	.12121	.00000	-.12104	.4972	.7714
2.5000	-2.52562	.83241	2.20000	.00000	-2.05788	.12956	.00000	-.11290	.5207	.7677
3.3333	-1.13018	.70786	2.30000	.00000	-2.18295	.13777	.00000	-.10011	.5309	.7689
4.1667	-.35177	.62905	2.30000	.00000	-2.24581	.14133	.00000	-.08941	.5314	.7524
5.0000	.51391	.55291	2.40000	.00000	-2.35535	.14773	.00000	-.08074	.5373	.7481
6.2500	1.49696	.47163	2.50000	.00000	-2.49086	.15563	.00000	-.07112	.5514	.7509
6.6667	1.68117	.45595	2.50000	.00000	-2.51565	.15710	.00000	-.06869	.5555	.7547
8.3333	3.02922	.36865	2.70000	.00000	-2.73792	.16992	.00000	-.06161	.5755	.7742
10.0000	3.96807	.30969	2.80000	.00000	-2.88687	.17721	.00000	-.05645	.5996	.7801
12.5000	5.06042	.23658	2.90000	.00000	-3.07011	.18687	.00000	-.05144	.6155	.7857
14.2857	5.39001	.21283	2.90000	.00000	-3.14219	.19157	.00000	-.05016	.6062	.7783
16.6667	5.76317	.17770	2.90000	.00000	-3.23069	.19853	.00000	-.04874	.6069	.7804
18.1818	5.97780	.15309	2.90000	.00000	-3.27987	.20285	.00000	-.04765	.6057	.7755
20.0000	6.72839	.10286	3.00000	.00000	-3.42641	.21245	.00000	-.04709	.6044	.7772
25.0000	7.17691	.06703	3.00000	.00000	-3.53823	.22097	.00000	-.04667	.6152	.7830
31.0000	7.00112	.06791	2.90000	.00000	-3.52780	.22143	.00000	-.04532	.6271	.7892
40.0000	6.77623	.06147	2.80000	.00000	-3.51436	.22369	.00000	-.04456	.6282	.7869
50.0000	6.29650	.07241	2.70000	.00000	-3.45328	.22311	.00000	-.04543	.6231	.7845
100.000	4.24595	.14544	2.60000	.00000	-3.14071	.21510	.00000	-.05128	.5625	.7374
PGA	3.49869	.19289	2.50000	.00000	-3.00815	.20682	.00000	-.05234	.5568	.7334
PGV	2.84051	.54156	2.10000	.00000	-2.47969	.18992	.00000	-.07781	.4470	-----

NOTE: PARAMETRIC SIGMA VALUES TAKEN FROM THE 1 CORNER VARIABLE STRESS DROP (MEDIUM) MODEL

Table 7  
SOUTH CAROLINA  
REGRESSION COEFFICIENTS FOR THE DOUBLE CORNER MODEL WITH SATURATION

Freq. Hz	C1	C2	C4	C5	C6	C7	C8	C10	Parametric	Total
									Sigma	Sigma
0.1000	-17.70361	2.06827	1.60000	.00000	-1.31801	.08712	.00000	-.32461	.3535	1.3235
0.2000	-13.92420	1.72207	1.80000	.00000	-1.45428	.09906	.00000	-.29911	.3736	1.1955
0.3333	-10.94321	1.43698	2.00000	.00000	-1.63284	.11719	.00000	-.23803	.3918	1.0469
0.5000	-8.83343	1.24320	2.10000	.00000	-1.77711	.13055	.00000	-.18835	.4162	.9591
0.6250	-7.76737	1.14287	2.10000	.00000	-1.85115	.13862	.00000	-.16740	.4286	.8866
1.0000	-5.33824	.93368	2.20000	.00000	-2.04663	.15785	.00000	-.14480	.4556	.8039
1.3333	-3.73678	.79317	2.30000	.00000	-2.19225	.17169	.00000	-.13937	.4708	.8102
2.0000	-1.84742	.62360	2.30000	.00000	-2.32294	.18424	.00000	-.13061	.5011	.7739
2.5000	-.55724	.50916	2.40000	.00000	-2.44529	.19431	.00000	-.12238	.5259	.7711
3.3333	.92868	.37406	2.50000	.00000	-2.58582	.20432	.00000	-.10951	.5377	.7737
4.1667	1.72573	.29401	2.50000	.00000	-2.65212	.20809	.00000	-.09876	.5392	.7580
5.0000	2.68457	.20711	2.60000	.00000	-2.77743	.21630	.00000	-.09004	.5456	.7538
6.2500	3.77386	.11416	2.70000	.00000	-2.93085	.22616	.00000	-.08037	.5599	.7568
6.6667	3.96591	.09800	2.70000	.00000	-2.95707	.22772	.00000	-.07792	.5639	.7606
8.3333	5.53031	-.01361	2.90000	.00000	-3.21501	.24453	.00000	-.07080	.5844	.7809
10.0000	6.60366	-.08665	3.00000	.00000	-3.38623	.25414	.00000	-.06561	.6093	.7878
12.5000	7.85421	-.17609	3.10000	.00000	-3.59574	.26651	.00000	-.06058	.6243	.7928
14.2857	8.21088	-.20169	3.10000	.00000	-3.67264	.27153	.00000	-.05926	.6149	.7846
16.6667	9.28186	-.28645	3.20000	.00000	-3.88204	.28695	.00000	-.05782	.6154	.7874
18.1818	9.52717	-.31412	3.20000	.00000	-3.93679	.29184	.00000	-.05671	.6137	.7817
20.0000	9.75655	-.33358	3.20000	.00000	-3.99128	.29606	.00000	-.05613	.6121	.7834
25.0000	10.24743	-.37291	3.20000	.00000	-4.11053	.30519	.00000	-.05567	.6224	.7886
31.0000	9.96722	-.35918	3.10000	.00000	-4.08417	.30364	.00000	-.05429	.6345	.7948
40.0000	9.64059	-.35408	3.00000	.00000	-4.05492	.30409	.00000	-.05350	.6346	.7917
50.0000	9.04691	-.33098	2.90000	.00000	-3.97551	.30155	.00000	-.05435	.6289	.7885
100.000	6.27888	-.20223	2.70000	.00000	-3.53646	.28388	.00000	-.06025	.5686	.7420
PGA	5.93818	-.18201	2.70000	.00000	-3.47772	.28050	.00000	-.06133	.5630	.7382
PGV	4.53013	.23834	2.20000	.00000	-2.81686	.25116	.00000	-.08693	.4489	-----

NOTE: PARAMETRIC SIGMA VALUES TAKEN FROM THE 1 CORNER VARIABLE STRESS DROP WITH SATURATION (MEDIUM) MODEL

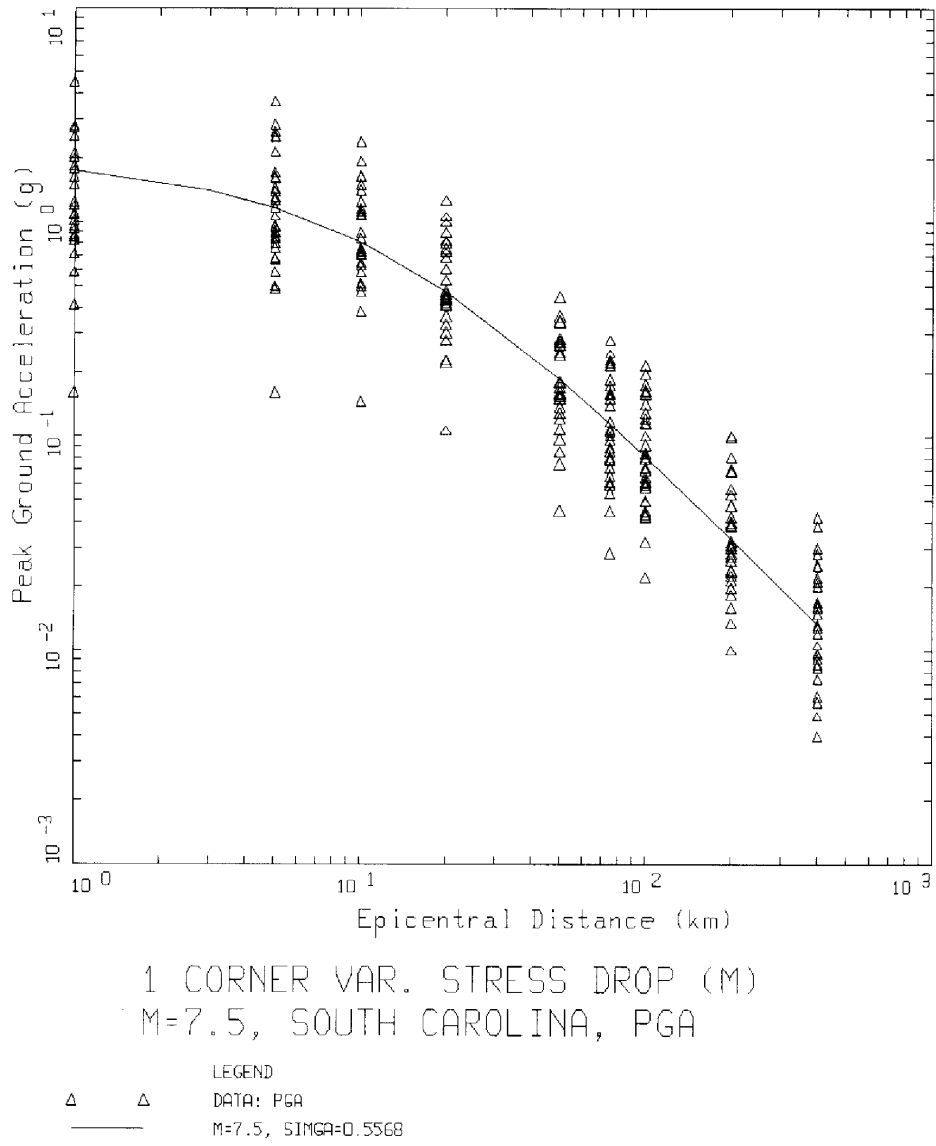
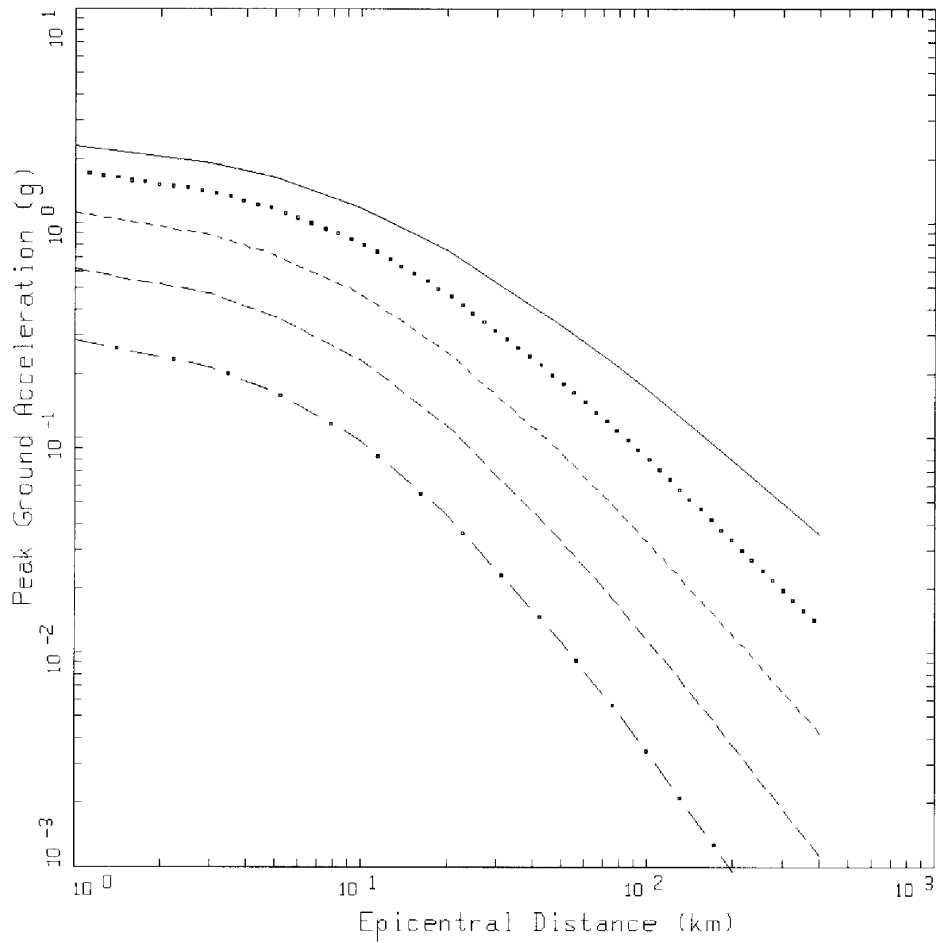


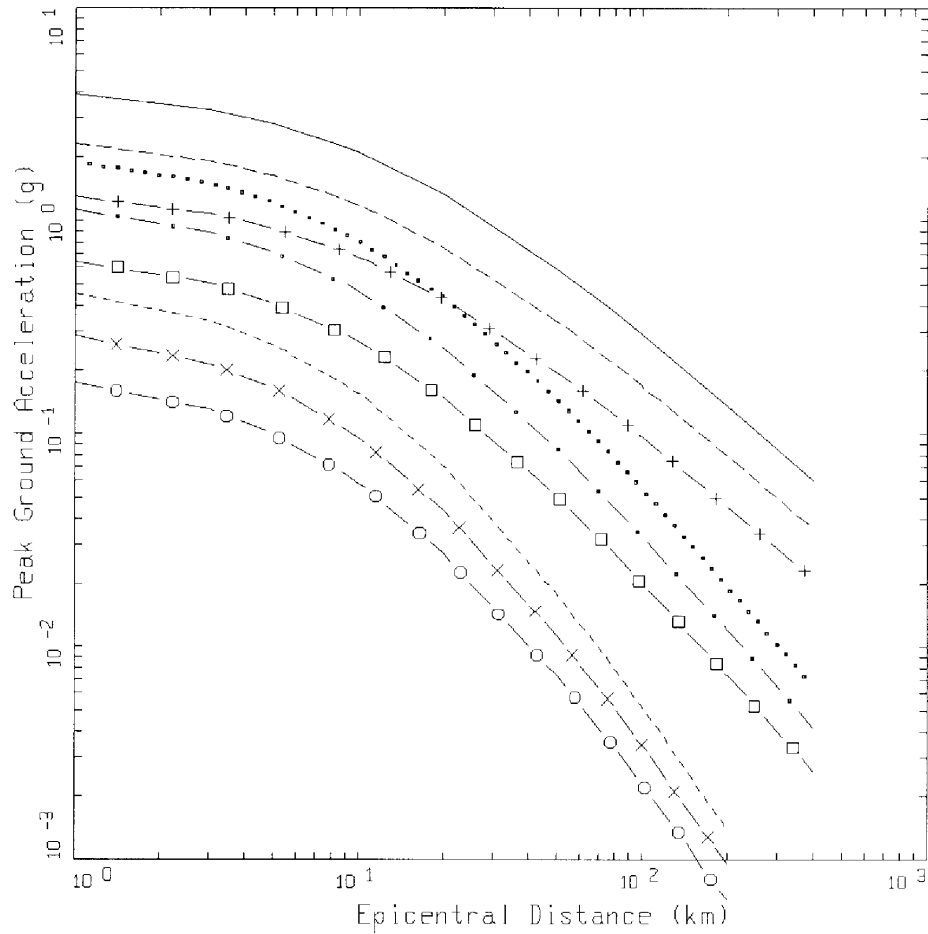
Figure 1. Peak acceleration estimates and regression fit at **M** 7.5 for the single corner model with variable (medium) stress drop, South Carolina.



1 CORNER VAR. STRESS DROP (M)  
SOUTH CAROLINA, PGA

- LEGEND
- M=8.5, SIGMA=0.5568
  - ..... M=7.5, SIGMA=0.5568
  - M=6.5, SIGMA=0.5568
  - · - · M=5.5, SIGMA=0.5568
  - - - - M=4.5, SIGMA=0.5568

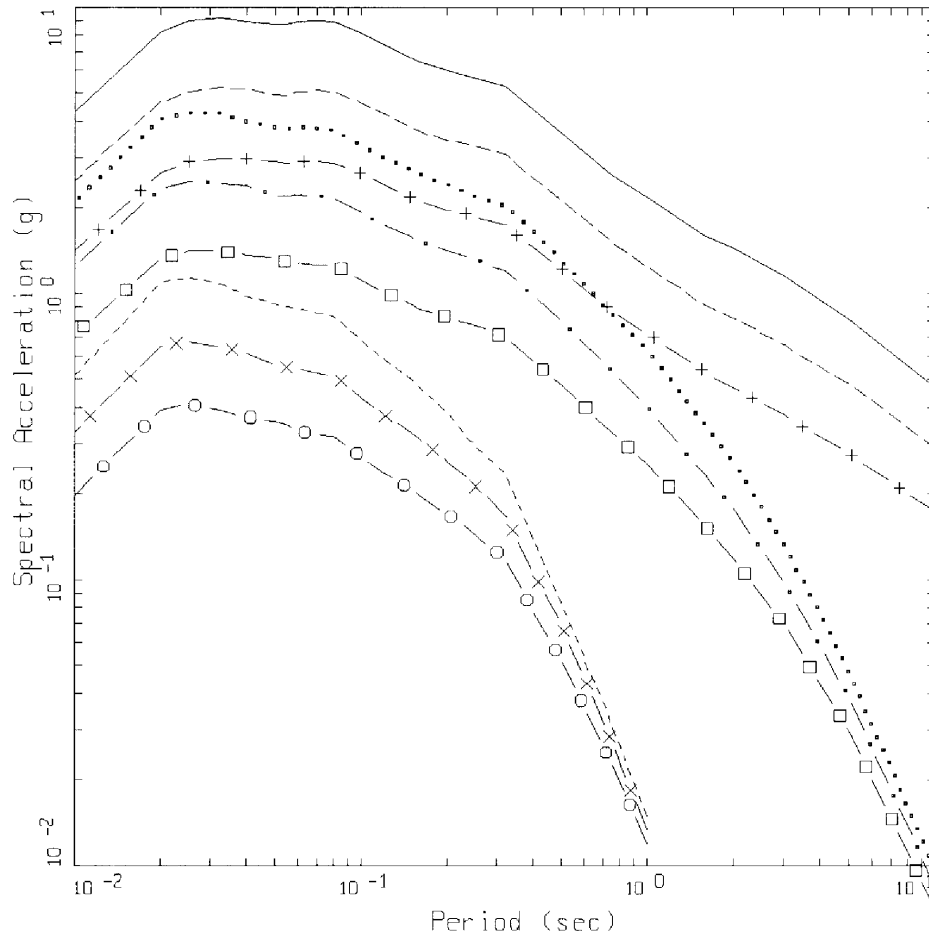
Figure 2a. Attenuation of median peak horizontal accelerations at **M** 4.5, 5.5, 6.5, 7.5 and 8.5 for the single corner model with variable (medium) stress drop, South Carolina.



1 CORNER VARIABLE STRESS DROP  
SOUTH CAROLINA, PGA

- LEGEND
- M=8.5, HIGH STRESS DROP, SIGMA=0.5568
  - ..... M=6.5, HIGH STRESS DROP, SIGMA=0.5568
  - M=4.5, HIGH STRESS DROP, SIGMA=0.5568
  - - - - M=8.5, MEDIUM STRESS DROP, SIGMA=0.5568
  - · - · M=6.5, MEDIUM STRESS DROP, SIGMA=0.5568
  - × - M=4.5, MEDIUM STRESS DROP, SIGMA=0.5568
  - + - M=8.5, LOW STRESS DROP, SIGMA=0.5571
  - □ - M=6.5, LOW STRESS DROP, SIGMA=0.5571
  - ○ - M=4.5, LOW STRESS DROP, SIGMA=0.5571

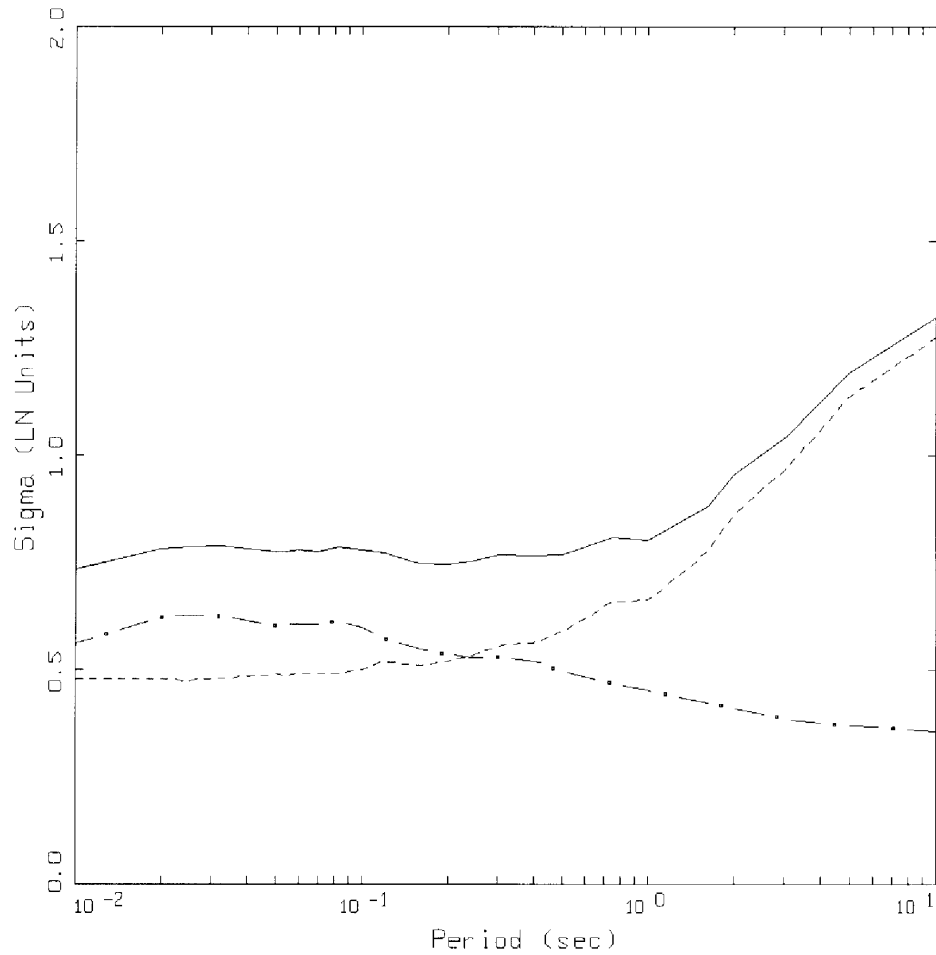
Figure 2b. Attenuation of median peak horizontal accelerations at **M** 4.5, 5.5, 6.5, 7.5 and 8.5 for the single corner model with variable stress drop, South Carolina, effect of stress drop.



1 CORNER VARIABLE STRESS DROP  
 DISTANCE=1KM, SOUTH CAROLINA, SA

LEGEND	
————	M=8.5, HIGH STRESS DROP
.....	M=6.5, HIGH STRESS DROP
-----	M=4.5, HIGH STRESS DROP
-----	M=8.5, MEDIUM STRESS DROP
— · —	M=6.5, MEDIUM STRESS DROP
— × —	M=4.5, MEDIUM STRESS DROP
— + —	M=8.5, LOW STRESS DROP
— □ —	M=6.5, LOW STRESS DROP
— ○ —	M=4.5, LOW STRESS DROP

Figure 3. Median response spectra (5% damping) at a distance of 1 km for magnitudes  $M$  4.5, 5.5, 6.5, 7.5, and 8.5 for the single corner model with variable stress drop, South Carolina, effect of stress drop.



1 CORNER VAR. STRESS DROP (M)  
 SOUTH CAROLINA, SIGMA

- LEGEND
- TOTAL SIGMA
  - • - PARAMETRIC SIGMA
  - · - MODELING SIGMA (BIAS CORRECTED)

Figure 4. Estimates of total variability (uncertainty) for the South Carolina attenuation model. Parametric variability is due to variation of variable (median) stress drop, single corner frequency point-source parameters (Table 2), and fit of regression model (Table 3a). Model variability is from validation exercises with 16 earthquakes ( $M$  5.3 to 7.4) at 500 sites over the fault distance range of 1 to 460 km (Appendix B).



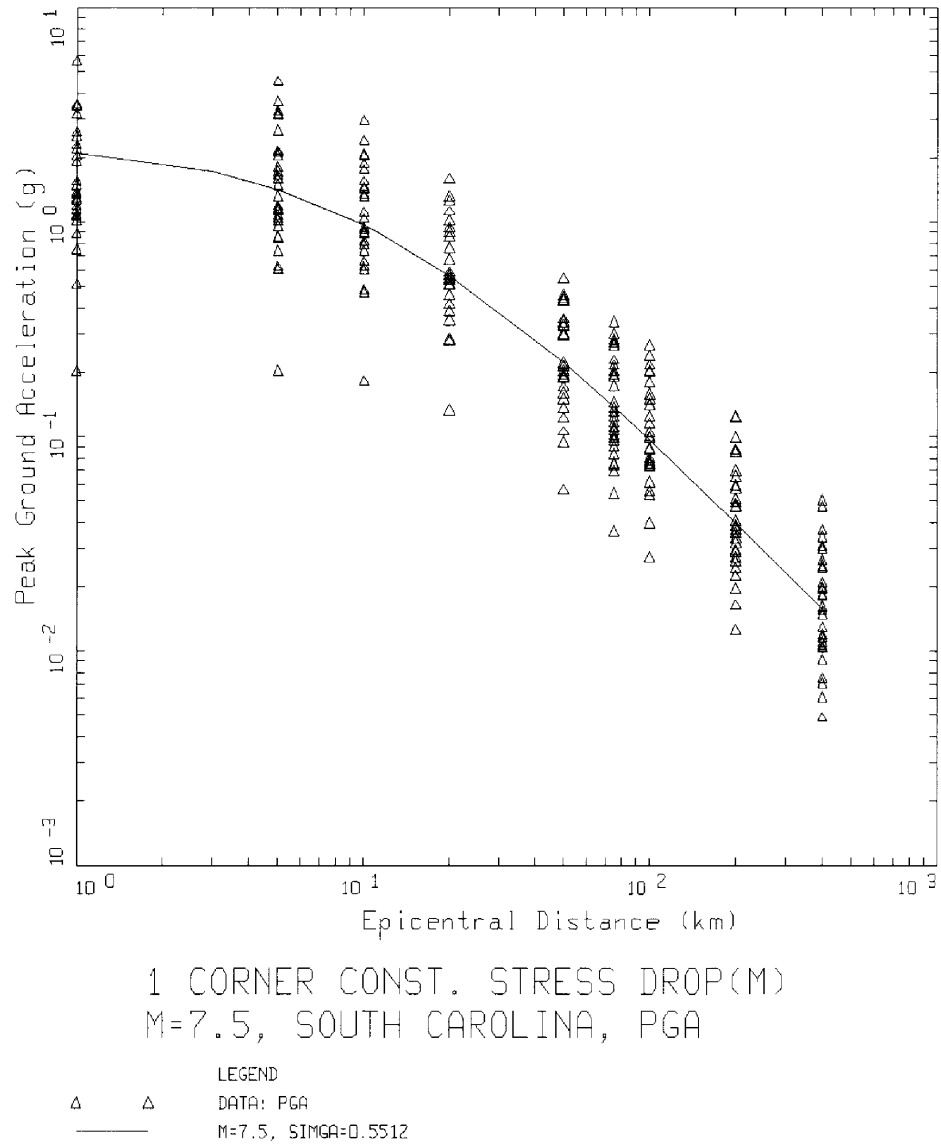
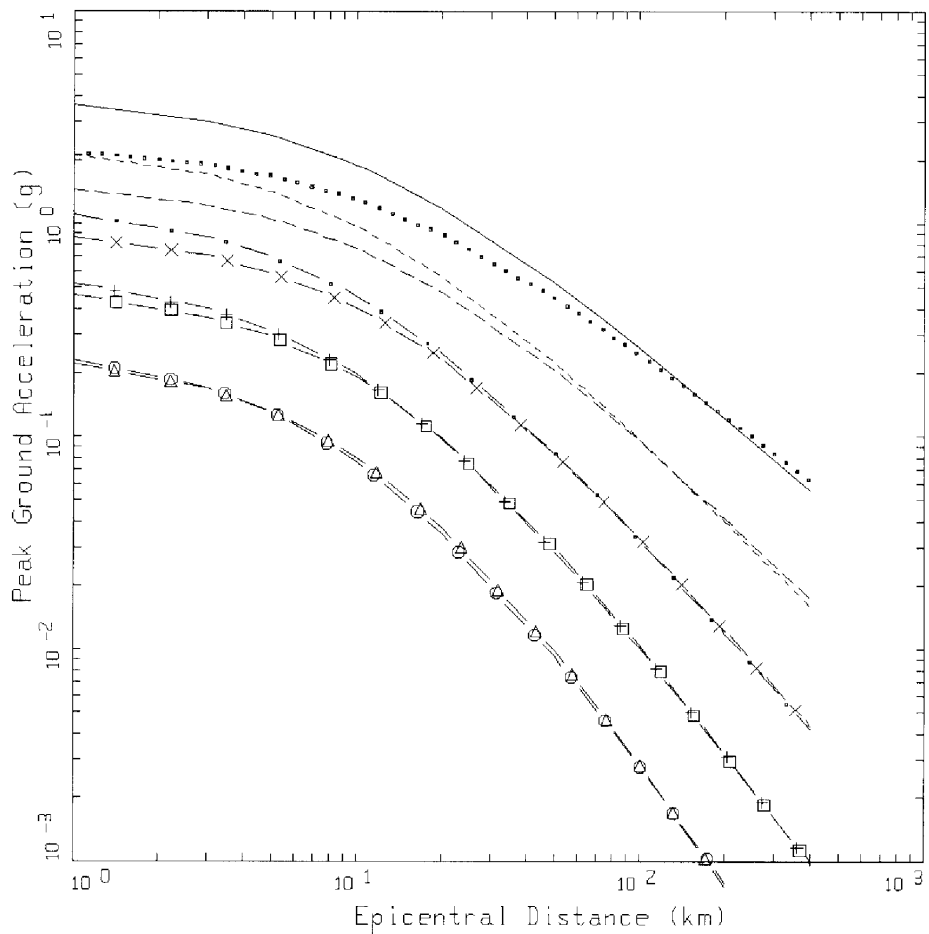


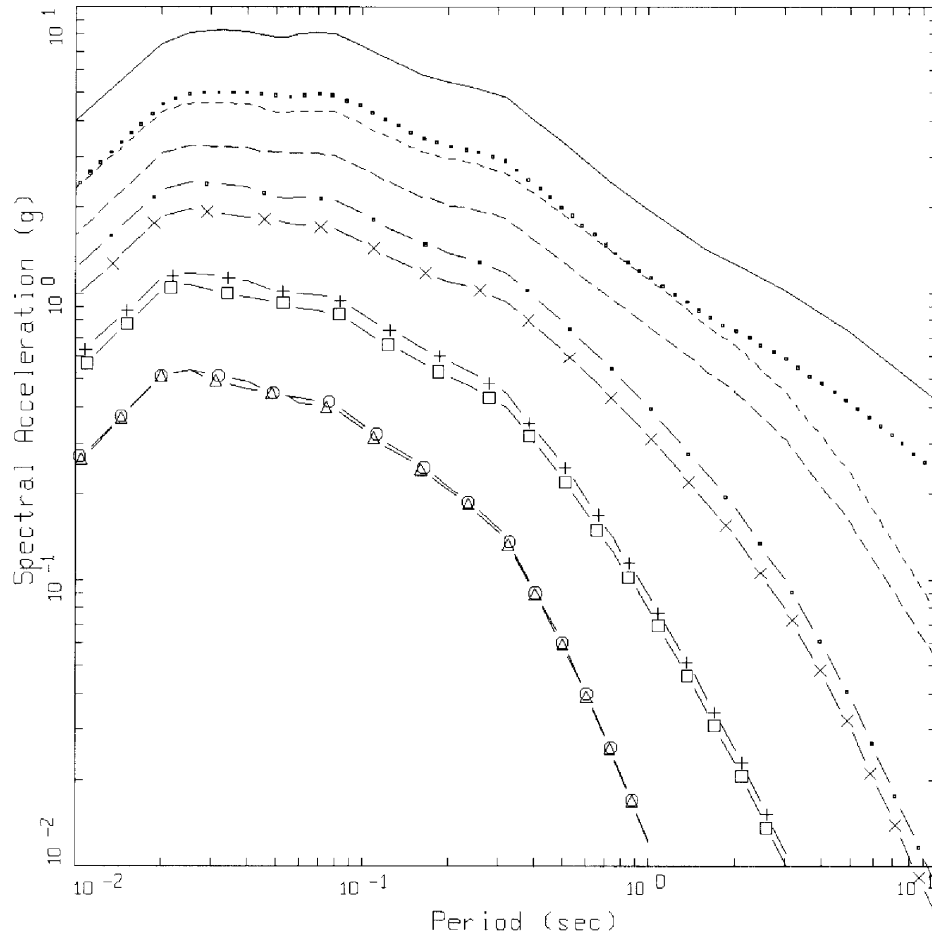
Figure 5. Peak acceleration estimates and regression fit at **M** 7.5 for the single corner model with constant (medium) stress drop, South Carolina.



1 CORNER CONST. STRESS DROP(M)  
SOUTH CAROLINA, PGA

- LEGEND
- M=8.5, SIGMA=0.5512
  - M=7.5, SIGMA=0.5512
  - • — M=6.5, SIGMA=0.5512
  - + — M=5.5, SIGMA=0.5512
  - ○ — M=4.5, SIGMA=0.5512
  - M=8.5 WITH SATURATION, SIGMA=0.5630
  - M=7.5 WITH SATURATION, SIGMA=0.5630
  - × — M=6.5 WITH SATURATION, SIGMA=0.5630
  - □ — M=5.5 WITH SATURATION, SIGMA=0.5630
  - △ — M=4.5 WITH SATURATION, SIGMA=0.5630

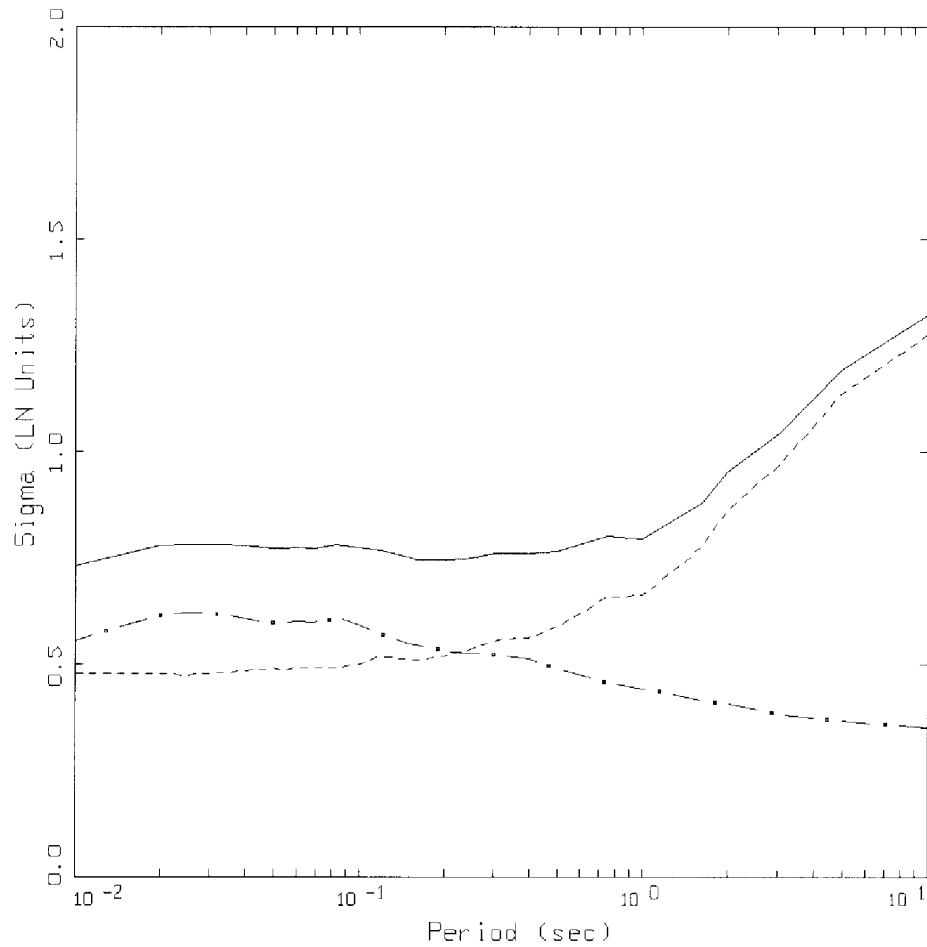
Figure 6. Attenuation of median peak horizontal accelerations at **M** 4.5, 5.5, 6.5, 7.5, and 8.5 for the single corner model with constant (medium) stress drop, with and without saturation, South Carolina.



1 CORNER CONST. STRESS DROP(M)  
 DISTANCE=1KM, SOUTH CAROLINA, SA

- LEGEND
- M=8.5
  - M=7.5
  - · - M=6.5
  - + - M=5.5
  - o - M=4.5
  - M=8.5 WITH SATURATION
  - M=7.5 WITH SATURATION
  - · · - M=6.5 WITH SATURATION
  - x - M=5.5 WITH SATURATION
  - □ - M=4.5 WITH SATURATION
  - △ - M=4.5 WITH SATURATION

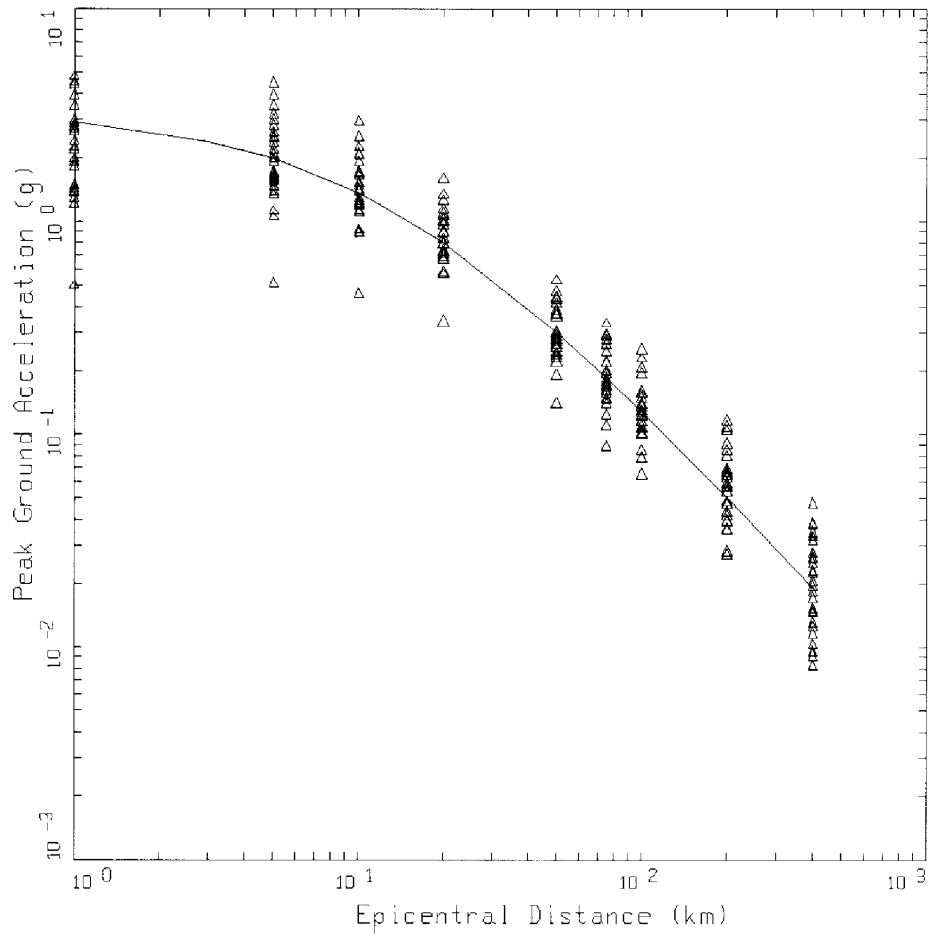
Figure 7. Median response spectra (5% damping) at a distance of 1 km for magnitudes **M** 4.5, 5.5, 6.5, 7.5, and 8.5 for the single corner model with constant (medium) stress drop, with and without saturation, South Carolina.



1 CORNER CONST. STRESS DROP(M)  
SOUTH CAROLINA, SIGMA

LEGEND  
 ——— TOTAL SIGMA  
 - · - PARAMETRIC SIGMA  
 - - - MODELING SIGMA (BIAS CORRECTED)

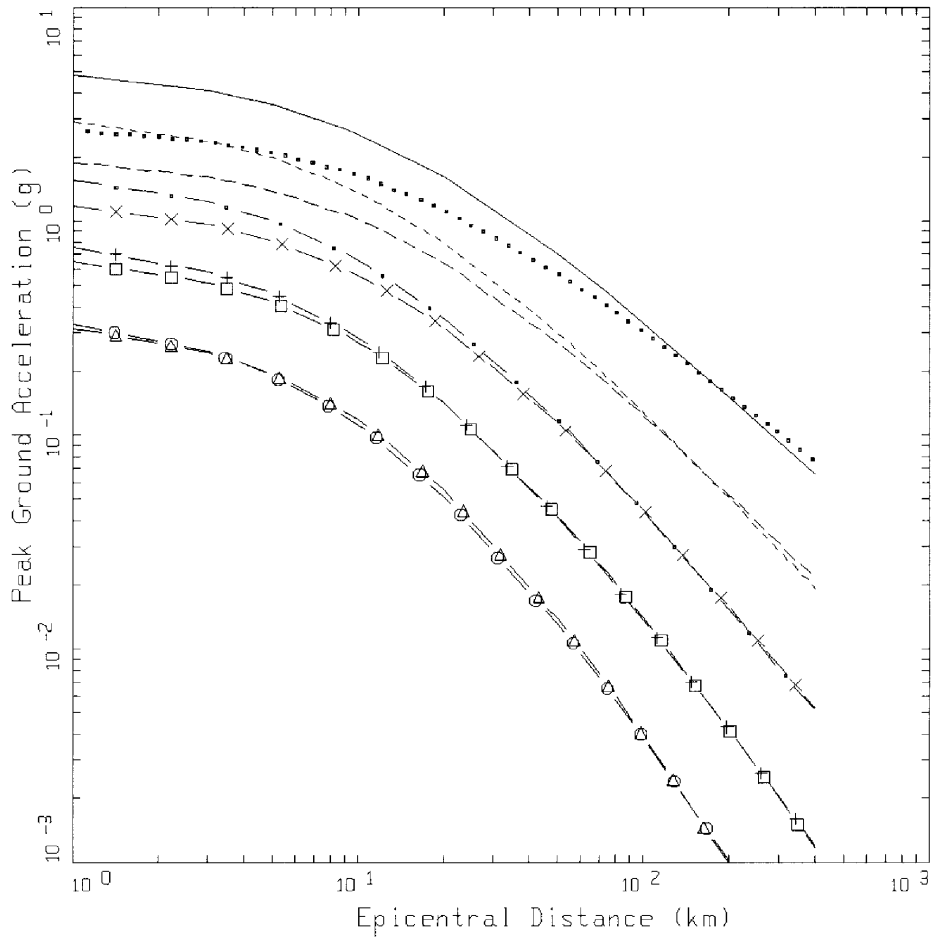
Figure 8. Estimates of total variability (uncertainty) for the South Carolina attenuation model. Parametric variability is due to variation of constant (medium) stress drop, single corner frequency point-source parameters (Table 2), and fit of regression model (Table 4a). Model variability is from validation exercises with 16 earthquakes ( $M$  5.3 to 7.4) at 500 sites over the fault distance range of 1 to 460 km (Appendix B).



2 CORNER  
M=7.5, SOUTH CAROLINA, PGA

LEGEND  
△ DATA: PGA  
— M=7.5, SIGMA=0.3814

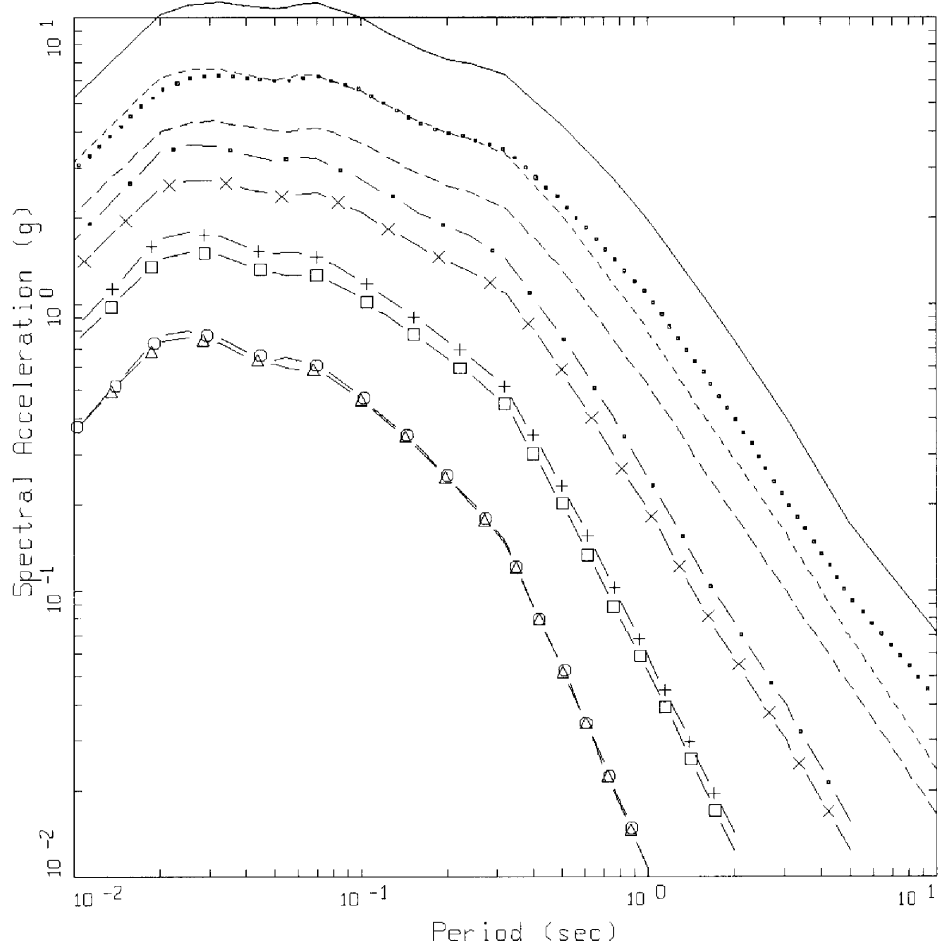
Figure 9. Peak acceleration estimates and regression fit at **M** 7.5 for the double corner model, South Carolina.



2 CORNER  
SOUTH CAROLINA, PGA

- LEGEND
- M=8.5, SIGMA=0.3814
  - M=7.5, SIGMA=0.3814
  - · - · M=6.5, SIGMA=0.3814
  - + - M=5.5, SIGMA=0.3814
  - o - M=4.5, SIGMA=0.3814
  - M=8.5 WITH SATURATION, SIGMA=0.4134
  - M=7.5 WITH SATURATION, SIGMA=0.4134
  - x - M=6.5 WITH SATURATION, SIGMA=0.4134
  - □ - M=5.5 WITH SATURATION, SIGMA=0.4134
  - △ - M=4.5 WITH SATURATION, SIGMA=0.4134

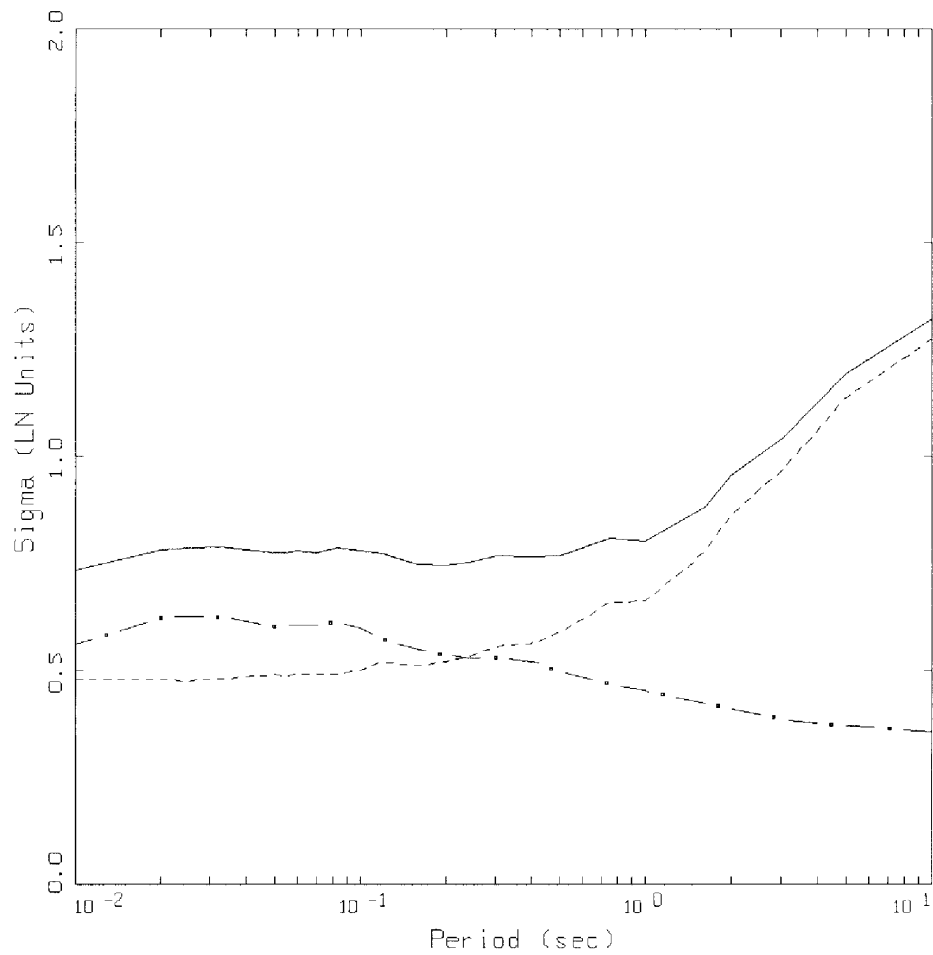
Figure 10. Attenuation of median peak horizontal accelerations at **M** 4.5, 5.5, 6.5, 7.5, and 8.5 for the double corner model, with and without saturation, South Carolina.



2 CORNER  
 DISTANCE=1KM, SOUTH CAROLINA, SA

- LEGEND
- M=8.5
  - - - M=7.5
  - · - M=6.5
  - + - M=5.5
  - ○ - M=4.5
  - · · M=8.5 WITH SATURATION
  - - - M=7.5 WITH SATURATION
  - × - M=6.5 WITH SATURATION
  - □ - M=5.5 WITH SATURATION
  - △ - M=4.5 WITH SATURATION

Figure 11. Median response spectra (5% damping) at a distance of 1 km for magnitudes **M** 4.5, 5.5, 6.5, 7.5, and 8.5 for the double corner model, South Carolina.



2 CORNER  
SOUTH CAROLINA, SIGMA

- LEGEND
- TOTAL SIGMA
  - · - PARAMETRIC SIGMA (TAKEN FROM 1 CORNER VAR. MEDIUM SD MODEL)
  - · - · MODELING SIGMA (BIAS CORRECTED)

Figure 12b. Estimates of total variability (uncertainty) for the South Carolina attenuation model. Parametric variability is due to variation of variable stress drop, single corner frequency point-source parameters (Table 2) and fit of regression model (Table 6a). Model variability is from validation exercises with 16 earthquakes ( $M$  5.3 to 7.4) at 500 sites over the fault distance range of 1 to 460 km using the single corner frequency model (Appendix B).





## APPENDIX A

### STOCHASTIC GROUND MOTION MODEL DESCRIPTION

#### Background

In the context of strong ground motion, the term "stochastic" can be a fearful concept to some and may be interpreted to represent a fundamentally incorrect or inappropriate model (albeit the many examples demonstrating that it works well; Boore, 1983, 1986). To allay any initial misgivings, a brief discussion seems prudent to explain the term stochastic in the stochastic ground motion model.

The stochastic point-source model may be termed a spectral model in that it fundamentally describes the Fourier amplitude spectral density at the surface of a half-space (Hanks and McGuire, 1981). The model uses a Brune (1970, 1971) omega-square description of the earthquake source Fourier amplitude spectral density. This model is easily the most widely used and qualitatively validated source description available. Seismic sources ranging from  $M = -6$  (hydrofracture) to  $M = 8$  have been interpreted in terms of the Brune omega-square model in dozens of papers over the last 30 years. The general conclusion is that it provides a reasonable and consistent representation of crustal sources, particularly for tectonically active regions such as plate margins. A unique phase spectrum can be associated with the Brune source amplitude spectrum to produce a complex spectrum which can be propagated using either exact or approximate (1-2- or 3-D) wave propagation algorithms to produce single or multiple component time histories. In this context the model is not stochastic, it is decidedly deterministic and as exact and rigorous as one chooses. A two-dimensional array of such point-sources may be appropriately located on a fault surface (area) and fired with suitable delays to simulate rupture propagation on an extended rupture plane. As with the single point-source, any degree of rigor may be used in the wave propagation algorithm to produce multiple component or average horizontal component time histories. The result is a kinematic<sup>1</sup> finite-source model which has as its basis a source time history defined as a Brune pulse whose Fourier amplitude spectrum follows an omega-square model. This finite-fault model would be very similar to that used in published inversions for slip models if the 1-D propagation were treated using a reflectivity algorithm (Aki and Richards, 1980). This algorithm is a complete solution to the wave equation from static offsets (near-field terms) to an arbitrarily selected high frequency cutoff (generally 1-2 Hz).

Alternatively, to model the wave propagation more accurately, recordings of small earthquakes at the site of interest and with source locations distributed along the fault of interest may be used as empirical Green functions (Hartzell, 1978). To model the design earthquake, the empirical Green functions are delayed and summed in a manner to simulate rupture propagation (Hartzell, 1978). Provided a sufficient number of small

---

<sup>1</sup>Kinematic source model is one whose slip (displacement) is defined (imposed) while in a dynamic source model forces (stress) are defined (see Aki and Richards 1980 for a complete description).

## APPENDIX A

earthquakes are recorded at the site of interest, the source locations adequately cover the expected rupture surface, and sufficient low frequency energy is present in the Green functions, this would be the most appropriate procedure to use if nonlinear site response is not an issue. With this approach the wave propagation is, in principle, exactly represented from each Green function source to the site. However, nonlinear site response is not treated unless Green function motions are recorded at a nearby rock outcrop with dynamic material properties similar to the rock underlying the soils at the site or recordings are made at depth within the site soil column. These motions may then be used as input to either total or effective stress site response codes to model nonlinear effects. Important issues associated with this approach include the availability of an appropriate nearby (1 to 2 km) rock outcrop and, for the downhole recordings, the necessity to remove all downgoing energy from the at-depth soil recordings. The downgoing energy must be removed from the downhole Green functions (recordings) prior to generating the control motions (summing) as only the upgoing wavefields are used as input to the nonlinear site response analyses. Removal of the downgoing energy from each recording requires multiple site response analyses which introduce uncertainty into the Green functions due to uncertainty in dynamic material properties and the numerical site response model used to separate the upgoing and downgoing wavefields.

To alleviate these difficulties one can use recordings well distributed in azimuth at close distances to a small earthquake and correct the recordings back to the source by removing wave propagation effects using a simple approximation (say  $1/R$  plus a constant for crustal amplification and radiation pattern), to obtain an empirical source function. This source function can be used to replace the Brune pulse to introduce some natural (although source, path, and site specific) variation into the dislocation time history. If this is coupled to an approximate wave propagation algorithm (asymptotic ray theory) which includes the direct rays and those which have undergone a single reflection, the result is the empirical source function method (EPRI, 1993). Combining the reflectivity propagation (which is generally limited to frequencies  $\#$  1-2 Hz due to computational demands) with the empirical source function approach (appropriate for frequencies  $\$$  1 Hz; EPRI, 1993) results in a broad band simulation procedure which is strictly deterministic at low frequencies (where an analytical source function is used) and incorporates some natural variation at high frequencies through the use of an empirical source function (Sommerville et al., 1995).

All of these techniques are fundamentally similar, well founded in seismic source and wave propagation physics, and importantly, they are all approximate. Simply put, all models are wrong (approximate) and the single essential element in selecting a model is to incorporate the appropriate degree of rigor, commensurate with uncertainties and variabilities in crustal structure and site effects, through extensive validation exercises. It is generally felt that more complicated models produce more accurate results, however, the implications of more sophisticated models with the increased number of parameters which must be specified is often overlooked. This is not too serious a consequence in modeling past earthquakes since a reasonable range in parameter space can be explored to give the "best" results. However for future predictions, this increased rigor may carry undesirable baggage in increased parametric variability (Roblee et al., 1996). The effects of lack of knowledge (epistemic uncertainty; EPRI, 1993) regarding parameter values for

## APPENDIX A

future occurrences results in uncertainty or variability in ground motion predictions. It may easily be the case that a very simple model, such as the point-source model can have comparable, or even smaller, total variability (modeling plus parametric) than a much more rigorous model with an increased number of parameters (EPRI, 1993). What is desired in a model is sufficient sophistication such that it captures the dominant and stable features of source, distance, and site dependencies observed in strong ground motions. It is these considerations which led to the development of the stochastic point- and finite-source models and, in part, leads to the stochastic element of the models.

The stochastic nature of the point- and finite-source RVT models is simply the assumption made about the character of ground motion time histories that permits stable estimates of peak parameters (e.g. acceleration, velocity, strain, stress, oscillator response) to be made without computing detailed time histories (Hanks and McGuire, 1981; Boore, 1983). This process uses random vibration theory to relate a time domain peak value to the time history root-mean-square (RMS) value (Boore, 1983). The assumption of the character of the time history for this process to strictly apply is that it be normally distributed random noise and stationary (its statistics do not change with time) over its duration. A visual examination of any time history quickly reveals that this is clearly not the case: time histories (acceleration, velocity, stress, strain, oscillator) start, build up, and then diminish with time. However poor the assumption of stationary Gaussian noise may appear, the net result is that the assumption is weak enough to permit the approach to work surprisingly well, as numerous comparisons with recorded motions and both qualitative and quantitative validations have shown (Hanks and McGuire, 1981; Boore, 1983, 1986; McGuire et al., 1984; Boore and Atkinson, 1987; Silva and Lee, 1987; Toro and McGuire, 1987; Silva et al., 1990; EPRI, 1993; Schneider et al., 1993; Silva and Darragh, 1995; Silva et al., 1997). Corrections to RVT are available to accommodate different distributions as well as non-stationarity and are usually applied to the estimation of peak oscillator response in the calculated response spectra (Boore and Joyner, 1984; Toro, 1985).

### Point-source Model

The conventional stochastic ground motion model uses an  $\omega$ -square source model (Brune, 1970, 1971) with a single corner frequency and a constant stress drop (Boore, 1983; Atkinson, 1984). Random vibration theory is used to relate RMS (root-mean-square) values to peak values of acceleration (Boore, 1983), and oscillator response (Boore and Joyner, 1984; Toro, 1985; Silva and Lee, 1987) computed from the power spectra to expected peak time domain values (Boore, 1983).

The shape of the acceleration spectral density,  $a(f)$ , is given by

$$a(f) = C \frac{f^2}{1 + \left(\frac{f}{f_0}\right)^2} \frac{MSUB0}{R} P(f) A(f) e^{-\frac{\pi f R}{\beta_0 Q(f)}} \quad (A-1)$$

where

## APPENDIX A

$$C = \left(\frac{1}{\rho_0 \beta_0^3}\right) \cdot (2) \cdot (0.55) \cdot \left(\frac{1}{\sqrt{2}}\right) \cdot \pi.$$

- $M_0$  = seismic moment,  
 $R$  = hypocentral distance,  
 $\beta_0$  = shear-wave velocity at the source,  
 $\rho_0$  = density at the source  
 $Q(f)$  = frequency dependent quality factor (crustal damping),  
 $A(f)$  = crustal amplification,  
 $P(f)$  = high-frequency truncation filter,  
 $f_0$  = source corner frequency.

C is a constant which contains source region density ( $\rho_0$ ) and shear-wave velocity terms and accounts for the free-surface effect (factor of 2), the source radiation pattern averaged over a sphere (0.55) (Boore, 1986), and the partition of energy into two horizontal components ( $1/\sqrt{2}$ ).

Source scaling is provided by specifying two independent parameters, the seismic moment ( $M_0$ ) and the high-frequency stress parameter or stress drop ( $\Delta\sigma$ ). The seismic moment is related to magnitude through the definition of moment magnitude  $\mathbf{M}$  by the relation

$$\log M_0 = 1.5 \mathbf{M} + 16.05 \quad (\text{Hanks and Kanamori, 1979}) \quad (\text{A - 2}).$$

The stress drop ( $\Delta\sigma$ ) relates the corner frequency  $f_0$  to  $M_0$  through the relation

$$f_0 = \beta_0 (\Delta\sigma/8.44 M_0)^{1/3} \quad (\text{Brune; 1970, 1971}) \quad (\text{A - 3}).$$

The stress drop is sometimes referred to as the high frequency stress parameter (Boore, 1983) (or simply the stress parameter) since it directly scales the Fourier amplitude spectrum for frequencies above the corner frequency (Silva, 1991; Silva and Darragh 1995). High ( $> 1$  Hz) frequency model predictions are then very sensitive to this parameter (Silva, 1991; EPRI, 1993) and the interpretation of it being a stress drop or simply a scaling parameter depends upon how well real earthquake sources (on average) obey the omega-square scaling (Equation A-3) and how well they are fit by the single-corner-frequency model (Atkinson and Silva, 1997). If earthquakes truly have single-corner-frequency omega-square sources, the stress drop in Equation A-3 is a physical parameter and its values have a physical interpretation of the forces (stresses) accelerating the relative slip across the rupture surface. High stress drop sources are due to a smaller source (fault) area (for the same  $\mathbf{M}$ ) than low stress drop sources (Brune, 1970). Otherwise, it simply a high frequency ( $f > f_0$ ) scaling or fitting parameter.

## APPENDIX A

The spectral shape of the single-corner-frequency  $\omega$ -square source model is then described by the two free parameters  $M_0$  and  $\Delta\sigma$ . The corner frequency increases with the shear-wave velocity and with increasing stress drop, both of which may be region dependent.

The crustal amplification accounts for the increase in wave amplitude as seismic energy travels through lower- velocity crustal materials from the source to the surface. The amplification depends on average crustal and near surface shear-wave velocity and density (Boore, 1986).

The P(f) filter is used in an attempt to model the observation that acceleration spectral density appears to fall off rapidly beyond some region- or site-dependent maximum frequency (Hanks, 1982; Silva and Darragh, 1995). This observed phenomenon truncates the high frequency portion of the spectrum and is responsible for the band-limited nature of the stochastic model. The band limits are the source corner frequency at low frequency and the high frequency spectral attenuation. This spectral fall-off at high frequency has been attributed to near-site attenuation (Hanks, 1982; Anderson and Hough, 1984) or to source processes (Papageorgiou and Aki, 1983) or perhaps to both effects. In the Anderson and Hough (1984) attenuation model, adopted here, the form of the P(f) filter is taken as

$$P(f, r) = e^{-\pi\kappa(r)f} \quad (\text{A-4}).$$

Kappa (r) ( $\kappa(r)$  in Equation A-4) is a site and distance dependent parameter that represents the effect of intrinsic attenuation upon the wavefield as it propagates through the crust from source to receiver. Kappa (r) depends on epicentral distance (r) and on both the shear-wave velocity ( $\beta$ ) and quality factor ( $Q_s$ ) averaged over a depth of H beneath the site (Hough et al., 1988). At zero epicentral distance kappa ( $\kappa$ ) is given by

$$\kappa(0) = \frac{H}{\beta Q_s} \quad (\text{A-5}),$$

and is referred to as  $\kappa$ .

The bar in Equation A-5 represents an average of these quantities over a depth H. The value of kappa at zero epicentral distance is attributed to attenuation in the very shallow crust directly below the site (Hough and Anderson, 1988; Silva and Darragh, 1995). The intrinsic attenuation along this part of the path is not thought to be frequency dependent and is modeled as a frequency independent, but site and crustal region dependent, constant value of kappa (Hough et al., 1988; Rovelli et al., 1988). This zero epicentral distance kappa is the model implemented in this study.

## APPENDIX A

The crustal path attenuation from the source to just below the site is modeled with the frequency- dependent quality factor  $Q(f)$ . Thus the distance component of the original  $\kappa(r)$  (Equation A-4) is accommodated by  $Q(f)$  and  $R$  in the last term of Equation A-1:

$$\kappa(r) = \frac{H}{\beta Q_s} + \frac{R}{\beta_0 Q(f)} \quad (\text{A-6}).$$

The Fourier amplitude spectrum,  $a(f)$ , given by Equation A-1 represents the stochastic ground motion model employing a Brune source spectrum that is characterized by a single corner frequency. It is a point source and models direct shear-waves in a homogeneous half-space (with effects of a velocity gradient captured by the  $A(f)$  filter, Equation A-1). For horizontal motions, vertically propagating shear-waves are assumed. Validations using incident inclined SH-waves accompanied with raytracing to find appropriate incidence angles leaving the source showed little reduction in uncertainty compared to results using vertically propagating shear-waves. For vertical motions, P/SV propagators are used coupled with raytracing to model incident inclined plane waves (EPRI, 1993). This approach has been validated with recordings from the 1989 **M** 6.9 Loma Prieta earthquake (EPRI, 1993).

Equation A-1 represents an elegant ground motion model that accommodates source and wave propagation physics as well as propagation path and site effects with an attractive simplicity. The model is appropriate for an engineering characterization of ground motion since it captures the general features of strong ground motion in terms of peak acceleration and spectral composition with a minimum of free parameters (Boore, 1983; McGuire et al., 1984; Boore, 1986; Silva and Green, 1988; Silva et al., 1988; Schneider et al., 1993; Silva and Darragh, 1995). An additional important aspect of the stochastic model employing a simple source description is that the region-dependent parameters may be evaluated by observations of small local or regional earthquakes. Region-specific seismic hazard evaluations can then be made for areas with sparse strong motion data with relatively simple spectral analyses of weak motion (Silva, 1992).

In order to compute peak time-domain values, i.e. peak acceleration and oscillator response, RVT is used to relate RMS computations to peak value estimates. Boore (1983) and Boore and Joyner (1984) present an excellent development of the RVT methodology as applied to the stochastic ground motion model. The procedure involves computing the RMS value by integrating the power spectrum from zero frequency to the Nyquist frequency and applying Parseval's relation. Extreme value theory is then used to estimate the expected ratio of the peak value to the RMS value of a specified duration of the stochastic time history. The duration is taken as the inverse of the source corner frequency (Boore, 1983).

Factors that affect strong ground motions such as surface topography, finite and propagating seismic sources, laterally varying near-surface velocity and  $Q$  gradients, and random inhomogeneities along the propagation path are not included in the model. While some or all of these factors are generally present in any observation of ground motion and may exert controlling influences in some cases, the simple stochastic point-source model appears to be robust in predicting median or average properties of ground motion (Boore

## APPENDIX A

1983, 1986; Schneider et al., 1993; Silva and Stark, 1993; Silva et al., 1997). The motivation for comprehensive validation exercises involving many earthquakes with a wide range in magnitudes, rupture distances, and site conditions is to capture unmodeled effects. The unmodeled effects which are random are captured in estimates of model uncertainty and those which are pervasive are captured in the estimates of model bias (see later sections). The combination of realistic, albeit simple, model physics with comprehensive validation exercises makes the stochastic point source ground motion model a powerful predictive and interpretative tool for engineering characterization of strong ground motion.

### Finite-source Model Ground Motion Model

In the near-source region of large earthquakes, aspects of a finite-source including rupture propagation, directivity source-receiver geometry, and saturation of high-frequency ( $\geq 1$  Hz) motions with increasing magnitude can be significant and may be incorporated into strong ground motion predictions. To accommodate these effects, a methodology that combines the aspects of finite-earthquake-source modeling techniques (Hartzell, 1978; Irikura 1983) with the stochastic point-source ground motion model has been developed to produce response spectra as well as time histories appropriate for engineering design (Silva et al., 1990; Silva and Stark, 1993; Schneider et al., 1993). The approach is very similar to the empirical Green function methodology introduced by Hartzell (1978) and Irikura (1983). In this case however, the stochastic point-source is substituted for the empirical Green function and peak amplitudes; PGA, PGV, and response spectra (when time histories are not produced) are estimated using random process theory.

Use of the stochastic point-source as a Green function is motivated by its demonstrated success in modeling ground motions in general and strong ground motions in particular (Boore, 1983, 1986; Silva and Stark, 1993; Schneider et al., 1993; Silva and Darragh, 1995) and the desire to have a model that is truly site- and region-specific. The model can accommodate a region specific  $Q(f)$ , Green function sources of arbitrary moment or stress drop, and site specific kappa values and soil profiles. The necessity for having available regional and site specific recordings distributed over the rupture surface of a future earthquake or modifying possibly inappropriate empirical Green functions is eliminated.

For the finite-source characterization, a rectangular fault is discretized into NS subfaults of moment  $M_0^S$ . The empirical relationship

$$\log(A) = \mathbf{M} - 4.0, \quad A \text{ in km}^2 \quad (\text{A-7})$$

is used to assign areas to both the target earthquake (if its rupture surface is not fixed) as well as to the subfaults. This relation results from regressing log area on  $\mathbf{M}$  using the data of Wells and Coppersmith (1994). In the regression, the coefficient on  $\mathbf{M}$  is set to unity which implies a constant static stress drop of about 30 bars (Equation A-9). This is consistent with the general observation of a constant static stress drop for earthquakes based on aftershock locations (Wells and Coppersmith 1994). The static stress drop,



## APPENDIX A

defined by Equation A-10, is related to the average slip over the rupture surface as well as rupture area. It is theoretically identical to the stress drop in Equation A-3 which defines the omega-square source corner frequency assuming the rupture surface is a circular crack model (Brune, 1970; 1971). The stress drop determined by the source corner frequency (or source duration) is usually estimated through the Fourier amplitude spectral density while the static stress drop uses the moment magnitude and an estimate of the rupture area. The two estimates for the same earthquake seldom yield the same values with the static generally being the smaller. In a recent study (Silva et al., 1997), the average stress drop based on Fourier amplitude spectra determined from an empirical attenuation relation (Abrahamson and Silva, 1997) is about 70 bars while the average static stress drop for the crustal earthquakes studied by Wells and Coppersmith (1994) is about 30 bars. These results reflect a general factor of about 2 on average between the two values. These large differences may simply be the result of using an inappropriate estimate of rupture area as the zone of actual slip is difficult to determine unambiguously. In general however, even for individual earthquakes, the two stress drops scale similarly with high static stress drops (> 30 bars) resulting in large high frequency (> 1 Hz for  $M \geq 5$ ) ground motions which translates to high corner frequencies (Equation A-3).

The subevent magnitude  $M_S$  is generally taken in the range of 5.0-6.5 depending upon the size of the target event.  $M_S$  5.0 is used for crustal earthquakes with  $M$  in the range of 5.5 to 8.0 and  $M_S$  6.4 is used for large subduction earthquakes with  $M > 7.5$ . The value of  $N_S$  is determined as the ratio of the target event area to the subfault area. To constrain the proper moment, the total number of events summed ( $N$ ) is given by the ratio of the target event moment to the subevent moment. The subevent and target event rise times (duration of slip at a point) are determined by the equation

$$\log \tau = 0.33 \log M_0 - 8.54 \quad (\text{A-8})$$

which results from a fit to the rise times used in the finite-fault modeling exercises, (Silva et al., 1997). Slip on each subfault is assumed to continue for a time  $\tau$ . The ratio of target-to-subevent rise times is given by

$$\frac{\tau}{\tau} = 10^{0.5(M-M_S)} \quad (\text{A-9})$$

and determines the number of subevents to sum in each subfault. This approach is generally referred to as the constant-rise-time model and results in variable slip velocity for nonuniform slip distributions. Alternatively, one can assume a constant slip velocity (as do Beresnev and Atkinson, 2002) resulting in a variable-rise-time model for heterogenous slip distributions. This approach was implemented and validations resulted in an overall “best” average slip velocity of about 70 cm/sec, with no significant improvement over a magnitude dependent rise time (Equation A-8). The feature is retained as an option in the simulation code.

## APPENDIX A

Recent modeling of the Landers (Wald and Heaton, 1994), Kobe (Wald, 1996) and Northridge (Hartzell et al. 1996) earthquakes suggests that a mixture of both constant rise time and constant slip velocity may be present. Longer rise times seem to be associated with areas of larger slip with the ratio of slip-to-rise time (slip velocity) being depth dependent. Lower slip velocities (longer rise times) are associated with shallow slip resulting in relatively less short period seismic radiation. This result may explain the general observation that shallow slip is largely aseismic. The significant contributions to strong ground motions appear to originate at depths exceeding about 4 km (Campbell, 1993; Boore et al., 1994) as the fictitious depth term in empirical attenuation relation (Abrahamson and Silva, 1997; Boore et al., 1997). Finite-fault models generally predict unrealistically large strong ground motions for large shallow (near surface) slip using rise times or slip velocities associated with deeper ( $> 4$  km) zones of slip. This is an important and unresolved issue in finite-fault modeling and the general approach is constrain the slip to relatively small values in the top 2 to 4 km. For the composite source model, the approach is to taper the subevent stress drop to zero at the ground surface (Yehua Zeng, personal communication 1999). This approach is also followed in the stochastic finite source model. For earthquakes with significant shallow slip, greater than 20% moment released in the top 5 km, expected short period ( $< 1 - 2$  second) motions are significantly lower (20 – 50%) than those of deep slip events, of the same magnitude (Silva et al., 1997). To capture this effect, shallow slip earthquakes are modeled with a 5 bar, rather than 30 bar subevent stress drop, over the entire rupture surface, based on the validation exercises (Silva et al., 1997). These results imply significantly different source processes affecting short periods between earthquakes which do not interact with low stresses associated with shallow rupture and those earthquakes which have deep rupture only. The implications to seismic hazard are obvious.

To introduce heterogeneity of the earthquake source process into the stochastic finite-fault model, the location of the sub-events within each subfault (Hartzell, 1978) are randomized as well as the subevent rise time ( $\sigma_{ln} = 0.8$ ). The stress drop of the stochastic point-source Green function is taken as 30 bars, consistent with the static value based on the **M** 5.0 subevent area using the equation

$$\Delta\sigma = \frac{7}{16} \left( \frac{M_e}{R_e^3} \right) \quad (\text{Brune, 1970, 1971}) \quad (\text{A-10})$$

where  $R_e$  is the equivalent circular radius of the rectangular sub-event.

Different values of slip are assigned to each subfault as relative weights so that asperities or non-uniform slip can be incorporated into the methodology. For validation exercises, slip models are taken from the literature and are based on inversions of strong motion as well as regional or teleseismic recordings. To produce slip distributions for future earthquakes, random slip models are generated based on a statistical asperity model with parameters calibrated to the published slip distributions. This approach has been validated by comparing the modeling uncertainty and bias estimates for the Loma Prieta and Whittier Narrows earthquakes using motion at each site averaged over several (30)

## APPENDIX A

random slip models to the bias and uncertainty estimates using the published slip model. The results show nearly identical bias and uncertainty estimates suggesting that averaging the motions over random slip models produces as accurate a prediction at a site as a single motion computed using the "true" slip model which is determined from inverting actual recordings.

The rupture velocity is taken as depth independent at a value of 0.8 times the shear-wave velocity, generally at the depth of the dominant slip. This value is based on a number of studies of source rupture processes which also suggest that rupture velocity is non-uniform. To capture the effects of non-uniform rupture velocity, a random component is added through the randomized location of the subevents within each subfault. The radiation pattern is computed for each subfault, a random component added, and the RMS applied to the motions computed at the site when modeling an average horizontal component. To model individual horizontal components, the radiation pattern for each subfault is used to scale each subfault's contribution to the final summed motion.

The ground-motion time history at the receiver is computed by summing the contributions from each subfault associated with the closest Green function, transforming to the frequency domain, and convolving with the appropriate Green function spectrum (Equation A-1). The locations of the Green functions are generally taken at center of each subfault for small subfaults or at a maximum separation of about 5 to 10 km for large subfaults. As a final step, the individual contributions associated with each Green function are summed in the frequency domain, multiplied by the RMS radiation pattern, and the resultant power spectrum at the site is computed. The appropriate duration used in the RVT computations for PGA, PGV, and oscillator response is computed by transforming the summed Fourier spectrum into the time domain and computing the 5 to 75% Arias intensity (Ou and Herrmann, 1990).

As with the point-source model, crustal response effects are accommodated through the amplification factor ( $A(f)$ ) or by using vertically propagating shear waves through a vertically heterogeneous crustal structure. Soil nonlinearity is accommodated through the equivalent-linear approximation. Propagation path damping, through the  $Q(f)$  model, is incorporated from each fault element to the site. Near-surface crustal damping is incorporated through the kappa operator (Equation A-1). To model crustal propagation path effects, the raytracing method of Ou and Herrmann (1990) is applied from each subfault to the site.

Time histories may be computed in the process as well by simply adding a phase spectrum appropriate to the subevent earthquake. The phase spectrum can be extracted from a recording made at close distance to an earthquake of a size comparable to that of the subevent (generally  $M$  5.0 to 6.5). Interestingly, the phase spectrum need not be from a recording in the region of interest (Silva et al., 1989). A recording in WNA (Western North America) can effectively be used to simulate motions appropriate to ENA (Eastern North America). Transforming the Fourier spectrum computed at the site into the time domain results in a computed time history which then includes all of the aspects of rupture propagation and source finiteness, as well as region specific propagation path and site effects.

## APPENDIX A

For fixed fault size, mechanism, and moment, the specific source parameters for the finite-fault are slip distribution, location of nucleation point, and site azimuth. The propagation path and site parameters remain identical for both the point- and finite-source models.

### Partition and assessment of ground motion variability

An essential requirement of any numerical modeling approach, particularly one which is implemented in the process of defining design ground motions, is a quantitative assessment of prediction accuracy. A desirable approach to achieving this goal is in a manner which lends itself to characterizing the variability associated with model predictions. For a ground motion model, prediction variability is comprised of two components: modeling variability and parametric variability. Modeling variability is a measure of how well the model works (how accurately it predicts ground motions) when specific parameter values are known. Modeling variability is measured by misfits of model predictions to recorded motions through validation exercises and is due to unaccounted for components in the source, path, and site models (i.e. a point-source cannot model the effects of directivity and linear site response cannot accommodate nonlinear effects). Results from a viable range of values for model parameters (i.e., slip distribution, soil profile,  $G/G_{\max}$  and hysteretic damping curves, etc). Parametric variability is the sensitivity of a model to a viable range of values for model parameters. The total variability, modeling plus parametric, represents the variance associated with the ground motion prediction and, because it is a necessary component in estimating fractile levels, may be regarded as important as median predictions.

Both the modeling and parametric variabilities may have components of randomness and uncertainty. Table A.1 summarizes the four components of total variability in the context of ground motion predictions. Uncertainty is that portion of both modeling and parametric variability which, in principle, can be reduced as additional information becomes available, whereas randomness represents the intrinsic or irreducible component of variability for a given model or parameter. Randomness is that component of variability which is intrinsic or irreducible for a given model. The uncertainty component reflects a lack of knowledge and may be reduced as more data are analyzed. For example, in the point-source model, stress drop is generally taken to be independent of source mechanism as well as tectonic region and is found to have a standard error of about 0.7 (natural log) for the CEUS (EPRI, 1993). This variation or uncertainty plus randomness in  $\Delta\sigma$  results in a variability in ground motion predictions for future earthquakes. If, for example, it is found that normal faulting earthquakes have generally lower stress drops than strike-slip which are, in turn, lower than reverse mechanism earthquakes, perhaps much of the variability in  $\Delta\sigma$  may be reduced. In extensional regimes, where normal faulting earthquakes are most likely to occur, this new information may provide a reduction in variability (uncertainty component) for stress drop, say to 0.3 or 0.4 resulting in less ground motion variation due to a lack of knowledge of the mean or median stress drop. There is, however, a component of this stress drop variability which can never be reduced in the context of the Brune model. This is simply due to the heterogeneity of the earthquake dynamics which is not

## APPENDIX A

accounted for in the model and results in the randomness component of parametric variability in stress drop. A more sophisticated model may be able to accommodate or model more accurately source dynamics but, perhaps, at the expense of a larger number of parameters and increased parametric uncertainty (i.e. the finite-fault with slip model and nucleation point as unknown parameters for future earthquakes). That is, more complex models typically seek to reduce modeling randomness by more closely modeling physical phenomena. However, such models often require more comprehensive sets of observed data to constrain additional model parameters, which generally leads to increased parametric variability. If the increased parametric variability is primarily in the form of uncertainty, it is possible to reduce total variability, but only at the additional expense of constraining the additional parameters. Therefore, existing knowledge and/or available resources may limit the ability of more complex models to reduce total variability.

The distinction of randomness and uncertainty is model driven and somewhat arbitrary. The allocation is only important in the context of probabilistic seismic hazard analyses as uncertainty is treated as alternative hypotheses in logic trees while randomness is integrated over in the hazard calculation (Cornell, 1968). For example, the uncertainty component in stress drop may be treated by using an N-point approximation to the stress drop distribution and assigning a branch in a logic tree for each stress drop and associated weight. A reasonable three point approximation to a normal distribution is given by weights of 0.2, 0.6, 0.2 for expected 5%, mean, and 95% values of stress drop respectively. If the distribution of uncertainty in stress drop was such that the 5%, mean, and 95% values were 50, 100, and 200 bars respectively, the stress drop branch on a logic tree would have 50, and 200 bars with weights of 0.2 and 100 bars with a weight of 0.6. The randomness component in stress drop variability would then be formally integrated over in the hazard calculation.

### Assessment of Modeling Variability

Modeling variability (uncertainty plus randomness) is usually evaluated by comparing response spectra computed from recordings to predicted spectra and is a direct assessment of model accuracy. The modeling variability is defined as the standard error of the residuals of the log of the average horizontal component (or vertical component) response spectra. The residual is defined as the difference of the logarithms of the observed average 5% damped acceleration response spectra and the predicted response spectra. At each period, the residuals are squared, and summed over the total number of sites for one or all earthquakes modeled. Dividing the resultant sum by the number of sites results in an estimate of the model variance. Any model bias (average offset) that exists may be estimated in the process (Abrahamson et al., 1990; EPRI, 1993) and used to correct (lower) the variance (and to adjust the median as well). In this approach, the modeling variability can be separated into randomness and uncertainty where the bias corrected variability represents randomness and the total variability represents randomness plus uncertainty. The uncertainty is captured in the model bias as this may be reduced in the future by refining the model. The remaining variability (randomness) remains irreducible for this model. In computing the variance and bias estimates only the

## APPENDIX A

frequency range between processing filters at each site (minimum of the 2 components) should be used.

### Assessment of Parametric Variability

Parametric variability, or the variation in ground motion predictions due to uncertainty and randomness in model parameters is difficult to assess. Formally, it is straightforward in that a Monte Carlo approach may be used with each parameter randomly sampled about its mean (median) value either individually for sensitivity analyses (Silva, 1992; Roblee et al., 1996) or in combination to estimate the total parametric variability (Silva, 1992; EPRI, 1993). In reality, however, there are two complicating factors.

The first factor involves the specific parameters kept fixed with all earthquakes, paths, and sites when computing the modeling variability. These parameters are then implicitly included in modeling variability provided the data sample a sufficiently wide range in source, path, and site conditions. The parameters which are varied during the assessment of modeling variation should have a degree of uncertainty and randomness associated with them for the next earthquake. Any ground motion prediction should then have a variation reflecting this lack of knowledge and randomness in the free parameters.

An important adjunct to fixed and free parameters is the issue of parameters which may vary but by fixed rules. For example, source rise time (Equation A-8) is magnitude dependent and in the stochastic finite-source model is specified by an empirical relation. In evaluating the modeling variability with different magnitude earthquakes, rise time is varied, but because it follows a strict rule, any variability associated with rise time variation is counted in modeling variability. This is strictly true only if the sample of earthquakes has adequately spanned the space of magnitude, source mechanism, and other factors which may affect rise time. Also, the earthquake to be modeled must be within that validation space. As a result, the validation or assessment of model variation should be done on as large a number of earthquakes of varying sizes and mechanisms as possible.

The second, more obvious factor in assessing parametric variability is a knowledge of the appropriate distributions for the parameters (assuming correct values for median or mean estimates are known). In general, for the stochastic models, median parameter values and uncertainties are based, to the extent possible, on evaluating the parameters derived from previous earthquakes (Silva, 1992; EPRI, 1993).

The parametric variability is site, path, and source dependent and must be evaluated for each modeling application (Roblee et al., 1996). For example, at large source-to-site distances, crustal path damping may control short-period motions. At close distances to a large fault, both the site and finite-source (asperity location and nucleation point) may dominate, and, depending upon site characteristics, the source or site may control different frequency ranges (Silva, 1992; Roblee et al., 1996). Additionally, level of control motion may affect the relative importance of  $G/G_{\max}$  and hysteretic damping curves.

## APPENDIX A

In combining modeling and parametric variations, independence is assumed (covariance is zero) and the variances are simply added to give the total variability.

$$\ln\sigma_T^2 = \ln\sigma_M^2 + \ln\sigma_P^2 \quad (\text{A-11}),$$

where

$\ln\sigma_M^2$  = modeling variation,

$\ln\sigma_P^2$  = parametric variation.

### Validation Of The Point- and Finite-Source Models

In a recent Department of Energy sponsored project (Silva et al., 1997), both the point- and finite-source stochastic models were validated in a systematic and comprehensive manner. In this project, 16 well recorded earthquakes were modeled at about 500 sites. Magnitudes ranged from **M** 5.3 to **M** 7.4 with fault distances from about 1 km out to 218 km for WUS earthquakes and 460 km for CEUS earthquakes. This range in magnitude and distance as well as number of earthquakes and sites results in the most comprehensively validated model currently available to simulate strong ground motions.

For these exercises, regional  $Q(f)$  models and point source stress drops were determined through inversions using the strong motion recordings (Silva et al., 1997). Small strain WUS rock and soil kappa values were set to 0.04 sec, the average from the inversions of small strain data. CEUS rock site kappa values were fixed at inversion values, which averaged about 0.02 sec and ranged from 0.004 to 0.06 sec. For the finite source parameters, slip models and nucleation points were taken from the literature (Silva et al., 1997). Point-source depths were taken as the depth of the center of the largest asperity in the slip models while point-source distance used the closest distance to the surface projection of the rupture surface.

A unique aspect of this validation is that rock and soil sites were modeled using generic rock and soil profiles and equivalent-linear site response. Validations done with other simulation procedures typically neglect site conditions as well as nonlinearity resulting in ambiguity in interpretation of the simulated motions.

### Point-Source Model

---

<sup>2</sup>Strong ground motions are generally considered to be log normally distributed.

## APPENDIX A

Final model bias and variability estimates for the point-source model are shown in Figure A1. Over all the sites (Figure A1) the bias is slightly positive for frequencies greater than about 10 Hz and is near zero from about 10 Hz to 1 Hz. Below 1 Hz, a stable point-source overprediction is reflected in the negative bias. The analyses are considered reliable down to about 0.3 Hz (3.3 sec) where the point-source shows about a 40% overprediction.

The model variability is low, about 0.5 above about 3 to 4 Hz and increases with decreasing frequency to near 1 at 0.3 Hz. Above 1 Hz, there is little difference between the total variability (uncertainty plus randomness) and randomness (bias corrected variability) reflecting the near zero bias estimates. Below 1 Hz there is considerable uncertainty contributing to the total variability suggesting that the model can be measurably improved as its predictions tend to be consistently high at very low frequencies ( $\neq$  1 Hz). This stable misfit may be interpreted as the presence of a second corner frequency for WNA sources (Atkinson and Silva, 1997).

### Finite-Source Model

For the finite-fault, Figure A2 shows the corresponding bias and variability estimates. For all the sites, the finite-source model provides slightly smaller bias estimates and, surprisingly, slightly higher variability for frequencies exceeding about 5 Hz. The low frequency ( $\neq$  1 Hz) point-source overprediction is not present in the finite-source results, indicating that it is giving more accurate predictions than the point-source model over a broad frequency range, from about 0.3 Hz (the lowest frequency of reliable analyses) to the highest frequency of the analyses.

In general, for frequencies of about 1 Hz and above the point-source and finite-source give comparable results: the bias estimates are small (near zero) and the variabilities range from about 0.5 to 0.6. These estimates are low considering the analyses are based on a data set comprised of earthquakes with  $M$  less than  $M$  6.5 (288 of 513 sites) and high frequency ground motion variance decreases with increasing magnitude, particularly above  $M$  6.5 (Youngs et al., 1995) Additionally, for the vast majority of sites, generic site conditions were used (inversion kappa values were used for only the Saguenay and Nahanni earthquake analyses, 25 rock sites). As a result, the model variability (mean = 0) contains the total uncertainty and randomness contribution for the site. The parametric variability due to uncertainty and randomness in site parameters: shear-wave velocity, profile depth,  $G/G_{\max}$  and hysteretic damping curves need not be added to the model variability estimates. It is useful to perform parametric variations to assess site parameter sensitivities on the ground motions, but only source and path damping  $Q(f)$  parametric variabilities require assessment on a site specific basis and added to the model variability. The source uncertainty and randomness components include point-source stress drop as well as source depth and finite-source slip model and nucleation point (Silva, 1992).

The general approach taken in these validations is to have few free parameters and accept a relatively large model misfit. This approach relaxes the need to develop appropriate distributions for poorly resolved parameters such as spatially varying rise times and rupture velocity as well as non-planar rupture surfaces (e.g. Landers, Kobe, and Kocaeli



## APPENDIX A

earthquakes). An alternative approach is to adjust these suites of parameters, which naturally improves the fits to recorded motions and results in smaller modeling uncertainties. However, unless independent information is available to constrain these parameters for future earthquakes, they must be appropriately counted as parametric variability. This may result in the total variability remaining comparable between the two approaches. This concept parallels the utility of increased model complexity, i.e., simple versus complex models. More complex models may increase an understanding of physical processes but, in the context of predicting motions due to the next earthquake, increased model complexity may not provide more accurate estimates of strong ground motions, again unless independent information is available to constrain potential ranges in some or all of the free parameters.

A summary of fixed and free parameters for the implementation of the stochastic point and finite source models presented here is listed in Table 2.

### Empirical Attenuation Model

As an additional assessment of the stochastic models, bias and variability estimates were made over the same earthquakes (except Saguenay since it was not used in the regressions) and sites using a recently developed empirical attenuation relation (Abrahamson and Silva, 1997). For all the sites, the estimates are shown in Figure A3. Interestingly, the point-source overprediction below about 1 Hz is present in the empirical relation perhaps suggesting that this suite of earthquakes possess lower than expected motions in this frequency range as the empirical model does not show this bias over all earthquakes (. 50) used in its development. Comparing these results to the point- and finite-source results (Figures A1 and A2) show comparable bias and variability estimates. For future predictions, source and path damping parametric variability must be added to the numerical simulations which will contribute a  $\sigma_{ln}$  of about 0.2 to 0.4, depending upon frequency, source and path conditions, and site location. This will raise the modeling variability from about 0.50 to the range of 0.54 to 0.64, about 10 to 30%. These values are still comparable to the variability of the empirical relation indicating that the point- and finite-source numerical models perform about as well as a recently developed empirical attenuation relation for the validation earthquakes and sites.

These results are very encouraging and provide an additional qualitative validation of the point- and finite-source models. Paranthetically this approach provides a rational basis for evaluating empirical attenuation models.

## APPENDIX A

### REFERENCES

- Abrahamson, N.A. and W.J. Silva (1997). "Empirical response spectral attenuation relations for shallow crustal earthquakes." *Seismological Research Let.*, 68(1), 94-127.
- Abrahamson, N.A., P.G. Somerville, and C.A. Cornell (1990). "Uncertainty in numerical strong motion predictions" *Proc. Fourth U.S. Nat. Conf. Earth. Engin.*, Palm Springs, CA., 1, 407-416.
- Aki, K. and P.G. Richards. (1980). "*Quantitative siesmology.*" W. H. Freeman and Co., San Francisco, California.
- Atkinson, G.M and W.J. Silva (1997). "An empirical study of earthquake source spectra for California earthquakes." *Bull. Seism. Soc. Am.* 87(1), 97-113.
- Anderson, J.G. and S.E. Hough (1984). "A Model for the Shape of the Fourier Amplitude Spectrum of Acceleration at High Frequencies." *Bulletin of the Seismological Society of America*, 74(5), 1969-1993.
- Atkinson, G.M. (1984). "Attenuation of strong ground motion in Canada from a random vibrations approach." *Bull. Seism. Soc. Am.*, 74(5), 2629-2653.
- Beresnev, I.A. and G. M. Atkinson (2002). "Source parameters of earthquakes in Eastern and Western North America." *Bull. Seism. Soc. Am.*, 92(2), 695-710.
- Boore, D.M., W.B. Joyner, and T.E. Fumal (1997). "Equations for estimating horizontal response spectra and peak acceleration from Western North American earthquakes: A summary of recent work." *Seism. Res. Lett.* 68(1), 128-153.
- Boore, D.M., W.B. Joyner, and T.E. Fumal (1994). "Estimation of response spectra and peak accelerations from western North American earthquakes: and interim report. Part 2. *U.S. Geological Survey Open-File Rept.* 94-127.
- Boore, D.M., and G.M. Atkinson (1987). "Stochastic prediction of ground motion and spectral response parameters at hard-rock sites in eastern North America." *Bull. Seism. Soc. Am.*, 77(2), 440-467.
- Boore, D.M. (1986). "Short-period P- and S-wave radiation from large earthquakes: implications for spectral scaling relations." *Bull. Seism. Soc. Am.*, 76(1) 43-64.
- Boore, D.M. and W.B. Joyner (1984). "A note on the use of random vibration theory to predict peak amplitudes of transient signals." *Bull. Seism. Soc. Am.*, 74, 2035-2039.
- Boore, D.M. (1983). "Stochastic simulation of high-frequency ground motions based on seismological models of the radiated spectra." *Bull. Seism. Soc. Am.*, 73(6), 1865-1894.

## APPENDIX A

- Brune, J.N. (1971). "Correction." *J. Geophys. Res.* 76, 5002.
- Brune, J.N. (1970). "Tectonic stress and the spectra of seismic shear waves from earthquakes." *J. Geophys. Res.* 75, 4997-5009.
- Campbell, K.W. (1993) "Empirical prediction of near-source ground motion from large earthquakes." in V.K. Gaur, ed., *Proceedings, Intern'l Workshop on Earthquake Hazard and Large Dams in the Himalya*. INTACH, New Delhi, p. 93-103.
- Cornell, C.A. (1968). "Engineering seismic risk analysis." *Bull. Seism. Soc. Am.*, 58, 1583-1606.
- Electric Power Research Institute (1993). "Guidelines for determining design basis ground motions." Palo Alto, Calif: Electric Power Research Institute, vol. 1-5, EPRI TR-102293.
- vol. 1: Methodology and guidelines for estimating earthquake ground motion in eastern North America.
  - vol. 2: Appendices for ground motion estimation.
  - vol. 3: Appendices for field investigations.
  - vol. 4: Appendices for laboratory investigations.
  - vol. 5: Quantification of seismic source effects.
- Hanks, T.C. (1982). " $f_{\max}$ ." *Bull. Seism. Soc. Am.*, 72, 1867-1879.
- Hanks, T.C. and R.K. McGuire (1981). "The character of high-frequency strong ground motion." *Bull. Seism. Soc. Am.*, 71(6), 2071-2095.
- Hanks, T.C. and H. Kanamori (1979). "A moment magnitude scale." *J. Geophys. Res.*, 84, 2348-2350.
- Hartzell, S., A. Leeds, A. Frankel, and J. Michael (1996). "Site response for urban Los Angeles using aftershocks of the Northridge earthquake." *Bull. Seism. Soc. Am.*, 86(1B), S168-S192.
- Hartzell, S.H. (1978). "Earthquake aftershocks as Green's functions." *Geophys. Res. Letters*, 5, 1-4.
- Hough, S.E., J.G. Anderson, J. Brune, F. Vernon III, J. Berger, J. Fletcher, L. Haar, T. Hanks, and L. Baker (1988). "Attenuation near Anza, California." *Bull. Seism. Soc. Am.*, 78(2), 672-691.
- Hough, S.E. and J.G. Anderson (1988). "High-Frequency Spectra Observed at Anza, California: Implications for Q Structure." *Bull. Seism. Soc. Am.*, 78(2), 692-707.

## APPENDIX A

- Irikura, K. (1983). "Semi-empirical estimation of strong ground motions during large earthquakes." *Bull. Disaster Prevention Res. Inst.*, Kyoto Univ., 33, 63-104.
- McGuire, R. K., A.M. Becker, and N.C. Donovan (1984). "Spectral Estimates of Seismic Shear Waves." *Bull. Seism. Soc. Am.*, 74(4), 1427-1440.
- Ou, G.B. and R.B. Herrmann (1990). "Estimation theory for strong ground motion." *Seism. Res. Letters*. 61.
- Papageorgiou, A.S. and K. Aki (1983). "A specific barrier model for the quantitative description of inhomogeneous faulting and the prediction of strong ground motion, part I, Description of the model." *Bull. Seism. Soc. Am.*, 73(4), 693-722.
- Roblee, C.J., W.J. Silva, G.R. Toro and N. Abrahamson (1996). "Variability in site-specific seismic ground-motion design predictions." in press.
- Rovelli, A., O. Bonamassa, M. Cocco, M. Di Bona, and S. Mazza (1988). "Scaling laws and spectral parameters of the ground motion in active extensional areas in Italy." *Bull. Seism. Soc. Am.*, 78(2), 530-560.
- Schneider, J.F., W.J. Silva, and C.L. Stark (1993). "Ground motion model for the 1989 M 6.9 Loma Prieta earthquake including effects of source, path and site." *Earthquake Spectra*, 9(2), 251-287.
- Silva, W.J., N. Abrahamson, G. Toro, and C. Costantino (1997). "Description and validation of the stochastic ground motion model." Submitted to Brookhaven National Laboratory, Associated Universities, Inc. Upton, New York.
- Silva, W.J. and R. Darragh (1995). "Engineering characterization of earthquake strong ground motion recorded at rock sites." Palo Alto, Calif:Electric Power Research Institute, TR-102261.
- Silva, W.J. and C.L. Stark (1993) "Source, path, and site ground motion model for the 1989 M 6.9 Loma Prieta earthquake." CDMG draft final report.
- Silva, W.J. (1992). "Factors controlling strong ground motions and their associated uncertainties." *Dynamic Analysis and Design Considerations for High Level Nuclear Waste Repositories*, ASCE 132-161.
- Silva, W.J. (1991). "Global characteristics and site geometry." Chapter 6 in *Proceedings: NSF/EPRI Workshop on Dynamic Soil Properties and Site Characterization*. Palo Alto, Calif.: Electric Power Research Institute, NP-7337.
- Silva, W. J., R. Darragh, C. Stark, I. Wong, J. C. Stepp, J. Schneider, and S-J. Chiou (1990). "A Methodology to Estimate Design Response Spectra in the Near-Source Region of Large Earthquakes Using the Band-Limited-White-Noise Ground Motion

## APPENDIX A

- Model". *Procee. of the Fourth U.S. Conf. on Earthquake Engineering*, Palm Springs, California. 1, 487-494.
- Silva, W.J., R.B. Darragh, R.K. Green and F.T. Turcotte (1989). *Estimated Ground Motions for a new madrid Event*. U.S. Army Engineer Waterways Experiment Station, Wash., DC, Misc. Paper GL-89-17.
- Silva, W. J. and R. K. Green (1988). "Magnitude and Distance Scaling of Response Spectral Shapes for Rock Sites with Applications to North American Environments." In *Proceedings: Workshop on Estimation of Ground Motion in the Eastern United States*, EPRI NP-5875, Electric Power Research Institute.
- Silva, W. J., T. Turcotte, and Y. Moriwaki (1988). "Soil Response to Earthquake Ground Motion," Electric Power Research Institute, Walnut Creek, California, Report No. NP-5747.
- Silva, W.J. and K. Lee (1987). "*WES RASCAL code for synthesizing earthquake ground motions.*" State-of-the-Art for Assessing Earthquake Hazards in the United States, Report 24, U.S. Army Engineers Waterways Experiment Station, Miscellaneous Paper S-73-1.
- Somerville, P.G., R. Graves and C. Saikia (1995). "TECHNICAL REPORT: Characterization of ground motions during the Northridge earthquake of January 17, 1994." *Structural Engineers Association of California (SEAOC)*. Report No. SAC-95-03.
- Toro, G. R. and R. K. McGuire (1987). "An Investigation into Earthquake Ground Motion Characteristics in Eastern North America." *Bull. Seism. Soc. Am.*, 77(2), 468-489.
- Toro, G. R. (1985). "Stochastic Model Estimates of Strong Ground Motion." In *Seismic Hazard Methodology for Nuclear Facilities in the Eastern United States*, Appendix B, R. K. McGuire, ed., Electric Power Research Institute, Project P101-29.
- Wald, D.J. (1996). "Slip history of the 1995 Kobe, Japan, earthquake determined from strong motion, teleseismic, and geodetic data." *J. of Physics of the Earth*, in press.
- Wald, D.J. and T.H. Heaton (1994). "Spatial and temporal distribution of slip for the 1992 Landers, California, earthquake." *Bull. Seism. Soc. Amer.*, 84(3), 668-691.
- Wells, D.L. and K.J. Coppersmith (1994). "New empirical relationships among magnitude, rupture length, rupture width, rupture area, and surface displacement." *Bull. Seism. Soc. Am.* 84(4), 974-1002.
- Youngs, R.R., N.A. Abrahamson, F. Makdisi, and K. Sadigh (1995). "Magnitude dependent dispersion in peak ground acceleration." *Bull. Seism. Soc. Amer.*, 85(1), 161-1, 176.

**APPENDIX A**

Table A.1 CONTRIBUTIONS TO TOTAL VARIABILITY IN GROUND MOTION MODELS		
	Modeling Variability	Parametric Variability
<p><b>Uncertainty</b> <i>(also Epistemic Uncertainty)</i></p>	<p><u>Modeling Uncertainty:</u> Variability in predicted motions resulting from particular model assumptions, simplifications and/or fixed parameter values.  <i>Can be reduced by adjusting or "calibrating" model to better fit observed earthquake response.</i></p>	<p><u>Parametric Uncertainty:</u> Variability in predicted motions resulting from incomplete data needed to characterize parameters.  <i>Can be reduced by collection of additional information which better constrains parameters</i></p>
<p><b>Randomness</b> <i>(also Aleatory Uncertainty)</i></p>	<p><u>Modeling Randomness:</u> Variability in predicted motions resulting from discrepancies between model and actual complex physical processes.  <i>Cannot be reduced for a given model form.</i></p>	<p><u>Parametric Randomness:</u> Variability in predicted motions resulting from inherent randomness of parameter values.  <i>Cannot be reduced a priori<sup>***</sup> by collection of additional information.</i></p>

---

\*\*\*Some parameters (e.g. source characteristics) may be well defined after an earthquakes.

## APPENDIX A

Table A.2

### FIXED AND FREE PARAMETERS

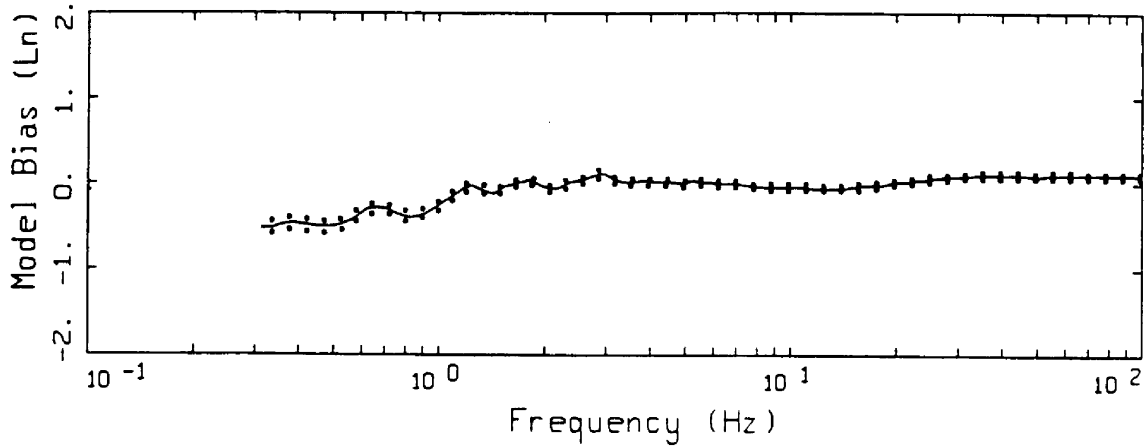
#### Fixed Parameters

Regional Crustal Model  
Rock and Soil Generic Profiles  
Kappa  
G/Gmax and Hysteretic Damping Curves  
Finite Source Rise Time  
Finite Source Rupture Velocity

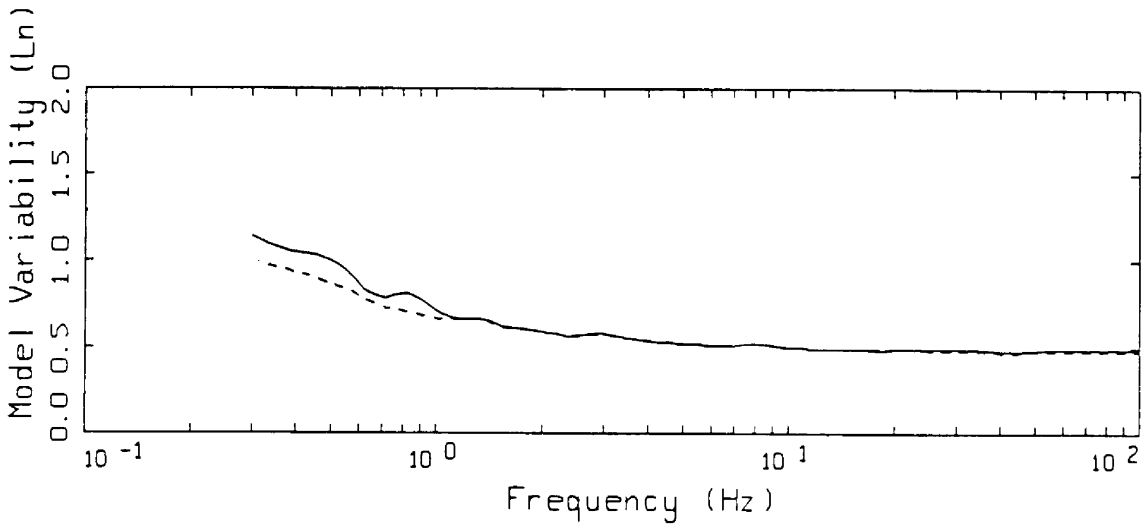
#### Free Parameters

Regional Q(f) Model  
Point Source Stress Drop and Depth  
Finite Source Slip Model and Nucleation Point

# APPENDIX A



LEGEND  
—— MODELING BIAS  
..... 90% CONFIDENCE INTERVAL OF MODELING BIAS  
..... 90% CONFIDENCE INTERVAL OF MODELING BIAS



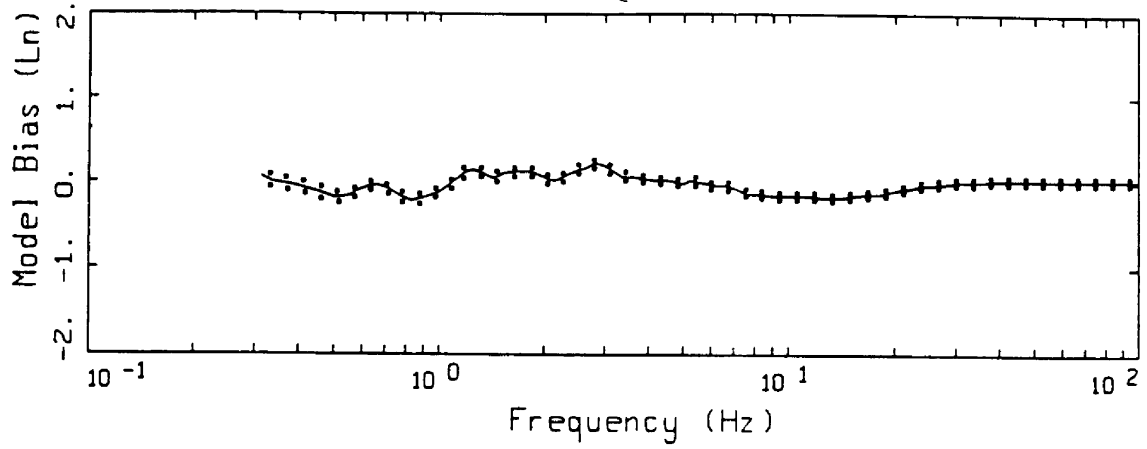
LEGEND  
—— MEAN=0.0  
----- BIAS CORRECTED

16 EARTHQUAKES POINT-SOURCE  
NONLINEAR, ALL 503 SITES

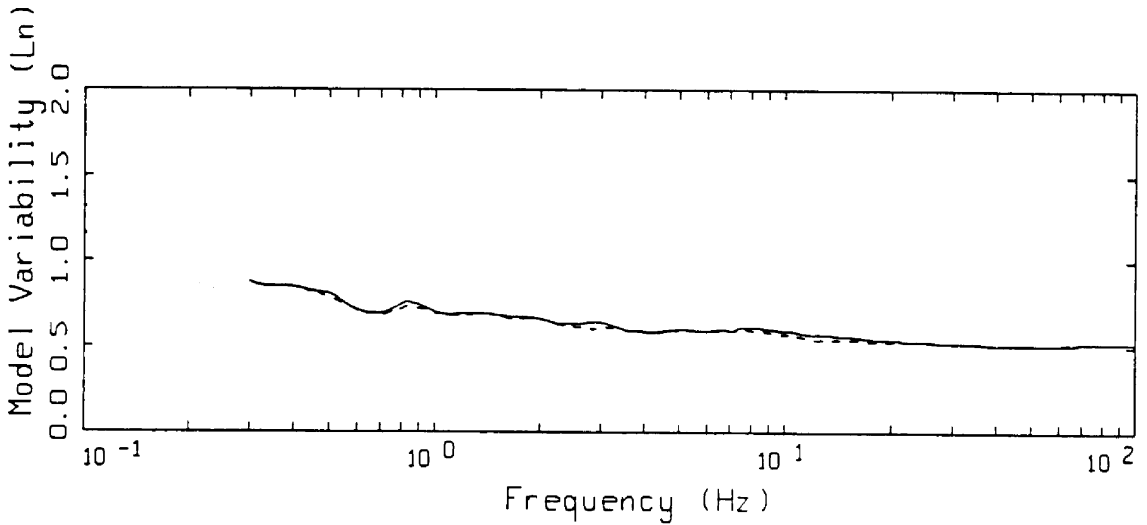
Figure A1. Model bias and variability estimates for all earthquakes computed over all 503 sites for the point-source model.



APPENDIX A



LEGEND  
 — MODELING BIAS  
 ..... 90% CONFIDENCE INTERVAL OF MODELING BIAS  
 ..... 90% CONFIDENCE INTERVAL OF MODELING BIAS



LEGEND  
 — MEAN=0.0  
 - - - - - BIAS CORRECTED

15 EARTHQUAKES FINITE-SOURCE  
 NONLINEAR, ALL 487 SITES

Figure A2. Model bias and variability estimates for all earthquakes computed over all 487 sites for the finite-source model.

APPENDIX A

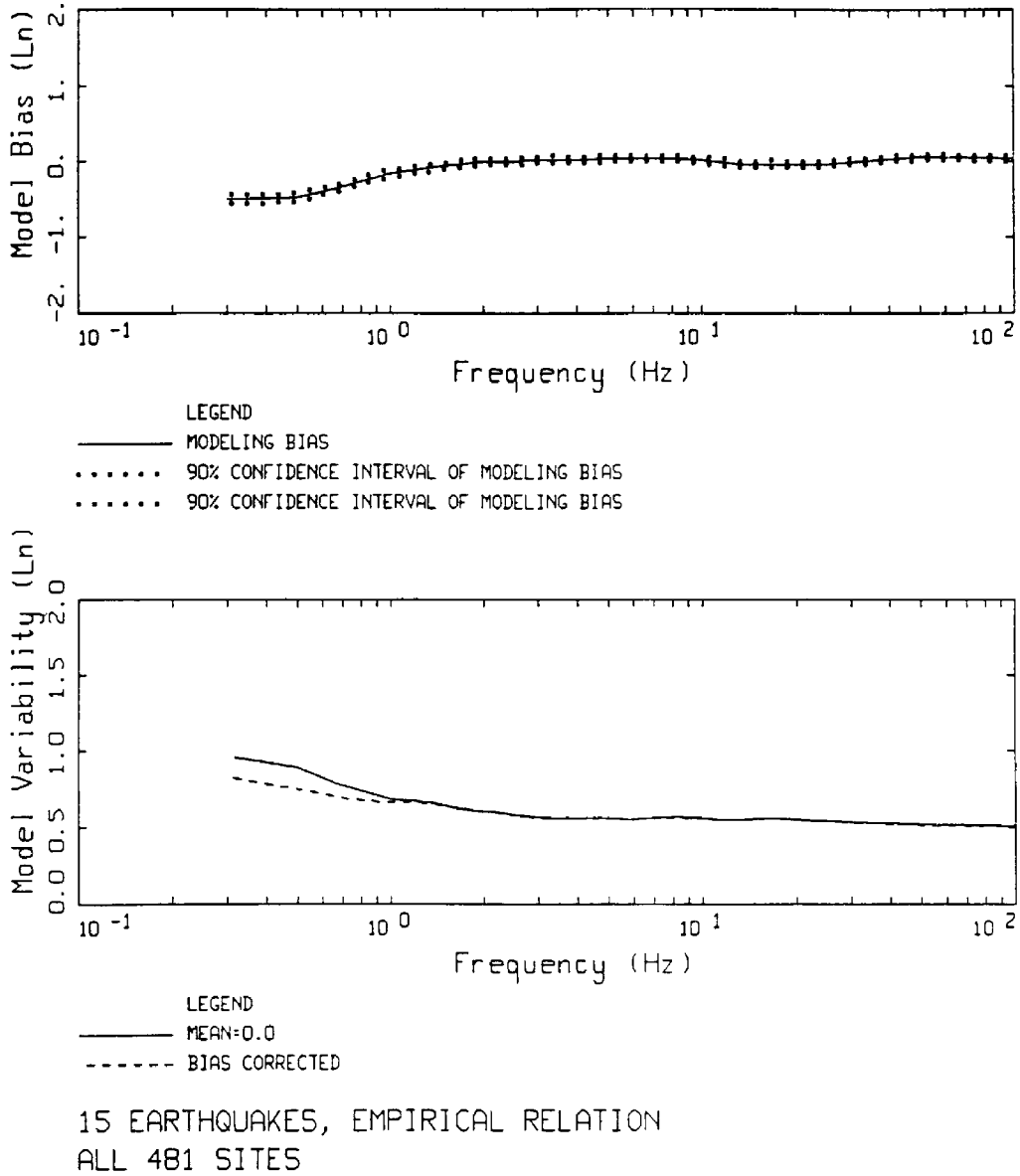


Figure A3. Model bias and variability estimates for all earthquakes computed over all 481 sites for the empirical model.

## **APPENDIX B**

### **SITE RESPONSE ANALYSIS METHOD**

#### **Development of Site Specific Soil Motions**

The conventional approach to estimating the effects of site-specific site conditions on strong ground motions involves development of a set (1, 2, or 3 component) of time histories compatible with the specified outcrop response spectra to serve as control (or input) motions. The control motions are then used to drive a nonlinear computational formulation to transmit the motions through the profile. Simplified analyses generally assume vertically propagating shear-waves for horizontal components and vertically propagating compression-waves for vertical motions. These are termed one-dimensional site response analyses.

#### **Equivalent-Linear Computational Scheme**

The computational scheme which has been most widely employed to evaluate one-dimensional site response assumes vertically-propagating plane shear-waves. Departures of soil response from a linear constitutive relation are treated in an approximate manner through the use of the equivalent-linear approach.

The equivalent-linear approach, in its present form, was introduced by Seed and Idriss (1970). This scheme is a particular application of the general equivalent-linear theory developed by Iwan (1967). Basically, the approach is to approximate a second order nonlinear equation, over a limited range of its variables, by a linear equation. Formally this is done in such a way that the average of the difference between the two systems is minimized. This was done in an ad-hoc manner for ground response modeling by defining an effective strain which is assumed to exist for the duration of the excitation. This value is usually taken as 65% of the peak time-domain strain calculated at the midpoint of each layer, using a linear analysis. Modulus reduction and hysteretic damping curves are then used to define new parameters for each layer based on the effective strain computations. The linear response calculation is repeated, new effective strains evaluated, and iterations performed until the changes in parameters are below some tolerance level. Generally a few iterations are sufficient to achieve a strain-compatible linear solution.

This stepwise analysis procedure was formalized into a one-dimensional, vertically propagating shear-wave code called SHAKE (Schnabel et al., 1972). Subsequently, this code has easily become the most widely used analysis package for one-dimensional site response calculations.

The advantages of the equivalent-linear approach are that parameterization of complex nonlinear soil models is avoided and the mathematical simplicity of a linear analysis is preserved. A truly nonlinear approach requires the specification of the shapes of hysteresis curves and their cyclic dependencies through an increased number of material parameters. In the equivalent-linear methodology the soil data are utilized directly and, because at each iteration the problem is linear and the material properties are frequency independent, the damping is rate independent and hysteresis loops close.

## APPENDIX B

Careful validation exercises between equivalent-linear and fully nonlinear formulations using recorded motions from 0.05 to 0.50g showed little difference in results (EPRI, 1993). Both formulations compared very favorably to recorded motions suggesting both the adequacy of the vertically propagating shear-wave model and the approximate equivalent-linear formulation. While the assumptions of vertically propagating shear-waves and equivalent-linear soil response certainly represent approximations to actual conditions, their combination has achieved demonstrated success in modeling observations of site effects and represent a stable, mature, and reliable means of estimating the effects of site conditions on strong ground motions (Schnabel et al., 1972; Silva et al., 1988; Schneider et al., 1993; EPRI, 1993).

To accommodate both uncertainty and randomness in dynamic material properties, analyses are typically done for the best estimate shear-wave velocity profile as well as upper- and lower-range profiles. The upper- and lower-ranges are usually specified as twice and one-half the best estimate shear-wave moduli. Depending upon the nature of the structure, the final design spectrum is then based upon an envelope or average of the three spectra.

For vertical motions, the SHAKE code is also used with compression-wave velocities and damping substituted for the shear-wave values. To accommodate possible nonlinear response on the vertical component, since modulus reduction and hysteretic damping curves are not generally available for the constrained modulus, the low-strain Poisson's ratio is usually fixed and strain compatible compression-wave velocities calculated using the strain compatible shear moduli from the horizontal component analyses combined with the low-strain Poisson's ratios. In a similar manner, strain compatible compression-wave damping values are estimated by combining the strain compatible shear-wave damping values with the low-strain damping in bulk or pure volume change. This process assumes the loss in bulk (volume change) is constant or strain independent. Alternatively, zero loss in bulk is assumed and the equation relating shear- and compression-wave damping ( $\eta_S$  and  $\eta_P$ ) and velocities ( $V_S$  and  $V_P$ )

$$\eta_P \approx \frac{4}{3} \frac{V_S}{V_P} \eta_S, \quad (\text{B-1})$$

is used.

### RVT Based Computational Scheme

The computational scheme employed to compute the site response for this project uses an alternative approach employing random vibration theory (RVT). In this approach the control motion power spectrum is propagated through the one-dimensional soil profile using the plane-wave propagators of Silva (1976). In this formulation only SH waves are

## APPENDIX B

considered. Arbitrary angles of incidence may be specified but normal incidence is used throughout the present analyses.

In order to treat possible material nonlinearities, an RVT based equivalent-linear formulation is employed. Random process theory is used to predict peak time domain values of shear-strain based upon the shear-strain power spectrum. In this sense the procedure is analogous to the program SHAKE except that peak shear-strains in SHAKE are measured in the time domain. The purely frequency domain approach obviates a time domain control motion and, perhaps just as significant, eliminates the need for a suite of analyses based on different input motions. This arises because each time domain analysis may be viewed as one realization of a random process. Different control motion time histories reflecting different time domain characteristics but with nearly identical response spectra can result in different nonlinear and equivalent-linear response.

In this case, several realizations of the random process must be sampled to have a statistically stable estimate of site response. The realizations are usually performed by employing different control motions with approximately the same level of peak accelerations and response spectra.

In the case of the frequency domain approach, the estimates of peak shear-strain as well as oscillator response are, as a result of the random process theory, fundamentally probabilistic in nature. For fixed material properties, stable estimates of site response can then be obtained with a single run.

In the context of the RVT equivalent-linear approach, a more robust method of incorporating uncertainty and randomness of dynamic material properties into the computed response has been developed. Because analyses with multiple time histories are not required, parametric variability can be accurately assessed through a Monte Carlo approach by randomly varying dynamic material properties. This results in median as well as other fractile levels (e.g. 16<sup>th</sup>, mean, 84<sup>th</sup>) of smooth response spectra at the surface of the site. The availability of fractile levels reflecting randomness and uncertainty in dynamic material properties then permits a more rational basis for selecting levels of risk.

In order to randomly vary the shear-wave velocity profile, a profile randomization scheme has been developed which varies both layer velocity and thickness. The randomization is based on a correlation model developed from an analysis of variance on about 500 measured shear-wave velocity profiles (EPRI, 1993; Silva et al., 1997). Profile depth (depth to competent material) is also varied on a site specific basis using a uniform distribution. The depth range is generally selected to reflect expected variability over the structural foundation as well as uncertainty in the estimation of depth to competent material.

To model parametric variability for compression-waves, the base-case Poisson's ratio is generally fixed. Suites of compatible random compression- and shear-wave velocities are then generated based on the random shear-wave velocities profiles.

## APPENDIX B

To accommodate variability in modulus reduction and hysteretic damping curves on a generic basis, the curves are independently randomized about the base case values. A log normal distribution is assumed with a  $\sigma_{\ln}$  of 0.35 at a cyclic shear strain of  $3 \times 10^{-2}\%$ . These values are based on an analysis of variance on a suite of laboratory test results. An upper and lower bound truncation of  $2\sigma$  is used to prevent modulus reduction or damping models that are not physically possible. The random curves are generated by sampling the transformed normal distribution with a  $\sigma_{\ln}$  of 0.35, computing the change in normalized modulus reduction or percent damping at  $3 \times 10^{-2}\%$  shear strain, and applying this factor at all strains. The random perturbation factor is reduced or tapered near the ends of the strain range to preserve the general shape of the median curves (Silva, 1992).

To model vertical motions, incident inclined compression- and shear (SV)-waves are assumed. Raytracing is done from the source location to the site to obtain appropriate angles of incidence. In the P-SV site response analyses, linear response is assumed in both compression and shear with the low-strain shear-wave damping used for the compression-wave damping (Johnson and Silva, 1981). The vertical and horizontal motions are treated independently in separate analyses. Validation exercises with a fully 3-D soil model using recorded motions up to 0.50%g showed these approximations to be validate (EPRI, 1993).

In addition, the site response model for the vertical motions has been validated at over 100 rock and soil sites for three large earthquakes: 1989 **M** 6.9 Loma Prieta, 1992 **M** 7.2 Landers, and the 1994 Northridge earthquakes. In general, the model performs well and captures the site and distance dependency of vertical motions over the frequency range of about 0.3 to 50.0 Hz and the fault distance range of about 1 to 100 km.

## APPENDIX B

### REFERENCES

- Electric Power Research Institute (1993). "Guidelines for determining design basis ground motions." Palo Alto, Calif: Electric Power Research Institute, vol. 1-5, EPRI TR-102293.
- vol. 1: Methodology and guidelines for estimating earthquake ground motion in eastern North America.
  - vol. 2: Appendices for ground motion estimation.
  - vol. 3: Appendices for field investigations.
  - vol. 4: Appendices for laboratory investigations.
  - vol. 5: Quantification of seismic source effects.
- Iwan, W.D. (1967). "On a class of models for the yielding behavior of continuous and composite systems." *J. Appl. Mech.*, 34, 612-617.
- Johnson, L.R. and W.J. Silva (1981). "The effects of unconsolidated sediments upon the ground motion during local earthquakes." *Bull. Seism. Soc. Am.*, 71, 127-142.
- Schnabel, P.B., J. Lysmer, and H.B. Seed (1972). *SHAKE: a Computer Program for Earthquake Response Analysis of Horizontally Layered Sites*. Earthq. Engin. Res. Center, Univ. of Calif. at Berkeley, EERC 72-12.
- Schneider, J.F., W.J. Silva, and C.L. Stark (1993). Ground motion model for the 1989 M 6.9 Loma Prieta earthquake including effects of source, path and site. *Earthquake Spectra*, 9(2), 251-287.
- Seed, H.B. and I.M. Idriss (1970). "Soil Moduli and Damping Factors for Dynamic Response Analyses," Earthq. Eng. Res. Center, Univ. of Calif. at Berkeley, Report No. UCB/EERC-70/10.
- Silva, W.J., N. Abrahamson, G. Toro, and C. Costantino (1997). "Description and validation of the stochastic ground motion model." Submitted to Brookhaven National Laboratory, Associated Universities, Inc. Upton, New York.
- Silva, W.J. (1992). "Factors controlling strong ground motions and their associated uncertainties." *Dynamic Analysis and Design Considerations for High Level Nuclear Waste Repositories*, ASCE 132-161.
- Silva, W. J., T. Turcotte, and Y. Moriwaki, (1988). "Soil Response to Earthquake Ground Motion," Electric Power Research Institute, Walnut Creek, California, Report No. NP-5747.
- Silva, W.J. (1976). "Body Waves in a Layered Anelastic solid." *Bull. Seis. Soc. Am.*, vol. 66(5), 1539-1554.